



<https://theses.gla.ac.uk/>

Theses Digitisation:

<https://www.gla.ac.uk/myglasgow/research/enlighten/theses/digitisation/>

This is a digitised version of the original print thesis.

Copyright and moral rights for this work are retained by the author

A copy can be downloaded for personal non-commercial research or study, without prior permission or charge

This work cannot be reproduced or quoted extensively from without first obtaining permission in writing from the author

The content must not be changed in any way or sold commercially in any format or medium without the formal permission of the author

When referring to this work, full bibliographic details including the author, title, awarding institution and date of the thesis must be given

Enlighten: Theses

<https://theses.gla.ac.uk/>
research-enlighten@glasgow.ac.uk

STRUCTURAL BASIS OF SUBSTRATE BINDING
TO HUMAN FACILITATIVE SUGAR TRANSPORTERS

A thesis submitted to the

FACULTY OF SCIENCE

for

the degree of

DOCTOR OF PHILOSOPHY

BY

SUSAN KANE

Division of Biochemistry and Molecular Biology

Institute of Biomedical and Life Sciences

University of Glasgow

February 1997

ProQuest Number: 10391274

All rights reserved

INFORMATION TO ALL USERS

The quality of this reproduction is dependent upon the quality of the copy submitted.

In the unlikely event that the author did not send a complete manuscript and there are missing pages, these will be noted. Also, if material had to be removed, a note will indicate the deletion.



ProQuest 10391274

Published by ProQuest LLC (2017). Copyright of the Dissertation is held by the Author.

All rights reserved.

This work is protected against unauthorized copying under Title 17, United States Code
Microform Edition © ProQuest LLC.

ProQuest LLC.
789 East Eisenhower Parkway
P.O. Box 1346
Ann Arbor, MI 48106 – 1346

Thesis
10820
Copy 2

Abstract.

Human GLUT5 has been heterologously expressed in *Xenopus* oocytes, allowing examination of its substrate selectivity and basic kinetic parameters. The K_m for zero-*trans* entry of D-fructose by GLUT5 is 22.5 mM, but 2-deoxy-D-glucose is not transported by this isoform. Additionally, transport of fructose is not inhibited by the presence of either deoxyglucose or D-glucose. Analysis of the effects of pH on transport indicate that deoxyglucose is not transported across the pH range. Furthermore, the K_m for transport of fructose remains constant under varying pH conditions.

The inhibitory effects of fused ring fructose analogues on the fructose transport of GLUT5 have also been determined. Fructose transport by GLUT5-expressing oocytes is not inhibited by the fused pyranose ring analogues, 1,5-anhydromannitol and L-sorbose. However, the fused furanose ring analogue, 2,5-anhydromannitol, does inhibit the transport of fructose by GLUT5 in the same system.

GLUT2/GLUT3 chimeras had been constructed previously. Expression of these mutants in *Xenopus* oocytes has allowed determination of their basic kinetic parameters, with a view to examine the structural basis for differential substrate selectivity between isoforms. K_m values for the transport of alternative substrates, fructose and galactose, have been determined for these chimeras, and compared with parameters previously measured for deoxyglucose. All parameters were compared with K_m values obtained for native GLUT2 and GLUT3 in the same system. Results indicate that helix 7 participates in fructose recognition by GLUT2, and the equivalent helix in GLUT3 is involved in high affinity deoxyglucose and galactose transport by this isoform.

A panel of nineteen GLUT3 mutants had been constructed previously, each incorporating substitution of an individual residue of helix 8 with alanine. These have been expressed in the *Xenopus* oocyte system, allowing analysis of their basic

kinetic properties. The K_m value for deoxyglucose entry was determined for each mutant and this compared to that of wild-type GLUT3. Only replacement of asparagine-315 with alanine altered this transport parameter with respect to the wild type value, producing a 4-fold elevation of K_m . This residue is polar and may be directly involved in the transport of glucose.

Acknowledgements.

My acknowledgements go to the following people, all of whom have made this strange PhD experience worthwhile.

Special thanks to Gwyn, my patient supervisor, for his unending encouragement, and for his unfailing faith in me which made all the difference. Contrary to popular belief, however, I am *not* to blame for his drastic hair loss, or for that world-weary expression he wears these days.

Equally special thanks also to Michael, without whose help and good humour, my thesis would not have been started- or finished, and the bit , , , , , in-between wouldn't have been so much fun.

Thanks also to: Lisa, who is a most excellent Guinness-drinking, spoon-playing mate, with whom I have enjoyed many an adventure; to all the brilliant people I have worked with in Lab C36, who are too numerous to mention (either Gwyn employs too many people, or I have worked here for way too long!), but especially to Alison, Sally, Callum, Margaret and Fiona, who have all been a great help to me at one time or another, and a great laugh, and to Tommy, whose colourful character is second only to his trousers. Thanks to Gwyn, Tommy, Lisa, Alison, Sally and Mikey, I *never* wandered lonely as a cloud!

Final and special acknowledgements go to Andrew, Brian and The Weather Parents for always making me laugh and got things in perspective when the plans went awry.

This thesis is dedicated with great affection to my Mum and Dad, who would have been just as proud of me had I gone to work in "The Biscuit Factory", but whose love, support and understanding have carried me all this way.

Abbreviations.

Ac	Acetate
Amp	Ampicillin
ASA-BMPA	2-N-(4-azidosalicyl)-1,3-bis(D-mannos-4-yloxy)propyl-2-amine
ATB-BMPA	2-N-[4-azi-2,2,2-trifluoroethyl)benzoyl]-1,3-bis(D-mannos-4-yloxy)-2-propylamine
ATP	adenosine 5'-triphosphate
BBM	brush border membrane
BLM	basolateral membrane
BMPA	1,3-bis-(D-mannos-4-yloxy)-2-propylamine
bp	base pairs
C-1	carbon position number 1.
cDNA	complementary deoxyribonucleic acid
CD	circular dichroism
CIP	calf intestinal phosphatase
CTP	cytidine 5'-triphosphate
CPM	counts per minute
DeGlc	deoxyglucose
DNA	deoxyribonucleic acid
dsDNA	double-stranded deoxyribonucleic acid
dNTPs	deoxyribonucleic nucleoside 5'-triphosphates
dITP	deoxyribonucleic thymidine 5'-triphosphate
DIT	dithiothreitol
EDTA	Diaminoethanetetra-acetic acid, disodium salt
FTIR	fourier-transforming infra-red
gav	average gravitational force
GLUT	glucose transporter

GTP	guanosine 5'-triphosphate
HEPES	<i>N</i> -2-hydroxyethylpiperazine- <i>N'</i> -2-ethane sulphonic acid
IAPS-forskolin	iodo-4-azidophenethylamido-7- <i>O</i> -succinyldeacetyl forskolin
IR	infra-red
K_i	inhibitory affinity constant
K_m	affinity constant
LB	Luria-Bertani
min	minutes
MOPS	3'-(<i>N</i> -morpholino)propanesulphonic acid
mRNA	messenger ribonucleic acid
NIDDM	non-insulin-dependent diabetes mellitus
NMR	nuclear magnetic resonance
PBS	phosphate-buffered saline
PCR	polymerase chain reaction
PEG	polyethylene glycol
RNA	ribonucleic acid
RNase A	ribonuclease A
rNTPs	ribonucleoside 5'-triphosphates
rpm	revolutions per minute
sec	seconds
SEM	standard error of the mean
SDS-PAGE	sodium dodecyl sulphate polyacrylamide gel electrophoresis
SGLT1	sodium-glucose-linked transporter 1
STE	saline-Tris-EDTA
STET	sucrose-triton X-100-EDTA-tris
TACS	terminator ammonium cycle sequencing
TAE	Tris-acetate-EDTA

TBE	Tris-borate-EDTA
TE	Tris-EDTA
TEMED	<i>N, N, N', N'</i> -tetramethylethylenediamine
Tris	tris(hydroxymethyl)aminoethane
rUTP	uridine 5'-triphosphate
UTR	untranslated regions
V_{\max}	theoretical maximum velocity
v/v	volume/ volume ratio
w/v	weight/ volume ratio

Contents.

	Page
Title	i
Abstract	ii
Acknowledgements	iv
Abbreviations	v
Contents	viii
List of Figures	xvi
List of Tables	xix
Chapter 1. Introduction.	
1.1 General Background.	2
1.2.1 Tissue-Specific Distribution of the Facilitative Glucose Transporter Family.	4
1.2.2 GLUT1	4
1.2.3 GLUT2	6
1.2.4 GLUT3	8
1.2.5 GLUT4	10
1.2.6 GLUT5	11
1.2.7 GLUT6	12
1.2.8 GLUT7	13
1.2.9 Homologous Transporters in Other Organisms.	14
1.3.1 Structure of the Mammalian Facilitative Glucose Transporter Family.	15
1.3.2 Topological Model of GLUT1.	17

1.4.1	The Single Site Conformational Change Model.	19
1.4.2.1	Kinetics of Transport of D-Glucose by GLUT1.	21
1.4.2.2	<i>Zero-Trans</i> Entry.	21
1.4.2.3	<i>Zero-Trans</i> Exit.	22
1.4.2.4	Equilibrium Exchange.	22
1.4.3.1	Reaction Mechanism of the Single Site Model.	23
1.4.3.2	Measurement of Steady State Rate Constants.	24
1.4.3.3	Measurement of Pre-Steady State Rate Constants.	25
1.4.3.4	Multiple Site Models.	27
1.5.1	Conformational Change in GLUT1: Detected by Changes in Intrinsic Fluorescence.	28
1.5.2	Changes in Proteolytic Susceptibility: Support for the Alternating Conformation Model.	30
1.5.3	Chemical Inactivation of GLUT1: Support for the Alternating Conformation Model.	32
1.6	Photoaffinity Labelling of GLUT1 by Conformation- Specific Ligands.	33
1.7	The Contribution of Molecular Biology to the Understanding of the Alternating Conformation Model.	36
1.8	The Role of the C-Terminal Half of the Transporter in the Formation of the Exofacial and Endofacial Binding Sites.	37
1.9	Molecular Model of the Tertiary Structure of GLUT1.	39
1.10	Oligomerisation of GLUT1.	40

1.11	Aims of this Study.	43
------	---------------------	----

Chapter 2. Materials and Methods.

2.1	Materials.	64
2.2	<i>In Vitro</i> Transcription of mRNA from Plasmid cDNA.	67
2.3	Using <i>Xenopus</i> Oocytes.	68
2.3.1	Handling <i>Xenopus</i> .	68
2.3.2	Anaesthesia.	69
2.3.3	Surgery.	69
2.3.4	Oocyte Isolation and Injection.	70
2.4	Sugar Transport in <i>Xenopus</i> Oocytes.	71
2.5	General Techniques for the Manipulation of DNA.	72
2.5.1	Plasmid Construction.	72
2.5.2	Linearisation of Plasmid cDNA.	73
2.5.3	Agarose Gel Electrophoresis of DNA.	73
2.5.4	Restriction Digestion of DNA.	75
2.5.5	Dephosphorylation of Double-Stranded DNA using Calf Intestinal Phosphatase.	76
2.5.6	Ligation of Double-Stranded DNA.	76
2.5.7	Preparation and Transformation of Competent <i>E.coli</i> DH5 α Cells.	76
2.5.8	Preparation of Small Amounts of Plasmid DNA from Transformed DH5 α Cells.	78
2.5.9	Calculation to Determine Plasmid DNA Concentration and Purity.	79
2.6	Recombinant Polymerase Chain Reaction.	80

2.6.1	Primary Polymerase Chain Reaction Using <i>Taq</i> DNA Polymerase.	80
2.6.1a	Synthesis of Oligonucleotides.	80
2.6.1b	Primary PCR: Reaction Conditions.	81
2.6.1c	Thermal Cycling.	81
2.6.1d	Secondary PCR: Reaction Conditions.	82
2.6.2	Polymerase Chain Reaction Using <i>Pfu</i> DNA Polymerase.	83
2.6.2a	Primary PCR: Reaction Conditions.	83
2.6.2b	Secondary PCR: Reaction Conditions.	84
2.6.2c	Thermal Cycling.	85
2.6.3	Polymerase Chain Reaction Using Vent DNA Polymerase.	86
2.6.3a	Primary PCR: Reaction Conditions.	86
2.6.3b	Secondary PCR: Reaction Conditions.	87
2.6.3c	Thermal Cycling.	88
2.6.4	Elution of DNA from Gel Fragments by Electrophoresis.	88
2.6.5	Preparation of Dialysis Tubing.	89
2.6.6	Purification of DNA Using Elutip-D Affinity Columns.	89
2.7	<i>Taq</i> DyeDeoxy™ Terminator Cycle Sequencing Protocol.	91
2.7.1a	Kit Reagents.	91
2.7.1b	Other Reagents.	91
2.7.2	Preparation of Templates.	92
2.7.3	Thermal Cycling.	93
2.7.4	Acrylamide Gel Preparation.	94
2.7.5a	Preparing the Gel Plates.	94
2.7.5b	Casting the Gel.	94
2.7.6	Setting up for a Run.	95
2.7.7	Sample Extraction and Precipitation.	96
2.7.8	Preparing and Loading the Samples.	96

2.7.9	Analysis of Samples.	97
Chapter 3.	Studies of the GLUT5 Isoform.	
3.1.1	Introduction.	107
3.1.2	Substrate Selectivity of GLUT5.	109
3.1.3	GLUT2, GLUT5 and SCLT1 in the Small Intestine.	111
3.1.4	Structural Requirements of Fructose Binding to GLUT5.	113
3.1.5	Studies of Other Fructose Transporters.	114
3.2	Aims of This Study.	116
3.3	Results.	117
3.3.1	Measurement of the K_m Value for the Transport of D-Fructose by Human GLUT5 in <i>Xenopus</i> Oocytes.	117
3.3.2	Determining the Substrate Selectivity of Human GLUT5 in <i>Xenopus</i> Oocytes.	118
3.3.3	The Effects of pH on the Substrate Selectivity of Human GLUT5 in <i>Xenopus</i> Oocytes.	118
3.3.4	The Effects of pH on the K_m for Fructose Transport by GLUT5 in <i>Xenopus</i> Oocytes at pH4.5.	118
3.3.5	Analysis of the Preferred Fructo- Ring Form Accepted by Human GLUT5.	119
3.5	Conclusions.	137
3.5.1	Kinetics and Substrate Selectivity of Human GLUT5 in <i>Xenopus</i> Oocytes.	137

3.5.2	The Effect of pH on the Substrate Selectivity of Human GLUT5 in <i>Xenopus</i> Oocytes.	137
3.5.3	Analysis of the Preferred Fructo-Ring Form Accepted by Human GLUT5.	138
3.6	Summary.	139
Chapter 4.	Kinetic Characterisation of GLUT2/GLUT3 Chimeric Transporters.	
4.1.1	Introduction.	142
4.1.2	Previous Studies of Regions Involved in Substrate Selectivity.	143
4.1.3	Kinetic Characterisation of Other Glucose Transporter Isoforms.	146
4.2	Methods.	148
4.3	Aims of this Study.	150
4.4.1	Results.	151
4.4.2	Measurement of Fructose Transport.	151
4.4.3	Measurement of Galactose Transport.	152
4.5.1	Discussion.	179
4.5.2	Analysis of the GLUT3 Series.	179
4.5.2a	Kinetics of DeGlc Transport in the GLUT3 Series.	179
4.5.2b	Fructose Recognition in the GLUT3 Series.	180
4.5.2c	Galactose Transport in the GLUT3 Series.	180

4.5.3	Analysis of the GLUT2 Series.	181
4.5.4	Maltose Inhibition of DeGlc Transport.	183
4.6	Conclusions.	186
4.6.1	Working Model for Substrate Recognition and Isoform Specific Kinetics.	186
4.6.1a	The Role of Helix 7.	186
4.6.1b	The Role of the N-Terminal Half of the Transporter.	188
4.6.1c	Possible Involvement of the Cytoplasmic C-Terminal Tail of GLUT2.	189
4.6.1d	Possible Role for the H7 _{end} -H10 _{end} Sequence.	190
4.6.2	Speculation as to How Helix 7 Interacts with Substrate.	191
4.6.3	Problems with this Study.	192
Chapter 5.	Construction of Second Generation Chimeras.	
5.1	Introduction.	196
5.2	Methods.	197
5.2.1	PCR- Primary Reactions.	197
5.2.2	PCR- Secondary Reactions.	198
5.2.3	Vectors and Cloning Procedure.	200
5.3	Results.	201
5.3.1	Results Using <i>Taq</i> DNA Polymerase.	201
5.3.2	Results Using <i>Pfu</i> DNA Polymerase.	202
5.3.3	Results Using <i>Vent</i> DNA Polymerase.	203
Chapter 6.	Kinetic Analysis of GLUT3 Helix 8 Mutants.	
6.1	Introduction.	217

6.2.1	Use of Site Directed Mutagenesis.	218
6.2.2	Substitution of Conserved Polar Residues.	219
6.2.3	Substitution of Conserved Tryptophan Residues.	222
6.2.4	Substitution of Conserved Proline Residues.	223
6.2.5	Substitution of Conserved Cysteine Residues.	225
6.2.6	Residues in Extramembraneous Regions.	226
6.2.7	The C-Terminal Cytoplasmic Tail.	226
6.2.8	Naturally Occurring Mutations.	229
6.2.9	Transmembrane Helix 8 of GLUT1.	230
6.3	Methods.	232
6.3.1	Alanine Scanning Mutagenesis.	232
6.3.2	Construction and Subcloning of the Helix 8 Mutants.	233
6.3.3	Expression of the Mutant Constructs in <i>Xenopus</i> Oocytes.	234
6.4	Results.	234
6.5	Conclusions.	251
6.6	Discussion.	251
Chapter 7.	Discussion.	257
	References.	264

List of Figures.

	Page
Figure 1.1 Comparison of Hydropathy Plots of GLUTs 1, 2, 3 and 5.	46
Figure 1.2 Topological Model of the Mammalian Facilitative Glucose Transporters.	48
Figure 1.3 Diagram of the Single Site Alternating Conformation Model of GLUT1.	50
Figure 1.4 Interaction of β -D-Glucose at the Exofacial Binding Site of GLUT1.	52
Figure 1.5 King-Altman Representation of the Transport Cycle of GLUT1.	54
Figure 1.6 Structures of Cytochalasin B and ATB-BMPA.	56
Figure 1.7 Diagram Showing the Proposed Model of GLUT1 Oligomerisation.	58
Figure 1.8 Diagram Showing Regions of Importance in the Transporter Structure.	60
Figure 1.9 Speculative Models of the Helical Packing Arrangement in the Tertiary Structure of GLUT1.	62
Figure 2.1 Diagram of pSP64T Vector.	101
Figure 2.2 Agarose Gel Analysis of <i>in vitro</i> Transcribed mRNA.	103
Figure 2.3 Cloning of Chimeric Constructs into pSP64T Vector.	105
Figure 3.1 Diagram Showing the Uptake and Efflux of Dietary Sugars Across an Intestinal Epithelial Cell.	121
Figure 3.2 Structures of Pyranose and Furanose Forms of β -D-Fructose and Fused Ring Fructo-Analogues.	123

Figure 3.3	Lineweaver-Burk Plot of Fructose Uptake by Human GLUT5-Injected Oocytes.	125
Figure 3.4	Graph Showing the Uptake of 0.1mM DeGlc by GLUT2-Injected, GLUT5-Injected and Control Oocytes.	127
Figure 3.5	Graph Showing the Inhibition of Uptake of 0.1mM Fructose by 100mM D-Glucose, L-Glucose or D-Fructose.	129
Figure 3.6	Graph Showing the Effect of pH on the Transport Activity of GLUT5-Injected Oocytes.	131
Figure 3.7	Lineweaver-Burk Plot of Fructose Transport by GLUT5-Injected Oocytes at pH 4.5.	133
Figure 3.8	Graph Showing the Inhibition of the Fructose Transport of GLUT5-Injected Oocytes by Fused Ring Fructose Analogues.	135
Figure 4.1	Diagram of the Recombinant PCR Used to Construct GLUT2/GLUT3 Chimeric Transporters.	154
Figure 4.2	Diagram Showing the Junction Points of the GLUT2 and GLUT3 Chimeric Series.	156
Figure 4.3	Lineweaver-Burk Plot of the Uptake of D-Fructose by Chimera G2(12Ed)-Injected Oocytes.	158
Figure 4.4	Lineweaver-Burk Plot of the Uptake of D-Fructose by Chimera G3(7St)-Injected Oocytes.	160
Figure 4.5	Lineweaver Burk-Plot of the Uptake of D-Galactose by Chimera G3(7St)-Injected Oocytes.	162
Figure 4.6	Lineweaver Burk-Plot of the Uptake of D-Galactose by Chimera G3(7Ed)-Injected Oocytes.	164
Figure 4.7	Lineweaver-Burk Plot of the Uptake of D-Galactose by Chimera G3(10Ed)-Injected Oocytes.	166

Figure 4.8	Lineweaver-Burk Plot of the Uptake of D-Galactose by Chimera G3(12Ed)-Injected Oocytes.	168
Figure 4.9	Structures of β -D-Glucose and β -D-Maltose.	170
Figure 4.10	King-Altman Diagram Showing the Competition of DeGlc and Maltose at the Exofacial Binding Site of the Transporter.	172
Figure 4.11	Diagram Showing Regions of the Transporter Structure Involved in Substrate Selectivity and Transport Kinetics.	174
Figure 4.12	Comparison of the Helix 7 Amino Acid Sequences of Human GLUTs 1, 2, 3, 4 and 5.	176
Figure 5.1	Diagram of Second Generation GLUT2/GLUT3 Chimeric Constructs.	206
Figure 5.2	Recombinant PCR Method Used to Construct Second Generation Chimeric Transporters.	208
Figure 5.3	Agarose Gel of Primary <i>Taq</i> PCR Fragments.	210
Figure 5.4	Agarose Gel of Secondary PCR Fragments, Unligated Vector and Ligated Chimeric Constructs.	212
Figure 6.1	Comparison of Amino Acid Sequences in Putative Transmembrane Helix 8 of the Facilitative Glucose Transporter Family.	236
Figure 6.2	Predicted α -Helical Structure of GLUT3 Transmembrane Helix 8.	238
Figure 6.3	Diagram Describing Recombinant PCR Approach.	240
Figure 6.4	Lineweaver-Burk Plot of the Uptake of DeGlc by Mutant Ile ³⁰⁵ -Injected Oocytes.	242
Figure 6.5	Lineweaver-Burk Plot of the Uptake of DeGlc by Mutant Asn ³¹⁵ -Injected Oocytes.	244

List of Tables.

		Page.
Table 2.1	Table of Buffers.	98
Table 2.2	Bacterial Media and Agar.	99
Table 3.1	Collected GLUT5 Data From Different Species and Different Expression Systems.	136
Table 4.1	Kinetic Parameters of the Glucose Transporter Family Expressed in <i>Xenopus</i> Oocytes.	177
Table 4.2	Kinetic Parameters for Transport of Substrates by GLUT2/ GLUT3 Chimeras.	178
Table 5.1	Oligonucleotides Used in the Recombinant PCR.	213
Table 5.2	Sequencing Primers.	215
Table 6.1	Effects of Point Mutation on the Transport Activity of Glucose Transporters: Collected Results From Other Studies.	245
Table 6.2	Kinetic Parameters of Helix 8 Mutants in Oocytes.	250

CHAPTER 1.

Introduction.

1.1 General Background.

The ability of cells to selectively transport molecules and ions across their plasma membranes is an important feature of the essential link between membrane physiology and cellular metabolism. This link is clearly demonstrated by the mechanisms that have evolved in living cells to mediate the uptake of the most metabolically important biological molecule on earth—glucose.

In mammalian cells, these mechanisms fall into two general categories (reviewed in Carruthers, 1990). The first of these is a protein-mediated diffusion mechanism which involves the rapid diffusion of glucose down its concentration gradient via a protein carrier molecule. This transport event is driven only by the concentration gradient and can be bidirectional. This is termed facilitative diffusion. The second type of mechanism is termed active transport. This type of system couples the transport of glucose with an energy-producing reaction such as the hydrolysis of ATP or the co-transport of an ion. The expression of these active transport carriers is restricted to the apical membrane in cells of the absorptive epithelia in the small intestine and the reabsorptive epithelia of the kidney tubules. In all other tissues the uptake of glucose is achieved by facilitated diffusion, which is possible due to the maintenance of a relatively high physiological blood glucose concentration—approximately between 5-10mM.

Studies performed by Widdas in 1952, examining the saturable nature of sugar transport into erythrocytes, and by LeFevre in 1961, examining the competition between sugars for transport, showed that the erythrocyte system displayed modified Michaelis-Menton saturation kinetics, in which the carrier acted as the enzyme and D-glucose as the substrate on the outside of the cell membrane and the product on the inside (LeFevre, 1961, Widdas, 1952). In these studies, differences were noted in the kinetics of sugar uptake into

different tissue types which hinted at the prospect of the existence of tissue specific isoforms.

Evidence that the mechanism of glucose transport was at least partially protein-dependent came from studies by Jung (Jung, 1971), who showed that erythrocyte ghosts retain the capacity to transport glucose, whereas the protein-bereft pure phospholipid component of fractionated erythrocytes do not. Further studies also showed that glucose uptake into erythrocytes could be inhibited very efficiently by low concentrations of cytochalasin B or phloretin. These compounds had K_i values of 140nM and 200nM respectively (Bloch, 1973, LeFevre & Marshall, 1959, Zoccoli *et al.*, 1978). Much of the early kinetic data was generated using the erythrocyte system as these cells were easy to manipulate and were available in large quantities. Several early studies, investigating the nature of the glucose binding site within the carrier, demonstrated that the reversible binding of glucose to the carrier was mediated by hydrogen bonding (Barnett *et al.*, 1973, Kahlenberg & Dolansky, 1972).

The purification of the erythrocyte transporter was achieved by two independent groups in the late 1970's. In 1977 Kasahara and Hinkle demonstrated that the protein they had purified could transport glucose when reconstituted into fractionated erythrocyte membranes, while in 1979, Baldwin *et al* showed that their purified protein could bind cytochalasin B (Baldwin *et al.*, 1979, Kasahara & Hinkle, 1977). Both these studies revealed the carrier to be a heterologously glycosylated integral membrane protein which, when analysed by SDS polyacrylamide gel electrophoresis, was found to migrate as a broad band of 55KDa in molecular mass. This could be reduced to a band of 46KDa upon endoglycosidase H treatment.

Reconstitution of this purified protein into phospholipid vesicles demonstrated that it was the carrier system in its entirety, as the kinetics of transport were identical to those of the native protein (Wheeler, 1981). This

reconstituted protein could also bind cytochalasin B with a stoichiometry ratio of 1:1 (Baldwin *et al.*, 1981, Baldwin *et al.*, 1979).

This purification of the protein led to the production of antibodies (Sogin & Hinkle, 1978), and its partial protein sequencing. These advancements allowed the isolation and sequencing of the cDNA from the human hepatoma (HepG2) cell line in 1985 by Mueckler *et al.*, and the subsequent cloning and sequencing of a further five functional isoforms of the carrier by various other groups (Mueckler, 1985).

The erythrocyte transporter, being the first to be cloned and sequenced, was later named GLUT1 (Fukumoto *et al.*, 1989), and the other isoforms were named GLUTs 2-7 according to the chronology of the isolation of their cDNAs. Six isoforms to date, GLUTs 1, 2, 3, 4, 5, and 7, comprise the mammalian facilitative glucose transporter family.

1.2.1 Tissue-Specific Distribution of the Facilitative Glucose Transporters.

The observation that different tissues have varying needs for glucose throughout the progressive stages of development, and that these tissues display subtly different kinetics for the uptake of D-glucose first led researchers to propose that a family of transporters might exist. To date, seven such isoforms have been identified and named GLUTs 1-7. GLUTs 1-5 and GLUT7 encode functional proteins, while GLUT6 is a pseudogene-like sequence.

1.2.2 GLUT1

GLUT1 was the first transporter isoform to be cloned and remains the only one to be purified in a functional form. GLUT1 is also referred to as the erythrocyte transporter due to its abundance in the erythrocyte membrane. It is also referred to as the brain-type or HepG2 transporter since the first clones

encoding it were isolated by screening rat brain tissue and the human hepatoma carcinoma (HepG2) cell line (Birnbaum *et al.*, 1986).

The cloning and sequencing of GLUT1 revealed a protein of 492 amino acid residues. Since then, cDNAs from other species have been isolated, including mouse (Kaestner *et al.*, 1989), rabbit (Asano *et al.*, 1988), and pig (Weiler Guttler *et al.*, 1989). All have been found to be 492 residues in length, and display 97% sequence identity with human GLUT1.

The production of oligonucleotides (enabled by the isolation of the cDNA) allowed the screening of tissues for the presence of GLUT1 mRNA. The relative GLUT1 protein levels in these tissues could also be measured using antibodies generated against the purified protein. The highest levels of GLUT1 were found in the membrane of erythrocytes where this transporter was found to constitute up to 7% of total membrane protein (Allard & Lienhard, 1985). High levels were also found in various blood-tissue barriers (Takata *et al.*, 1990) such as the blood-brain and blood-nerve barriers, the placenta syncytiotrophoblast, and several blood-eye barriers. GLUT1 was also found in virtually every other tissue, albeit at very low levels.

The physiological significance of such high levels of GLUT1 in erythrocytes is unknown. At physiological temperature, the K_m of GLUT1 for the uptake of D-glucose is approximately 7mM (Lowe & Walmsley, 1986), which is close to physiological glucose concentrations. It is for this reason that GLUT1 has been proposed to be responsible for the basal uptake of glucose into cells. However, at this rate of uptake the maximum transport capacity of the erythrocyte is 12,000 fold greater than the rate of cellular glucose utilisation.

One possible explanation for this is derived from the following observations: GLUT1 is the transporter which is expressed in foetal tissues, including heart, liver and brown fat. In adults, these tissues have very low levels of GLUT1 and the predominant transporter is GLUT4 (Asano *et al.*, 1988). Also, it has previously been noted that in most foetal animals the

erythrocytes have a very high capacity for D-glucose transport. In these animals, with the exception of primates, this capacity is lost soon after birth (Widdas, 1955). Therefore, it has been suggested that GLUT1 may function in the foetus to mediate the transfer of D-glucose across the placenta into the intracellular space of the erythrocyte, and that this process still occurs to a lesser extent across the blood-tissue barriers in primates (Jacquez, 1984).

Another unusual observation is the elevation of GLUT1 levels in transformed cells and indeed in all cultured cell lines. However, it has been noted that mitogens and growth factors can stimulate transcription of the GLUT1 gene (Merrall *et al.*, 1993), as can a state of starvation (reviewed in Gould & Holman, 1993). Since cultured cells are subjected constantly to these conditions, it is thought that this mechanism may be responsible for elevated GLUT1 levels in these cells.

1.2.3 GLUT2.

Due to the very low levels of GLUT1 found in liver tissue, and because of the distinct glucose transport kinetics exhibited by this tissue, it was suspected that another transporter isoform was present in hepatocytes.

Using GLUT1 cDNA oligonucleotides in low stringency hybridisation screening of hepatocyte DNA libraries, the GLUT2 cDNA was isolated (Fukumoto *et al.*, 1988). GLUT2 cDNAs have since been isolated from rat (Thorens, 1988), and mouse (Suzue *et al.*, 1989). These cDNAs encode molecules which are 522, 523 and 524 amino acid residues long, respectively, and share 88% amino acid sequence identity with each other. Human GLUT2 and human GLUT1 share 55% sequence identity and have virtually superimposable hydropathy plots. Most diversity between the two isoforms occurs in the extreme C-terminus and in the large loop that separates putative

transmembrane helices 1 and 2. In GLUT2 there is an additional 32 residues in this loop, which doubles its size with respect to the GLUT1 loop.

The screening of tissues for GLUT2 protein revealed high levels of GLUT2 in the β -cells of the islets of Langerhans in the pancreas (Orci, 1989, Thorens, 1988), in the transepithelial cells of the intestine and kidney tubules (Thorens, 1990), and in the hepatocytes of the liver. The molecular weight of the GLUT2 protein differs between tissues, being 53, 55, 57, and 61kDa in liver, β -cell, kidney, and intestine tissues respectively. This is thought to be the result of differences in the extent of glycosylation of GLUT2 in the various tissue types. Like GLUT1, the large extracellular loop of GLUT2 contains a single asparagine residue which is a potential site for *N*-linked glycosylation (Thorens, 1988).

The role of GLUT2 in the liver is important as it allows this organ to accumulate glucose for conversion to glycogen when blood glucose levels are high. Moreover, when blood glucose levels are low, glucose is produced by the liver's glucose yielding processes- glycogeneolysis and gluconeogenesis, and is released into the blood with identical kinetics to those of glucose uptake. GLUT2 is a low affinity/high capacity "enzyme" both for D-glucose entry and exit (reviewed in Elliott & Craik, 1983), and it is present in the hepatocyte membrane in large quantities. It therefore allows the release and uptake of glucose to occur in a rapid and non-saturable manner, thus enabling the liver to fulfil its important role in blood glucose homeostasis.

Interestingly, GLUT2 is found in the islets of Langerhans in the pancreas, but its expression is absolutely restricted to the β -cells (Orci, 1989, Thorens, 1988). These are the cells which secrete insulin in response to elevated blood glucose levels. Insulin secretion is achieved by transcription of the insulin gene which is in turn regulated by glucose uptake and metabolic processing in the β -cell. It has therefore been suggested that GLUT2 plays an important role in this process. Since GLUT2 is a low affinity/high capacity

enzyme, the uptake of glucose over the range of physiological concentrations (5-15mM) will be non-saturable, and furthermore, the rate will be directly proportional to the concentration of glucose in the blood. This has led to the speculation that GLUT2 allows glucokinase (which has a relatively low K_m for glucose of 6mM) (Vischer *et al.*, 1987) to be the rate-limiting step in β -cell glucose metabolism. Some as yet unidentified downstream product of this pathway may provide the signal that directly regulates the transcription of the insulin gene. Glucokinase may therefore act as the "blood glucose sensor" of the β -cell (reviewed in Gould & Holman, 1993).

GLUT2 seems to play an important role in glucose homeostasis wherever it is found. In the epithelia of the intestine and the kidney tubules, the high capacity transport property of GLUT2 ensures the efficient transfer of glucose down its concentration gradient into the bloodstream, the high concentration of glucose in the epithelial cells being achieved by the active transport of glucose from the lumen of these structures into the epithelial cells themselves, via active transport mechanisms.

1.2.4 GLUT3

The isolation of GLUT3 cDNA from human skeletal muscle DNA libraries was achieved using the same low stringency hybridisation techniques employed previously for the isolation of GLUT2 cDNA (Kayano *et al.*, 1988).

The GLUT3 protein was found to be 496 residues in length, displaying 64% and 51% sequence identity with GLUT1 and GLUT2 respectively (Kayano *et al.*, 1988).

Northern blot analysis of human tissues showed almost ubiquitous expression of GLUT3 mRNA with the highest levels found in neuronal and brain tissue, and in these tissues especially high levels were found in the cerebral areas (Kayano *et al.*, 1988). High levels of mRNA were also found in

the placenta and kidney (Kayano *et al.*, 1988). However, studies using an antibody raised against the carboxy-terminus of GLUT3 showed that, while the protein is present in neuronal and brain tissues, it is present only in very low levels in heart, placenta and liver, and is almost undetectable in kidney (Gould *et al.*, 1992, Shepherd, 1992a).

Analysis of GLUT3 protein distribution in other species, such as monkey, rabbit, rat and mouse (Maher *et al.*, 1992, Nagamatsu, 1992, Yano, 1991) have illustrated that the tissue distribution of GLUT3 mRNA and protein is exclusively restricted to brain and neuronal tissue. GLUT3 mRNA and protein are also expressed in cultured neuronal cell lines.

The apparent anomaly between rodent and human GLUT3 mRNA tissue distribution may perhaps be due to contamination of the human tissues with neuronal tissue in the northern blot analysis. It is also possible however, that a post transcriptional regulation mechanism operates in human non neuronal tissues.

It has been suggested that the role of GLUT3 in neuronal and brain tissue is a specific and important one: the brain is absolutely dependent upon glucose as its sole energy source since it is unable to derive energy from the hydrolysis of fatty acids. Furthermore, it has been found that glucose concentrations in the extracellular fluids of the brain are lower than those found in blood plasma (Lund-Anderson, 1979). The K_m value for zero-trans entry (see section 1.4.2.2) of 2-deoxyglucose into *Xenopus* oocytes via GLUT3 is ~1.4mM (Colville *et al.*, 1993b), a value which is relatively low with respect to GLUT1 which has a K_m value of 7mM (Lowe & Walmsley, 1986). Therefore GLUT3 has a greater efficiency for glucose transport under hypoglycaemic conditions. The co-expression of GLUT1 and GLUT3 in the brain tissue would therefore allow the high efficiency transport of glucose over the entire physiological range of blood glucose concentrations, with GLUT1 working at its

highest capacity when blood glucose levels are high, and GLUT3 transporting glucose more efficiently when blood glucose levels are low.

1.2.5 GLUT4

Studies involving the use of 3T3-L1 adipocytes showed that upon insulin stimulation the rate of glucose uptake increased between 12- and 15-fold. It was also noted however, that the increase in GLUT1 at the plasma membrane was only around 4-fold. Therefore GLUT1 could not be entirely responsible for this increase in transport ability in these cells. After feverish activity to clone the isoform responsible for this insulin stimulated transport, the cDNA for what is now referred to as GLUT4 was eventually isolated simultaneously by several groups. It was cloned from human (Fukumoto *et al.*, 1989, James *et al.*, 1989), rat (Birnbaum, 1989, Charron *et al.*, 1989), and mouse (Kaestner *et al.*, 1989) cDNA libraries.

The cDNA for human GLUT4 was found to encode a protein of 509 residues in length, which shared 65% sequence identity with GLUT1. Once again their hydropathy plots were superimposable (Fukumoto *et al.*, 1989, James *et al.*, 1989), with the exception of the amino-terminus of GLUT4 which was extended by an additional twelve amino acid residues with respect to GLUT1. Other more variable regions between these isoforms occur in the large extracellular loop which separates putative transmembrane regions 1 and 2: in the GLUT4 isoform this loop is longer.

Studies on rat adipocytes reported a 20- to 30-fold increase in D-glucose uptake upon insulin stimulation, while rat muscle cells exhibited a 7-fold increase (Ploug, 1987). The increase in glucose uptake by human adipocytes and human skeletal muscle cells in response to insulin was even lower: 2- to 4-fold (Pederson & Gliemann, 1981), and 2-fold (Dohm *et al.*, 1988). Kinetic data from these experiments has shown that the increase in transport capacity observed

in these tissues in response to insulin is brought about by a change in the V_{\max} and not K_m (Holman *et al.*, 1990, May & Mikulecky, 1982, Simpson & Cushman, 1986, Taylor & Holman, 1981, Whitesell & Gliemann, 1979). Although there was, and still is, speculation that this increase in the V_{\max} of the transporter is achieved by intrinsic activation of the transporter protein, it is now largely established that this increase in transport capacity is achieved by recruitment of a large number of transporters to the plasma membrane from an intracellular pool, the exact nature and location of which is still unknown. This has been shown to occur in both fat (Cushman & Wardzala, 1980, Suzuki & Kono, 1980), and skeletal muscle (Hirshman *et al.*, 1990, Klip *et al.*, 1987).

Equilibrium exchange studies on GLUT4 have reported K_m values for 3-O-methyl-D-glucose of 1.8mM (Keller *et al.*, 1989), and 4.3mM (Nishimura, 1993). Therefore at low physiological glucose concentrations, GLUT4 is responsible for the majority of glucose uptake in human tissues. Upon insulin stimulation, the number of transporters increases at the plasma membrane and the result is an increase in the glucose transport capacity of the cell.

1.2.6 GLUT5

Using low stringency hybridisation to screen a human jejunal DNA library, Kayano *et al* isolated a cDNA with a GLUT-like sequence (Kayano *et al.*, 1990). This cDNA was found to encode a protein of 501 amino acid residues in length and which is the most divergent of the GLUT sequences so far: there is only 42%, 40%, 39%, and 42% sequence identity between this isoform, referred to as GLUT5, and GLUTs 1-4 respectively.

Northern blot analysis of human tissues revealed that GLUT5 mRNA is present at high levels in the epithelia of the small intestine and the kidney, in the testes and spermatozoa, and at lower levels in skeletal muscle and adipose

tissue (Kayano *et al.*, 1990). Immuno-blot and immunohistochemical studies have shown that GLUT5 protein is present in human muscle, testes and spermatozoa, the adipocyte plasma membrane, the small intestine, the kidney and heart (Burant *et al.*, 1992, Shepherd, 1992b).

The presence of GLUT5 in enterocytes was at first puzzling since there did not seem to be a need for an additional glucose transporter in this cell: the sodium linked glucose transporter SGLT1 in the enterocyte is capable of high efficiency transport and accumulation of glucose against its concentration gradient. However, Burant *et al* expressed human GLUT5 in *Xenopus* oocytes and demonstrated that this isoform is a fructose transporter, and has virtually no ability to transport glucose (Burant *et al.*, 1992).

It is thought that GLUT5 is restricted to the brush border membrane of enterocytes, where it mediates the uptake of dietary fructose from the lumen of the gut, although some evidence exists to suggest that GLUT5 may also be present on the basolateral membrane of human enterocytes (Davidson *et al.*, 1992, Hundal *et al.*, 1992). Once inside the enterocyte, fructose is transported out of the cell by GLUT2, the isoform present on the basolateral membrane (Thorens, 1990).

Other cDNAs from species such as rat (Rand, 1993) and rabbit (Miyamoto *et al.*, 1994) have also been isolated, and studies on these homologues have provided conflicting evidence as to whether GLUT5, in these species, can transport glucose and bind cytochalasin B. These studies will be discussed in detail in Chapter 3.

1.2.7 GLUT6

A cDNA was isolated in 1990 which was found to have 70% sequence identity with GLUT3, and was named GLUT6 (Kayano *et al.*, 1990). However, further analysis of this isoform found multiple termination codons in the

cDNA sequence, and so this gene does not encode a functional protein (Kayano *et al.*, 1990). It has been suggested that the GLUT6 pseudogene-like sequence might have arisen from a gene duplication event involving the GLUT3 gene sequence, thus explaining the high degree of homology between these two sequences.

1.2.8 GLUT7

GLUT7 cDNA was isolated in 1992 from a rat DNA library (Waddell, 1992). This isoform was found to be 528 amino acid residues in length, and displayed 68% sequence identity with rat GLUT2. Rat GLUT2 and GLUT7 were found to be identical at three separate sequence locations, and there appeared to be very little base drift over much larger areas of the remaining sequence. Although these sequences do not coincide with the intron-exon boundaries of the GLUT2 gene, it is still possible that GLUT2 and GLUT7 mRNAs are generated by an unknown splicing mechanism (Waddell, 1992). One of the differences between these sequences is the presence of a six amino acid targeting motif (KKxKxx) at the C-terminus of the GLUT7 sequence, which is believed to be responsible for targeting this isoform to the endoplasmic reticulum.

GLUT7 was found to be present in the microsomal fraction of rat hepatocytes, and it was found to localise to the endoplasmic reticulum when expressed in COS-7 cells (Waddell, 1992).

The liver plays a crucial role in blood-glucose homeostasis. As previously described, it is responsible for the uptake and release of glucose from and into the blood, via the GLUT2 isoform which is present on the surface of hepatocytes. However, the terminal step in glycogeneolysis and gluconeogenesis is the dephosphorylation of glucose-6-phosphate by glucose-6-phosphatase, and this process occurs in the lumen of the hepatocyte

endoplasmic reticulum. So glucose must traverse this membrane first before it can reach the cytosol for transport out of the hepatocyte via GLUT2. It has been suggested that GLUT7 mediates the transport of glucose out of the hepatocyte endoplasmic reticulum.

Waddell *et al* are to date, the only group to have successfully cloned this transporter cDNA. This, together with the fact that there are large stretches of sequence identical to that of GLUT2, and extremely low level of base drift over large areas of the remaining sequence, leaves doubt as to whether this cDNA may be a cloning artefact. Therefore the existence of GLUT7 awaits confirmation from other sources.

1.2.9 Homologous Transporters in Other Organisms.

In 1992 it was observed that glucose transporters shared homology with a number of bacterial transport proteins (Griffith *et al.*, 1992). Using the sequences of several known transporters: TetC protein (the tetracycline resistance protein of Gram-negative bacteria); TetL (the tetracycline resistance protein of Gram positive bacteria); AraF (a sugar transporter of *E. coli*); GLUT2; and CitA (the citrate transporter of Gram-negative bacteria), Griffith *et al* searched databases for proteins with homologous sequences. It was shown that a high level of homology existed between sequences from these proteins and a variety of other proteins from several different species. These included active and passive transporters of eukaryotic and prokaryotic organisms, sugar/H⁺ symporters from higher plants, green algae, protozoans, yeasts, cyanobacteria and eubacteria (reviewed in Griffith *et al.*, 1992, Henderson *et al.*, 1992). Although these transporters differed in substrate specificity, the mechanism of transport and the presence of fairly highly conserved stretches of sequence within their cDNAs allowed the inclusion of these proteins into a transporter "superfamily". Also included in this group are the bacterial tetracycline and

citrate transporters, and the fungal quinate transporters as well as the GLUTs. However some transporters, such as the mammalian sodium-linked glucose transporters and the bacterial ATP- and phosphoenol pyruvate-utilising active transporters, are, surprisingly, not included in this superfamily.

All members of the superfamily have similar hydropathy plots to those of the mammalian glucose transporters, and, despite the differences in sequence length between the members of this group, they are all believed to have a structure which spans the membrane twelve times, with a large central cytoplasmic loop between helices 6 and 7 (Figure 1.2).

Transporters most closely related to GLUT1 by sequence include AraE- the H⁺/L-arabinose symporter of *E.coli*, XylE- the H⁺/D-xylose symporter of *E.coli*, and GalP- the galactose transporter of *E.coli*. These share 23%, 27%, and 25% sequence identity with GLUT1 respectively. GalP and AraE also bind cytochalasin B. GalP shares the same sensitivity of GLUT1 to the inhibitor forskolin (Martin *et al.*, 1994). Moreover, cytochalasin B photolabelled GalP can be proteolytically digested to yield labelled fragments similar in size to those produced by labelling and digestion of GLUT1 (Cairns *et al.*, 1987).

It is not known if the lactose permease of *E.coli* is a member of the superfamily, as it appears to share very little sequence identity with GLUT1. However, it too, has twelve predicted transmembrane helices, and although the percentage of sequence identity with GLUT1 is low, lac permease possesses many of the motifs which are highly conserved in this superfamily (Buchel *et al.*, 1980).

1.3.1 Structure of the Mammalian Facilitative Glucose Transporters.

When the GLUT1 primary sequence was subjected to hydropathy analysis (Mueckler, 1985), the pattern was found to contain twelve regions each approximately 21 residues in length. These were long enough to be possible

hydrophobic or amphipathic membrane spanning α -helices. According to this structure, the N- and C-termini were predicted to lie on the same side of the membrane in addition to a large central loop which separated transmembrane regions 6 and 7. Another large loop between transmembrane segments 1 and 2 was predicted to lie on the opposite side of the membrane from the central loop. Proteolytic digestion studies have shown that the N- and C-termini and the large central loop are cytoplasmically disposed, and the other large loop between transmembrane regions 1 and 2 is exofacial (Cairns *et al.*, 1987, Mueckler, 1985).

Following the isolation of the cDNAs for the other transporter isoforms, the same hydropathy analysis has been performed on these sequences and it has been shown that the traces are all virtually superimposable. The hydropathy plots of GLUTs 1, 2, 3, 4 and 5 are shown in Figure 1.1. The sequences that are most conserved between the isoforms lie within the transmembrane regions and the least conserved areas least conserved lie in the N- and C-terminal regions and in the two large loops. Five of the transmembrane helices are predicted to be amphipathic: transmembrane regions 3, 5, 7, 8 and 11, and it has been suggested that these helices may form a hydrophilic pore across the lipid bilayer through which D-glucose might move during transport (Mueckler, 1985). The large intracellular loop between helices 6 and 7 divides the structure into two "halves", although whether this division is relevant in the tertiary structure is not known. The other cytoplasmic loops are short, only eight residues long and, as a result, probably restrict movement of the transmembrane helices. The extracellular loops are less conserved in size and sequence than the cytoplasmic loops, probably allowing flexibility of the protein during transport. It has been suggested that constraints imposed by the short loops at the cytoplasmic side of the membrane may cause a bunching effect of the helices, so that the structure at

the extracellular side of the membrane is more open and relaxed, possibly exposing the exofacial sugar binding site.

There are several conserved sequences within the transporter cDNA: there is a GRR(K) motif present between transmembrane regions 1 and 2, which is repeated again between transmembrane regions 7 and 8. ExxxxxxR is conserved between transmembrane regions 4 and 5, and repeated again between transmembrane regions 10 and 11. There is also a conserved PESPR sequence in the cytoplasmic loop between transmembrane helices 6 and 7, which is similar to the motif in the C-terminal cytoplasmic tail -PETKG. This repetition of conserved motifs may suggest the evolution of the transporter protein from an ancestral six transmembrane helix membrane protein by a gene duplication event (Baldwin & Henderson, 1989, Maiden *et al.*, 1987). Together with the fact that the cytoplasmic loops are so short and probably restrain the possible tertiary structure of the protein, this duplication suggests that the protein may well adopt a bilobular structure, with six helices in each domain (Hodgson *et al.*, 1992). This has been observed to occur with the *E.coli* lactose permease protein. This protein is also a transporter molecule with a membrane spanning structure that is proposed to be similar to the GLUTs. Low resolution electron microscopy studies on this protein have shown it to be arranged in the membrane in two discrete domains (Li & Tooth, 1987).

1.3.2 Topological Model of GLUT1.

The topological model of GLUT1 shown in Figure 1.2 is largely based upon the results of hydropathy plot analyses on the amino acid sequence of the protein (Figure 1.1). This model was originally proposed by Mueckler *et al* (Mueckler, 1985). The "positive inside" rule of protein folding states that in mono- or polytopic membrane proteins, there is likely to be a prevalence of

positively charged amino acids in the cytoplasmic domains of the protein. This model of the GLUT1 transporter is consistent with the "positive inside" rule.

Several biochemical and biophysical studies have lent support to this model. Proteolytic digestion of GLUT1 in erythrocyte membranes with trypsin yields several proteolytic fragments. Analysis of these fragments with peptide specific antisera shows that they correspond to the C-terminal region (residues 451-492) and the large loop between putative transmembrane helices 6 and 7 (residues 207-271) (Cairns *et al.*, 1987). The native transporter is known to be susceptible to proteolytic cleavage by trypsin only at the cytoplasmic surface, and so it was deduced that the C-terminus and the large loop between helices 6 and 7 were cytoplasmically disposed.

The site of *N*-linked glycosylation has been shown to be residue Asn⁴⁵ which lies in the loop between helices 1 and 2. This loop is predicted to be extracellular (Cairns *et al.*, 1987, Mueckler, 1985).

Studies on GLUT1 in *Xenopus* oocytes have shown that Cys⁴²⁹ can be labelled externally by the impermeant sulphhydryl reagent bis-(maleimidomethyl)-ether-L-[³⁵S]cysteine (May *et al.*, 1990, Wellner *et al.*, 1992). This residue must therefore be extracellular and since it lies in the loop at the top of helix 12, that loop must also be extracellular. This is consistent with Muecklers' model.

Studies of GLUT1 in intact erythrocytes have shown that residue Lys³⁰⁰ which is predicted to lie in the exofacial loop between helices 7 and 8, can be labelled externally by the impermeant biotinylation reagent sulphosuccinimidyl-6-(biotinamido)-hexanoate (NHS-LC-biotin), and so this loop is also exofacial, as predicted (Preston & Baldwin, 1993).

Fourier Transform Infra-Red spectroscopy is a method whereby the α -helical, the β -sheet structure and the random coil content of membrane proteins can be estimated when the proteins are in dilute aqueous media. This technique, together with circular dichroism studies, revealed that GLUT1

contains a large proportion of α -helix, with a lesser β -sheet content (Chin *et al.*, 1986). These studies also measured the tilt angle of the helices from the plane of the membrane bilayer, and noted that this angle is perpendicular to the membrane, but is reduced upon the binding of D-glucose to the protein.

Further support for the topology of Muecklers' model was obtained in 1994 when Hresko *et al.* published an elegant study which established the orientation of each of the soluble domains of the protein (Hresko *et al.*, 1994). These workers used a mutagenesis scanning technique in which they inserted an epitope into each of the soluble domains of an aglyco-GLUT1 construct. This GLUT1 construct had the Asn⁴⁵ residue, the site of potential glycosylation, mutated to Thr⁴⁵, a substitution which abolishes glycosylation. The epitope which was inserted into the hydrophilic domains of this construct corresponded to the glycosylation consensus sequence (Asn-x-Thr/Ser) of GLUT4. Since N-linked glycosylation occurs exclusively on the side of the membrane which is exposed to the lumen of the endoplasmic reticulum, only the epitope tagged loops that are exofacial can be glycosylated. Expression of these mutants in *Xenopus* oocytes showed quite convincingly that the Muecklers' model was correct; only those loops which were predicted to be exofacial were, in fact, glycosylated.

1.4.1 The Single Site Conformational Change Model.

It was shown in the 1970's that sugars with bulky C-4 groups (with respect to glucose), such as maltose and 4,6-O-ethylidene D-glucose, or sugars with bulky C-6 groups such as 6-O-propyl-D-glucose could inhibit the transport of D-glucose by erythrocytes. It was shown further, however, that these sugars could only effect inhibition of glucose entry when present extracellularly (Baker & Widdas, 1973, Barnett *et al.*, 1975). Similarly, *n*-propyl- β -D-

glucopyranoside could inhibit only glucose efflux when present inside the cell (Barnett *et al.*, 1975).

These studies eluded to the idea that there may be two glucose binding sites on the transporter, one exofacial and one endofacial, and that these are structurally different because influx and efflux of glucose are susceptible to inhibition by different sugar analogues.

More recent evidence for the separation of these binding sites has come from transporter-specific ligands that bind to only one site. Cytochalasin B is a compound that is thought to bind to the endofacial binding site, since it inhibits glucose efflux in a competitive manner (Cairns *et al.*, 1987). IAPS-Forskolin is also thought to interact with the endofacial site (Wadzinski *et al.*, 1987). ATB-BMPA, a bismannose derivative, is proposed to bind to the exofacial binding site, since it can inhibit sugar influx in a competitive manner (Clark & Holman, 1990). For further discussion of these ligands see section 1.6.

It is thought that the exofacial and the endofacial binding sites cannot be occupied simultaneously, and indeed, the formation of one is suspected to preclude formation of the other (reviewed Baldwin, 1993).

The single site alternating conformation model is represented by the diagram shown in Figure 1.3. What is not clear from the available evidence for this model is whether these binding sites, although conformationally different, are absolutely structurally separate.

Molecular modelling studies, based on the ability of sugar analogues to inhibit glucose influx and efflux, have produced a model describing how glucose sterically occupies each of these putative binding pockets.

This model is shown in Figure 1.4. Glucose is proposed to enter the exofacial binding pocket with its C-1 carbon atom going in first, and the C-4 last. When it leaves the endofacial pocket it is thought to leave C-1 first. It is thought that glucose efflux occurs by the direct reverse of this procedure, with glucose

entering the endofacial binding pocket C-4 first and leaving the exofacial site, C-1 last (Barnett *et al.*, 1975).

1.4.2.1 Kinetics of Transport of D-Glucose by GLUT1.

Most of the work investigating the kinetics of transport by the glucose transporters has been performed on GLUT1. This is due to the functional purification of this isoform which is made possible by the ready availability of erythrocytes and their ease manipulation (Kasahara & Hinkle, 1977). However, it is thought that despite differences in sugar specificity, kinetic parameters, targeting patterns, ligand binding, hormonal regulation and tissue-specific distribution, the other isoforms of the GLUT family will share the same general mechanism as that of GLUT1.

In the following sections, a model is proposed which describes the general mechanism of transport. In these sections, and in subsequent chapters of this thesis, kinetic terms are used to describe the behaviour of the transporter within this model. These are listed and explained below. The terms *cis* and *trans* refer to the side of the membrane from which transport is measured and the opposite side, respectively.

1.4.2.2 Zero-*Trans* Entry.

This term refers to the simplest type of assay to measure the transport activity of a carrier. In all of the flux experiments listed here, the movement of substrate is traced by the addition of small amounts of radioactive substrate. This is known as the radiolabel or tracer. The measurement of zero-*trans* entry involves the pre-incubation of cells expressing the transporter in a substrate-free medium for a suitable period of time that ensures that the concentration of substrate in the cytosol of the cell is as low as possible. The external sugar

concentration is varied for each measurement. The initial transport rate of substrate into the cell should be linear since the cytosolic substrate concentration is zero. Only initial rates of sugar transport are measured, before *trans* → *cis* transport starts to occur. Therefore, the kinetic parameter being measured is the substrate binding affinity at the exofacial binding site (K_m outside) and the maximum velocity of substrate uptake under infinitely high substrate concentrations (V_{max} entry).

1.4.2.3 Zero-Trans Exit.

This term refers to the type of assay which measures the exit of substrate from cells at initial rates of transport. In this measurement, the cells are pre-incubated in varying concentrations of substrate until equilibrium is reached, at which point the medium is rapidly aspirated off and replaced with another without substrate. Initial rates of substrate efflux are determined by measuring the amount of radioactive tracer that has been transported out of the cell. This assay measures the affinity of the endofacial substrate binding site (K_m inside) and the V_{max} for sugar exit.

1.4.2.4 Equilibrium Exchange.

In this type of assay the concentration of cytosolic substrate in the cell is equal to that of the surrounding medium. This is achieved by pre-incubation of cells in medium containing the substrate at various concentrations for a period of time that allows the substrate to equilibrate between the external medium and the cytosol. Uptake or efflux of tracer-labelled substrate is measured at various substrate concentrations, but the concentration of substrate on the outside of the cell is always equal to that of the cytosol. In this way, K_m and V_{max} for substrate exchange (for entry or efflux) can be measured.

1.4.3.1 Reaction Mechanism of the Single Site Model.

The simplest model which describes the transport cycling of GLUT1 is known as the single site alternating conformer model. This was initially developed as a symmetric carrier model by Widdas (Widdas, 1952), but was later adjusted to the asymmetric model to account for the observed asymmetry of D-glucose transport by GLUT1 (Geck, 1971). This model, shown in Figure 1.5 as a King-Altman diagram, describes the re-orientation of a single substrate binding site between two conformations: an outward-facing conformation (T_O), and an inward facing conformation (T_I). This cycling can occur in the presence or the absence of substrate. The re-orientation of the loaded transporter (T_S) from the outward-facing conformation (T_{OS}) to the inward facing conformation (T_{IS}) is responsible for the movement of substrate into the cell. This mechanism (in reverse) applies to efflux of substrate from the cell, the direction of the net transport flux being driven purely by the direction of the substrate concentration gradient.

In this model, it is important to note that the rate constants that describe the movement of the loaded transporter (k_2, k_{-2}) are both greater than those describing the movement of the empty transporter (k_1, k_{-1}). The dissociation constants of the substrate bound at the exofacial and the endofacial site are not necessarily equal. Furthermore, it has been shown by NMR studies, that the rates of association and dissociation of D-glucose at either binding site, are greater than those of the re-orientation of loaded or unloaded transporter (Wang, 1986). In short, the slowest step in the cycle is the re-orientation of the unloaded transporter. It is also important that the rate of re-orientation of the loaded carrier is faster than the reorientation of the empty carrier, and that movement of the loaded carrier from the outward facing to the inward facing

conformation is faster than the reverse of this step. This is important in explaining the phenomenon of *trans*-acceleration (section 1.4.3.3).

1.4.3.2 Measurement of Steady State Rate Constants.

Evidence in support of this model has come from the measurement of steady-state and pre-steady state GLUT1 kinetics. The steady state kinetics have been determined by measuring the zero-*trans* entry, zero-*trans* exit and equilibrium exchange constants of GLUT1 in erythrocytes over a range of temperatures (Lowe & Walmsley, 1986).

The kinetics of GLUT1 are temperature dependent, displaying lower K_m and V_{max} values at lower temperatures. However, the transporter always displays simple, hyperbolic Michaelis-Menton kinetics (i.e. simple Michaelis-Menton kinetics, but "modified" to account for the fact that the "enzyme" is a transporter, and the substrate is a transported sugar, which is not structurally modified by the action of the enzyme). It has been demonstrated that the temperature dependence of the zero-*trans* Michaelis constants observed at low temperatures is not due to a change in the affinities of the exofacial and endofacial binding sites, but as a result of differences in the rate constants for transporter re-orientation. Therefore, at 0°C for example, there is an asymmetric distribution of outward facing and inward facing transporters which is a direct result of the inequality of re-orientation rate constants (k_1 , k_{-1} , and k_2 , k_{-2}). Thus, in the absence of glucose, only 6% of the transporter population is predicted to be in an outward-facing conformation (T_O). At physiological temperature, the proportion of outward-facing transporters increases to 40%, as a direct change in the rate constants (k_1 , k_{-1}) that govern re-orientation of the transporter from the inward-facing to the outward-facing conformation.

It has been suggested that the temperature dependence of GLUT1 is the consequence of the large endothermic enthalpy and positive entropy changes associated with the re-orientation of the transporter from an inward-facing conformation to an outward-facing conformation (Walmsley, 1987).

1.4.3.3 Measurement of Pre-Steady State Rate Constants.

Pre-steady state values have been obtained using purified GLUT1 reconstituted into leaky vesicles (Appleman & Lienhard, 1989). Unidirectional conversions from one conformational state to another (half turnovers) can be observed by monitoring changes in protein fluorescence upon the addition of specific inhibitors which orientate the transporters into a particular conformation. This is possible since each conformation displays a slightly different pattern of intrinsic fluorescence at 336nm. Such studies have utilised site specific ligands such as 4,6-*O*-ethylidene-D-glucose, an external ligand, and phenyl- β -D-glucoside, an internal ligand. By adding saturating concentrations of 4,6-*O*-ethylidene-D-glucose at 10°C, the population of transporter molecules is pulled rapidly into the outward facing conformation (T_0), and trapped in this state. At 10°C it is possible to measure the time taken for the transporters to achieve this conformation (i.e. $T_i \rightarrow T_0$). The rate constants for this event, k_2 and k_{-1} , are determined by performing the above in the presence and absence of glucose respectively. In this way it is possible to measure single half turnovers of the transporter. The $T_0(\pm s) \rightarrow T_i(\pm s)$ step can be measured by the addition of the internal ligand phenyl- β -D-glucoside, and the rate constants k_3 and k_1 can be measured by performing the above in either the presence or the absence of glucose respectively.

The values obtained for rate constants using this technique are shown in Figure 1.5 legend. Importantly, the relative rates of each step are in the order of $k_2 > k_3 > k_1 > k_{-1}$ -the slowest step being the re-orientation of empty carrier.

The dissociation constants of the substrate at the exofacial binding site and the endofacial binding site (K_{so} and K_{si} respectively), have been calculated by the application of these rate constants to the observed kinetic models. It has been calculated that at 37°C the value of K_{so} is ~10mM, and K_{si} is 23mM (Lowe & Walmsley, 1986). Therefore, the rate of dissociation of substrate at the exofacial site is greater than this event at the endofacial site.

Taken together, these values explain the phenomenon of *trans*-acceleration. It has been shown that the presence of substrate on the *trans*- (opposite) side of the membrane actually stimulates transport of tracer into the cell. This is thought to occur by the following mechanism: under *zero-trans* conditions, the initial flux of D-glucose is uni-directional, and is limited by the slowest step in the cycle, re-orientation of the empty carrier. However, as the substrate accumulates on the *trans* side of the membrane, and the state of equilibrium exchange approaches, the overall rate of transport increases because the empty carrier re-orientation step is bypassed. Instead, the carrier re-orientates itself in an occupied state and this is a faster event. This mechanism in effect, increases the number of unoccupied transporters in the outward facing conformation (T_o), and therefore increases transport rate. However, it should be noted that it is the flux of tracer that can be shown to increase. The net flux of substrate across the membrane remains constant, as the transport of every molecule of substrate into the cell is followed by the efflux of another. This is the mechanism by which *trans*-acceleration occurs, the phenomenon exhibited by GLUT1, and many other transport proteins. It has been suggested that GLUT2 and GLUT4 do not display this behaviour (Gould & Holman, 1993). However, it is difficult to measure this property of a transport protein unless it can be purified and reconstituted into phospholipid vesicles, where the transport kinetics are easier to measure, and equilibrium of substrate with the water space of the vesicle is slower. This has not been

possible for the other isoforms as they have not been purified to a functional form. GLUT3 and GLUT5 have not been investigated for this property.

1.4.3.4 Multiple-Site Models.

Carruthers has shown that inconsistencies exist between the kinetic data from GLUT1 studies and the predicted values obtained using integrated rate equations applied to the one site alternating conformation model (Carruthers, 1990). He has proposed several alternative models to explain these discrepancies, each of which is based upon the assumption that the transporter possesses two glucose binding sites which are present on opposite sides of the membrane simultaneously (Carruthers, 1991). Evidence for such a two site carrier comes from studies of erythrocyte glucose transporters where it has been demonstrated that the transporter molecules can bind cytochalasin B and then bind exofacial ligands, such as maltose, 4,6-*O*-ethylidene-D-glucose, or phloretin simultaneously (Helgerson & Carruthers, 1987). Also, it has been shown that the effects of each of these compounds on the inhibition of D-glucose transport by each of the other compounds, suggests that in addition to the two sites existing simultaneously, the binding of one ligand exhibits negative cooperativity on the binding of the second ligand (Carruthers & Helgerson, 1991).

However, as discussed by Baldwin (Baldwin, 1993), most of the kinetic data does agree with the one site asymmetric model, if allowances are made for the different measurement techniques, and for the fact that sugars may not display "ideal" behaviour.

Also, fluorescence, proteolytic digestion, chemical inactivation and most ligand binding studies all support the single site alternating conformation model. These are discussed below. However, Carruthers has also suggested an explanation for the discrepant data, which can incorporate the one site model.

This involves oligomerisation of GLUT1 transporter molecules, and it is discussed in section 1.10.

1.5.1 Conformational Change in GLUT1 Detected by Changes in Intrinsic Fluorescence.

The wavelength of fluorescence emissions from tryptophan residues within proteins is dependent upon the polarity of the surrounding environment, that is, whether the residue is in a hydrophilic or a hydrophobic environment. This property of tryptophan can therefore be exploited in the investigation of transmembrane proteins.

GLUT1 has six tryptophan residues throughout its sequence (Mueckler, 1985). Examination of the intrinsic tryptophan fluorescence of GLUT1 has shown that these residues are distributed in both hydrophobic and hydrophilic environments. These experiments also indicate that there is a difference in intrinsic fluorescence of exofacially and endofacially orientated transporters, as demonstrated with the use of site-specific ligands. It has been shown that at specific wavelengths, the tryptophan fluorescence of exofacially-orientated transporter is 20% less than the endofacial conformation (Krupka, 1972, Pawagi & Deber, 1990).

Intrinsic fluorescence of membrane proteins can be quenched by the addition of small hydrophilic molecules such as potassium iodide, and measurements of quenching efficiency can be used to assess the position and accessibility of fluorescent groups. Such measurements of GLUT1 have shown that not all of the emissions can be quenched by the addition of potassium iodide. This result indicates that most of the tryptophan residues are located within the membrane bilayer and are therefore inaccessible to the potassium iodide, whilst those responsible for that part of the signal that can be quenched,

are present in a more hydrophilic and accessible environment (Pawagi & Deber, 1990).

It was shown that in the presence of glucose the quenching of fluorescence is reduced. This result indicates that the binding and transport of D-glucose causes the movement of one or more tryptophan residues from a hydrophilic environment to a hydrophobic environment (Chin *et al.*, 1992, Pawagi & Deber, 1990). This reduction in quenching is not observed when the transporter binds cytochalasin B or maltose. Therefore, this probably represents a transition state in the transport process which involves the movement of the vulnerable tryptophan into the membrane bilayer, where it is shielded from quenching. These results are consistent with the idea of large segments of the protein moving to induce a large conformational change associated with transport catalysis.

These observations are also consistent with data from circular dichroism spectroscopy studies. It has been shown that the binding of D-glucose results in a 10% increase in the α -helical content of the GLUT1 protein. The addition of cytochalasin B can reverse this effect. The binding of maltose, however, leads to a 10% reduction in the α -helical content (Pawagi & Deber, 1987, Pawagi & Deber, 1990). Taken together, these studies support the suggestion that maltose stabilises the transporter in an outward-facing conformation, while D-glucose induces a change to the inward-facing conformation.

The movement of tryptophan(s) from a solvent accessible environment into the lipid bilayer is likely to occur via the movement of one of the transmembrane helices. Pawagi and Deber have predicted that the segment of GLUT1 most likely to be able to exist as a hydrophilic loop or as an α -helix, is that comprised of residues 378-398. This sequence lies within helix 10. The presence of several proline and glycine residues is thought to contribute to the flexibility of this segment (Pawagi & Deber, 1990).

Tryptophan residues Trp³⁸⁸ and Trp⁴¹² lie within or close to this predicted dynamic segment. They also lie in the proximity to the cytochalasin B binding site, and exhibit a fluorescence excitation wavelength similar to that required for cytochalasin B photoactivation (Holman & Midgley, 1985). These residues have therefore been implicated in the glucose transport mechanism. Substitution of both Trp³⁸⁸ and Trp⁴¹² in GLUT1 has been shown to result in a drastic loss of transport activity, and perturbation of the endofacial binding site as indicated by a loss of cytochalasin B binding and photolabelling (Inukai *et al.*, 1994) (section 6.2.3).

1.5.2 Changes in Proteolytic Susceptibility: Support for the Alternating Conformation Model.

Proteolytic digestion of GLUT1 by trypsin occurs at the cytoplasmic face, and produces two large membrane embedded protein fragments, and two soluble peptides which correspond to the C-terminus (amino acid residues 457-492) and the large cytoplasmic loop between helices 6 and 7 (residues 213-269) (Cairns *et al.*, 1987, Gibbs *et al.*, 1988). The rate of proteolytic digestion is reduced in the presence of ligands that reversibly bind to the exofacial binding site such as maltose, 4,6-*O*-ethylidene-D-glucose and phloretin (Gibbs *et al.*, 1988, King *et al.*, 1991). Also, it has been shown that photoaffinity labelling of GLUT1 by the impermeant bismannose compound AIB-BMPA almost completely protect the protein from cleavage by thermolysin (Clark & Holman, 1990).

These effects suggest that, when the glucose transporter becomes stabilised in an outward facing conformation by the action of ligand binding to the exofacial site, the associated conformational change in the protein has resulted in

a relocation of the proteolytic cleavage points on the cytoplasmic loop and tail so that they are now inaccessible to enzyme attack.

Conversely, the reversible binding of ligands to the endofacial binding site causes an increase in the rate of proteolysis. Presumably this is because the opening of the endofacial site to accept the endofacial ligands results in exposure of the cleavage points at the cytoplasmic face and thus increases their susceptibility to proteolytic attack. The presence of intracellular glucose also increases the rate of digestion by the same mechanism.

In following this line of argument it might be expected that the presence of cytochalasin B on the endofacial side of the membrane would greatly increase the rate of digestion, but this does not occur with tryptic digestion (Gibbs *et al.*, 1988, King *et al.*, 1991). It is possible that, because cytochalasin B is a large, bulky molecule, steric hindrance may block accessibility of the proteases to the cleavage points. However, digestion with thermolysin occurs when cytochalasin B is bound to the transporter, but not when ATB-BMPA is bound (Holman *et al.*, 1986). The binding of cytochalasin B presumably exposes the thermolysin cleavage points, while the binding of ATB-BMPA pulls them toward the membrane bilayer into a protected position.

It has been shown that if GLUT1 is subjected to tryptic digestion first and then exposed to cytochalasin B, then the remaining membrane embedded protein fragments can still bind the ligand (Cairns *et al.*, 1987), and therefore the C-terminal tail and the large cytoplasmic loop probably not involved in the formation of the cytochalasin B binding site.

However, the exofacial ligand ATB-BMPA, cannot bind to the protein after it has been subjected to proteolytic digestion (Clark & Holman, 1990). It would seem that at least part of the cytoplasmic C-terminal tail is important in the formation of the outward facing conformation. This has been further demonstrated by the construction of a GLUT1 mutant which has the last 37 amino acid residues deleted from its cytoplasmic C-terminal tail (Oka, 1990). This mutant

can still bind cytochalasin B, and therefore its endofacial binding site must still be intact, but it cannot transport deoxyglucose, and furthermore it cannot bind the exofacial ligand ATB-BMPA. This mutant, it would seem, is locked in an inward-facing conformation. Deletion of the last 12 amino acid residues by comparison, produced a functional protein -so it appears that residues 455-480 are important for the ability of the molecule to undergo conformational change (section 6.2.7).

1.5.3 Chemical Inactivation of GLUT1: Support for the Alternating Conformation Model.

The chemical inactivation of GLUT1 and the patterns of ligand protection almost mirror those described for ligand protection from proteolytic digestion of the protein.

Early studies investigating GLUT1 in intact erythrocytes showed that the rate of irreversible chemical inactivation by the amino group-modifying reagent 1-fluoro-2,4-dinitrobenzene can either be increased by the presence of extracellular glucose, or decreased by the presence of intracellular glucose (Edwards, 1973).

The inactivation of GLUT1 by *n*-propyl- β -D-glucopyranoside, a molecule which is known to bind to the endofacial binding site, is accelerated by the presence of intracellular glucose (Barnett *et al.*, 1973). Also, protection from inactivation by this molecule can be afforded by the binding of exofacial ligands such as maltose, 4,6-O-ethylidene-D-glucose, phloretin, and 6-O-alkyl galactose (Baker & Widdas, 1973, Barnett *et al.*, 1975, Krupka, 1971).

Similarly, modification of the exofacial cysteine residue (Cys⁴²⁹) by the impermeant sulphhydryl group-modifying agent p-chloromercuribenzenesulphonate (pCMBS), leads to inactivation of the transporter (May *et*

al., 1990, Wellner *et al.*, 1992), and this rate of modification can be increased by the presence of exofacial ligands such as maltose and phloretin.

This effect is presumably due to the transient stabilisation of the transporter in an outward facing conformation, brought about by exofacial ligand binding, resulting in the exposition of Cys⁴²⁹ to the modifying agent. This likely occurs because Cys⁴²⁹ is not directly adjacent to the exofacial binding site although its accessibility is linked to the unfolding of the exofacial binding site, thereby allowing the modifying agent to attack the Cys⁴²⁹ residue without steric hindrance from the various exofacially bound ligands.

The rate of inactivation can also be decreased in the presence of cytochalasin B, which stabilises the transporter in an inward facing conformation (Krupka, 1971, May, 1988, May, 1989).

These studies suggest that when the transporter is in an outward facing conformation (i.e. when exofacial ligands are bound), Cys⁴²⁹ is in an exposed and probably hydrophilic environment. When the transporter adopts an inward facing conformation (i.e. when endofacial ligands are bound), some movement may occur in helix 10 which results in Cys⁴²⁹ being buried in the membrane bilayer. Alternatively, movement may occur in the other loops which results in the protection of Cys⁴²⁹, but the steric constraints imposed by the short length of the exofacial loops makes this unlikely.

1.6 Photoaffinity Labelling of GLUT1 by Ligands that Bind to a Specific Conformational Shape.

Cytochalasin B, a fungal metabolite, has been shown to bind GLUT1 in a D-glucose inhibitable manner, with a ratio of binding of one molecule of cytochalasin B per GLUT1 polypeptide chain (Baldwin & Lienhard, 1989). Cytochalasin B can also be photoactivated by ultraviolet light, and can photolabel GLUT1 (Shanahan, 1982).

As discussed previously, the binding of cytochalasin B to the endofacial binding site increases the susceptibility of GLUT1 to proteolytic digestion by thermolysin (Karim *et al.*, 1987).

Later studies in which [³H] cytochalasin B was used to bind to and label the transporter, then treated with proteolytic enzymes to release the labelled fragment, suggested that the site of labelling was contained within amino acid residues 389-412. These residues lie in the loop connecting helices 10 and 11, and within helix 11 itself (Holman & Rees, 1987).

This entire sequence is thought to also contain the endofacial glucose binding site, and it is often assumed that the endofacial binding sites for glucose and for cytochalasin B are one and the same. The rationale behind this thought is based upon the fact that glucose and cytochalasin B can competitively inhibit each other's binding to the endofacial site. Also, the binding moiety of cytochalasin B has an arrangement of oxygen atoms that is superimposable with that of glucose, and is therefore proposed to interact with the endofacial binding site, via the formation of hydrogen bonds, in the same manner as glucose.

Forskolin is also proposed to have this same arrangement of oxygen atoms, and has also been demonstrated to specifically label glucose transporters (Sergeant & Kim, 1985, Shanahan *et al.*, 1987). Binding of forskolin is D-glucose and cytochalasin B inhibitable. This compound may therefore interact with the endofacial glucose binding site, however, the sidedness of forskolin binding has not been confirmed by kinetic transport studies.

Studies of the related bacterial transporters (section 1.2.9) suggest that the cytochalasin B binding site and the forskolin binding site may not be analogous. The *E.coli* galactose/H⁺ symporter GalP and the arabinose/H⁺ symporter AraE can both bind cytochalasin B whilst the xylose/H⁺ symporter XylE can not. Forskolin, if the binding site was shared with cytochalasin B, should show the same pattern of binding between these transporters- but does

not. Forskolin can bind to GalP only, it cannot bind to either AraE or XylE (Henderson *et al.*, 1992). However, this may be due to differences in the binding pockets of these transporters regarding how easily they can accept large bulky molecules such as forskolin and cytochalasin B.

IAPS forskolin is a lipophilic 7-substituted derivative of forskolin which, unlike the original compound, does not activate adenylate cyclase (Joost *et al.*, 1988). When GLUT1 is labelled with [³H]-IAPS forskolin and then proteolytically cleaved, a labelled fragment is produced which corresponds to amino acid residues 369-389. These residues lie within helix 10 (Wadzinski *et al.*, 1990). The site of labelling in GLUT4 with IAPS forskolin has been assigned to helix 9 (Hellwig *et al.*, 1992). This sequence is not identical to that labelled by cytochalasin B but it does lie in very close proximity to it. It is also possible that this sequence is important in the structural formation of the cytochalasin B binding site pocket, even though the residues are not directly labelled by this molecule.

Site directed mutagenesis studies have investigated the importance of tryptophan residues Trp³⁸⁸ and Trp⁴¹² in the glucose transport mechanism. The importance of these tryptophans is implicated by their proximity to the region of cytochalasin B binding (i.e. residues 265-456), and because they have a fluorescence excitation wavelength similar to that required for photoactivation of cytochalasin B (Holman & Rees, 1987) (Inukai *et al.*, 1994). The results of these studies have suggested a model for the labelling of GLUT1 in which cytochalasin B can photolabel either Trp³⁸⁸ or Trp⁴¹². See also section 6.2.3 for further discussion.

ATB-BMPA is a hydrophilic, impermeant ligand which was specifically designed to interact with the exofacial glucose binding site and be photoreactive (Holman & Midgley, 1985, Midgley *et al.*, 1985). Binding of this compound is D-glucose inhibitable, and also can be displaced by 4,6-O-ethylidene-D-glucose or cytochalasin B. Proteolytic studies of photolabelled

GLUT1 have suggested that the sequence that contains the ATB-BMPA binding site is within amino acid residues 301-330 (Davies *et al.*, 1991). These residues lie within helix 8. Site directed mutagenesis studies have shown that the binding of ATB-BMPA to GLUT1 can be abolished by the substitution of the glutamine residue Gln²⁸² in helix 7 by leucine. Cytochalasin B binding in this mutant was comparable to wild type, which suggests that the exofacial and endofacial binding site are structurally separate (Hashiramoto *et al.*, 1992). The site of binding and the site of photolabelling need not be identical, therefore, ATB-BMPA probably binds to Gln²⁸² in helix 7, but photolabels another site in helix 8.

1.7 The Contribution of Molecular Biology to the Understanding of the Transport Mechanism of GLUT1.

Site directed mutagenesis has proved to be a valuable tool in the study of the facilitative glucose transporters. It has been shown that it is possible to disrupt either the exofacial or the endofacial binding site by the substitution of key amino acid residues, without causing perturbation of the other. The substitution of Gln²⁸² in helix 7 of GLUT1 with leucine for example, causes perturbation of the exofacial binding site, without causing any detectable structural disruption of the endofacial binding site (Hashiramoto *et al.*, 1992). The substitution of Tyr²⁹³ in GLUT1, on the other hand, results in disruption of the endofacial binding site, without affecting exofacial ligand binding (Mori *et al.*, 1994). These studies further demonstrate that the exofacial and endofacial binding sites are structurally distinct and separate. Gln²⁸² and Tyr²⁹³ of GLUT1 are thought to be essential in the ability of the transporter to undergo the conformational change associated with transport. The substitution of these residues is thought to lock the transporter in an inward facing or an outward facing conformation, respectively. Therefore, the substitutions do not exactly

disrupt the structure of the respective binding sites, rather, they prevent their formation (see section 6.2.2).

The C-terminal cytoplasmic tail has also been shown to be important in the conformational change mechanism. Deletion of the last 37 amino acid residues from the C-terminal tail of GLUT1 results in a molecule which is locked in an inward-facing conformation (Oka, 1990). The endofacial binding site in this molecule remains intact, but the transporter cannot achieve the conformational change necessary to expose the exofacial binding site. This study will be discussed later, section 6.2.7. Transport activity in all of these conformationally locked mutants is abolished.

1.8 The Role of the C-terminal "Half" of the Transporter in Formation of the Exofacial and Endofacial Binding Sites.

Site-directed mutagenesis has identified several key amino acid residues which are involved in the exofacial and endofacial binding sites of the transporter (Chapter 6). However, it is interesting to note that all but one of the residues found to be important in ligand binding and conformational change, are located within the C-terminal "half" of the transporter (i.e. from the start of the amino terminus to the start of helix 7). The only residue outwith the C-terminal domain, whose substitution has been shown to have any effect on ligand binding, is Gln¹⁶¹ (helix 5). Substitution of this residue with aspartate reduces the transport activity of the molecule, which is caused by a decrease in the catalytic turnover of the protein. The ability of this molecule to bind the exofacial ligand 4,6-O-ethylidene-D-glucose is also reduced. This may indicate that Gln¹⁶¹ is involved in the exofacial binding site, however, this is unlikely since the affinity of the exofacial binding site for D-glucose was unaffected, and the decrease in transport activity exhibited by the mutant was associated with a decrease in catalytic turnover. The reduced affinity for 4,6-O-ethylidene-D-

glucose is probably due to a more general structural disruption rather than a specific effect from loss of this residue. Since most of the amino acid substitutions found to affect ligand binding are located in the C-terminal half of the protein, it is likely that the residues directly involved in formation of the glucose binding sites are located here also. Evidence from ligand binding and proteolytic digestion studies have also suggested that the sites of ligand binding are located within this half of the protein.

The length of the cytoplasmic C-terminal tail is crucial in the conformational change mechanism (Muraoka, 1995). The cytoplasmic C-terminal tail of GLUT1 stretches from the end of the twelfth helix to the carboxy terminus, and is 42 amino acid residues in length. Of these a minimum structure of 18 residues is essential for conformational change. However, the C-terminal tail has also been implicated by several studies as being partly responsible in determining isoform-specific kinetics (Katagiri *et al.*, 1992, Buchs, 1995, Due, 1995). This aspect of transporter function is further discussed in Chapter 5.

The lack of information on the role of the N-terminal "half" of the transporter has prompted one group to investigate this. Cope *et al* have produced a study in which cDNAs encoding the N-terminal and C-terminal "halves" of GLUT1 are expressed either separately or together in Sf9 (*Spodoptera frugiperida* clone 9) insect cells (Cope *et al.*, 1994). It has been shown that, when expressed alone, the C-terminal half is not capable of binding either the exofacial ligand ATB-BMPA, or the endofacial ligand cytochalasin B. Identical results are obtained when the N-terminal domain is expressed in isolation. However, if both constructs are expressed together in the same cell, ligand binding is restored.

These results suggest that although the endofacial and exofacial binding sites have been mapped to regions in the C-terminal half of the protein, this domain is not sufficient to form these binding pockets. It has been suggested

therefore, that the N-terminal half of the protein may be necessary to provide a packing surface against which the helices of the C-terminal half of the protein can correctly arrange themselves, forming a stable structure to expose either the endofacial or the exofacial binding site.

1.9 Molecular Model of the Tertiary Structure of GLUT1.

Several studies have demonstrated that the protein undergoes a large conformational change, and that this change is too large to be mediated by the localised movement of amino acid side chains alone. It has been suggested that helix 10 is a highly mobile region. The conserved sequence within this helix (Phe³⁷⁸-Trp³⁸⁸) is thought to be a pivotal point of flexibility (Pawagi & Deber, 1990). Movement may occur around this point which allows the helices to orientate themselves to expose, alternatively, the endofacial and exofacial binding sites.

When the transporter is in the inward facing conformation, it is believed that helices 11 and 12 pack against the exofacial binding site which is composed of sequences which lie within helices 7, 8, and 9. When the transporter is in an outward facing conformation it is thought that helices 11 and 12 pack against the endofacial binding site which is composed of sequences in the base of helix 10.

Molecular modelling studies (Osguthorpe & Holman, unpublished work) also suggest that the base of helix 12 and the C-terminal tail will pack against the base of helix 10 (which contains the endofacial binding site), and block this site when the transporter is in the outward facing conformation. This model would explain why the C-terminally truncated mutant is locked in an inward facing conformation, and why the length of the tail is critical in determining the ability of the molecule to form the exofacial binding site: presumably the cytoplasmic tail is necessary to pack against the endofacial

binding site and block it. Therefore, in the C-terminally deleted mutant, the tail is not long enough to block the endofacial binding site, and so the endofacial binding site stays permanently exposed.

The tertiary structure of the glucose transporter, despite the extensive mutagenesis studies, remains largely a matter of speculation. Recently, Zeng *et al* have proposed two models describing the helical packing of the protein (Zeng *et al.*, 1996). These models are computer generated, making use of recent advances in protein structure prediction algorithms. A diagram of these is shown in Figure 1.9. In generating these models, the authors of this study propose that they have taken into account the physical dimensions and water accessibility of the channel, the length of the loops between the helices, the macrodipole orientation in the four helix bundle motif and the helix packing energy. In each of these models, it is predicted that five helices, either helices 3, 4, 7, 8 and 11, (model 1) or 2, 5, 11, 8 and 7 (model 2) bundle together to line the channel, with the remaining helices packing around the outside of the channel. Each of these models has a high level of compatibility with the available mutagenesis data. However, in the absence of crystallographic evidence, details of the tertiary structure of the protein cannot be determined with any degree of certainty.

1.10 Oligomerisation of GLUT1.

It has been shown by Carruthers that GLUT1 protein, recovered from erythrocytes by cholate solubilisation of membranes and purified by the application of size exclusion chromatography and sucrose gradient ultracentrifugation, can be reconstituted into proteoliposomes which then display transport activity and D-glucose inhibitable cytochalasin B binding (Hebert & Carruthers, 1991). Furthermore, it has been shown through measurement of the sizes of these particles, that, under different reducing

membrane proteins
α crystals
- high res. structure.

conditions, GLUT1 exists in complexes of either dimers or tetramers. Hydrodynamic studies of cholate solubilised GLUT1, the use of conformationally-specific antibodies, and chemical cross-linking studies of membrane resident GLUT1 have suggested that native GLUT1 exists in the tetrameric form (Hebert & Carruthers, 1992). In this tetrameric state, the GLUT1 complex binds one molecule of cytochalasin B per two molecules of GLUT1, and presents at least two binding sites to D-glucose. When this complex is reduced to the dimeric form, cytochalasin B binds with a stoichiometry of one molecule per one GLUT1 molecule and the dimer presents a single population of binding sites for glucose. Carruthers' model for interaction of monomeric subunits is shown in Figure 1.7. In the dimer, the monomeric subunits can isomerise between the exofacial and endofacial binding sites independently of each other. Cytochalasin B binds to the endofacial conformation thus giving rise to the observation that, in the dimeric form, GLUT1 binds cytochalasin B with a stoichiometry of 1:1 (Hebert & Carruthers, 1992). In the tetrameric state however, Carruthers has proposed that the conformationally active parts of each monomer are constrained by the interaction of the subunits. This results in the coupled isomerisation between the exofacial and endofacial conformations in the two dimers which comprise the tetramer, so that each dimer presents an exofacial binding site and an endofacial binding site simultaneously. The binding sites are arranged in an antiparallel manner (Figure 1.7). Thus, when one subunit isomerises from the inward to the outward facing conformation, this induces the isomerisation of the adjacent subunit in the opposite direction. Carruthers proposes that the GLUT1 tetramer is 2-8-fold catalytically more active than the dimer. This model has been shown to fit most of the kinetic data on substrate binding (Hebert & Carruthers, 1992). Presumably, the physiological advantage of this system is that the slowest step in the transport cycle- the re-orientation of empty carrier, is made faster by the coupled isomerisation of the adjacent

subunit, thereby increasing the rate of catalytic turnover. This model may also explain the differences observed in the kinetics of purified reconstituted GLUT1 and the kinetics of GLUT1 in intact erythrocytes, where it has been shown that the catalytic turnover (K_{cat}) of the reconstituted protein is 20-fold lower than that of native transporter in erythrocytes (Connolly *et al.*, 1985, Hebert & Carruthers, 1992, Wheeler, 1981).

The tetrameric structure is proposed to be stabilised by the presence of a single intramolecular disulphide bridge between Cys³⁴⁷ and Cys⁴²¹ (Zottola *et al.*, 1995). However, a recent publication describes a GLUT1 cysteineless-mutant which is reported to retain wild type kinetics (Due *et al.*, 1995a). This mutant must therefore be capable of accelerated exchange, so the role of the putative disulphide bridge in facilitating accelerated exchange is not clear.

There is some evidence in support of this model from the expression of glucose transporters in heterologous cell types. Pessino *et al* produced a study in which two GLUT1/GLUT4 chimeric glucose transporters were each shown to co-immunoprecipitate with native GLUT1 from CHO cells (Pessino, 1991). The chimeric transporters were composed of GLUT1 sequence with either the C-terminal 29 residues, or the C-terminal 294 residues substituted with GLUT4 sequence. The antibody used in the immunoprecipitation was raised against a GLUT4 C-terminal peptide. This suggests that the sequence important in the interaction of the subunits is present in the first 199 residues of GLUT1. No co-immunoprecipitation of native GLUT4 and native GLUT1 was detected in 3T3-L1 cells using this antibody, suggesting that GLUT1 can form homodimers but not heterodimers *in vivo*.

It has been shown that GLUT2 and GLUT3 can be heterologously expressed in oocytes, where they display differing kinetic profiles (Burant & Bell, 1992a, Colville *et al.*, 1993b). These transporters can be expressed simultaneously in this system, and the resulting kinetic pattern can be separated into two components attributable to each of the isoforms. This

indicates that, at least in this system, heterodimers are not formed (Burant & Bell, 1992a).

1.11 Aims of This Study.

The purpose of this study is initially to characterise the basic kinetic parameters of fructose transport by human GLUT5 when expressed in the *Xenopus* oocyte system. Little is known about this isoform, and previous studies which have measured the kinetics of transport and substrate specificity have thrown up conflicting results. It has previously been demonstrated that GLUT2, the only other glucose transporter isoform capable of fructose transport, accepts fructose in the furanose ring form. Since it is not known how fructose is bound by GLUT5, or which ring form is preferred, it is intended to determine this by using fructose analogues which are locked in either the furanose or pyranose ring forms, in inhibition studies. It is also intended to examine the effects of pH on the function of GLUT5, since this isoform is expressed in tissues of the mammalian body which are exposed to a wide range of pH values.

The structural basis of fructose recognition in GLUT2, and indeed the basis for substrate selectivity and isoform specific kinetics of both GLUT2 and GLUT3 will be investigated by the characterisation of a series of GLUT2/GLUT3 chimeric transporters. These will be expressed in the *Xenopus* oocyte system, which will allow the measurement of the kinetics of transport of fructose, deGlc and galactose.

In an effort to further investigate the structural basis of substrate binding in isoforms other than GLUT1, GLUT3 has been chosen as a template for site directed mutagenesis. A series of mutants have been constructed where each amino acid residue in helix 8 of GLUT3 is individually replaced with alanine. It is intended to express these mutant constructs in the *Xenopus* oocyte system,

and to measure the K_m value for the transport of deoxyglucose. It is hoped that this characterisation might identify residues involved in substrate binding in GLUT3.

The GLUT2/GLUT3 chimeric constructs used in this work have been made by Dr Margaret Arbuckle, and the GLUT3 helix 8 point mutants have been made by Dr Michael J. Seatter. Additionally, some of the characterisation of these mutants was performed by the above, and it is noted in this thesis where it is included.

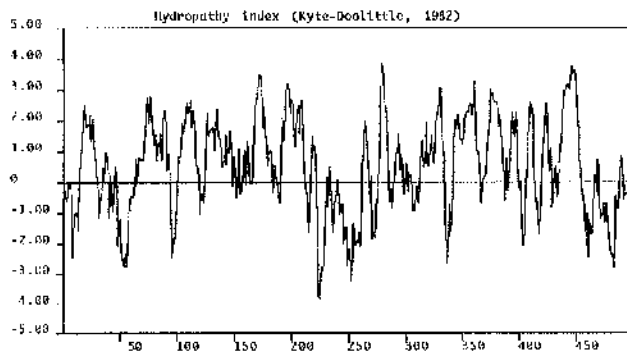
Figure 1.1

Hydropathy Plots of GLUTs 1, 2, 3 and 5.

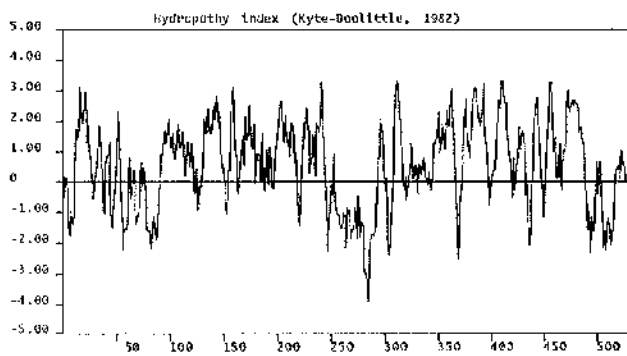
This diagram shows the hydropathy plots of GLUTs 1, 2, 3, and 5. The plots are virtually superimposable, and this is thought to reflect a similar membrane topology and a common mechanism of action. The topological model of GLUT1 shown in Figure 1.2 is largely based on this analysis.

Figure 1.1-
Hydropathy Plots of GLUTs 1, 2, 3 & 5.

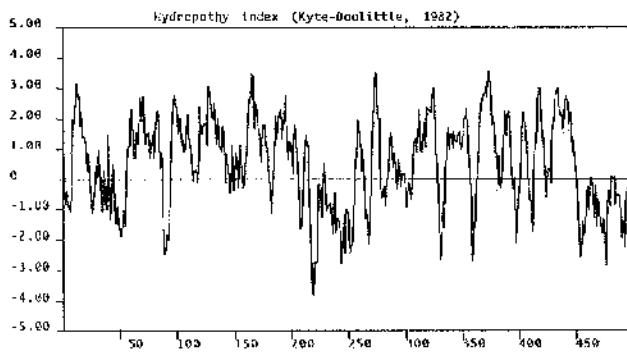
GLUT1 (rat)



GLUT2 (human)



GLUT3 (human)



GLUT5 (human)

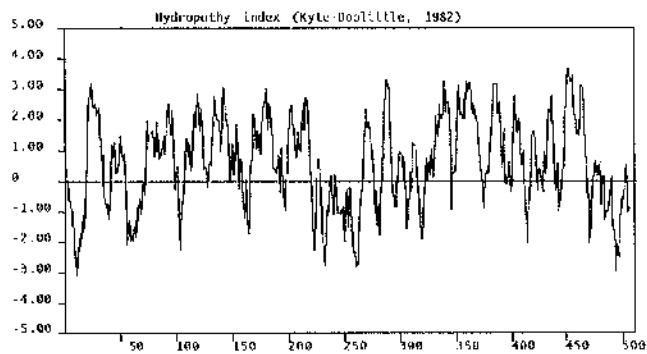


Figure 1.2

Topological Model of the Mammalian Facilitative Glucose Transporters.

This model is based on the results of hydropathy analysis of GLUT1 (Mueckler, 1985), and has been confirmed by glycosylation scanning mutagenesis. Since the hydropathy plots of GLUT1 and GLUTs 2, 3, 4, and 5 are virtually superimposable, so it is assumed that this model is applicable to all the isoforms in the glucose transporter family. The diagram shows the twelve predicted transmembrane helices as boxes, numbered 1-12. The amino- and carboxy-termini (labelled NH₂ and COOH respectively) are on the cytoplasmic face of the membrane. The N- and C-terminal "halves" of the structure are separated by the large central cytoplasmic loop between helices 6 and 7. The other large loop is exofacial, and connects helices 1 and 2. This loop contains a site for N-linked glycosylation. This site is labelled "CHO" in the diagram. Invariant residues are shown by their single letter abbreviations, and filled circles represent invariant polar residues which are predicted to be membrane located.

Figure 1.2

Topological Model of the Mammalian Facilitative Glucose Transporters

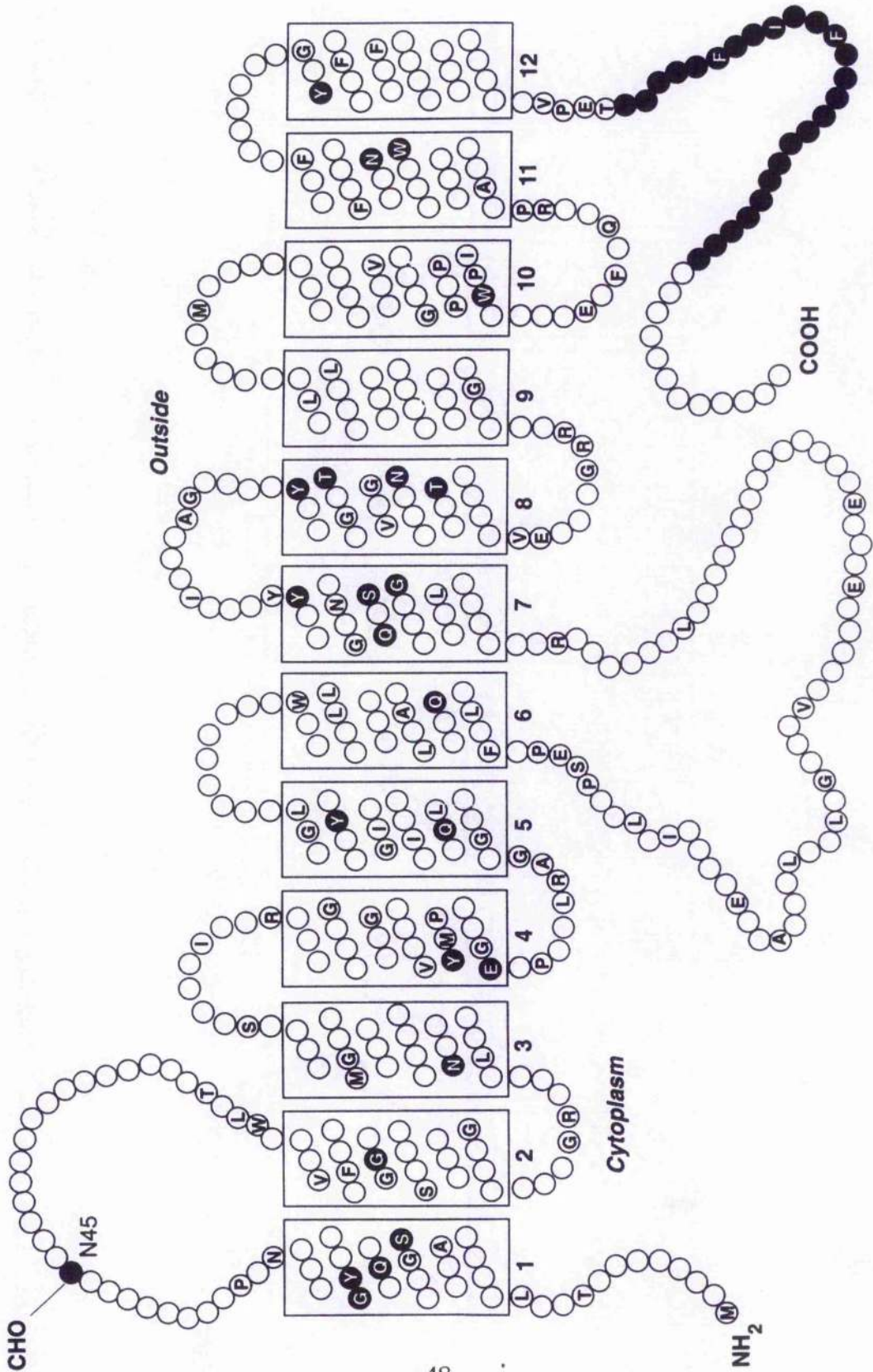


Figure 1.3

Diagram Describing the Single Site Alternating Conformation Model of GLUT1.

This diagram describes the conformational changes in GLUT1 (and in the other isoforms), which are associated with the transport of D-glucose. The diagram shows the binding of glucose to the outward-facing transporter, the conformational change which closes the exofacial binding site, opens the endofacial binding site, and which results in the transport of glucose to the other side of the membrane, the dissociation of glucose from the endofacial binding site, and the re-orientation of the carrier to the outward-facing conformation. This diagram is purely schematic, and does not attempt to represent the actual changes in the transporter structure.

Figure 1.3

Diagram of the Single Site Alternating Conformation Model of GLUT1.

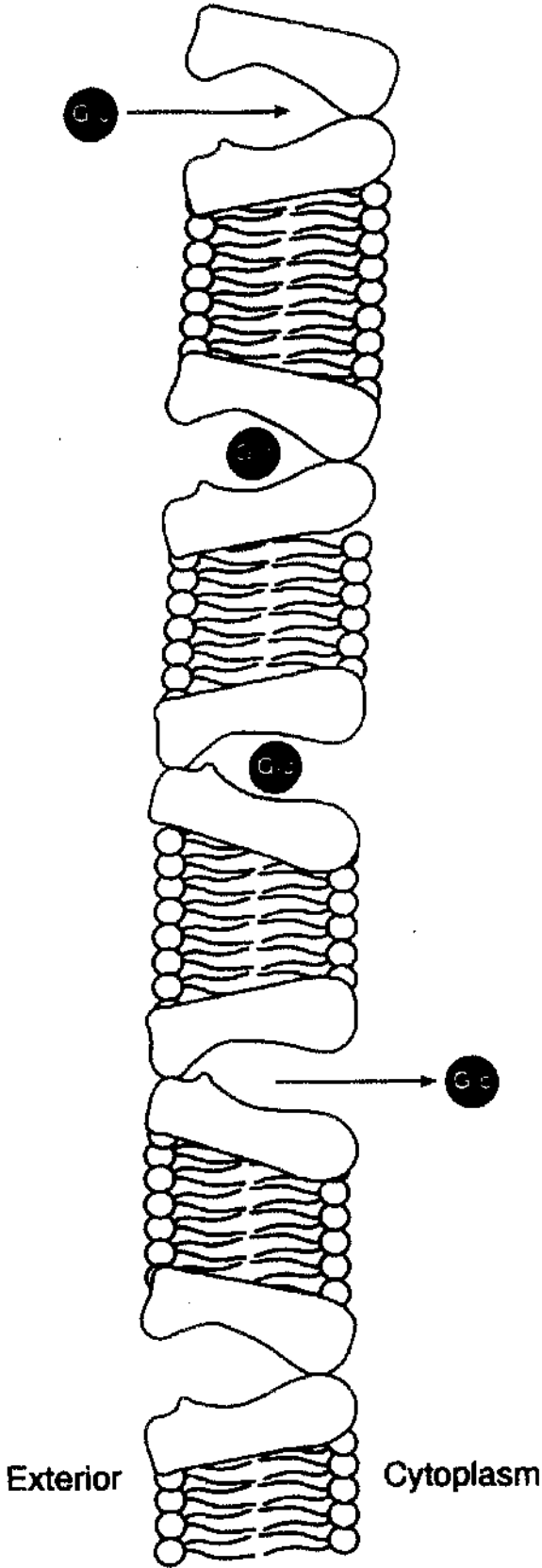


Figure 1.4

Interaction of β -D-glucose at the Exofacial Binding Site of GLUT1.

This diagram of the hydrogen bonding interactions of β -D-glucose with the exofacial binding site of GLUT1, is based on a model proposed by Barnett *et al.* Hydrogen bonds form between the transporter and the sugar hydroxyls of carbons C-1, C-3 and C-4. The oxygen of the sugar is also involved. Possible hydrophobic interactions between the transporter and the sugar at the C-6 position have also been suggested (Barnett *et al.*, 1973). Hydrogen bonds are represented by dotted lines, and the C-6 hydrophobic interactions are illustrated as a dashed area.

Figure 1.4

Interaction of β -D-Glucose at the Exofacial Binding Site of GLUT1.

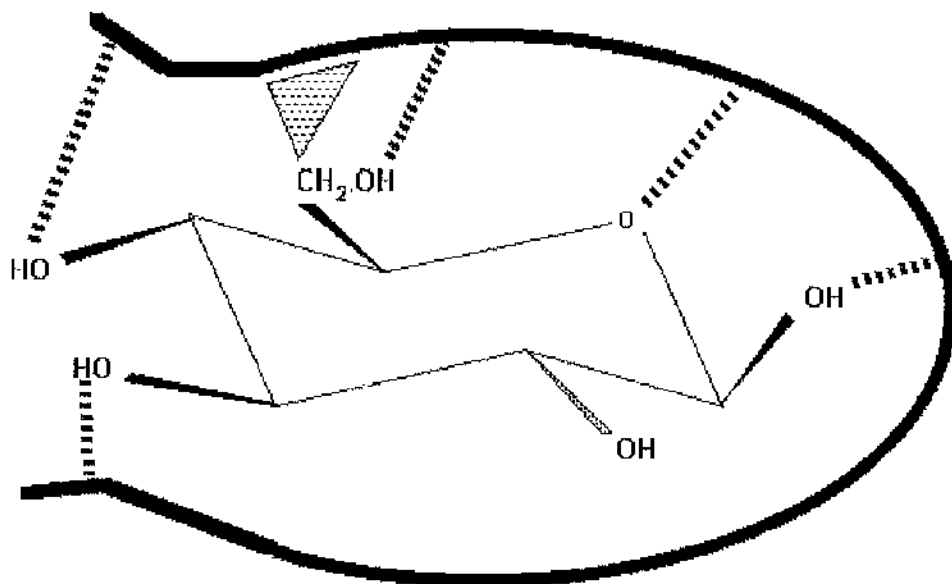


Figure 1.5

King-Altman Representation of the Transport Cycle of GLUT1.

This figure shows a King-Altman diagram of the alternating conformation model of GLUT1. T_o represents the transporter in the outward-facing conformation, in the absence of substrate. T_oS represents the transporter in the outward-facing conformation, in the presence of substrate. T_i , and T_iS represent the transporter in the inward-facing conformation, in the absence and the presence of substrate, respectively. K_{S_o} and K_{S_i} represent the dissociation constants of substrate (i.e. D-glucose), at the exofacial and endofacial binding sites, respectively. The rate constant for the re-orientation of the unloaded transporter from the outward-facing conformation to the inward-facing conformation is denoted as k_1 . Re-orientation of the empty carrier from the inward-facing conformation to the outward-facing conformation is denoted as k_{-1} . The rate constants for the movement of loaded transporter from the outward-facing conformation to the inward-facing conformation and back again, are denoted as k_2 , and k_{-2} , respectively. The values of these constants, measured for GLUT1 at 0°C are shown below (Lowe & Walmsley, 1986).

Rate Constant	Value at 0°C (s ⁻¹)
k_1	12.1 ± 0.98
k_{-1}	0.726 ± 0.498
k_2	1113 ± 498
k_{-2}	90 ± 3.47

Figure 1.5

King-Altman Representation of the Transport Cycle of GLUT1.

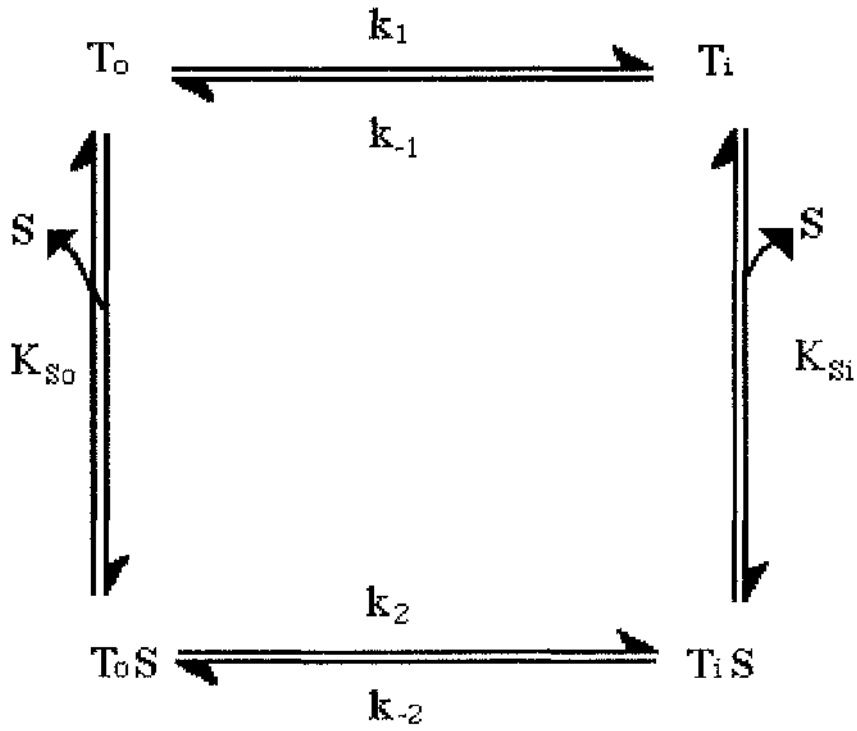


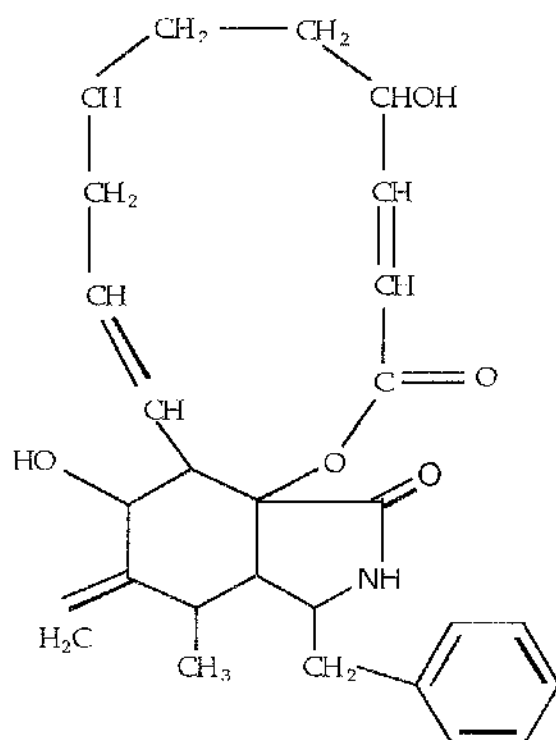
Figure 1.6

Structures of Cytochalasin B and ATB-BMPA.

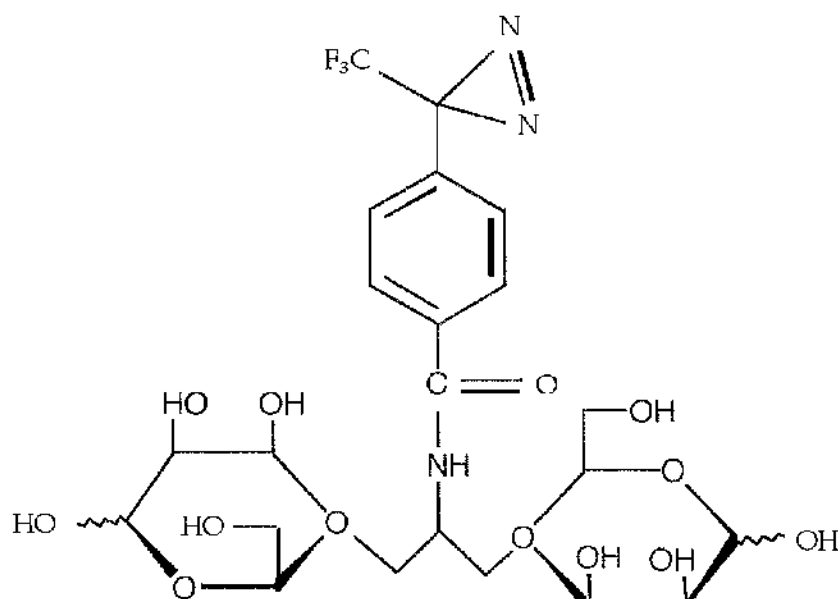
This diagram shows the structures of cytochalasin B and ATB-BMPA. These compounds interact competitively with glucose at the endofacial and exofacial binding sites, respectively. They are also thought to bind to and photolabel the transporter, specifically at these sites.

Figure 1.6

Structures of Cytochalasin B and ATB-BMPA.



Cytochalasin B



ATB-BMPA

Figure 1.7

Diagram Showing the Proposed Model of GLUT1 Oligomerisation.

This diagram shows a representation of the two oligomeric structures that GLUT1 can exist in, as described in the model proposed by Carruthers. GLUT1 can exist as a dimer or a tetramer. Each of the two molecules of GLUT1 that exist in the dimer can isomerise independently of the other. Hence in this situation, both transporters can be outward-facing or inward-facing at the same time. Alternatively, one may be outward-facing whilst the other is inward-facing. In the tetrameric form however, the isomerisation of each of the subunits is linked to the others. The tetramer is effectively composed of two dimers of GLUT1, but the subunits of these dimers are linked, so that isomerisation of one subunit results in the isomerisation of the adjacent subunit. Therefore, in the tetramer, two of the GLUT1 subunits will be outward-facing, and two will be inward-facing. Glucose binding to any of these subunits will induce conformational change in that subunit, and also in the adjacent subunits. The result of this is that every re-orientation of a GLUT1 subunit from the outward-facing conformation to the inward-facing conformation is accompanied by the linked movement of another subunit into the outward-facing conformation. The diagram indicates that from the evidence put forward by Carruthers, tetrameric GLUT1 can be converted to dimeric GLUT1 under reducing conditions (Herbert and Carruthers, 1992).

Figure 1.7

Diagram Showing the Proposed Model of GLUT1 Oligomerisation.

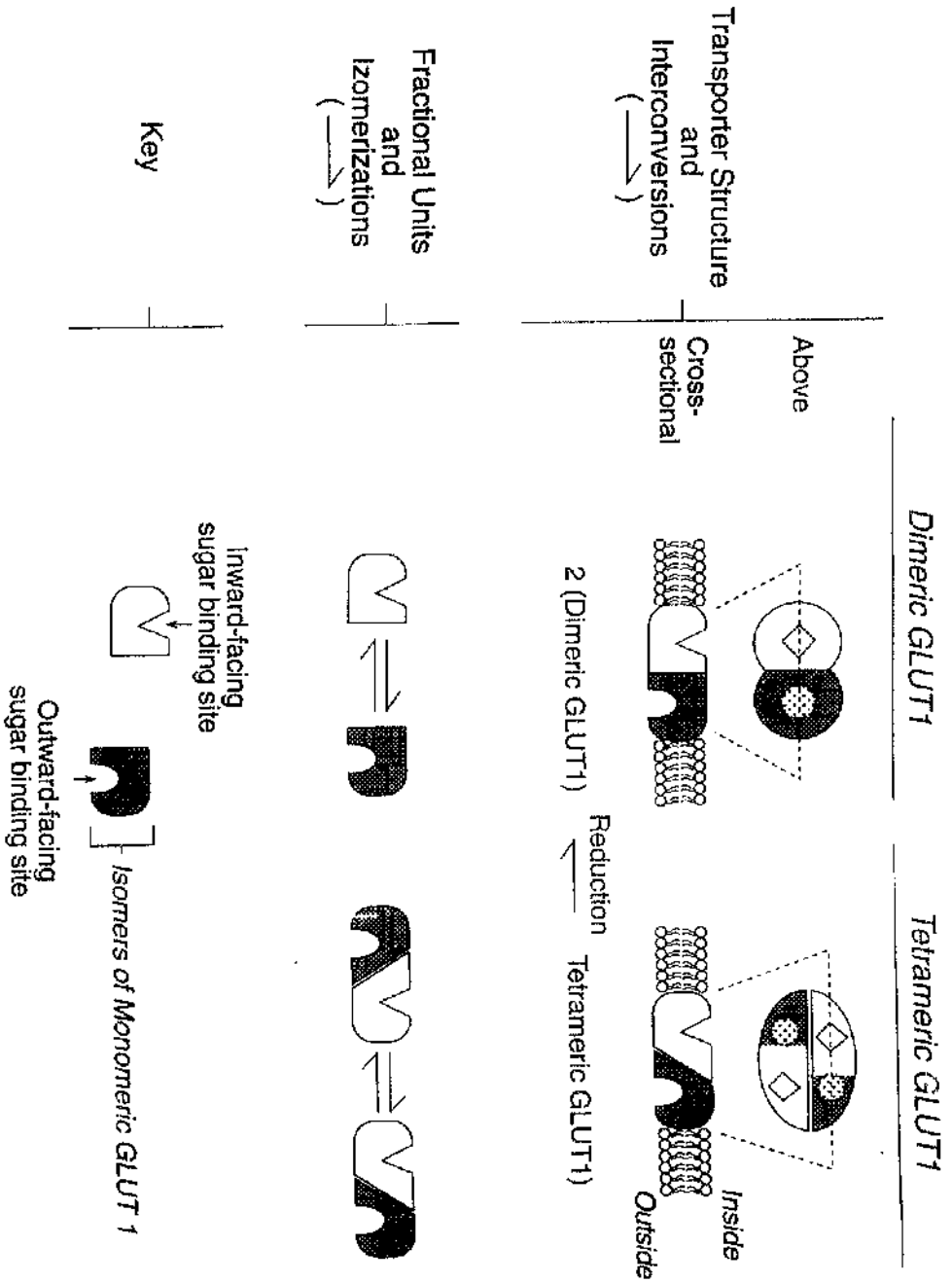


Figure 1.8

Diagram Showing Regions of Importance in the Transporter Structure.

This diagram shows regions of the transporter which have been shown to be involved in formation of the exofacial and endofacial binding sites, as demonstrated by studies using conformational-specific ligands ATB-BMPA, Forskolin, and cytochalasin B. Also shown in this diagram are regions important in the ability of the molecule to undergo conformational change.

Figure 1.8

Diagram Showing Regions of Importance in the Transporter Structure.

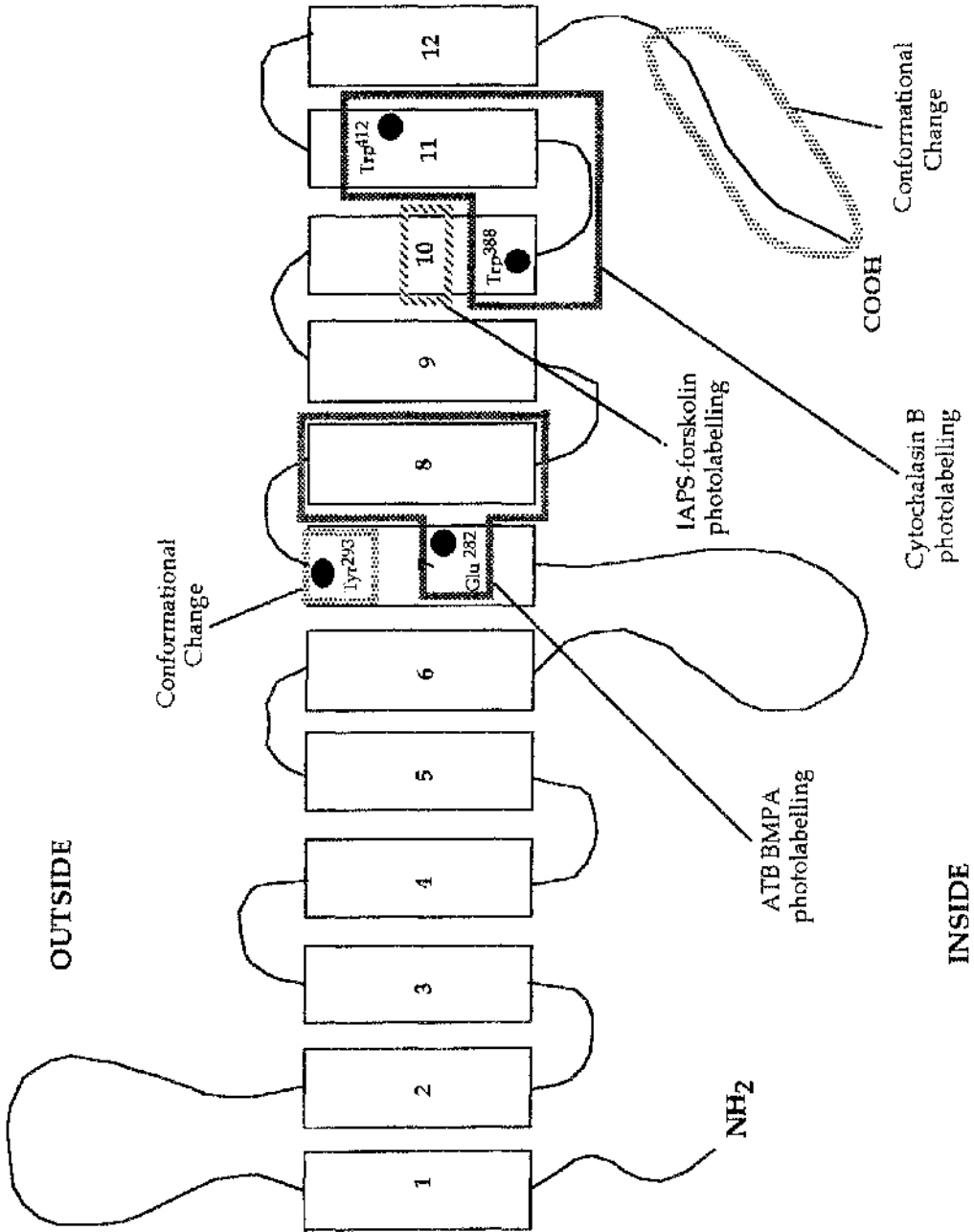


Figure 1.9

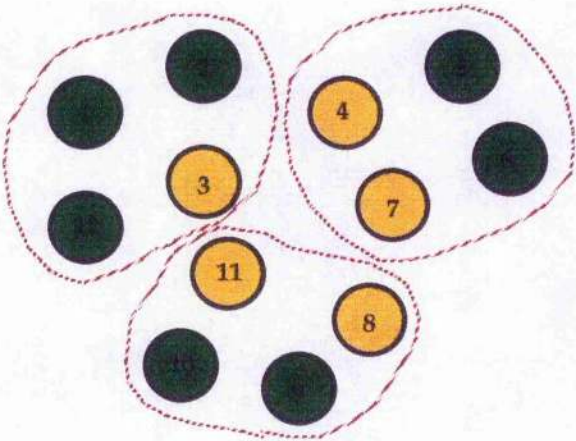
Speculative Models of the Helical Packing in the Tertiary Structure of GLUT1.

This diagram shows a representation of two speculative helical packing models for GLUT1, proposed by Zeng *et al.* Both of these computer generated models take into account various physical constraints on the possible tertiary structure. Macrodipoles arranged in antiparallel orientations within four-helix bundles are proposed to provide electrostatic stability. In both models in this diagram, the four-helix bundle arrangements are indicated by red dotted lines. The helices proposed to line the membrane spanning channel are shown in yellow, and the surrounding helices, in green. In model 2 helix 6 is distant to helix 7, and this distance is possible because of the long cytoplasmic loop between these helices. This model therefore, not only suggests a role for the large cytoplasmic loop, but also accounts for the bilobular structure which has been observed experimentally for other transport proteins, such as the lac permease of *E.coli.* (Zeng *et. al.*, 1996).

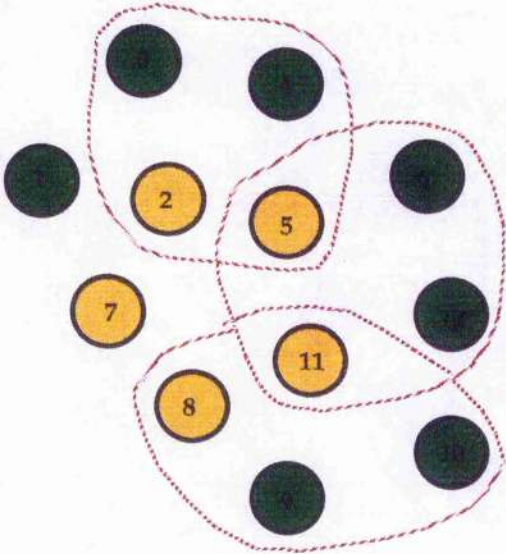
Figure 1.9

Speculative Models of the Helical Packing in the Tertiary Structure of GLUT1.

Model 1



Model 2



CHAPTER 2.

Materials and Methods.

2.1 Materials.

Adult female *Xenopus laevis* were obtained from either Blades Biologicals, Edenbridge, Kent, UK, or directly from South Africa, (African *Xenopus* Facility, PO Box 118, Noordhoek, Republic of South Africa). "Frog Brittle" was also obtained from Blades Biologicals.

Tricaine Methane Sulphonate, MS222 was supplied by Thompson & Joseph Ltd., Norwich, UK.

Chromic sterile catgut[®] was supplied by Ethicon Ltd., London, UK.

2-deoxy-D-glucose, 3- D-galactose, β -D-fructose, L-arabinose, D-mannose, phloretin, kanamycin, ampicillin, tetracycline, dithiothreitol, cytochalasin B, 1,5-anhydro-D-mannitol and 2,5-anhydro-D-mannitol were supplied by Sigma Chemical Company, Poole, Dorset, UK, and L-sorbose was supplied by Pfanstiehl Laboratories Inc., Waukegan, IL, USA.

Ammonium formate, and chloroform (Analytical Reagent) were supplied by BDH, Poole, UK.

Bacto[®]-tryptone, Bacto[®]-agar and Bacto[®]-yeast extract were supplied by Difco, East Molesey, Surrey, UK.

Tris was supplied by Boehringer Mannheim GmbH., Lewes, East Sussex, UK.

Agarose (electrophoresis grade), DNA ligase and 5x ligase buffer were supplied by Gibco BRL, Paisley, UK.

Lambda ladder (*Bst*E II digested) and ribonuclease A were supplied by New England Biolabs, Hitchin, Herts, UK.

Sequencing grade urea, Tris, EDTA, de-ionised formamide, TEMED and Mixed Bed Resin were obtained from International Biotechnologies Inc. Ltd. (IBI), Cambridge, UK.

National Diagnostics Sequagel-6[™] 6% sequencing gel solution and Sequagel[™] Complete Buffer Reagent were obtained from BS&S, Edinburgh, UK.

Ultima-flo AF scintillant was obtained from Canberra Packard Ltd., Pangbourne, Berks., UK.

Taq DyeDeoxy™ Terminator Cycle Sequencing kits and sequencing-grade phenol/chloroform/H₂O (68:18:14) was obtained from Applied Biosystems Inc. (ABI), Warrington, Cheshire, UK.

Elutip-D DNA purification columns (Schleicher & Schuell) were obtained from Anderman Ltd, London, UK.

Permacel™ tape was obtained from Genetic Research Instruments, Dunmow, Essex, UK.

Alconox™ detergent was supplied by Aldrich Chemical Company Ltd., Gillingham, Dorset, UK.

'Native' *Pfu* DNA polymerase and 'Native' *Pfu* polymerase 10x buffer were obtained from Stratagene, Cambridge, UK.

Vent DNA polymerase was supplied by New England Biolabs Inc., Beverly, MA.

All restriction enzymes and corresponding 10x buffers, *Taq* DNA polymerase with supplied 10x buffer and MgCl₂, calf intestinal alkaline phosphatase and 10x buffer, polynucleotide kinase and polynucleotide kinase 10x buffer, rNTPs, dNTPs, nuclease-free H₂O, 5x transcription buffer, dithiothreitol (DTT), RNasin, RNA ladder (360-9,490 bases) and SP6 RNA polymerase were supplied by Promega, Southampton, UK.

[2,6-³H]2-deoxy-D-glucose, [U-¹⁴C]D-fructose and [U-³H]D-galactose were supplied by DuPont NEN, Stevenage, Herts, UK.

"Sculptor™ *in vitro* mutagenesis system- RPN 1526" kits and [³²P]dATP (5000 Ci/mmole; 10 mCi/ml) were supplied by Amersham International plc., Aylesbury, Bucks, UK.

Dialysis tubing (Visking size 1-8/32") was supplied by Medicell International Ltd, London, UK.

Sterile Acrodisc® 0.2 µm filters were supplied by Gelman Sciences Ltd., Northampton, UK.

Sodium diguanosine triphosphate, GpppG (5' Cap) was supplied by Pharmacia, Milton Keynes, UK.

All oligonucleotides (Tables 5.1 and 5.2) were synthesised by Dr. V. Math, Department of Biochemistry, University of Glasgow.

Unless indicated otherwise, all remaining chemicals were supplied by Fisons, Loughborough, UK.

2.2 *In Vitro* Transcription of mRNA from Plasmid cDNA.

All work with mRNA was performed with sterile equipment whilst wearing gloves. Ribonucleases which can degrade mRNA can be found on the skin and elsewhere, and as these are very stable enzymes, this precaution was taken to avoid potential degradation of the mRNA. All reagents were thawed on ice. A nucleotide stock (2.5 mM rATP, 2.5 mM rCTP, 2.5 mM rUTP and 0.5 mM rGTP) was diluted from stock 100 mM ribonucleotides. The following reagents were added to a sterile microfuge tube in the order shown, at room temperature:-

- 75 μ l ribonuclease-free H₂O
- 40 μ l 5x transcription buffer
- 20 μ l 100 mM dithiothreitol (DTT)
- 5 μ l RNasin (a synthetic inhibitor of ribonuclease)
- 40 μ l nucleotide mix (see above)
- 10 μ l GpppG (5' Cap) (25 units/100 μ l).
- 10 μ l linearised plasmid cDNA (~ 1 μ g/ml)
- 1.5 μ l SP6 polymerase (25 units)

This gave a total volume of 200 μ l (before enzyme addition). The tube was placed in a 37°C water bath for a 1 hour incubation, after which a further 1.0 μ l of SP6 polymerase was added, mixed and incubated at 37°C for 30 min. At this point the reaction was centrifuged in a microfuge to collect the condensate and then 1 volume of phenol/chloroform [1:1 (v/v)] added. This was vortexed for 1 min and centrifuged in a microfuge for a further 1 min. The upper aqueous phase, which contained both mRNA and cDNA, was carefully collected into a clean tube. 100 μ l of chloroform/isoamyl-alcohol (24:1) was added to the solution, before vortexing, centrifuging, and again collecting the aqueous phase. This procedure was repeated, before finally adding 0.3 volumes of 5 M potassium acetate and 2.5 volumes of ice-cold absolute ethanol to precipitate the

nucleic acid. The reaction was mixed and placed at -20°C for approximately 2 hours, or at -80°C for 20 minutes, then centrifuged in a microfuge for 30 min. The pellet was washed with 1 ml 70% ethanol and centrifuged as above (the 70% ethanol was made up using ribonuclease-free water). All traces of ethanol were removed from the pellet by drying under vacuum. The pellet was resuspended in 35 μl of ribonuclease-free H_2O . 5 μl of this was mixed with 3 μl of 5x DNA gel loading buffer (Table 2.1) and loaded into a 1% agarose gel overlaid with 1x TAE running buffer (Table 2.1). 5 μl of 100 $\mu\text{g}/\text{ml}$ *Bst*E II-cut lambda ladder DNA was loaded into an adjacent well and the current adjusted to 50 mA so that negatively charged nucleic acids migrated toward the positive electrode. Electrophoresis was carried out until the dye-front was half to two thirds across the gel, then 20 μl of 10 mg/ml ethidium bromide added per litre of running buffer. The bands were visualised by viewing the gel under ultra-violet light. A typical photograph of mRNA on a 1% agarose gel is shown in Figure 2.2.

2.3 Using *Xenopus* Oocytes.

2.3.1 Handling *Xenopus*.

Adult female *Xenopus laevis* (average length 15 cm) were kept in aquaria at a constant temperature of $16-18^{\circ}\text{C}$ on a 12 hour day/night cycle. The animals were housed 2-4 per tank, in distilled water in a quiet environment. They were fed once weekly with raw chopped sheep heart and the aquaria cleaned the following day. Alternatively they were fed Blades Biologicals "Frog Brittle". Each animal was kept for at least one month before operating to allow acclimatisation to its new environment. Oocytes were generally satisfactory after this initial period, however during the summer poor oocytes were frequently encountered, coincident with seasonal variability of the female cycle in these animals.

2.3.2 Anaesthesia.

The anaesthetic was prepared by dissolving 0.75 g Tricaine Methane Sulphonate (MS222) in 500 ml distilled water. 25 ml of 0.5 M sodium bicarbonate was added to ensure that the pH of the anaesthetic approached neutrality and hence was acceptable for the animal. The animal to be operated on was placed in the tank with the anaesthetic and supervised to ensure that it did not drown. Typically, animals were unconscious after 5-10 min. The animal was placed on its back and observed. If it did not move, it was judged to be unconscious.

2.3.4 Surgery.

Home Office Project and Individual Animal Handling Licenses were required for work on *Xenopus*. The surgery was generally performed by Dr Micheal Seatter, and occasionally by Dr Fiona Thomson and Dr. Gwyn Gould. The animal was placed on its back and, using a sharp scalpel, a centimetre-long incision was made in the dermis and then another one directly underneath in the abdominal wall. A small clump of oocytes was removed using fine watchmaker's forceps and small scissors. These were placed into a petri-dish containing Barths buffer (Table 2.1). Oocytes were determined to be healthy if they fulfilled several important criteria. Oocytes had to be approximately 1 mm in diameter; required well-defined animal (dark) and vegetal (light) poles, with a sharp distinction at the boundary; required no discoloured patches; and had to exhibit a certain robustness when manipulated. These were defined as stage V and VI oocytes. If the oocytes were judged to be healthy, enough were removed from the toad as required for injection and non-injected controls. The animal was then sewn up using chromic sterile catgut, with a single stitch in the abdominal wall and two stitches in the dermis. The animal was then placed on its front in a recovery tank containing 2-3 mm of distilled water until it fully

regained consciousness, when it was returned to its own holding tank. A minimum period of no less than three months was allowed to pass before operating on the same animal: after this second operation the animal was sacrificed.

2.3.4 Oocyte Isolation and Injection.

Oocytes were removed from adult female *Xenopus laevis* and individually dissected. This involved removing the oocytes from the connective tissue and blood vessels which provide the oocytes with nutrients and remove toxic wastes. Oocytes were placed into a petri-dish, immersed in Barths buffer (Table 2.1), to maintain the environment as close to *in vivo* conditions as possible. Using a binocular microscope and fine watchmakers forceps, stage V and VI oocytes were removed from their connective tissue and then transferred to a container with fresh Barths buffer. Damaged oocytes were immediately discarded to minimise the exposure of healthy oocytes to proteases. Generally, 2-3 times as many oocytes were isolated than actually required since a percentage of the population would be expected to die before they were assayed. Oocytes were selected as required for injection with 50 nl of *in vitro* transcribed mRNA encoding GLUT2, GLUT3, GLUT5 or a mutant transporter, or to act as non-injected "control" oocytes.

The injection apparatus consisted of a 10 μ l micro-injector (Drummond Scientific Co.); six inch long capillary tubes; a micro-manipulator (Narishige, Japan); a needle-puller (World Precision Instruments); a binocular microscope with separate light source; a petri-dish with a SpectraMesh grid (Fischer); and paraffin oil. Gloves were worn at all times to prevent contamination of the mRNA by ribonuclease present on fingertips. A capillary tube was placed in the needle-puller and by a combination of heating and pulling produced needles with a bore size of about 2 μ m. The tip of one was broken off near the end with

fine forceps and, using a syringe and 25 gauge needle, filled with paraffin oil. This was attached to the micropipette (set at about 1.5 μ l) and secured in the micro-manipulator. GLUT mRNA was placed into a 1.5 ml microfuge tube and pulsed for 30 sec in a microfuge to remove any debris or insoluble material. About 7 μ l of mRNA was taken from the supernatant and placed onto a sterile microfuge tube lid. The micropipette was lowered so that the end of the needle was submerged in the droplet, and the mRNA taken up slowly into the needle. Oocytes were placed on a grid in a petri-dish with Barths buffer and orientated so that the pale vegetal pole was uppermost. They were injected with a precise volume of mRNA (50 nl) and then removed to a separate container. The oocytes were incubated in Barths buffer for 48-72 hours prior to assay, transferring to fresh buffer every 12 hours. Non-injected oocytes were treated in an identical fashion. After this period, oocytes were assayed for the ability to transport the sugars appropriate for the experiment.

2.4 Sugar Transport in *Xenopus* oocytes.

Groups of between 6 and 10 oocytes were incubated in 0.45 ml Barths buffer (Table 2.1) at room temperature in 13.5 ml centrifuge tubes. Transport (zero-trans entry) was initiated by the addition of 50 μ l of [2,6- 3 H]2-deoxy-D-glucose, [3 H]D-galactose, or [U- 14 , C]D-fructose to give a specified final sugar concentration with an activity of \sim 1 μ Ci/ml. After a designated time, usually 15 or 30 min, the transport of sugar into the oocytes was quenched by rapid aspiration of the media and three washes with 5 ml ice-cold 150 mM phosphate buffered saline, pH 7.4, (1xPBS, Table 2.1) containing 0.1 mM phloretin (a potent transport inhibitor). The oocytes were dispensed individually into scintillation vials using a pipettman and a tip which had the end cut off, and then 1ml of 1% sodium dodecyl sulphate (SDS) added. The vials were covered with Cling Film and left overnight at room temperature to solubilise the oocytes, before the

4, 5' α 3'
untrans
 β -globi
me cap?

addition of 4 ml scintillation fluid and subsequent measurement of radioactive uptake by a scintillation counter. For each group of GLUT-injected oocytes assayed at a particular sugar concentration, a group of non-injected oocytes were assayed under identical conditions. This control gave a value for radioactive sugar transport by native oocyte glucose transporters plus background radiation levels. Hence, the rate of uptake in GLUT-injected oocytes less the rate of transport in control (non-injected) oocytes gave a value corresponding to specific transport by heterologous transporters. Transport with a variety of sugar concentrations was measured for each assay so that Lineweaver-Burk plots could be constructed, and K_m and K_i values determined. For assays involving the inhibition of radioactive sugar uptake by another sugar, the oocytes were exposed to the inhibitor in 0.45 ml Barths buffer at least 15 min prior to addition of labelled sugar.

2.5 General Techniques for the Manipulation of DNA.

2.5.1 Plasmid Construction.

The human glucose transporter constructs used for the preparation of mRNA have been described previously (Kayano *et al.*, 1990). Human GLUTs 2, 3 and 5 were in pSP64T (Kreig & Melton, 1984) and named pHTL217, pSPGT3, and pHGLUT5 respectively. These constructs contain the protein coding region of the cDNA flanked by 89 bp of 5'- and 141 bp of 3'-untranslated sequence from the *Xenopus* β -globin gene (Kayano *et al.*, 1990) (Figure 2.1). The plasmid contains a SP6 RNA polymerase promoter at the 5' end of the transporter sequence and a sequence encoding ampicillin resistance.

2.5.2 Linearisation of Plasmid cDNA.

pHTL217, pSPGT3, pHGLUT5 or any of the chimeric or point mutation constructs, were specifically restricted once at the 3' end of the cDNA, downstream of the coding sequence. This had the effect of linearising the plasmid, so that the efficiency of subsequent mRNA synthesis reactions were increased by ensuring that the SP6 RNA polymerase used did not continue synthesis of mRNA after transcription of the transporter. The choice of restriction enzyme depended on the particular plasmid and transporter. GLUT3 and the helix 8 point mutation constructs were linearised using *Xba* I, GLUT2 and the chimeric constructs by *Sal* I, and GLUT5 by *Hind*III. 10 μ g of plasmid cDNA was digested in a total volume of 20 μ l overnight at 37°C (section 2.5.4). 1 μ l of this reaction was loaded onto a 1% agarose gel and electrophoresed to confirm linearisation (section 2.5.3). From this point onwards, all work was done using sterile microfuge tubes whilst wearing gloves. 100 μ l of ribonuclease-free H₂O was added to the tube, the solution extracted with 1 volume of phenol/chloroform (1:1), then twice with chloroform/isoamyl-alcohol (24:1). The cDNA was precipitated by the addition of 0.3 volumes of 5 M potassium acetate and 2.5 volumes of absolute ethanol, and incubation at -20°C for at least 1 hour. The tube was centrifuged in a microfuge for 30 min at 4°C, the pellet resuspended in 1 ml 70% ethanol, centrifuged again in a microfuge for 30 min, and the pellet finally resuspended in 10 μ l of ribonuclease-free H₂O. This was ready to be used in a mRNA synthesis reaction (section 2.2).

2.5.3 Agarose Gel Electrophoresis of DNA.

Various gel volumes, combs and agarose concentrations were used. The gel volume was governed by the number of samples, the volume of the samples and to a lesser extent the required degree of separation of the DNA bands. The

choice of comb depended only on the volume of the samples. The concentration of agarose used varied depending on the molecular weight of the DNA band to be visualised- high agarose concentrations aided the separation of low molecular weight bands, and lower agarose concentrations give better separation with higher molecular weight bands. Typical concentrations used were 1.0% and 1.6% (w/v).

Example:- for a 100 ml 1.0% Agarose Gel.

An appropriate gel base was selected and the ends secured with tape to prevent gel leakage. 1.0 g of agarose was weighed out and distilled water added to a total volume of 100 ml. This was heated in a microwave oven until the solution just boiled and left to cool until hand hot. 2 ml of 50xTAE buffer (Table 2.1) was added to the gel solution and mixed. The contents were poured onto the gel base, the comb inserted and the gel left to set for about 20 min. The tape was then removed and the entire gel and its base placed into the electrophoresis tank so that the wells were nearest to the negative electrode. About 1 litre of 1xTAE buffer (Table 2.1) was added to the chamber so that the entire gel was submerged, and then the comb was removed. To each sample, 1/4 volume of 5x DNA gel-loading buffer (Table 2.1) was added and mixed. The samples were loaded into the wells by pipetting directly above them- the glycerol in the sample buffer ensured that the samples were more dense than the buffer and therefore the samples sank into the wells. 10 μ l of loading buffer containing 25 μ g/ml *Bst*E II-cut lambda ladder DNA was loaded into an adjacent well. The electrodes were connected so that the negative electrode was closest to the sample wells. The samples were electrophoresed at 50-100 mA using an LKB 2197 power supply until the dye front had migrated two thirds of the way along the gel towards the positive electrode, then 50 μ l of 10 mg/ml ethidium bromide was added per litre of running buffer, and left at room temperature for 30- 45 min. The DNA was

visualised by ultra-violet light using an Ultraviolet Products Inc. transilluminator, and the size of any DNA band checked by its relative migration to the lambda ladder. The gel was then photographed using a Mitsubishi video copy processor.

2.5.4 Restriction Digestion of DNA.

Restriction digestion of DNA was performed by the addition of restriction enzymes to DNA in the appropriate buffer, optimising salt concentration and pH for individual enzymes. Generally, from 0.5-10 μg of DNA was digested per reaction. The total reaction volume was 10 μl per 1 μg DNA and the quantity of enzyme added equal to 1 unit per 1 μg DNA. The reaction was carried out by the addition of 1 volume of 10x buffer to 9 volumes diluted DNA solution, before the addition of enzyme. This was incubated for 3 hours at 37 °C (or otherwise depending on the particular enzyme). For digestions with more than one enzyme, the reaction was carried out as usual with the first enzyme (the one which utilises lower salt concentrations), and then salt added to the reaction to optimise conditions for the second digestion which was subsequently carried out. Alternatively, if both enzymes utilised approximately the same optimum reaction conditions, both digests could be carried out simultaneously. The reactions were then added to 1/4 volume of 5x DNA gel loading buffer and the solution loaded onto an appropriate agarose gel. This was electrophoresed, stained with ethidium bromide and DNA bands visualised as described above (section 2.5.3). Any bands of interest were excised from the gel with a scalpel and purified as described (sections 2.6.4, 2.6.6).

2.5.5 Dephosphorylation of Double-Stranded DNA using Calf Intestinal Phosphatase.

Plasmid DNA was digested with the appropriate restriction enzyme for 3hrs and then treated with RNase A for 15 min at 37°C (section 2.5.4). The mix was then made up to a volume of 100 μ l with dephosphorylation buffer (1 mM ZnCl₂, 1 mM MgCl₂, 10 mM Tris-HCl pH 8.8) and 10 units of Calf Intestinal Phosphatase (CIP) was added (10X amount recommended by Promega, the supplier). After incubation at 37°C for 2hrs, plasmid cDNA was isolated from the enzyme reagents by phenol extraction and precipitation (section 2.5.2), and DNA was resuspended in 20 μ l of H₂O.

2.5.6 Ligation of Double-Stranded DNA.

cDNA fragments were ligated to plasmid DNA by the following procedure. In order to increase the efficiency of ligation, the reaction was performed with a high GLUT cDNA: plasmid DNA molar ratio, (between 3:1 and 10:1). 100 ng of plasmid DNA which had been CIP-treated was added to GLUT cDNA at the appropriate molar ratio, and the mix incubated at 60°C for 5 min. After pulsing the samples briefly in a microfuge, an aliquot of 5x concentrated ligation buffer and 3 units of T4 DNA ligase were added, and the samples then incubated overnight at 16°C. Competent bacteria were then transformed with 5- 10 μ l of the ligation reaction as described (section 2.5.7).

2.5.7 Preparation and Transformation of Competent *E. coli* DH5 α cells.

A colony was picked from a freshly grown plate of DH5 α cells, and used to inoculate 3 mls of 2xYT medium in a universal container (Table 2.1). After an overnight incubation at 37°C in a shaking incubator, 200 μ l of the resulting

culture was removed and used to inoculate 50 mls of 2xYT medium which was contained in a 500 ml culture flask (-this ensured good aeration of the growing culture). This culture was placed in at 37°C in a shaking incubator for 2 hrs, or until an O.D. of 0.2 was reached.

The cells were then harvested by transferring the 50 ml culture to a sterile plastic 50 ml Falcon tube, and spinning at 3K for 10 mins in a Beckman benchtop centrifuge. After carefully discarding the supernatant, the cell pellet was gently resuspended in 2 mls of TSB buffer (Table 2.1). This cell suspension was incubated on ice for 10 mins, after which 200 µl aliquots were removed and transferred to sterile 1.5 ml eppendorf tubes. At this point the cells were competent for transformation by the following method.

Plasmid DNA was then added to the 200 µl aliquots of cells -typically 1 and 7 µl depending upon the concentration of the DNA. The cells and the DNA were mixed together by gently flicking the eppendorf tube, then transferred back to ice and incubated for at least 5 mins and no longer than 30 mins. 800 µl of TSB+glucose (Table 2.1) was then added to each of the 200 µl transformation reactions, gently mixed by flicking, and transferred to a shaking incubator at 37°C for at least 1 hr (-this allows expression of the ampicillin resistance gene on the pSPGT plasmid). The cells were collected by microfuging the eppendorf tubes for 30 secs, removing 800 µl of the supernatant, and gently resuspending the cell pellet in the remaining 200 µl volume. This 200 µl volume was then removed and plated out onto 2xYT agar plates which had ampicillin added at a concentration of 50 µgml⁻¹ (Table 2.1). The plates were allowed to dry, then were placed upside-down in a 37°C incubator and left overnight.

2.5.8 Preparation of Small Amounts of Plasmid DNA from Transformed *E.coli* DH5 α cells.

Any colony of interest was picked from the agar plate by stabbing with a sterile pipette tip, and used to inoculate a universal container containing 3 mls of 2xYT culture medium. This was grown up overnight at 37°C in a shaking incubator, after which 1.5 mls of culture was removed and placed in a sterile microfuge tube. The tube was microfuged for 30 secs to pellet the cells, the supernatant removed, and the pellet resuspended in 100 μ l of STEE buffer (Table 2.1). 20 μ l of a 10 mg/ml lysozyme solution was added and mixed thoroughly by vortexing before being placed in a boiling water bath for 50 secs. Once removed, the tube was microfuged immediately for 10 mins, and the resulting lysis pellet removed with a sterile cocktail stick. At this point in the procedure the DNA could be precipitated from the solution by the addition of 60 μ l of isopropanol followed by a 5 min incubation at -20°C, and the DNA pelleted by spinning for 10 mins in a microfuge. Removal of the isopropanol and air drying of the eppendorf tube for 15 mins would yield a DNA pellet which could be resuspended in an appropriate volume of sterile water-typically 20 μ l. This method of extraction was used if the purity of the DNA was not important, alternatively, if cleaner DNA was required, the sample could be purified by a phenol/chloroform extraction procedure followed by ethanol precipitation. This was the method most frequently used. One phenol extraction, two phenol/chloroform (1:1 v/v) extractions, and two chloroform/ isoamylalcohol (24:1 v/v) washes of the supernatants were performed, retaining each time the upper aqueous phase. After the final wash, 0.3 volumes of 3 M sodium acetate and 2.5 volumes of 100% ethanol were added to precipitate the DNA. This was incubated at -20°C for at least an hour before pelleting the DNA by centrifugation for 30 min in a microfuge. The ethanol was removed, the pellet washed with 70% ethanol and centrifuged for a further 30 min, before drying

under vacuum. The pellet was resuspended in 20 μ l of sterile water. 1 μ l of this was added to 1 ml of sterile water and the absorbance measured at 260 nm. The concentration was determined from the calculation below.

2.5.9 Calculation to Determine the Plasmid DNA Concentration and Purity.

absorbance value of 1.0 at 260 nm = 50 μ g/ml of dsDNA.

absorbance value of "y" at 260 nm = "y" x 50 μ g/ml of dsDNA.

absorbance at 260 nm = "Z"

absorbance at 280 nm

DNA has a lower protein concentration and has a higher purity when the value of "Z" is nearer to 2.0.

2.6 Recombinant Polymerase Chain Reaction.

2.6.1 Primary Polymerase Chain Reactions using *Taq* DNA Polymerase.

2.6.1a Synthesis of Oligonucleotides.

Oligonucleotides (60'-61'mers) with sequence composed in part of GLUT2 and part GLUT3 from various helical regions in the C-terminal half of the transporter protein were synthesised (Dr. V. Math, Department of Biochemistry, University of Glasgow). Pairs of oligonucleotides were constructed: one sequence representing the sense strand and another the complementary sequence, both of which had GLUT2 or GLUT3 binding sequences and GLUT3 or GLUT2 "tails". These will be referred to subsequently as internal primers. Additionally, two oligonucleotides (37'mers) were constructed which had positive polarity and sequence complementary to the antisense strands of the untranslated region at the 5' ends of GLUT2 and GLUT3. Likewise, antisense oligonucleotides (37'mers) were synthesised which bound to the positive strands of cDNA at the untranslated region at the 3' ends of GLUT2 and GLUT3 (Figure 5.3). Both these oligonucleotides incorporated a *Sal* I restriction site at their 5' ends (Table 5.1) and are subsequently referred to as external primers.

2.6.1b Primary PCR: Reaction Conditions.

1.6 μ g	"internal" primer.
1.6 μ g	"external" primer.
10 ng	template dsDNA
2 μ l	nucleotide mix (20 mM dATP, 20 mM dGTP, 20 mM dTTP, 20 mM dCTP)
10 μ l	10x <i>Taq</i> polymerase reaction buffer.
6 μ l	25 mM MgCl ₂
2.0 units	<i>Taq</i> polymerase
sterile water to give a final volume of 100 μ l	

Reactions were carried out in 0.5 ml microfuge tubes, adding the *Taq* polymerase last. Upon completion of the thermal cycling (see below), 20 μ l of 5x DNA gel loading buffer was added to each reaction and mixed, before loading the entire reaction mixture onto a 1.5% agarose gel. Following electrophoresis, cDNA bands were excised, electro-eluted (section 2.6.4), purified and ethanol precipitated (section 2.6.6), combining the contents of 3-6 reactions, and finally resuspending each pellet into 40 μ l of sterile water. 5 μ l of this was then electrophoresed on another 1.5% agarose gel to determine the recovery of purified primary product.

2.6.1c Thermal Cycling.

The tubes were placed in a Techne PJC-3 Thermal Cycler with a heated lid. The following procedure was programmed into the machine:-

Initial Extension 95°C 3 min

Cycling- (30 cycles total, with a 1°C/sec ramp rate.)

Separation 95°C 1 min

Reannealing X°C 1 min

Extension 72°C 2 min

Final Extension 72°C 10 min

Soak 4°C Hold

"X" = 0-5°C below the melting temperature of the oligonucleotide having the lower melting temperature.

2.6.1d Secondary PCR: Reaction Conditions.

0.8 µg "external-sense" primer

0.8 µg "external-antisense" primer

1-2 µl template (5' primary product)-approx 100ng

1-2 µl template (3' primary product)-approx 100ng

2 µl nucleotide mix (20 mM dATP, 20 mM dGTP, 20 mM dTTP,
20 mM dCTP)

10 µl 10x *Taq* polymerase reaction buffer

4 µl 25 mM MgCl₂

2.0 units *Taq* polymerase

sterile water to give a final volume of 100 µl

Secondary reactions were carried out in a similar way to primary reactions except that there were two primary product templates instead of one. The 3' end of the 5' primary product (encoding the N-terminal portion of the protein) and

the 5' end of the 3' primary product (encoding the C-terminal portion of the protein) were single-stranded, complementary and overlapped (Figure 5.2). The first few cycles of the chain reaction involved the association of the two primary products as well as the polymerisation. The reactions were treated exactly in the same way as the primary reactions, except that the final pellet was resuspended in 10 μ l of sterile water.

2.6.2 Polymerase Chain Reaction using *Pfu* DNA Polymerase.

2.6.2a Primary PCR: Reaction Conditions.

0.8 μ g	"internal" primer.
0.8 μ g	"external" primer.
100 ng	template dsDNA
1 μ l	nucleotide mix (20 mM dATP, 20 mM dGTP, 20 mM dTTP, 20 mM dCTP)
10 μ l	10x <i>Pfu</i> DNA polymerase reaction buffer
2.5 units	<i>Pfu</i> DNA polymerase
sterile water to give a final volume of 100 μ l	

Oligonucleotides used were identical to those used with reactions involving *Taq* DNA polymerase. Reactions were carried out in 0.5 ml microfuge tubes, adding the *Pfu* polymerase to the reactions after the initial 10 min annealing step. This is referred to as "Hot Start PCR". Upon completion of the thermal cycling (section 2.6.2c), 20 μ l of 5x DNA gel loading buffer was added to each reaction and mixed, before loading the entire reaction mixture onto a 1.5% agarose gel. Following electrophoresis, DNA bands were excised, electro-eluted (section 2.6.4), purified and ethanol precipitated (section 2.6.6), combining the contents of 3-6 reactions and finally resuspending each pellet into 40 μ l of

sterile water. 5 μ l of this was then electrophoresed on another 1.5% agarose gel to determine the recovery of purified primary product.

2.6.2b Secondary PCR: Reaction Conditions.

0.8 μ g	"external- sense" primer
0.8 μ g	"external- antisense" primer
1-2 μ l	template (5' primary product)-approx 200ng
1-2 μ l	template (3' primary product)-approx 200ng
1 μ l	nucleotide mix (20 mM dATP, 20 mM dGTP, 20 mM dTTP, 20 mM dCTP)
10 μ l	10x <i>Pfu</i> DNA polymerase reaction buffer
2.5 units	<i>Pfu</i> DNA polymerase
sterile water to give a final volume of 100 μ l	

Secondary reactions were carried out in a similar way to primary reactions except that there were two primary product templates instead of one. The 3' end of the 5' primary product (encoding the N-terminal portion of GLUT3) and the 5' end of the 3' primary product (encoding the C-terminal portion of GLUT3) were single-stranded, complementary and overlapped (Figure 5.2). The first few cycles of the chain reaction involved the association of the two primary products as well as the polymerisation between the two external primers, but uses the same reaction protocol as that used for the generation of primary products with *Pfu* polymerase. The reactions were treated exactly in the same way as the primary reactions, except that the final pellet was resuspended in 10 μ l of sterile water.

2.6.2c Thermal Cycling.

The tubes were placed in a Techne PHC-3 Thermal Cycler with a heated lid. The following procedure was programmed into the machine:-

Initial Extension 95°C 10 min

Addition of Pfu DNA polymerase.

Cycling- (3 cycles total, with a 1°C/sec ramp rate.)

Separation 95°C 1 min

Reannealing 37°C 5 min

Extension 72°C 5 min

Cycling- (27 cycles total, with a 1°C/sec ramp rate.)

Separation 95°C 1 min

Reannealing 56°C 2 min

Extension 72°C 5 min

Final Extension 72°C 10 min

Soak 4°C Hold

2.6.3 Polymerase Chain Reactions using Vent DNA Polymerase. †

2.6.3a Primary PCR: Reaction Conditions.

0.8 μ g	"internal" primer.
0.8 μ g	"external" primer.
5-50 ng	template dsDNA (optimised for each reaction)
2 μ l	nucleotide mix (20 mM dATP, 20 mM dGTP, 20 mM dTTP, 20 mM dCTP)
10 μ l	10x Vent DNA polymerase reaction buffer
2-5 μ l	MgSO ₄ (25 mM stock) (optimised for each reaction)
2.5 units	Vent DNA polymerase
sterile water to give a final volume of 100 μ l	

Oligonucleotides used were identical to those used with reactions involving *Taq* and *Pfu* DNA polymerase. Reactions were carried out in 0.5 ml microfuge tubes, adding the Vent polymerase to the reactions after the initial 10 min annealing step. This is referred to as "Hot Start PCR" (section 5.3.2). Upon completion of the thermal cycling (section 2.6.3.c), 20 μ l of 5x DNA gel loading buffer was added to each reaction and mixed, before loading the entire reaction mixture onto a 1.5% agarose gel. Following electrophoresis, DNA bands were excised, electro-eluted (section 2.6.4), purified and ethanol precipitated (section 2.6.6), combing the contents of 3-6 reactions and finally resuspending each pellet into 40 μ l of sterile water. 5 μ l of this was then electrophoresed on another 1.5% agarose gel to determine the recovery of purified primary product.

2.6.3b Secondary PCR: Reaction Conditions.

0.8 μ g	"external- sense" primer
0.8 μ g	"external- antisense" primer
1-2 μ l	template (5' primary product)-approx 100 ng
1-2 μ l	template (3' primary product)-approx 100 ng
2 μ l	nucleotide mix (20 mM dATP, 20 mM dGTP, 20 mM dTTP, 20 mM dCTP)
10 μ l	10x Vent DNA polymerase reaction buffer
2.5 μ l	MgSO ₄ (25mM stock) (optimised for each reaction)
2.5 units	Vent DNA polymerase
sterile water to give a final volume of 100 μ l	

Secondary reactions were carried out in a similar way to primary reactions except that there were two primary product templates instead of one.

2.6.3c Thermal Cycling.

The tubes were placed in a Techne PHC-3 Thermal Cycler with a heated lid. The following procedure was programmed into the machine:-

Initial Extension 95°C 10 min

Addition of Vent DNA polymerase.

Cycling- (27 cycles total, with a 1°C/sec ramp rate.)

Separation 95°C 1 min

Reannealing 56°C 2 min

Extension 72°C Y min

Final Extension 72°C 10 min

Soak 4°C Hold

"Y" = time in minutes calculated for each fragment on the basis of 1 min per Kbp DNA.

2.6.4 Elution of DNA from Gel Fragments by Electrophoresis.

The gel fragment containing the DNA band of interest was put into dialysis tubing (section 2.6.5) which had been clipped shut at one end. Then 1 ml of TAE buffer was added to the tubing and the other end secured, ensuring that no air bubbles remained within. This tubing was then placed into an electrophoresis tank containing 1 litre of TAE buffer. The tubing was laid at an angle perpendicular to the direction of current and the voltage increased to 150 V for 2 hours. Next, the voltage polarity was reversed so that the current flowed in the opposite direction for 30 sec to ensure that the cDNA was removed from the membrane and was present in solution. The solution was removed from

the tubing with a sterile pasteur pipette and placed into a 5 ml "bijou" tube. Then a further 1 ml of TAE buffer was added to the tubing and pumped up and down vigorously to remove any residual cDNA, before adding this to the same bijou tube.

2.6.5 Preparation of Dialysis Tubing.

Dialysis tubing (Visking size 1-8/32") was cut into lengths of approximately 6 cm. 10 g of this was placed in a beaker with 500 ml of 2% sodium hydrogen carbonate, 10 mM EDTA and boiled for 10 min. The solution was then poured away and the tubing washed twice in distilled water. The tubing was stored at 4°C in 50% ethanol, 50% water, 1 mM EDTA. When required, the tubing was washed by boiling briefly in distilled water.

2.6.6 Purification of DNA using Elutip-D Affinity Columns.

Components:-

High salt solution (see below)

Low salt solution (see below)

Sterile 10 ml syringes

Sterile 1 ml syringes

Sterile Acrodisc® 0.2 µm filters

Elutip-D columns

Low salt solution

0.2 M NaCl

20 mM Tris, pH 7.4

1 mM EDTA

High salt solution

1 M NaCl

20 mM Tris, pH 7.4

1 mM EDTA

This procedure could be used to purify both PCR fragments or plasmid DNA. A 10 ml syringe was loaded with 2 ml of high salt solution, the Elutip-D column attached to the syringe and the solution passed through the column to remove any DNA which might be present. A second syringe was loaded with 5 ml low salt solution and this was passed down the column to remove all traces of high salt solution. The DNA sample in TAE buffer was taken up into the same syringe. A 0.2 μm filter was attached between this syringe and the column and the DNA passed through the column at a flow rate no faster than 1 ml/min. The column was then washed with 3 ml of low salt solution, again using the same syringe and filter. Finally the DNA was eluted from the column in 0.4 ml of high salt solution into a sterile microfuge tube. 1.2 ml of ethanol was added to the tube, mixed and incubated at -20°C for 1 hour. The precipitated DNA was collected by centrifugation in a microfuge tube for 30 min, washed with 70% ethanol, centrifuged again for another 30 min, the pellet dried and resuspended in a suitable volume of sterile water, generally 20 μl .

2.7 *Taq* DyeDeoxy™ Terminator Cycle Sequencing Protocol.

This protocol was used with the Applied Biosystems *Taq* DyeDeoxy™ Terminator Cycle Sequencing Kit, in conjunction with the Applied Biosystems Model 373A Automated Sequencer.

2.7.1a Kit Reagents.

100 µl	G DyeDeoxy™ Terminator
100 µl	A DyeDeoxy™ Terminator
100 µl	T DyeDeoxy™ Terminator
100 µl	C DyeDeoxy™ Terminator
100 µl	dNTP mix- (750 µM dGTP, 150 µM dATP, 150 µM dTTP, 150 µM dCTP)
400 units	AmpliTaq® DNA Polymerase, 8 units/µl
400 µl	5x Terminator Ammonium Cycle Sequencing (TACS) Buffer- (400 mM Tris-HCl, 10 mM MgCl ₂ , 100 mM (NH ₄) ₂ SO ₄ pH 9.0)
6 µg	pGEM®-3Zf(+) double-stranded DNA Control Template, 0.2 µg/µl
50 µl	-21M13 Forward Primer, 0.8 pmoles/µl

2.7.1b Other Reagents.

Distilled water

De-ionised formamide

Phenol/H₂O/Chloroform (68:18:14, v/v/v)

Alconox™ detergent

Ethanol

- A/ Gel Reagents- Sequagel-6™ 6% Sequencing Gel Solution
 Sequagel™ Complete Buffer Reagent
- B/ Gel Reagents- 40% Acrylamide stock solution (19:1 Acrylamide:
 Bisacrylamide)
- Other Reagents- 10xTBE Buffer (8.2 g EDTA, 107.8 g Tris, 55.0 g Boric acid
 per litre)
 10% Ammonium persulphate
 50 mM EDTA
 TEMED
 Urea
 dH₂O
 Mixed Bed Resin

2.7.2 Preparation of Templates.

Plasmid dsDNA was prepared from colonies as described previously (section 2.5.8). The quantities of template and sequencing oligonucleotide primers used per reaction were 2 μ g dsDNA template and 3.2 pmoles of primer. The primers used are listed in Table 5.2.

In either case the combined volume of template and primer did not exceed 10.5 μ l since 9.5 μ l of reaction premix was added to bring the final volume to 20 μ l. The total volume was adjusted to 20 μ l by the addition of sterile water. A reaction premix sufficient for 20 reactions consisted of:-

Reagents

5x TACS Buffer	80 μ l
dNTP mix	20 μ l
DyeDeoxy™ A Terminator	20 μ l
DyeDeoxy™ T Terminator	20 μ l
DyeDeoxy™ G Terminator	20 μ l
DyeDeoxy™ C Terminator	20 μ l
AmpliTaq® DNA Polymerase	10 μ l

The reagents were mixed in a 0.5 ml microfuge tube-

Reaction Premix	9.5 μ l
* Template DNA	5.0 μ l
** Primer	4.0 μ l
dH ₂ O	<u>1.5 μl</u>
Final volume	20 μ l

* ssDNA solution concentration = 0.2 mg/ml

dsDNA solution concentration = 0.4 mg/ml

** Primer concentration with ssDNA template = 0.4 pmoles/ μ l

Primer concentration with dsDNA template = 0.8 pmoles/ μ l

2.7.3 Thermal Cycling.

The tubes were placed in a Techne PHC-3 Thermal Cycler with a heated lid. The following procedure was programmed into the machine:-

Initial Extension	96°C	3 min
Cycling		
Separation	96°C	30 sec
Reannealing	50°C	15 sec
Extension	60°C	4 min
(30 cycles total, with a 1°C/sec ramp rate.)		
Soak	4°C	Hold

2.7.4 Acrylamide Gel Preparation.

The gel needed at least 2 hours polymerisation time before pre-running so the gel was prepared whilst the reactions underwent thermal cycling.

2.7.5a Preparing the Gel Plates.

The plates, spacers and comb were washed with Alconox™ and dH₂O. Only the plates were then wiped with absolute ethanol. The plates were aligned with the spacers between them along the outside of the longer edges. The plates were clamped in that position and Permacel™ tape applied along the short bottom edges of the plates and the lower ends of both longer edges so that the corners were covered and a seal was formed. The plates were balanced on a rest so that open top was raised and the angle between the plane of the plates and that of the desktop surface was 30-45°.

2.7.5b Casting the Gel.

This involved using Gel Reagents A. 80 ml of Sequagel-6™ 6% Sequencing Gel Solution was mixed with 20 ml of Sequagel™ Complete Buffer

Reagent and 0.8 ml of 10% ammonium persulphate solution was added while stirring. The gel was immediately poured between the glass plates up to the top edge of the notched plate, with the aid of a 60 ml syringe. All air bubbles were removed by tapping the plates or with the aid of a Promega "Bubble Hook". The plates were lowered so that they were lying flat on the bench and the gel casting comb carefully inserted. The comb was secured by clamping the top of the gel with two binder clamps. It was left to polymerise completely- this took at least 2 hours.

2.7.6 Setting Up for a Run.

All the clamps and tape were removed from the gel plates and the casting comb carefully taken out. Excess acrylamide was cleaned off the plates which were then washed with Alconox™, distilled water and ethanol making sure that the plates were especially clean in the region where the laser read (about a third of the way from the bottom of the plates). A 24-well-shark's tooth comb was carefully placed on the gel surface so that it indented the gel but did not puncture it. The 373A DNA Sequencer and the Macintosh IIfx computer were switched on. The gel was placed onto the lower buffer chamber and the beam-stop rack locked. The "Start Pre-run" button on the 373A keypad was pressed followed by "Plate Check". "Scan" and "Map" on the Macintosh Menu were opened. If the baselines were flat, then there was judged to be no dirt on the plates- if they were not then the plates were cleaned again. Next, "Abort Run" was pressed and the upper buffer chamber and the alignment brace were secured. 1.5 litres of 1xTBE buffer, pH 8.3 was prepared and about half added to the upper buffer chamber and the remainder poured into the bottom chamber. The wells were rinsed with a syringe fitted with a 18-gauge needle containing 1x TBE buffer. The electrode leads were attached and "Start Pre-run" and then "Pre-

run Gel" selected. Pre-running took at least 5 min but longer if required. "Abort Run" was pressed to stop.

2.7.7 Sample Extraction and Precipitation.

After the cycling (section 2.7.3) was complete, 80 μ l of sterile water was added to each reaction mixture. 100 μ l of phenol/water/chloroform (68:18:14, v/v/v) was added to each tube and vortexed for at least 1 min, and then centrifuged for 2 min in a microfuge. The upper aqueous phase was retained, discarding the lower organic phase. This process was repeated. The extracted aqueous phase was transferred to a fresh microfuge tube and precipitated by the addition of 15 μ l of 2 M sodium acetate and 300 μ l of absolute ethanol (stored at -20°C). Tubes were vortexed to mix the contents and then placed at -20°C for 30 min to ensure complete precipitation. The tubes were centrifuged in a microfuge for 15 min to pellet the cDNA, the pellets washed in 70% ethanol, and dried by centrifugation under vacuum.

2.7.8 Preparing and Loading the Samples.

4 μ l of de-ionised formamide/10 mM EDTA was added to each of the samples and mixed well. This was heated at 90°C for 2 min, and placed onto ice immediately. The wells of the gel (section 2.7.5b) were flushed out with 1xTBE and 4 μ l of each odd-numbered sample added to its corresponding well in the gel. The door was closed and "Start Run" pressed. This was left for 10 min. "Interrupt Run" was pressed and all the wells flushed out again. The even-numbered samples were loaded and the sequencer restarted. "Collect" on the Controller panel on the Macintosh display was clicked and the details of the samples filled out on a "New Sample Sheet".

2.7.9 Analysis of Samples.

The samples were electrophoresed at a constant temperature of 40°C for 12 hours, passing through the "read window" area of the gel where laser light was periodically passed along this area of the gel. The resulting fluorescence emitted by the DyeDeoxy™ Terminator dyes over a period of time were measured by the 373A sequencer and incorporated by the ABI Data Collection Program on the Macintosh IIfx computer. After the data was collected, it was analysed by the ABI Data Analysis Program. Sequences were determined by use of this program. When different sequences were generated by the use of various sequencing primers (Table 5.2) with the same template cDNA, these were compared using the GeneJockey II (Biosoft) program.

Table of Buffers.

Buffer	Constituents
50xTris-acetate (TAE) buffer	242 g Tris base; 57.1 ml glacial acetic acid, 100 ml 0.5 M EDTA, pH 8.0
10xTris-borate (TBE) buffer	108 g Tris base; 55.0 g Boric acid; 40 ml 0.5 M EDTA, pH 8.0
TE buffer (pH 8.0)	10 mM Tris.Cl, pH 8.0, 1 mM EDTA, pH 8.0
STET buffer	8% w/v sucrose; 0.5% w/v TritonX-100; 50mM EDTA (pH8); 10mM Tris, pH8.
10xPhosphate Buffered Saline (PBS)	80 g NaCl; 2 g KCl; 14.4 g Na ₂ HPO ₄ ; 2.4 g KH ₂ PO ₄ , pH 7.4
TSB (Transformation and Storage Buffer).	L-Broth +10% w/v PEG (Mol Wt 3350), 5% w/v DMSO, 10mM MgCl ₂ , 10mM MgSO ₄ .
TSB + Glucose	As TSB + 20mM glucose.
5x DNA gel-loading buffer	0.25% w/v bromophenol blue; 30% w/v glycerol in water
Barths buffer	88 mM NaCl; 1 mM KCl; 2.4 mM NaHCO ₃ ; 0.82 mM MgSO ₄ ; 0.41 mM CaCl ₂ ; 0.33 mM Ca(NO ₃) ₂ ; 5 mM HEPES-NaOH, pH 7.6.

Table 2. 2 Bacterial Media and Agar.

Type	Constituents (per litre)
Luria-Bertani medium (LB)	10 g Tryptone (Bactotryptone); 5 g Yeast extract; 10 g NaCl
2xYT medium	16 g Tryptone; 10 g Yeast extract; 5 g NaCl
LB plates	10 g Tryptone; 5 g Yeast extract; 10 g NaCl, 15 g Agar
2xYT plates	16 g Tryptone; 10 g Yeast extract; 5 g NaCl, 15 g Agar

Figure 2.1

Diagrammatic Representation of pSP64T Vector.

GLUT2 cDNA was ligated to *Bgl*III DNA linkers and cloned into the untranslated regions of the *Xenopus* β -globin gene, which had previously been cloned into the multiple cloning site of pSP64 (Kreig & Melton, 1984). GLUT3 cDNA was cloned into pSP64T as a *Bgl* II/*Bam*H I fragment into the untranslated regions of the *Xenopus* β -globin gene, and GLUT5 was force cloned into the *Bgl* II site in the β -globin gene. The 5' untranslated region (UTR) is 89 bp long and the 3' untranslated region is 141 bp long. These function to stabilise the *in vitro* synthesised mRNA in *Xenopus* oocytes. The GLUT cDNA and its flanking sequences are located 3' of the SP6 polymerase promoter.

Figure 2.1

Diagram of GLUT cDNAs in pSP64T Vector.

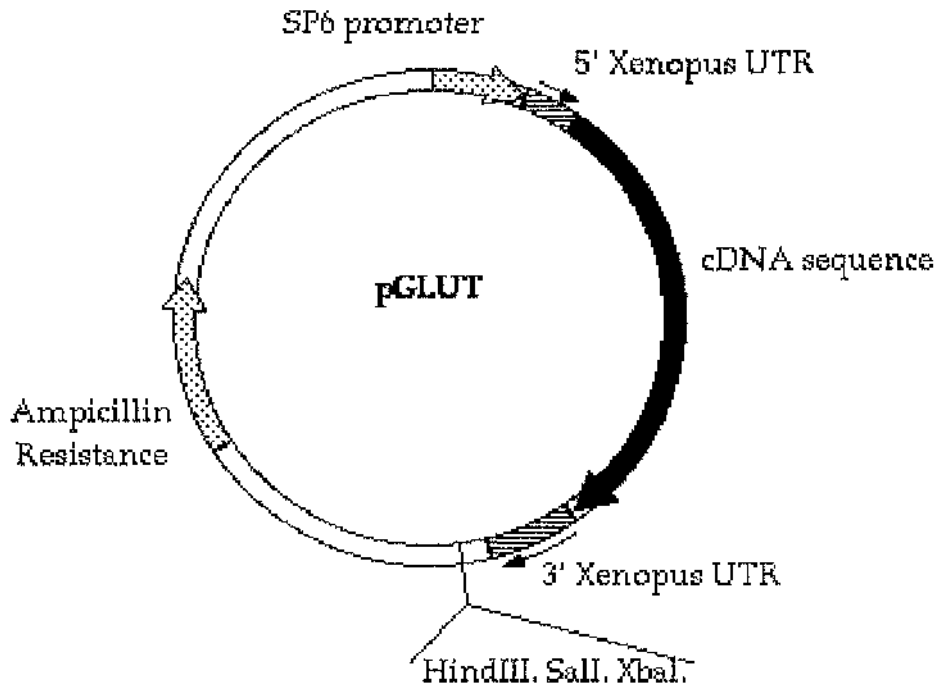


Figure 2.2

This shows a photograph of 2 μ l samples of *in vitro* synthesised mRNA which have been electrophoresed on a 1% denaturing agarose gel and stained with ethidium bromide. Lane 1 shows DNA markers (not applicable to RNA sizes), lanes 2, 3 and 4 show samples of GLUT2/GLUT3 chimeric mRNA. The size of all mRNA bands are approximately 1,700 bases.

Figure 2.2

1% Agarose Gel Showing *in vitro* Transcribed mRNA.

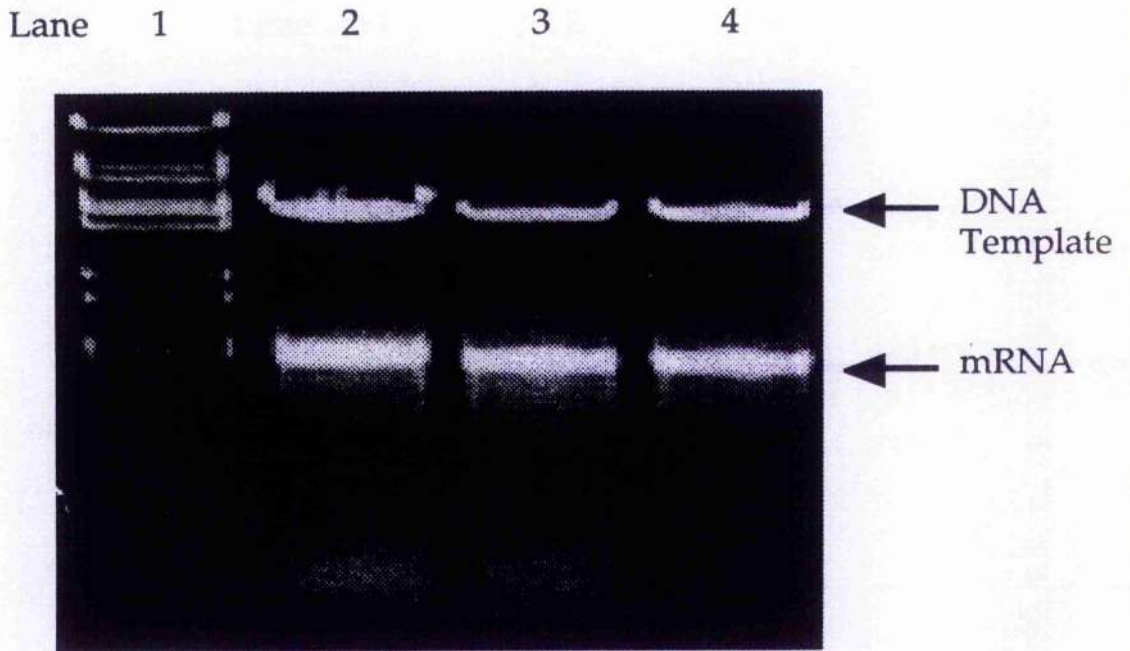


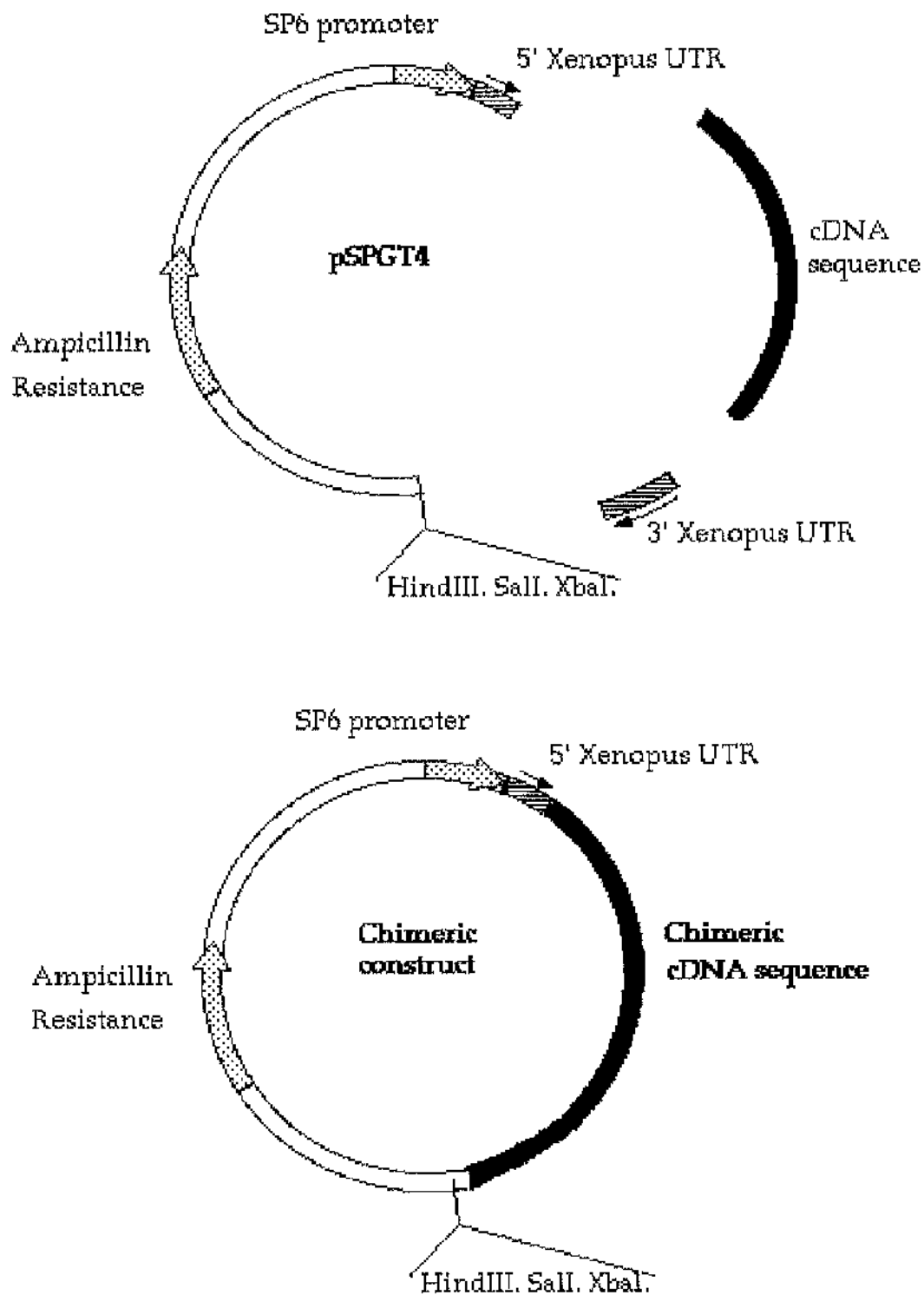
Figure 2.3

Diagram Showing Cloning of Chimeric PCR Products into the pSP64T Vector Backbone.

The pSP64T vector backbone was obtained by restricting pSPGT4 with *Sal* I. This released a fragment which corresponded to the coding region of GLUT4, a 200bp fragment corresponding to the 3' untranslated region of the *Xenopus* β -globin gene, and a 3Kb fragment which corresponded to the remainder of the pSP64T vector. This was alkaline phosphatase treated, and ligated to *Sal* I restricted PCR products as described. The ampicillin resistance gene was used to screen against background colonies arising from untransfected cells.

Figure 2.3

Cloning of Chimeric PCR Products into the pSP64T Vector Backbone.



CHAPTER 3.

Studies of the GLUT5 Isoform.

3.1.1 Introduction.

The cDNA of human GLUT5, isolated from a human jejunal DNA library, encodes a protein of 501 amino acid residues in length. With the exception of GLUT7, GLUT5 is the least well characterised isoform of the GLUT family. It is also the most divergent, displaying only between 39% and 42% amino acid sequence identity with GLUTs 1, 2, 3 and 4. Northern blot analyses have shown that human GLUT5 mRNA is present at high levels in the small intestine, the kidney, testis and spermatozoa, and at lower levels in muscle tissue and in the plasma membrane of adipocytes (Kayano *et al.*, 1990). Western blot analysis and immunohistochemical studies have shown that human GLUT5 protein is present in the small intestine, testis kidney, heart, brain and in the plasma membrane of adipocytes (Burant *et al.*, 1992, Shepherd, 1992b).

Burant *et al* have expressed human GLUT5 in *Xenopus* oocytes and shown that this isoform is a high capacity fructose transporter, which displays virtually no ability to transport glucose (Burant *et al.*, 1992). This surprising property of GLUT5 explains its presence in the epithelia of the small intestine (Davidson *et al.*, 1992) It has been shown that human GLUT5 is localised to the brush border membrane (BBM) of jejunal epithelial cells, where it is thought to mediate the uptake of dietary fructose from the gut lumen, in a facilitative manner.

It had been suspected prior to the isolation and characterisation of GLUT5 that there might be a fructose carrier in the gut which was independent of the sodium/glucose co-transporter SGLT1, since individuals with genetic mutations in this carrier were still capable of fructose metabolism (Wright *et al.*, 1991).

GLUT2 is also found in enterocytes (Thorens, 1990). This isoform is also capable of fructose transport, as has been demonstrated by its expression in

oocytes (Gould *et al.*, 1991). GLUT2 however, is restricted to the basolateral membrane (BLM), where it is thought to mediate the efflux of glucose and fructose from these cells into the blood (Thorens, 1990). A diagram of this movement of sugars across the epithelium is shown in Figure 3.1. A recent study has shown that GLUT5 may also be present on the basolateral membrane of human enterocytes (Hundal *et al.*, 1992). There is no evidence to suggest that GLUT5 is found on the basolateral membrane of rat or rabbit enterocytes.

The role of GLUT5 in human spermatocytes may be in mediating the uptake of fructose whilst the sperm is still in the seminal fluid. It has been reported that human spermatocytes use fructose when in the seminal fluid, and that there is a shift in the metabolic requirements from fructose to glucose when the spermatocytes enters the female reproductive tract (Peterson & Freund, 1975). It has also been suggested that the utilisation of fructose may be associated with the mechanisms which prevent acrosomal breakdown of the plasma membrane of the spermatocyte, while it is in the seminal fluid. This is thought to prevent premature activation of the spermatocyte, although it is not understood how this happens (Rogers & Perreault, 1990).

The role of GLUT5 in brain and kidney is unclear: these organs receive very little fructose as the primary site for fructose metabolism is the liver. Furthermore, in humans, GLUT5 is apparently absent from the liver. As far as it is understood, fructose transport into and out of this organ is mediated solely by GLUT2 (Thorens, 1990).

Northern blot analysis of tissues for rat GLUT5 mRNA has shown that the transcript can be found in intestine, kidney and brain tissue (Rand, 1993). It has been shown that rat spermatocytes utilise fructose as a metabolic energy source (Hussain, 1989), and so the absence of GLUT5 mRNA in testicular tissue is surprising. Similar experiments on rabbit tissues have shown that GLUT5 mRNA is found at high levels in the intestine and kidney (Miyamoto *et al.*,

1994). It is not yet clear if these results are indicating a species difference in tissue specific GLUT5 distribution.

Recently, the presence of human GLUT5 has been detected in insulin responsive tissues (Hundal *et al.*, 1992, Shepherd, 1992b), and although it has been demonstrated that fructose is transported into adipose cells (Halperin & Cheema-Dhadli, 1982), and muscle (Ahlborg & Bjorkman, 1990), the role of fructose metabolism in these tissues is unclear. Also, human GLUT5 has also been detected in the cerebral microganglia (Maher *et al.*, 1994). The ambient fructose levels are low in these cells however, and so this may indicate that human GLUT5 facilitates the transport of another, as yet undefined substrate (Maher *et al.*, 1994).

3.1.2 Substrate Selectivity of GLUT5.

Studies utilising the *Xenopus* oocyte expression system have yielded conflicting evidence on the preferred substrate of GLUT5. As previously described, human GLUT5 exhibits high efficiency fructose uptake and displays almost no ability to transport D-glucose, when expressed in oocytes. Additionally, the transport of D-fructose is insensitive to inhibition by D-glucose and cytochalasin B (Burant & Bell, 1992a). However, Shepherd *et al* have shown that cytochalasin B can photolabel a protein from small intestine membrane fractions which is immunoprecipitated by a GLUT5 antibody (Shepherd, 1992b). Cytochalasin B has been shown to competitively inhibit glucose efflux from erythrocytes, and therefore is proposed to interact with the endofacial glucose binding site of GLUT1 (section 1.6). The site of cytochalasin B photolabelling is not necessarily the same as the binding site, and so it is possible that cytochalasin B can photolabel GLUT5 but does not bind to the endofacial fructose binding site. Therefore, the endofacial fructose binding site in GLUT5 may not be analogous to the endofacial glucose binding

site in the other isoforms. Table 3.1 describes differences in reported properties of human GLUT5, and GLUT5 from other species, when expressed in different expression systems.

Studies of GLUT5 from rat and rabbit highlight ambiguity regarding the substrate selectivity of this isoform. It has been shown that rat GLUT5, when expressed in *Xenopus* oocytes, is capable of glucose transport in addition to fructose transport (Rand, 1993). Similar results have been reported for sugar uptake in oocytes expressing rabbit GLUT5 (Miyamoto *et al.*, 1994). Miyamoto *et al* reported that fructose uptake by rabbit GLUT5 in *Xenopus* oocytes could be inhibited by D-glucose and by D-galactose (Table 3.1).

However, when the properties of either rat or rabbit GLUT5 are studied in brush border membrane vesicles, the results conflict with those derived from studies using the oocyte system. The fructose transport kinetics of rabbit GLUT5 in BBM vesicles are similar to those of GLUT5 expressed in oocytes. In BBM vesicles however, fructose uptake via GLUT5 cannot be inhibited by D-glucose or by D-galactose. Furthermore, oocytes injected with total jejunal rabbit GLUT5 mRNA also displayed fructose uptake which was insensitive to inhibition by D-glucose and D-galactose (Miyamoto *et al.*, 1994). Recently it has been shown that rat GLUT5 in BBM vesicles displayed fructose transport which was not inhibited by D-glucose or phloretin (Corpe *et al.*, 1996).

This has led to speculation of the involvement of another protein which may be associated with the regulation of GLUT5 substrate specificity. It has been suggested that such a protein (which is presumably absent in oocytes) might associate with GLUT5 in such a way that the glucose binding site is either modified or in some way made inaccessible (Miyamoto *et al.*, 1994). As yet, there is no evidence in the literature to support this speculation.

The cDNA from rat GLUT5 has recently been transfected into CHO cells (Inukai *et al.*, 1995). In this expression system, rat GLUT5 mediates the efficient uptake of fructose and displays no glucose transport activity at all.

Furthermore, in this study GLUT5 could not be photolabelled with cytochalasin B.

In addition to the conflicting results on the apparent species-specific ability of GLUT5 to transport glucose and bind cytochalasin B, there is also some disagreement in the literature regarding the K_m for fructose *zero-trans* entry into BBM vesicles. (For a description of kinetic terms, see section 1.4.2.1) This kinetic parameter has been calculated to be 18mM in rabbit (Schultz & Strecker, 1970), 4mM in guinea pig (Mavrias & Mayer, 1973), 17mM in hamster (Honneger & Semenza, 1973), and 110mM in rat (Crouzoulon & Korieh, 1991, Sigrist-Nelson & Hopfer, 1974) experiments. Other studies with rat GLUT5, expressed in CHO cells, have shown the K_m to be 10-15mM (Inukai *et al.*, 1995). The discrepancies between these studies may be due to the procedures used to obtain BBM vesicles. It is difficult to obtain pure BBM vesicles without any contamination from the basolateral membrane. Therefore, it is possible that the high K_m values measured, especially in the rat experiments, may be due to a GLUT2 contamination from basolateral membrane fractions, since GLUT2 has a high K_m for fructose transport (Colville *et al.*, 1993b).

3.1.3 GLUT2, GLUT5, and SGLT1 in the Small Intestine.

The tissue specific distribution of GLUT5 in human, rat and rabbit differs slightly as described above. However, in all of these species GLUT5 is present in the brush border membrane of small intestine and kidney epithelial cells. SGLT1, the sodium/glucose co-transporter is also expressed on the BBM of these cells. It is widely accepted that these transporters act in concert to facilitate the uptake of dietary sugars from the lumen of the small intestine into enterocytes. Transport from the enterocytes into adjacent cells occurs across the basolateral membrane via GLUT2. In human, rat and rabbit epithelial cells the expression of GLUT2 is exclusively restricted to the

basolateral membrane. It is thought that GLUT2 mediates the efflux of both glucose and fructose from enterocytes (Figure 3.1), although in humans GLUT5 may also be expressed on the BLM (Hundal *et al.*, 1992).

In the human small intestine GLUT5 is expressed in both the duodenum and the jejunum (proximal and distal gut). Recently, a study of the sodium/glucose co-transporter, SGLT1, has shown that the transport properties of this carrier change as the pH of the gut changes (Hirayama *et al.*, 1994). When the carrier is present in the proximal end of the small intestine where the pH is low, it uses H^+ in the co-transport of glucose. In this situation SGLT1 acts as a low affinity/high capacity transporter. When the carrier is present in the distal end of the gut where the pH is higher, a Na^+ ion can be used instead of a proton. In this situation SGLT1 acts as a high affinity/low capacity transporter. This situation makes physiological sense: in the distal end of the gut, the concentration of glucose will be low, and therefore a carrier with a high catalytic turnover is not necessary. However, a carrier which does have a high affinity for its substrate is an advantage. SGLT1 in this situation is able to scavenge the remaining glucose from the gut lumen, thus increasing the overall efficiency of glucose uptake.

Since GLUT5 is also expressed throughout the small intestine and is therefore subject to a range of pHs, it is possible that the properties of GLUT5 may change in response to pH changes.

Additionally, human GLUT5 is expressed in spermatozoa where it is thought to be responsible for the uptake of fructose by the spermatocyte prior to ejaculation. Once the spermatocyte enters the female reproductive tract, where the pH of its environment changes, the metabolic substrate becomes glucose (Peterson & Freund, 1975). Therefore, one of the aims of this study is to examine whether pH can affect the substrate preference of GLUT5 when expressed in oocytes.

3.1.4 Structural Requirements of Fructose Binding to GLUT5.

The transfection of rat GLUT5 cDNA into CHO cells enabled Inukai *et al* to measure and compare the parameters of fructose and glucose transport by this isoform to those of rabbit GLUT1, which had also been transfected into this cell line (Inukai *et al.*, 1995). Subsequently, Inukai *et al* produced a panel of rat GLUT5/rabbit GLUT1 chimeric transporter constructs which were expressed in the CHO cell line. The rationale of this was to define the domains of the transporter structure which are necessary for fructose transport by GLUT5, and glucose transport by GLUT1. This approach is analogous to that chosen by this laboratory to study fructose transport by GLUT2 (Chapter 4). The results of this study suggested that the presence of two regions of GLUT5 were mandatory for fructose transport: the entire N-terminal half of the protein up to the sixth helix, and the C-terminal cytoplasmic tail. In contrast, the middle intracellular loop and the C-terminal half of the protein, from helix 7 through to helix 11, were necessary for glucose transport. Furthermore, replacing either the N-terminal half of GLUT1 or the C-terminal cytoplasmic tail of GLUT1 with the corresponding sequence of GLUT5, produced no marked effects on glucose transport activity. From this it was suggested that the structural requirements for fructose transport are more stringent than those for glucose transport among the glucose transporter family. However, it could be the case that the sequences important in GLUT5 are more widely distributed throughout the protein, rather than clustered in restricted regions.

This situation differs from that of fructose transport by GLUT2, where it has been shown that helix 7 is essential for fructose transport activity in this isoform (Chapter 4). Additionally, the conclusion that the C-terminal cytoplasmic tail is not involved in glucose transport by GLUT1 is also contentious (sections 4.1.2 and 6.2.7). It is possible that the C-terminal tail of

GLUT5 has the necessary sequences to complement the essential sequences in the C-terminal half of GLUT1.

3.1.5 Studies of Other Fructose Transporters.

It has been reported that the hexose transporter of the parasite *Trypanosoma brucei* transports D-glucose and D-fructose with equal efficiency (Fry *et al.*, 1993). Furthermore it has been shown that this transporter accepts D-glucose in the pyranose ring form, and D-fructose in the furanose ring form. In aqueous solutions D-fructose exists predominantly (~70%) in the pyranose ring form (Fry *et al.*, 1993), and so it is rather surprising that this transporter has evolved to transport both glucopyranose and fructofuranose with equal efficiency. It was also shown in this study that the trypanosome transporter accommodates glucopyranose and fructofuranose by binding to hydrogen bonds directed at the C-3, C-4 positions and ring oxygen positions, although the oxygen can be substituted by nitrogen without any great effect. Hydrogen bonding at the C-2 position is less important.

The substrate binding requirements of GLUT2 have been investigated (Colville *et al.*, 1993a). GLUT2 can transport both fructose and glucose but does so with unequal efficiency. D-glucose is a competitive inhibitor of D-fructose transport by GLUT2, and vice versa, therefore these substrates probably share the same exofacial binding site, or at least the regions involved in the exofacial binding sites overlap. It has been shown that GLUT2, like the trypanosome transporter, also binds the pyranose ring form of D-glucose and the furanose ring form of D-fructose (Colville *et al.*, 1993a). Hydrogen bonding at carbon positions C-1, C-3, and C-4 have been shown to be important in the binding of D-glucose to the exofacial binding site of GLUT2, whereas, it has been shown these interactions occur with the C-3 and C-4 positions but not with the C-2 position of D-fructose. (Colville *et al.*, 1993a)

It is not known whether GLUT5 binds fructose in the pyranose or the furanose ring form. In the GLUT1/GLUT5 chimeric study discussed above, it was suggested that the regions essential for fructose transport in GLUT5 differ from those necessary in transport of glucose by GLUT1. The regions of GLUT5 involved in fructose transport also differ from the regions of GLUT2 involved in fructose transport (Chapter 4). Therefore, given that fructose exists predominantly in the pyranose form in aqueous solutions, and that GLUT5 is a high efficiency fructose transporter, it is possible that this isoform may transport fructose in the pyranose ring form. Additionally, since the transport of fructose by human GLUT5 is not inhibited by cytochalasin B, and the transport of fructose by GLUT2 is, then this may suggest that the endofacial fructose binding site of GLUT5 may not be analogous to the endofacial fructose binding site in GLUT2.

It would therefore be instructive to investigate the structural requirements for fructose binding to GLUT5. To determine which ring form is accepted by GLUT5 it is proposed to make use of fructose analogues which are locked in either fused pyranose or furanose ring forms (Figure 3.2).

3.2 Aims of This Study.

1. To establish a K_m value for the transport of D-fructose by human GLUT5 when expressed in *Xenopus* oocytes.
2. To assess the substrate selectivity of human GLUT5 in oocytes.
3. To test the kinetics and substrate selectivity of GLUT5 over a range of temperatures and pH values.
4. To determine the preferred fructo- ring form of GLUT5.

3.3 Results.

3.3.1 Measurement of the K_m Value for the Transport of D-Fructose by Human GLUT5 in *Xenopus* Oocytes.

The K_m value for the transport of D-fructose by GLUT5 was determined by measuring the rate of uptake of trace radiolabelled sugar over a range of external sugar concentrations into oocytes which had been injected with GLUT5 mRNA at least 48 hrs prior to the assay. Lineweaver-Burk plots were constructed, and K_m values for zero-*trans* uptake were determined from the equation of the line. This calculation is as follows:

Equation of a straight line : $y = mx + c$.

Therefore, when $y = 0$,

$$x = -c/m$$

The point at which the line cuts the x axis = $1/-K_m$.

When $y=0$,

$$x = [1/-K_m]$$

$$\text{then } K_m = -1/[-c/m]$$

Figure 3.3 shows a Lineweaver-Burk plot of D-fructose transport by GLUT5. The data used to construct this graph was taken from a typical experiment. The K_m value for this transport event was found to be $22.5 \pm 10 \text{mM}$. This figure is the mean of at least three independent determinations, in which different batches of cRNA and different oocyte populations were used.

3.3.2 Determining the Substrate Selectivity of Human GLUT5 in *Xenopus* Oocytes.

The transport rate of GLUT5 injected oocytes was determined for the uptake of 0.1 mM D-fructose and 0.1 mM deGlc. Also, the effects of the addition of 100 mM L-glucose, D-glucose or D-fructose on these transport rates were examined. The results are shown in Figure 3.4.

3.3.3 The Effects of pH on the Substrate Selectivity of Human GLUT5 in *Xenopus* Oocytes.

To investigate the effects of pH on the substrate specificity of GLUT5, the uptake of 0.1mM D-fructose or 0.1mM deGlc by GLUT5 injected oocytes was measured over a range of pH values. The results are shown in Figure 3.5. The uptake of D-fructose was unaffected by reducing the pH from 7.5 to 4.5. Also, the lack of glucose transport displayed by the GLUT5 isoform in oocytes remained unchanged at lower pH.

3.3.4 The Effects of pH on the K_m for Fructose Transport by GLUT5 in *Xenopus* Oocytes at pH 4.5.

The K_m for fructose transport by human GLUT5 at pH 4.5 was determined by measuring the rate of uptake of trace radiolabelled fructose, over a range of external sugar concentrations as described. A typical Lineweaver Burk plot is shown in Figure 3.7.

3.3.5 Analysis of the Preferred Fructo- Ring Form Accepted by Human GLUT5.

To establish whether GLUT5 accepts fructose in the furanose (5-membered) or the pyranose (6-membered) ring form, the uptake of D-fructose by GLUT5 injected oocytes was measured in the presence and absence of various fructose analogues. The effects of inhibition of fructose uptake by the fructose analogues 1,5-Anhydromannitol, 2,5-Anhydromannitol and L-sorbose were measured. The results of this study are shown in Figure 3.8.

Figure 3.1.

Diagram Showing the Uptake and Efflux of Dietary Sugars Across an Intestinal Epithelial Cell.

The uptake of dietary D-glucose across the enterocytes of the small intestine occurs via the sodium-glucose co-transporter SGLT1. This transporter utilises the energy gained from the transport of a Na^+ ion down its concentration gradient, to transport one glucose molecule into the cell against its concentration gradient. The gradient of Na^+ ions in the cell is maintained by the sodium/potassium exchange pump. The uptake of dietary fructose occurs via facilitative transport by GLUT5. These transporters are present on the brush border membrane of these cells which is exposed to the lumen of the small intestine. The efflux of both sugars from these cells across the basolateral membrane is mediated by GLUT2.

Figure 3.1

Diagram Showing the Uptake and Efflux of Dietary Sugars Across an Intestinal Epithelial Cell.

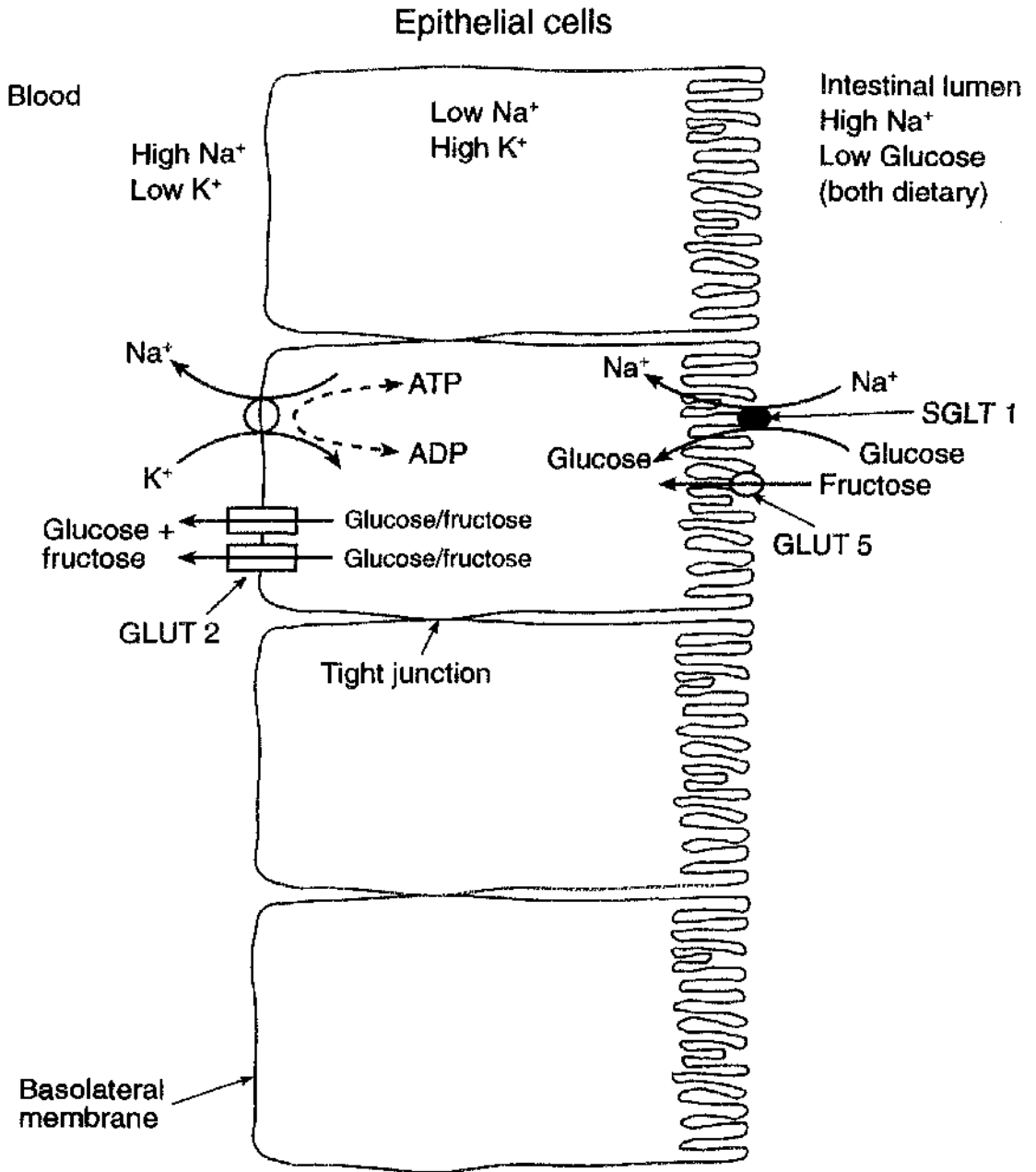


Figure 3.2

Structures of Pyranose and Furanose Forms of β -D-Fructose, and Fused-Ring Fructose Analogues.

This diagram shows a comparison of pyranose and furanose forms of fructose, and the structures of fused-ring fructose analogues. Compound I is β -D-fructofuranose (5-membered ring form of D-fructose), Compound II is fructopyranose (6-membered ring form of D-fructose), Compound III is 2,5 anhydromannitol (fused 5-membered ring fructose analogue), Compound IV is 1,5 anhydro-D-mannitol (fused 6-membered ring fructose analogue), and Compound V is α -L-sorbopyranose (L-sorbose -6-membered ring analogue).

Figure 3.2

Structures of Pyranose and Furanose Forms of β -D-Fructose, and Fused-Ring Fructose Analogues.

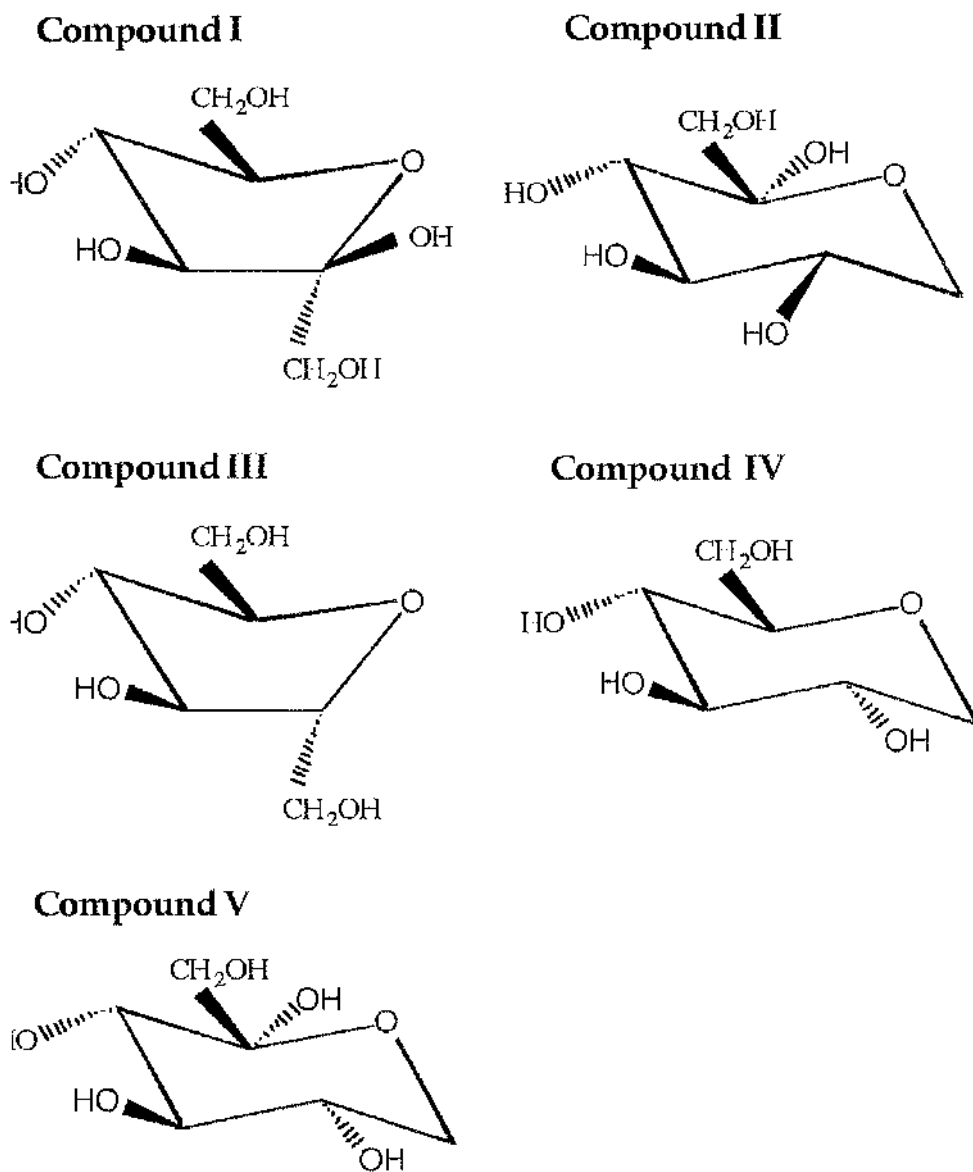


Figure 3.3

Lineweaver-Burk Plot of Fructose Uptake by Human GLUT5-Injected Oocytes.

Each point is the mean of the transport rate determined from groups of at least 10 oocytes (section 2.4). Rate of transport was determined by exposure of the oocytes to radiolabeled fructose for 60 mins and the counts per minute determined as described (section 2.4). For each experiment endogenous oocyte transport was measured by a parallel incubation of uninjected "control" oocytes in trace radiolabeled fructose. The values obtained for the control oocytes at each concentration were subtracted from the values obtained from the chimera-injected oocytes to obtain the heterologous transport rate. Transport rates in control oocytes were typically 10% of the injected oocytes. Error bars are excluded for clarity, but the range of error was typically 10%. The data shown here is representative of at least four separate experiments.

Figure 3.3

Lineweaver-Burk Plot of Fructose Uptake by Human GLUT5-Injected Oocytes.

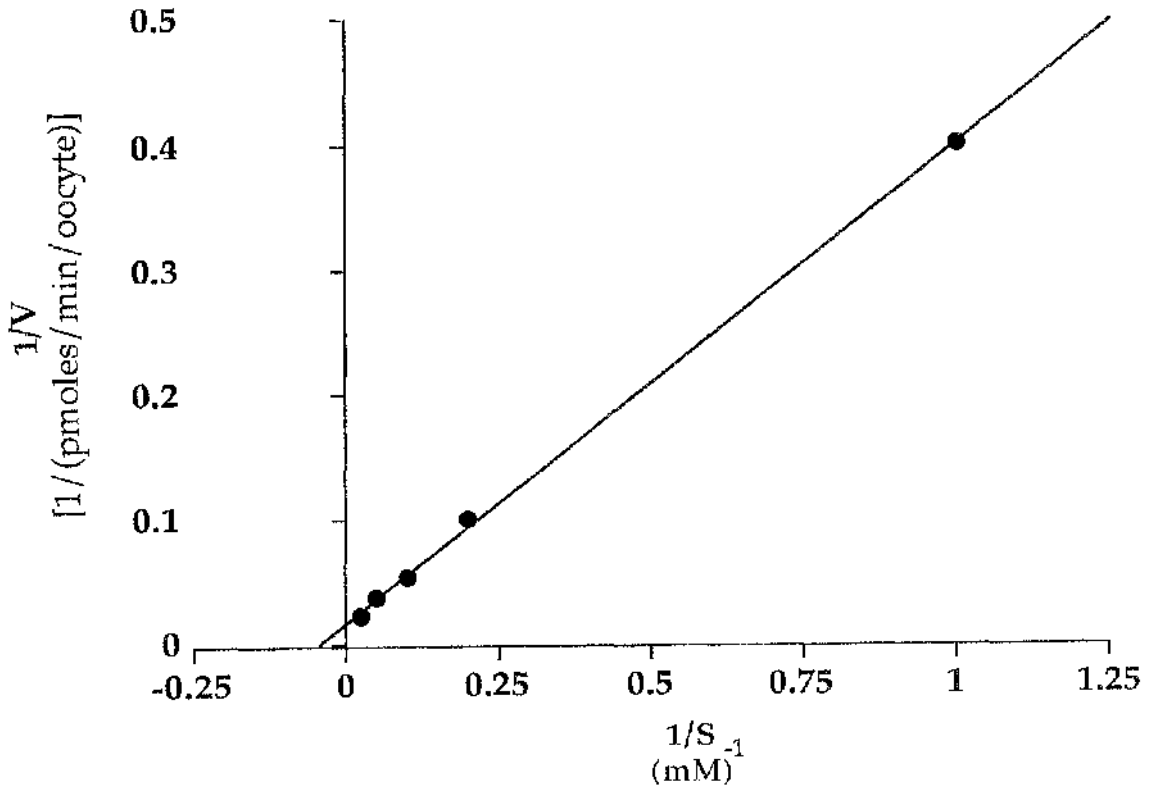


Figure 3.4

Graphs showing the Uptake of 0.1mM DeGlc by GLUT2-Injected, GLUT5-Injected and Control Oocytes.

This graph shows the uptake of 0.1mM [³H]2-deoxy-D-glucose into *Xenopus* oocytes injected with either GLUT2 or GLUT3 mRNA. Uptake was measured over a 30 min time period. The rate of uptake into non-injected, control oocytes is also shown to illustrate the low level of deGlc transport into GLUT5-injected oocytes. Each column represents the transport rate into at least 10 oocytes \pm SEM. This graph is representative of at least three experiments. Transport rate varies with each oocyte batch due to differing levels of protein expression, however, this graph is typical in that deGlc uptake by GLUT5 is consistently lower or equal to level of uptake by non-injected oocytes.

Figure 3.4

Graphs showing the Uptake of 0.1mM DeGlc by GLUT2-Injected, GLUT5-Injected and Control Oocytes.

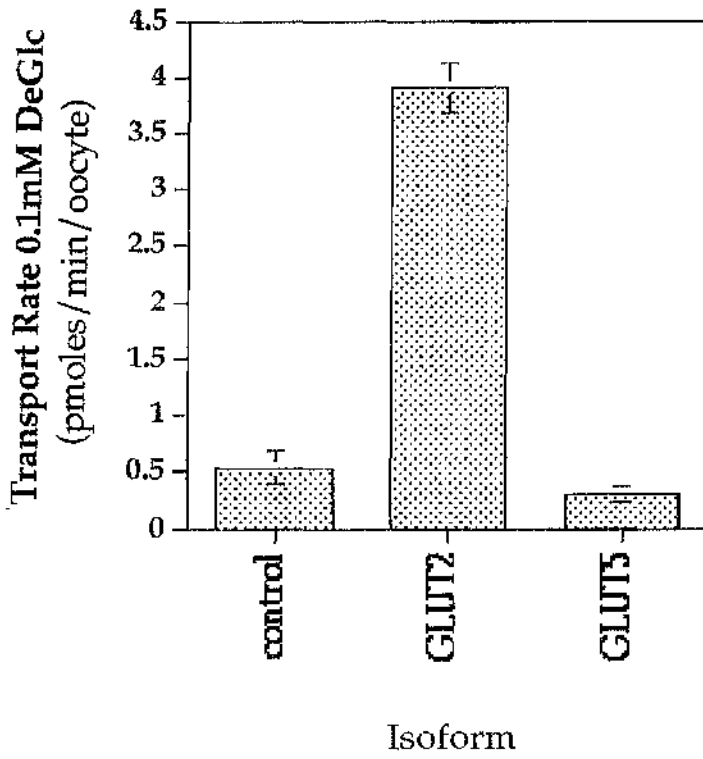


Figure 3.5

Graph Showing the Inhibition of Uptake of 0.1mM Fructose by 100mM D-Glucose, L-Glucose or D-Fructose.

This graph shows the uptake of 0.1mM D-fructose by GLUT5-injected oocytes, and the inhibition of this uptake by D-fructose, D-glucose and L-glucose, when added at a concentration of 100mM. Rates of uptake into non-injected oocytes are subtracted from rates of uptake into GLUT5-injected oocytes. Each column represents the uptake of fructose into at least 10 oocytes \pm SEM from a representative experiment (if $n > 3$). Uptake in this experiment was measured over a 60 min time period. Oocytes were exposed to competing sugar 10 mins prior to the addition of trace radiolabelled fructose.

Figure 3.5

Graph Showing the Inhibition of Uptake of 0.1mM Fructose by 100mM D-Glucose, L-Glucose or D-Fructose.

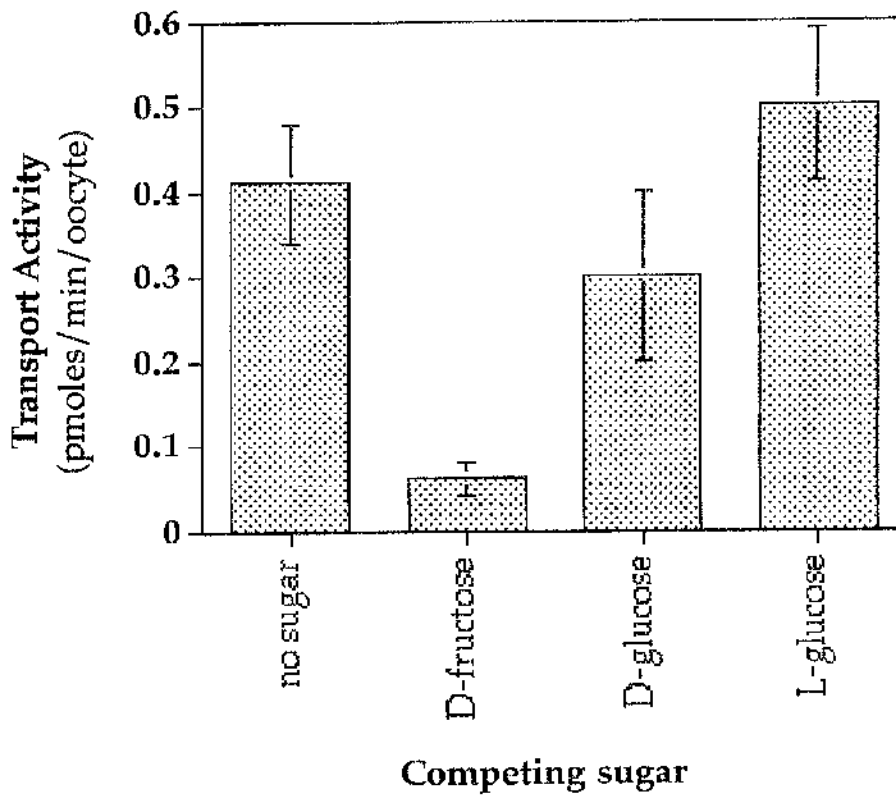


Figure 3.6

Graph Showing the Effects of pH on the Transport Activity of GLUT5-Injected Oocytes.

This graph shows the rate of uptake of 0.1mM D-fructose by GLUT5 injected oocytes, when incubated in transport medium of different pH values. The rate of uptake into non-injected oocytes is subtracted from the rate of uptake into non-injected oocytes. Each column represents the transport rate of at least 10 oocytes \pm SEM, from a representative experiment (if n >3). Uptake was measured over a 60 min time period.

Figure 3.6

Graph Showing the Effects of pH on the Transport Activity of GLUT5-Injected Oocytes.

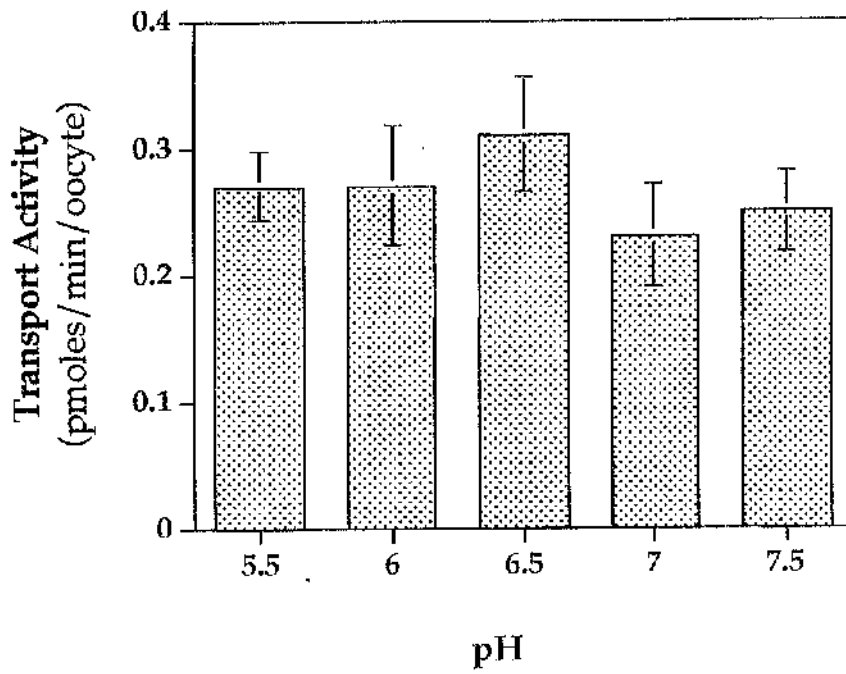


Figure 3.7

Lineweaver-Burk Plot of Fructose Transport by GLUT5-Injected Oocytes at pH 4.5.

Transport rates of D-fructose into GLUT5-injected oocytes were measured exactly as described, with the exception that the transport medium in the assay was adjusted to pH 4.5. This plot was constructed as described in section 3.3.1. Note that this experiment was only performed once, however, the K_m value obtained was, within the limits of experimental error, identical to the K_m value obtained for GLUT5-injected oocytes at pH 7.5 in the same experiment, on the same batch of oocytes.

Figure 3.7

Lineweaver-Burk Plot of Fructose Transport by GLUT5-Injected Oocytes at pH 4.5.

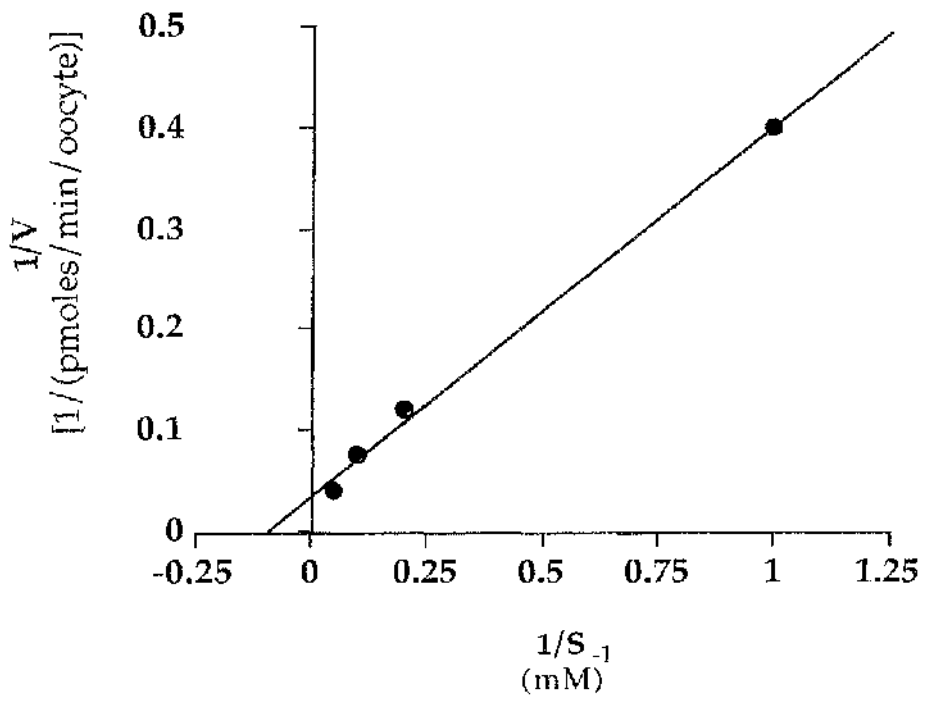


Figure 3.8

Graph Showing the Inhibition of Fructose Transport by GLUT5-Injected Oocytes, by Fused-Ring Fructose Analogues.

This graph shows the uptake of 0.1mM D-fructose by GLUT5-injected oocytes, and the inhibition of this uptake by fused-ring analogues. L-sorbose and 1,5 anhydromannitol are fused pyranose ring forms, while 2,5 anhydromannitol is a fused furanose ring structure. These compounds were added at a concentration of 50 mM. Rates of uptake into non-injected oocytes have been subtracted from rates of uptake into GLUT5-injected oocytes. Each column represents the uptake of fructose into at least 15 oocytes \pm SEM from a representative experiment (if $n > 3$). Uptake in this experiment was measured over a 60 min time period. Oocytes were exposed to competing analogue 10 mins prior to the addition of trace radiolabelled fructose.

Figure 3.8

Graph Showing the Inhibition of Fructose Transport by GLUT5-Injected Oocytes, by Fused-Ring Fructose Analogues.

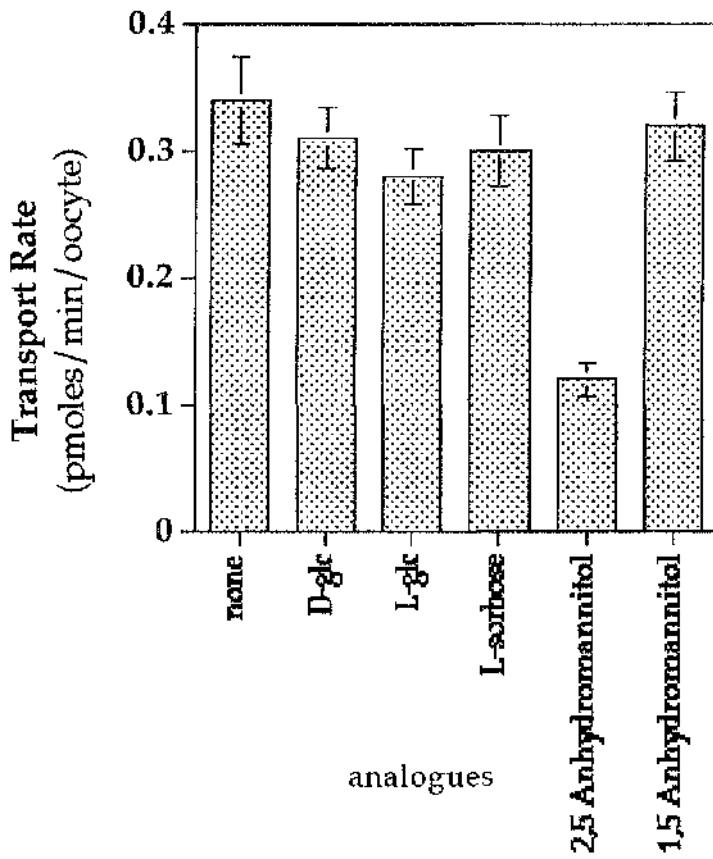


Table 3.1
Collected GLUT5 Data From Different Species And Different Expression Systems.

Species of GLUT5	Expression system	FructoseK _m (mM)	D-glc inhib _D of Fructose transport.	Glucose transport.	Cyto. B. photolab'ing	Cyto. B. inhib _D of transport	Reference
human	Oocytes + cRNA	6	NO	NO	NO	NO	(Parrant, 1992)
rat	Oocytes + cRNA	n.d.	YES	YES (deGlc)	NO	YES (deGlc)	(Rand, 1993)
rat	BBM vesicles	n.d.	NO	NO	n.d.	YES (fructose)	(Corpe, 1996)
rat	transfected CHO cells	10-15	NO	NO	NO	NO	(Inukai, 1995)
Rabbit	Oocytes + cRNA	11	YES (also D-gal)	YES	n.d.	n.d.	(Miyamoto, 1994)
rabbit	Oocytes + total jejunal RNA	n.d.	NO	n.d.	n.d.	n.d.	(Miyamoto, 1994)
rabbit	BBM vesicles	9	NO (neither gal)	NO	YES	NO	(Miyamoto, 1994)
rabbit	BBM vesicles	18	n.d.	n.d.	n.d.	n.d.	(Schultz, 1970)
guinea pig	BBM vesicles	4	n.d.	n.d.	n.d.	n.d.	(Mavrias, 1973)
hamster	BBM vesicles	17	n.d.	n.d.	n.d.	n.d.	(Honneger, 1973)

n.d. not determined.

Cyto. B photolab'ing : cytochalasin B photolabeling.

Cyto. B inhib_D : cytochalasin B inhibition of deGlc, D-glucose or D-fructose

3.5 Conclusions.

3.5.1 Kinetics and Substrate Selectivity of Human GLUT5 in *Xenopus* Oocytes.

The K_m value for fructose transport was measured as 22.5 ± 10 mM. This value is similar, although slightly higher to that reported by Burant *et al* (Burant *et al.*, 1992).

The substrate preference of human GLUT5 in the oocyte system was investigated. It was found that GLUT5 could not transport deGlc, and the presence of 50 mM or 150 mM D-glucose or L-glucose did not inhibit the transport of D-fructose. This is also in agreement with data from Burant *et al.*

3.5.2 The Effect of pH on Substrate Selectivity of Human GLUT5 in *Xenopus* Oocytes.

The effects of pH on the transport of D-fructose and deGlc were measured. It was found that a decrease in pH from 7.5 to 4.5 had no effect on the fructose transport activity of GLUT5. The K_m for fructose uptake at pH 4.5 was determined. There was no change in this value when measured at this pH compared to the K_m at pH 7.5. Also, there was no increase in the transporter's ability to transport deGlc. The substrate specificity of GLUT5 is therefore, unchanged throughout this pH range. It was not possible to measure the effect of lowering the pH below 4.5 as this would have deleterious effects on the oocyte membrane (Dr. Amir Ahmed, personal communication). Therefore, in this respect, this experiment does not completely replicate the conditions in the small intestine, especially the proximal end of the small intestine where the pH will be lower than 4.5. Nevertheless, if a decrease in pH did induce a change in either affinity of GLUT5 for fructose or glucose, it would be expected

that at pH 4.5, such an effect would be detectable. It is perhaps interesting in itself, that such a large decrease in pH does not affect the transporters activity.

3.5.3 Analysis of the Preferred Fructo- Ring Form Accepted by Human GLUT5.

The ability of fused ring fructose analogues L-sorbose, 1,5 anhydromannitol, and 2,5 anhydromannitol to inhibit the uptake of D-fructose has been studied. 1,5 anhydromannitol is a fused ring pyran- analogue of fructose, and 2,5 anhydromannitol is fused in the furan- ring form. L-sorbose exists mainly in the pyranose ring form. The structures of these compounds are shown in Figure 3.2. Figure 3.8 shows the inhibitory effects of these analogues on the transport of 0.1 mM D-fructose. As can be seen from this graph, the presence of 50 mM L-sorbose or 50 mM 1,5 anhydromannitol does not inhibit D-fructose transport at all. These analogues are in the fused pyran- ring form. Therefore, this indicates that there is no competition of these analogues for the binding site of D-fructose. The furan- fused ring analogue however, does compete with D-fructose for the exofacial binding site of GLUT5. This is demonstrated by the (~65%) inhibition of fructose transport by 50 mM 2,5 anhydromannitol. The results of these experiments indicate that GLUT5 transports D-fructose in the furanose ring form.

3.6 Summary.

The kinetics of transport and substrate specificity of GLUT5 have been poorly studied, and previous work on this isoform from different species and in different expression systems has yielded widely conflicting results (see table 3.1). The kinetic parameters and substrate specificity of human GLUT5 have been reported in only one previous study (Burant *et al.*, 1992). Therefore, we have measured a K_m value for the uptake of D-fructose by human GLUT5 in the *Xenopus* oocyte system, and found this value to be 22.5 ± 10 mM. This value is similar to that reported by Burant *et al.* We have also tested the substrate specificity of human GLUT5 in the oocyte system, specifically to determine if this isoform can transport deGlc or if the transport of D-fructose is D-glucose inhibitable. Our results support those of Burant *et al* in that we have detected no glucose transport activity in this isoform, and D-fructose transport was not inhibited by 100mM D-glucose.

The intestinal Na^+ -glucose cotransporter, SGLT1, has been shown to vary its affinity for substrate according to the pH of the intestine. Since GLUT5 is expressed in a variety of pH environments, both throughout the gut and elsewhere in human tissues, we investigated the effects of varying pH of the transport medium of GLUT5-injected oocytes. This was found to have no effect on the transport activity or affinity of human GLUT5 for fructose, as measured by K_m . Furthermore, no deGlc transport activity was observed regardless of pH.

It has been shown previously for GLUT2, that fructose is transported in the furanose form, and glucose in the pyranose form (Colville *et al.*, 1993a). It has also been shown that the fructose transporter of the parasite *Trypanosoma brucei*, can transport fructose in the furanose and the pyranose ring-form (Fry *et al.*, 1993). Previous studies, utilising the chimeric transporter approach, have investigated the structural requirements of GLUT1 and GLUT5 for the transport of both D-glucose and D-fructose. This work has shown that the

regions of GLUT1 required for glucose transport differ greatly from the regions of GLUT5 required for fructose transport. On the basis of these observations, we proposed that the substrate binding sites of these isoforms may not be analogous. Therefore, we have investigated the ring-form of fructose transported by human GLUT5. Preliminary studies have shown that fructose is transported in the furanose ring form, as demonstrated by the inhibition of fructose transport by the fused-furanose ring analogue, 2,5 anhydromannitol. Therefore, this situation may be analogous to the transport of fructose by GLUT2. Further inhibition studies with hydroxyl-substituted fructose analogues with GLUT2 and GLUT5 will provide more information on the structural requirements of fructose binding to these isoforms.

CHAPTER 4.

Kinetic Characterisation of GLUT2/GLUT3 Chimeric Transporters.

4.1.1 Introduction.

The mechanism by which GLUT1 undergoes conformational change during transport catalysis has been well studied (Chapter 1, sections 1.4-1.7). Much of the work on GLUT1 has also focused on mapping the exofacial and endofacial glucose binding sites. These sites have been shown to be structurally separate, and are located in different regions of the protein. ATB-BMPA, the exofacial ligand photolabels GLUT1 in the region of helices 7 and 8 (Davies *et al.*, 1991), whereas cytochalasin B, the endofacial ligand, photolabels a region between helices 10 and 11 (Holman & Rees, 1987). The structural separation of the sites has further been proposed on the basis of kinetic studies and inhibitor selectivity.

From ligand binding and proteolytic digestion studies, it has been shown that the C-terminal half of GLUT1 contains sufficient sequence information to bind cytochalasin B and ATB-BMPA. However, studies utilising the baculovirus system to express "half" GLUT1 molecules have suggested that the binding of these ligands can only occur if the C-terminal half of GLUT1 is co-expressed with an independent construct encoding the N-terminal half (Cope *et al.*, 1994). Therefore, it is proposed that while the six helices of the C-terminal half of GLUT1 are probably directly involved in formation of the glucose binding sites, the N-terminal half is necessary for correct structural packing of the C-terminal helices (section 1.8).

The importance of the C-terminal half of GLUT1 in substrate binding has also been implicated by site directed mutagenesis studies. An account of the details of this work is given in Chapter 6. According to Muecklers topological model of GLUT1 (Figure 1.2), helices 3, 5, 7, 8 and 11 are moderately amphipathic, and therefore able to form a channel through which glucose could pass during transport. Within each of these helices there are several polar residues which would be able to participate in hydrogen bonding with

the sugar molecule. Site directed mutagenesis has identified several residues important in exofacial and endofacial sugar binding, and in conformational flexibility. However, all but one of these residues reside in the C-terminal half of the molecule. In Figure 1.9, two putative models are described for the arrangement of helices which form the transmembrane channel (section 1.9). These models are speculative, however, it is interesting to note that they both include the C-terminal helices 7, 8, and 11 in the formation of the transporter channel.

4.1.2 Previous Studies of Regions Involved in Substrate Selectivity.

The topology of GLUT1 has been well characterised (section 1.3.2), and many studies have been conducted which support the alternating conformation model. The exofacial and the endofacial sugar binding sites of GLUT1 have been mapped to defined regions (section 1.6), and the kinetics of sugar transport exhaustively measured (section 1.4.2.1).

The hydropathy plots of each of the isoforms in the glucose transport family are virtually superimposable (Figure 1.1). Therefore, although the bulk of the work has focused on GLUT1, it is thought that the topology and transport mechanism of the other isoforms are similar, if not identical to those of GLUT1.

However, there is very little published work which investigates the substrate binding sites of the other isoforms, each of which has a distinct substrate selectivity (Table 4.1). There are obviously differences in the way each isoform binds and transports substrate. Such differences determine for example, why only GLUT2 and GLUT5 can recognise and transport fructose, or why GLUT3 can bind and transport D-galactose with such high affinity. (Fructose "recognition" is used here to mean that these transporter isoforms possess the sequence information which facilitates fructose binding.) Previous

work on GLUT1 has also largely ignored another area of interest: what structural features of the protein determine the isoform-specific kinetics.

There are few studies in the literature which attempt to answer these questions, and those which have, have produced conflicting results. Inukai *et al* have performed a study which examines the structural basis of the substrate specificity of GLUT5 and GLUT1 (Inukai *et al.*, 1995). This study involved the expression of chimeric GLUT1/GLUT5 constructs in CHO cells. The results from this study suggested that two large regions of the GLUT5 protein were essential for the ability of these chimeric molecules to transport fructose. These regions were the entire N-terminal "half" of the protein- from the N-terminus up to the end of the sixth helix, and the C-terminal cytoplasmic tail- from the end of helix 12 to the carboxy-terminus. (From here on, the cytoplasmic C-terminal tail may be referred to as the "C-tail".) For the ability of the chimeras to transport glucose, the middle cytoplasmic loop (between helices 6 and 7), and the C-terminal "half" of the protein (from helix 7 to the end of helix 11) were essential. Moreover, the ability to transport glucose was not affected by replacing the N-terminal half of GLUT1, or the C-tail of GLUT1 with the corresponding regions of GLUT5. This study however, only examined the substrate preference of the chimeric molecules, and did not examine the effects of the replacement of specific regions on the kinetics of sugar transport.

The C-terminal cytoplasmic tail of each of the isoforms is variable in size and sequence. This observation suggested to Katagiri *et al* that this region of the transporter may play a role in determining specific kinetics of each isoform. Therefore, Katagiri *et al* have constructed a chimeric molecule in which the last 42 amino acids of the cytoplasmic tail of GLUT1 are replaced with those of GLUT2 (Katagiri *et al.*, 1992). This construct has been expressed in CHO cells, and the K_m for deGlc shown to be 3-fold higher than that of wild-type GLUT1. From this, it has been inferred that in this chimera, the C-

terminal tail of GLUT2 confers "GLUT2 -like" kinetic properties on the GLUT1 molecule.

There are, however, some problems with this study: CHO cells, the expression system this group have chosen to use, express endogenous GLUT1, and so the accurate measurement of kinetics in this system is difficult. Therefore, although the K_m of this chimera has increased to 3-fold that of the GLUT1 wild type, it is difficult to know if this value is representative of a GLUT2 K_m value, when measured in this system. Additionally, accurate estimation of the number of transporters at the cell surface is necessary to relate measured V_{max} to turnover number. Such estimations are difficult at best, and the subcellular fractionation procedure employed by Katagiri may not be ideal in this regard.

However, Due *et al* have also produced a study which suggests that the last 29 amino acid residues of the C-terminal tail are important in determining the affinity of GLUT1 (Due *et al.*, 1995b). It was shown that replacement of the last 29 residues of the GLUT1 C-terminal tail, with those of GLUT4, has the effect of reducing the V_{max} of the transporter. Also, if the last 29 or 73 amino acid residues of GLUT4 are replaced with those of GLUT1, the V_{max} increases to almost half of that of GLUT1, and the affinity for substrate decreases by half. This study was performed in *Xenopus* oocytes, and again, in this system accurate determination of the number of transporters at the cell surface is difficult (section 4.6.3). Determining the parameter of V_{max} therefore, may not be accurate.

It has been shown that swapping the C-terminal tail of murine GLUT1 with that of murine GLUT4 results in abolition of the GLUT1 property of accelerated exchange (sections 1.4.2.1-1.4.3.4). However, replacing the GLUT4 tail with GLUT1 does not confer the property of accelerated exchange onto the GLUT4 molecule (Dauterive *et al.*, 1996). This study was also performed in *Xenopus* oocytes. Therefore, in addition to the problems of accurately

measuring V_{\max} , there are difficulties inherent in measuring the property of accelerated exchange outwith a cell-free system (section 1.4.3.3).

Further evidence for the involvement of the C-terminal tail in isoform-specific kinetics, comes from a study by Buchs *et al* (Buchs *et al.*, 1995). In this study, replacement of the last 30 residues of the carboxy-terminus of GLUT4 with those of GLUT2, results in a transporter which displays an affinity for 3-O-methyl glucose which is intermediate between GLUT4 and GLUT2. Moreover, replacement of the entire C-terminal half of GLUT4 (from the start of the large middle loop) with corresponding sequence of GLUT2 results in a transporter which displays transport kinetics highly similar to GLUT2.

On the basis of the studies discussed above, it may not be possible to assume that the regions of the transporter structure that confer isoform specific substrate selectivity are the same as those involved in isoform specific transport kinetics. Additionally, the extent of the involvement of the C-terminal tail and other regions in the substrate selectivity and kinetics of GLUT1 is not clear. It may be that the importance of these regions vary between isoforms.

The purpose of this chapter is to determine the structural basis of substrate selectivity and transport kinetics in the GLUT2 and GLUT3 isoforms.

4.1.3 Kinetic Characterisation of the Other Glucose Transporter Isoforms.

Endogenous expression of multiple GLUT isoforms is common to most cell types and for this reason it is difficult to measure the kinetics of the other isoforms in their native cell. However, the availability of cDNAs for these isoforms has enabled the heterologous expression of the transporters in the *Xenopus* oocyte system. These cells have a very low level of background endogenous transport, which allows the accurate measurement of isoform specific kinetics. A summary of the extensive kinetic characterisation of the

various isoforms performed in this expression system by this and other laboratories is presented in Table 4.1.

The transport kinetics of all the isoforms are quite distinct, but the GLUT2 and GLUT3 isoforms are particularly disparate. GLUT2 has a high K_m for the zero-*trans* entry of deGlc into oocytes (11.2mM), while GLUT3 has a relatively low K_m for this transport event (1.4mM). The K_m values of these isoforms for 3-*O*-methylglucose equilibrium exchange are equally distinct (42.3mM and 10.6mM respectively) and their substrate selectivities are also unique: only GLUT2 is capable of fructose uptake for example, while GLUT3 is a high affinity galactose transporter. GLUT2 can also transport galactose, but with a much lower affinity.

As discussed below, these distinctions were chosen as the basis of an assay to identify regions involved in substrate selectivity and high affinity deGlc transport.

4.2 Methods.

In an effort to identify the structural features of the protein which dictate the substrate selectivity and the affinity deGlc, GLUT2 and GLUT3 were chosen as suitable candidates for the generation of chimeric molecules. Using a PCR based approach outlined in Figure 4.1, a panel of constructs were engineered by Margaret Arbuckle, cloned into the pSP64T vector (Figure 2.1), and expressed in the *Xenopus* oocyte system. These are shown in Figure 4.2, and are presented as two separate series of constructs. The first of these series (the GLUT2 series), are essentially GLUT2 molecules in which lengths of sequence from the start of helix 7 to the end of the C-terminal cytoplasmic tail, have been replaced by the equivalent sequences of GLUT3. Investigation of the GLUT2-series of mutants should delineate sequences important for the "GLUT2-like" property of fructose recognition. Mirror image constructs have also been produced and are shown as the GLUT3-series of mutants in Figure 4.2. These constructs are GLUT3 molecules in which various lengths of sequence in the C-terminal half are replaced with those of GLUT2. The junction points of these chimeras are identical to those in the GLUT2-series. Analysis of these chimeras should identify the regions important in the "GLUT3-like" properties of high affinity deGlc and high affinity galactose transport. Furthermore, because these two series of mutants are mirror images, then the data resolved from either of the series should reflect and substantiate the data from the other. Therefore, the involvement of a particular sequence in fructose recognition, for example, should be detected in both the GLUT2 series and the GLUT3 series.

This approach focuses on the investigation of the C-terminal half of the protein (i.e. from the start of the seventh helix to the end of the C-terminal tail). The rationale behind this is based on evidence from structural studies of GLUT1, where helices in the C-terminal half have been found to be important

both in ligand binding and in mediating conformational change in the protein (sections 1.6 and 1.8). On the basis of this, it seems likely that the sequence information that is important in determining the kinetic parameters and substrate preferences of the other isoforms will also be found in this half of the molecule.

Preliminary characterisation of these constructs through their expression in the oocyte system has been successful in identifying regions of importance for the kinetic parameters of deGlc transport. This data is presented in Table 4.2 in conjunction with the results obtained in this study. Note that the deGlc kinetic data and maltose inhibition values presented in this table were obtained by Dr. Margaret Arbuckle in this laboratory. Also included are values of these kinetic parameters for the wild type proteins, which were measured by previous workers in this group (Colville *et al.*, 1993b), and in some cases confirmed in parallel experiments with the chimeric species.

4.3 Aims of this study.

1. To measure the K_m for D-fructose uptake in those chimeras which are capable of fructose recognition.
2. To measure the K_m for galactose transport for the GLUT3 chimeras.
3. To build a model of substrate selection by the GLUT2 and GLUT3 isoforms, on the basis of the results obtained from the above.

4.4.1 Results.

The K_m values of D-fructose and D-galactose uptake were determined by measuring the rate of transport of trace radiolabelled sugar over a range of external sugar concentrations into oocytes that had been incubated in sugar free medium for at least 48 hours (section 2.4). By measuring rates of *zero-trans* entry as a function of substrate concentration, Lineweaver-Burk plots were constructed, and the K_m values determined from the equation of the line as described (section 3.3.1).

Oocytes were exposed to radioactive fructose or galactose for 60 and 30 minutes respectively. Previous studies have shown that accumulation of radiolabel increases linearly with time over this time period (Colville *et al.*, 1993b). These experiments also demonstrated that no significant amount of radiolabeled non-phosphorylated sugar accumulated in the oocyte during this time period. Such studies indicate that transport across the membrane is the true rate limiting step and this measurement is not compounded by rates of sugar phosphorylation by hexokinase.

The graphs presented in Figures 4.3-4.8 are each representative of one of at least three separate measurements. K_m values \pm SEM calculated from a number of such experiments are shown in Table 4.2.

4.4.2 Measurement of Fructose Transport.

Figure 4.3 shows a representative Lineweaver-Burk plot of fructose transport by G2(12Ed). The K_m values for this chimera was calculated to be 139 ± 21 mM respectively. This value is shown in the context of wild type values in Table 4.2.

A Lineweaver-Burk plot of fructose transport by the only member of the GLUT3 series capable of fructose recognition- G3(7St), is shown in Figure 4.4. The K_m value for this chimera was calculated to be 365 ± 21 mM (Table 4.2).

4.4.3 Measurement of Galactose Transport.

Figures 4.5-4.8 show Lineweaver-Burk plots of galactose transport by the GLUT3 series of chimera: G3(7St), G3(7Ed), G3(10Ed), and G3(12Ed) respectively. The K_m values measured for these mutants were 25.4 ± 2.1 mM, 2.55 ± 0.4 mM, 2.8 ± 0.9 mM, and 4.8 ± 0.9 mM respectively (Table 4.2).

Figure 4.1

Diagram of Recombinant PCR Used to Construct GLUT2/GLUT3 Chimeric Transporters.

This diagram describes the PCR method used to construct the first generation chimeric transporters. The generation of GLUT2- and GLUT3-based primary products is achieved by using wild type GLUT2 and GLUT3, along with appropriate primers in separate reactions. The external primers for each of these reactions have tails which encode *Sal* I restriction sequences, and the internal primers have tails which are complementary in sequence to the opposite primary PCR fragment. Therefore, as can be seen from the diagram, in the secondary PCR, the primary fragments themselves act as templates: upon strand dissociation and re-annealing, the overlapping tail regions bind, and the sequence is extended to produce a full length construct. Prior to ligation into a suitable vector, the PCR products are restricted with *Sal* I. This produces sequence overhangs which enables cloning into the *Sal* I restricted vector. This diagram specifically shows the construction of a representative GLUT2 series member, however, the GLUT3 series constructs were made in a similar way, with GLUT3 acting as the template for generation of primary fragment "a", and GLUT2 for primary fragment "b". In this diagram, GLUT2 sequence is represented in black ink, and GLUT3 in red.

Figure 4.1 Recombinant PCR Approach.

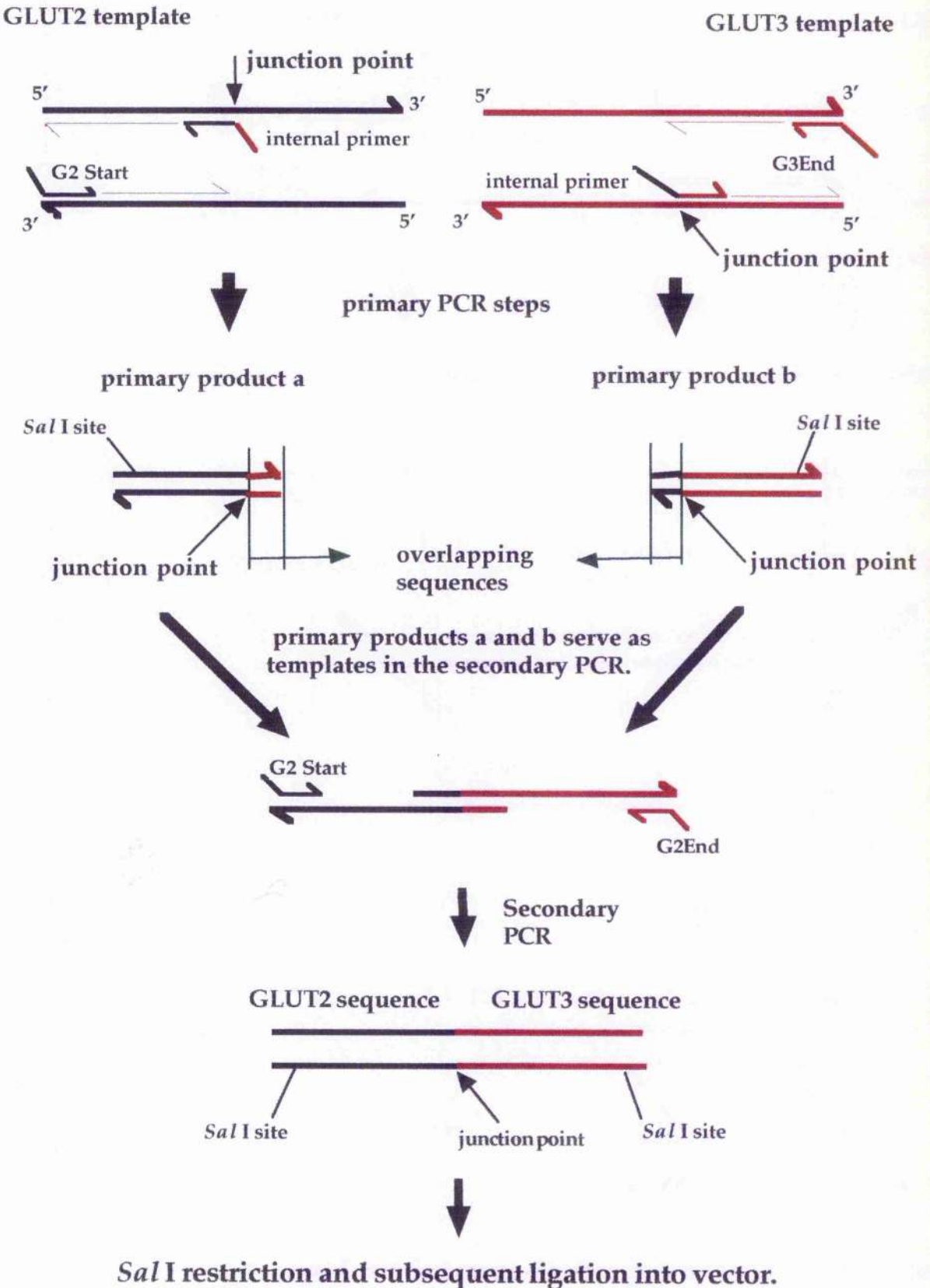


Figure 4.2

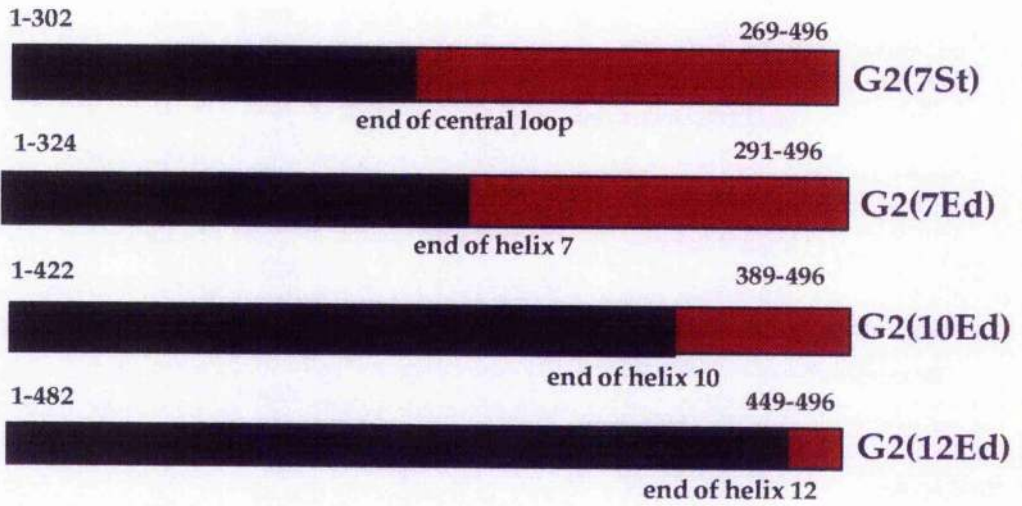
Diagram Showing the Junction Points of the GLUT2 and GLUT3 Series Chimeras.

This diagram shows the junction points of the GLUT2 and the GLUT3 chimeras. GLUT2 sequence is shown in black ink, and GLUT3 in red. The amino acid numbers shown correspond to either GLUT2 cDNA sequence or GLUT3 cDNA sequence, and refer to the sequences above which they are positioned. The first member of the GLUT2 series shown therefore is G2(7St). The GLUT2 portion of this chimera stretches from the N-terminus of GLUT2 to the end of the central loop, i.e. GLUT2 amino acids 1-302. The remaining portion is GLUT3 sequence from the end of the (GLUT3) central loop to the end of the C-terminus, i.e. GLUT3 amino acids 269-496.

Figure 4.2

Diagram Showing the Junction Points of the GLUT2/GLUT3 Chimeric Transporters.

GLUT2 SERIES



GLUT3 SERIES

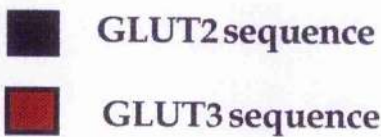
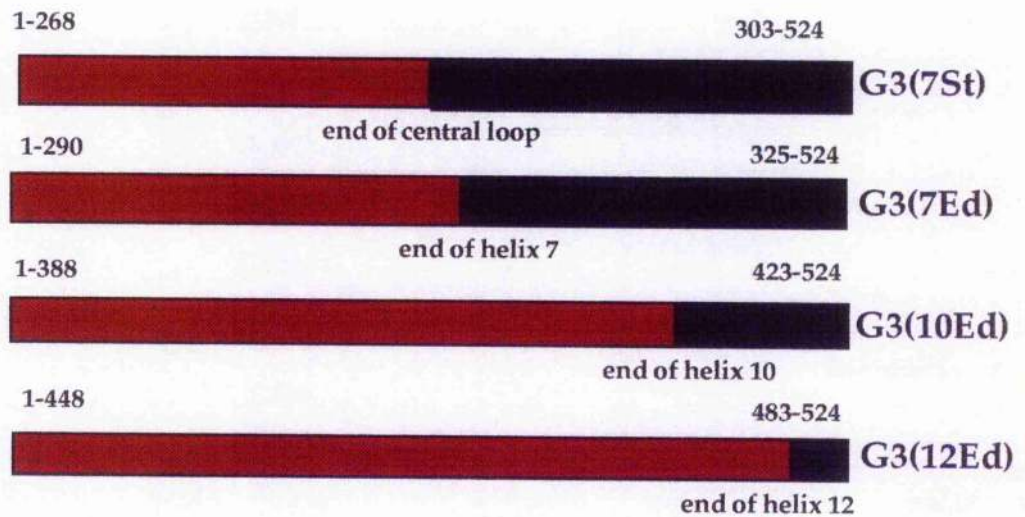


Figure 4.3.

Lineweaver-Burk Plot of the Uptake of D-Fructose by G2(12Ed)-Injected Oocytes.

Each point is the mean of the transport rate determined from groups of at least 10 oocytes. (section 2.4). Rate of transport was determined by exposure of the oocytes to radiolabeled fructose for 60 mins and the counts per minute determined as described (section 2.4). For each experiment endogenous oocyte transport was measured by a parallel incubation of uninjected "control" oocytes in trace radiolabeled fructose. The values obtained for the control oocytes at each concentration were subtracted from the values obtained from the chimera-injected oocytes to obtain the heterologous transport rate. Transport rates in control oocytes were typically 10% of the injected oocytes. Error bars are excluded for clarity, but the range of error was typically 10%. The data shown in this particular plot and in other plots presented in this chapter, are representative of at least four separate experiments.

Figure 4.3.

Lineweaver-Burk Plot of D-Fructose Transport by Chimera G2(12Ed)-Injected Oocytes.

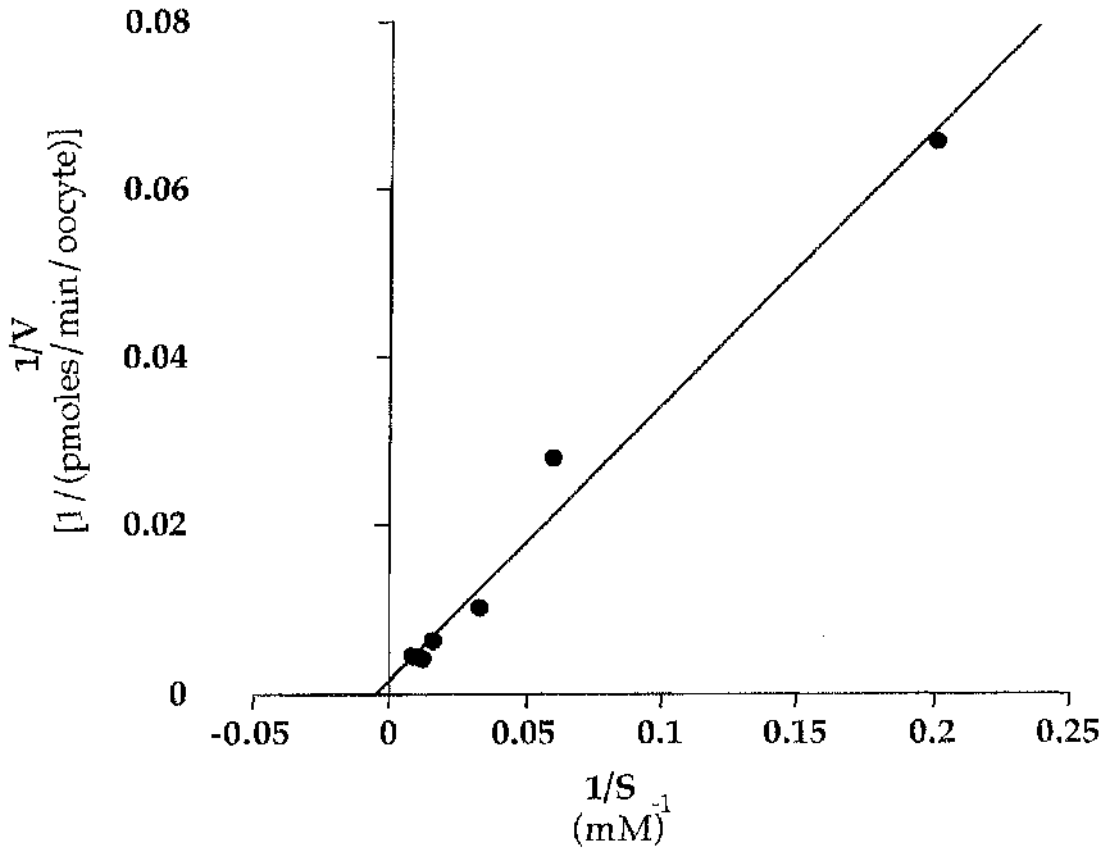


Figure 4.4

Lineweaver-Burk Plot of the Uptake of D-Fructose by Chimera G3(7St)-Injected Oocytes.

In the plot from this representative experiment, values for the transport rate of D-fructose by G3(7St) expressing oocytes were determined as described. Each point is the mean of at least 10 individual oocytes at each substrate concentration. Values are corrected for endogenous oocyte transport as described (Figure legend 4.3). The range of error was typically 10%, but error bars are omitted for clarity. Note that not all data points are shown.

Figure 4.4.

Lineweaver-Burk Plot of the Uptake of D-Fructose by Chimera G3(7St)-Injected Oocytes.

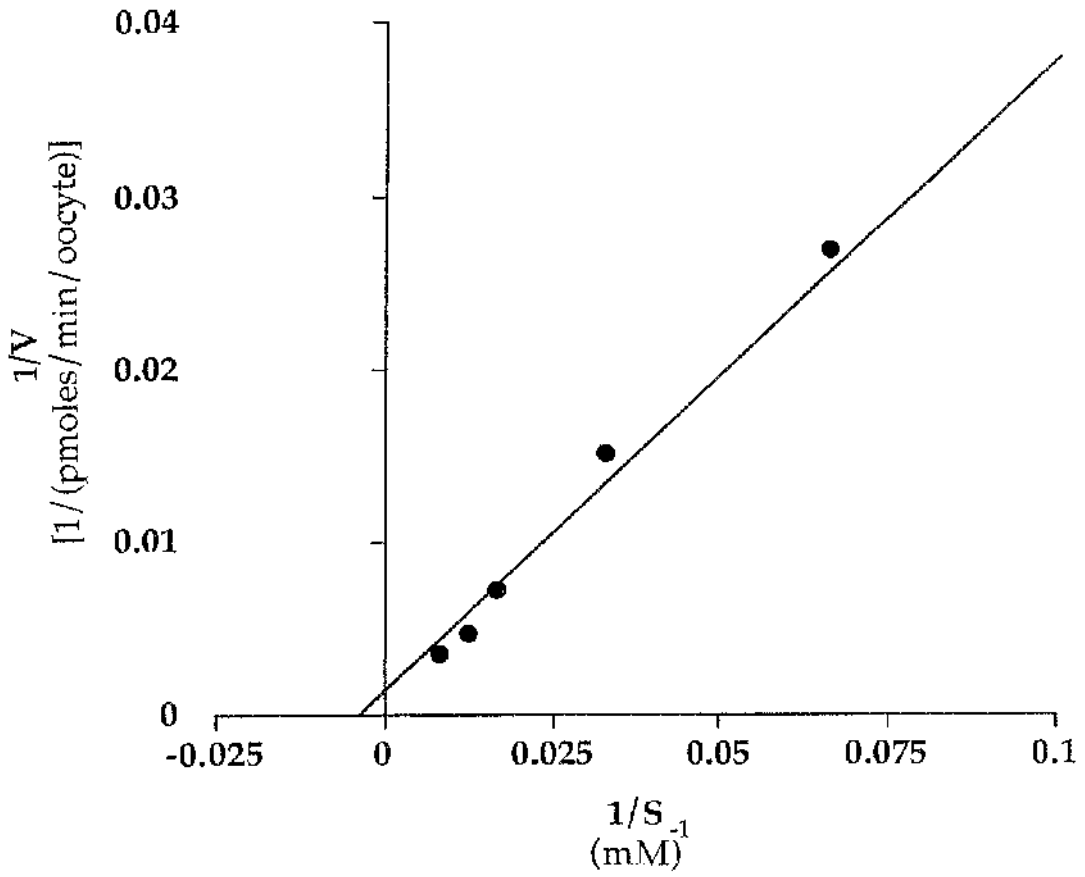


Figure 4.5.

Lineweaver-Burk Plot of the Uptake of D-Galactose by Chimera G3(7St)-Injected Oocytes.

In the plot from this representative experiment, values for the transport rate of D-galactose by G3(7St) expressing oocytes were determined as described. Each point is the mean of at least 10 individual oocytes at each substrate concentration. Values are corrected for endogenous oocyte transport as described (Figure legend 4.3). The range of error was typically 10%, but error bars are omitted for clarity. Note that not all data points are shown.

Figure 4.5.

Lineweaver-Burk Plot of the Uptake of D-Galactose by Chimera G3(7St)-
Injected Oocytes.

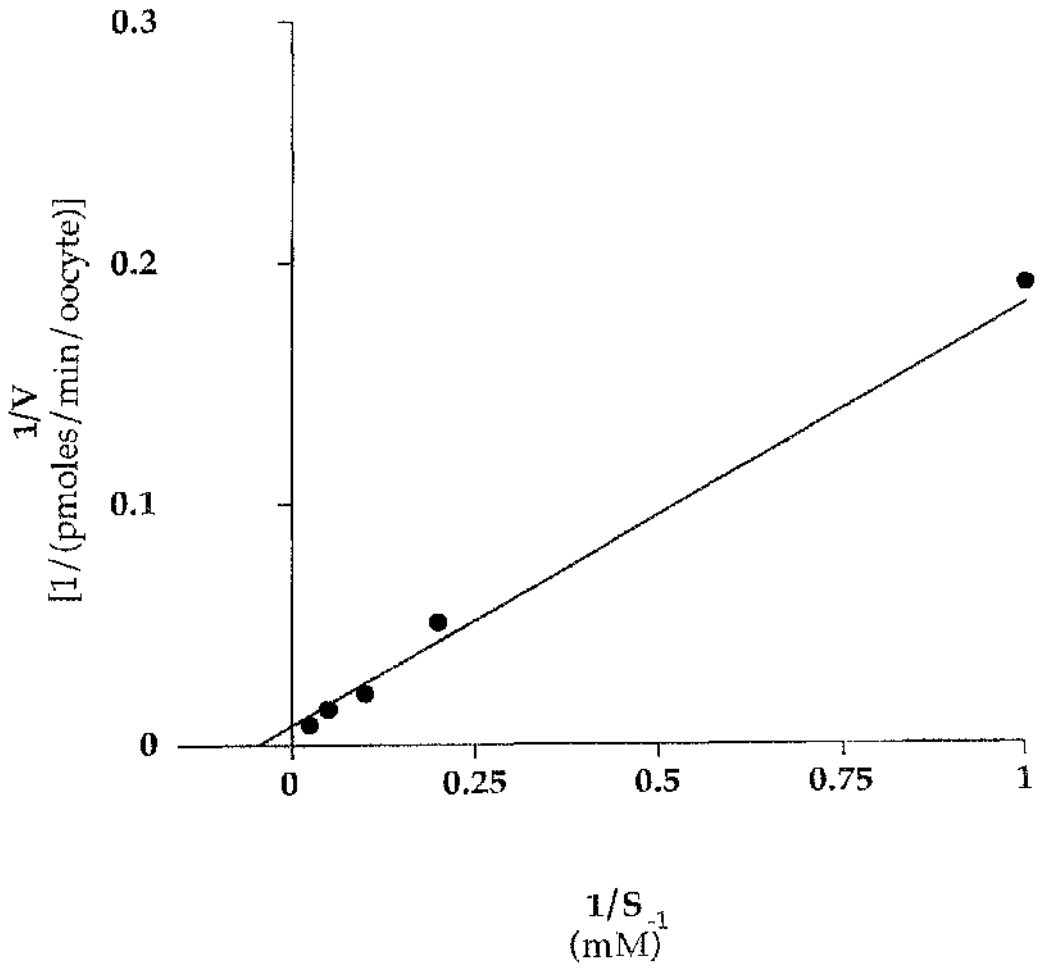


Figure 4.6.

Lineweaver-Burk Plot of the Uptake of D-Galactose by Chimera G3(7Ed)-Injected Oocytes.

In the plot from this representative experiment, values for the transport rate of D-galactose by G3(7Ed) expressing oocytes were determined as described. Each point is the mean of at least 10 individual oocytes at each substrate concentration. Values are corrected for endogenous oocyte transport as described (Figure legend 4.3). The range of error was typically 10%, but error bars are omitted for clarity. Note that not all data points are shown.

Figure 4.6

Lineweaver-Burk Plot of the Uptake of D-Galactose by Chimera G3(7Ed)-
Injected Oocytes.

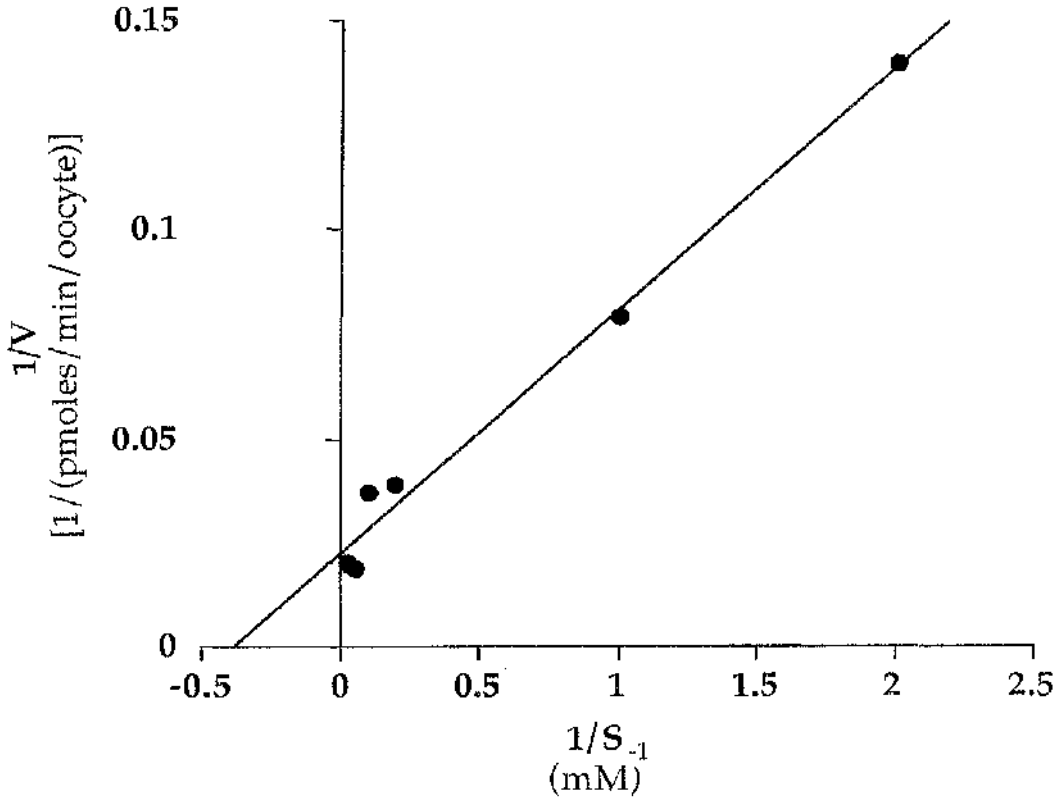


Figure 4.7.

Lineweaver-Burk Plot of the Uptake of D-Galactose by Chimera G3(10Ed)-Injected Oocytes.

In the plot from this representative experiment, values for the transport rate of D-galactose by G3(10Ed) expressing oocytes were determined as described. Each point is the mean of at least 10 individual oocytes at each substrate concentration. Values are corrected for endogenous oocyte transport as described (Figure legend 4.3). The range of error was typically 10%, but error bars are omitted for clarity. Note that not all data points are shown.

Figure 4.7.

Lineweaver-Burk Plot of the Uptake of D-Galactose by Chimera G3(10Ed)-
Injected Oocytes.

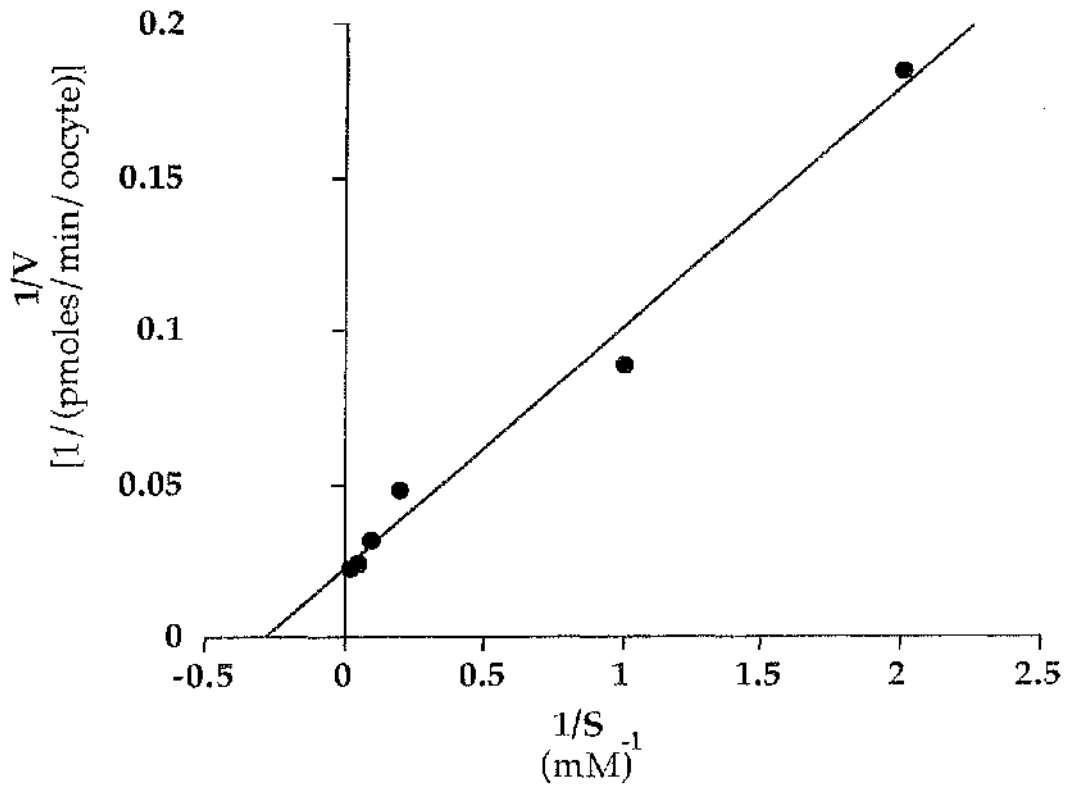


Figure 4.8

Lineweaver-Burk Plot of the Uptake of D-Galactose by Chimera G3(12Ed)-Injected Oocytes.

In the plot from this representative experiment, values for the transport rate of D-galactose by G3(12Ed) expressing oocytes were determined as described. Each point is the mean of at least 10 individual oocytes at each substrate concentration. Values are corrected for endogenous oocyte transport as described (Figure legend 4.3). The range of error was typically 10%, but error bars are omitted for clarity. Note that not all data points are shown.

Figure 4.8

Lineweaver-Burk Plot of the Uptake of D-Galactose by Chimera G3(12Ed)-
Injected Oocytes.

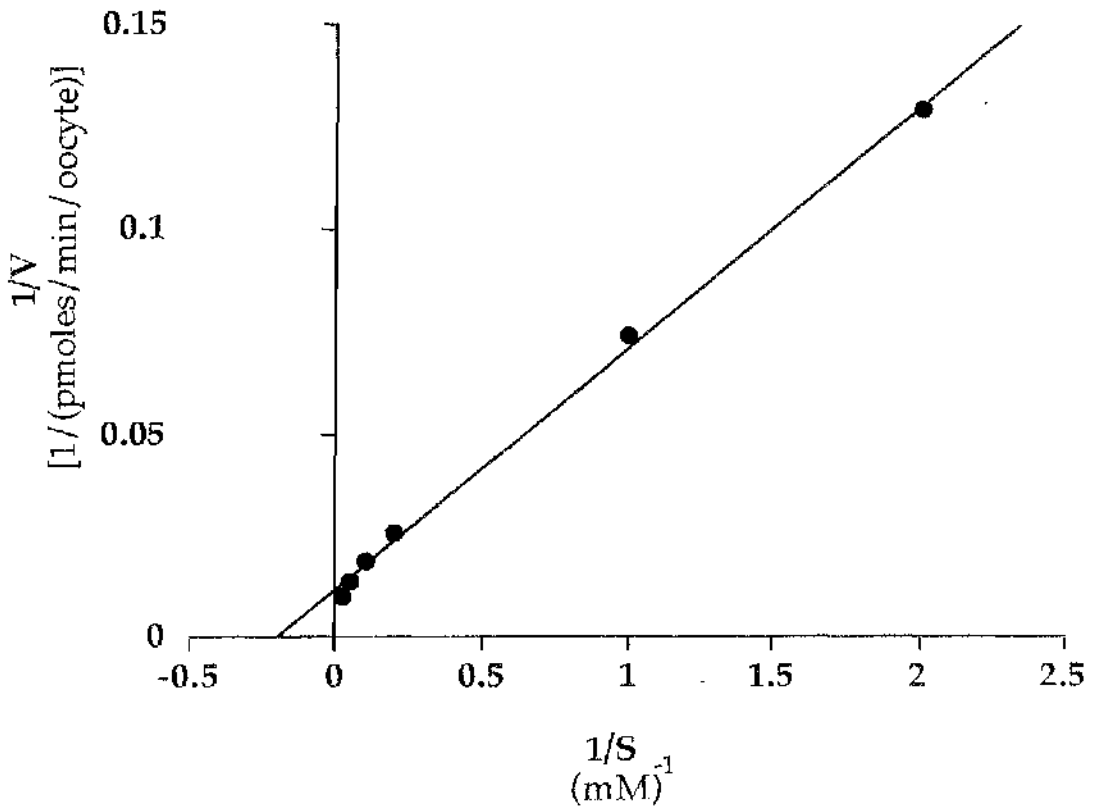


Figure 4.9

Structures of β -D-Glucose and β -D-Maltose.

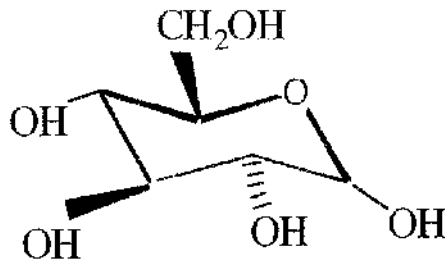
This diagram shows the structures of β -D-glucose (Compound I) and β -D-maltose (Compound II). As can be seen from these structures, maltose is a disaccharide of D-glucose in α (1-4) glycosidic linkage. Maltose is used as an inhibitor of sugar transport as it can bind to the transporter is not transported.

The C-1 position of the first glucose "subunit" of maltose enters the exofacial binding pocket of the transporter in a D-glucose-like manner. The sugar hydroxyls at positions C-3 and C-6 are also analogous, so it is expected that these will interact with the binding site in a " β -D-glucose-like" manner. However, the bond with the C-4 hydroxyl will not be formed because this carbon is involved in the glycosidic linkage with the other glucose "subunit" of maltose. This other glucose unit effectively acts as a large bulky group at the C-4 position of the first glucose unit, which prevents closing of the transporter around the sugar molecule. It is also possible that the interaction of the C-3 and C-6 carbons with the exofacial binding site may also be affected by the presence of the large bulky group at the C-4 position.

Figure 4.9

Structures of β -D-Glucose and β -D-Maltose.

Compound I



Compound II

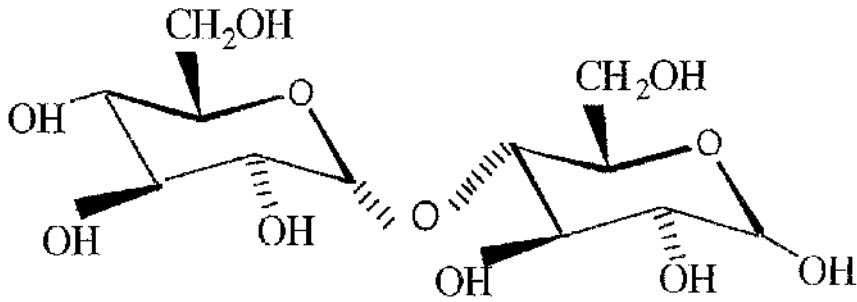


Figure 4.10

King-Altman Diagram Showing the Competition of DeGlc and Maltose at the Exofacial Binding Site of the Transporter.

This model shown in this diagram is based on kinetic data which has been established for GLUT1, although it is generally believed that this model will also apply to the other isoforms. The diagram describes the cycling of the transporter from an outward-facing conformation- T_o to an inward-facing conformation- T_i , and back again, either in the presence or absence ($\pm S$) of deGlc. K_{so} and K_{si} represent the dissociation constants at the outward-facing and inward-facing sites respectively, and k_1 , k_2 , k_{-1} and k_{-1} describe the rate constants of the steps indicated. This schematic also describes the competition between deGlc and maltose. It can be seen from the diagram that this event is mediated at the exofacial binding site. Maltose binds at the exofacial binding site (i.e. T_o), but is not transported to the other side of the membrane. Therefore the rate constants which govern this event are not dependent on the movement of the loaded carrier to the inward-facing conformation (k_2), dissociation of the sugar (K_{si}), or re-orientation of the empty carrier (k_{-1}). The kinetics of deGlc transport are dependent on all of these steps. Therefore, while the interaction of deGlc at the exofacial binding site is influenced by other steps in the transport cycle, the interaction of maltose is dependent only on the rate of association and dissociation of this sugar at the exofacial site. Hence, when the ability of maltose to inhibit deGlc transport is measured, the resulting K_i value which is generated is independent of transporter turnover number.

Figure 4.10.

King-Altman Diagram Showing the Competition of DeGlc and Maltose at the Exofacial Binding Site of the Transporter.

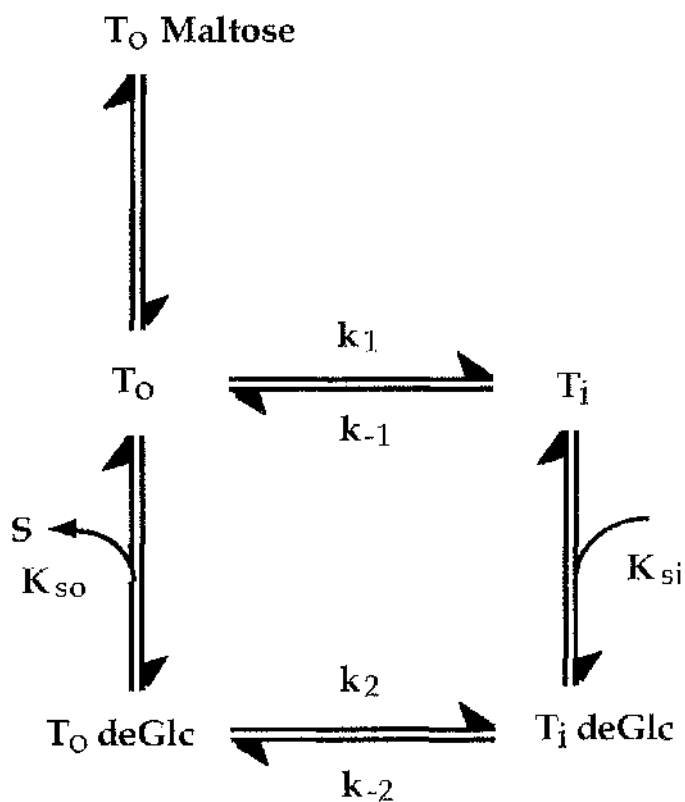


Figure 4.11

Diagram Showing Regions of the Transporter Structure Involved in Substrate Selectivity and Transport Kinetics.

This diagram is based on the results of the chimera work. The N-terminal helices (shown in blue), are indicated in this model to be important in structural packing. We have shown that this region of the transporter influences the transport kinetics of GLUT2 and GLUT3 in an isoforms-specific manner. However, we also propose that this influence is probably due to general structural stability, rather than a direct involvement. This suggestion is supported by previous work by others, which suggests that this region of the transporter is not directly involved in forming the exofacial or endofacial binding sites, but is required for correct structural packing of helices in the C-terminal half which play a more intimate role in substrate binding (Cope *et al.*, 1994).

Helix 7 (indicated in red), has been shown to contain information which is absolutely required for fructose recognition by GLUT2. Furthermore, sequence information contained the helix 7 of GLUT3 is responsible for the high affinity deGlc transport property of this isoform.

The region shown in yellow has been indicated by the chimera data to be of influence in the affinity of GLUT2 and GLUT3 for maltose. This may indicate a possible interaction between this region and the C-4 sugar hydroxyl, although further work is needed to characterise the nature of this involvement.

The regions which are not involved in substrate selectivity (as indicated by our experiments) are shown in grey. Note that although the loops connecting the helices in the N-terminal half, and in the C-terminal half are not colour-coded, they may also be involved in the various functions.

Figure 4.11

Diagram Showing Regions of the Transporter Structure Involved in Substrate Selectivity and Transport Kinetics.

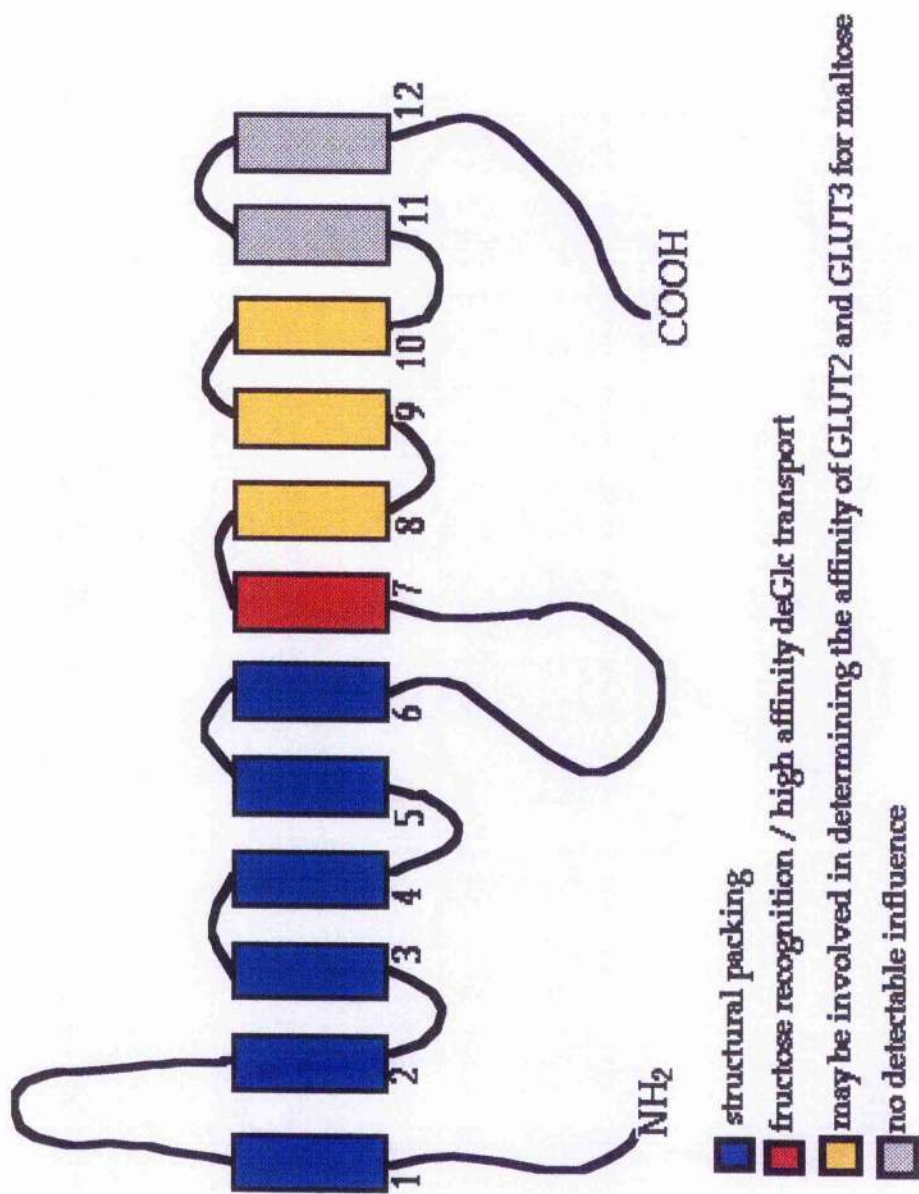


Figure 4.12

Comparison of the Helix 7 Amino Acid Sequences of Human GLUTs 1, 2, 3, 4 and 5.

This diagram shows a comparison of the helix 7 amino acid sequences of GLUTs 1, 2, 3, 4 and 5. There is a high level of conservation in this helix throughout the family. However, notably GLUTs 1, 3 and 4, which are all high affinity deGlc transporters, have a conserved QLS motif, while GLUT2 and GLUT3 do not. This may indicate that this motif is important in high affinity deGlc transport. GLUTs 2 and 5 are capable of fructose transport, while the other family members are not. The QLS motif is also absent from other fructose transporters such as the transporter of the parasite *Trypanosoma brucei*. Recently, it has been shown that the corresponding HVA motif in GLUT2 is responsible for fructose recognition (M.J.Seatter and G.W.Gould-unpublished data).

Figure 4.12

Comparison of the Helix 7 Amino Acid Sequences of Human GLUTs 1, 2, 3, 4 and 5.

ILIAVVL QLS QQLSGINAVFY	GLUT1
IIISIVL QLS QQLSGINAVFY	GLUT3
LIIAVVL QLS QQLSGINAVFY	GLUT4
ILVALML HVA QQFSGINGIFY	GLUT2
LLSIIVL MGG QQLSGVNAIYY	GLUT5

Table 4.1

Kinetic Parameters of the Glucose Transporter Family Expressed in Oocytes.

	K_m (mM)		
Isoform	DeGlc zero- <i>trans</i> entry (mM)	3-O-MG equilibrium exchange (mM)	Alternative substrates
GLUT1	6.9 \pm 1.5	20.9 \pm 2.9	Galactose (K_m 17mM)
GLUT2	11.2 \pm 1.1	42.3 \pm 4.1	Fructose (K_m 66mM)
GLUT3	1.4 \pm 0.06	10.6 \pm 1.3	Galactose (K_m 8.5mM)
GLUT4	4.6 \pm 0.3	1.8	Not studied in oocytes
GLUT5	n.d.	n.d.	Fructose* (K_m 6mM)

The data from this table were taken from results published in a number of studies (reviewed in Gould & Holman 1993).

n.d. - not determined, substrate not transported.

* Fructose is the preferred substrate of GLUT5, not the alternative substrate.

Table 4.2

Kinetic Parameters for Transport of Substrates by GLUT2/GLUT3 chimeras.

construct	K _m deGlc (mM)	K _i maltose (mM)	Fructose transport?	K _m fructose (mM)	K _m galactose (mM)
<i>GLUT2</i>	11.2±1.1	125±24	yes	76±11	92±8.4
<i>GLUT3</i>	1.4±0.06	28±2.5	no	n.d.	6.2±1.5
<i>G2(7S0)</i>	-	-	-	-	-
<i>G2(7E d)</i>	8.5±2.1		yes		
<i>G2(10E d)</i>	-	-	-	-	-
<i>G2(12E d)</i>	9.5±3.4	133±21	yes	139±21	-
<i>G3(7S0)</i>	8.3±0.3	135±15	yes	365±21	25.4±2.1
<i>G3(7E d)</i>	1.4±0.03	69±7	no	n.d.	2.55±0.4
<i>G3(10E d)</i>	1.05±0.07	26±4	no	n.d.	2.8±0.9
<i>G3(12E d)</i>	1.89±0.35	25±6.1	no	n.d.	4.8±0.88

Italics wild type values include for comparison.

n.d. not determined, substrate not transported.

4.5.1 Discussion.

From previous preliminary characterisation of these chimeras, it has been shown that helix 7 is important in fructose recognition by GLUT2 and high affinity deGlc recognition by GLUT3. The data from studies in this chapter have supported these initial proposals and have further defined the following conclusions:

4.5.2 Analysis of the GLUT3 series.

4.5.2a Kinetics of DeGlc Transport in the GLUT3 Series.

Previous studies of the GLUT3 series chimeras (Table 4.2), have identified helix 7 as a region of importance in high affinity deGlc transport. This is demonstrated by G3(7St): this construct has a K_m value for deGlc transport of 7.3mM, which is higher than that of wild type GLUT3 (1.4mM), and is approaching that of wild type GLUT2 (11.2mM). If the sequence of GLUT3 is replaced with that of GLUT2 at any point after the *end* of helix 7, i.e. G3(7Ed), G3(10Ed) or G3(12Ed), then the resulting transporter is capable of high affinity deGlc recognition. The K_m values measured for deGlc transport by constructs G3(7Ed), G3(10Ed) and G3(12Ed) are virtually indistinguishable from the wild type GLUT3 K_m value. These data argue a role for helix 7 in determining isoform-specific kinetics of deGlc transport. The aim of the work presented in this chapter was to examine the substrate selection of these chimeras.

4.5.2b Fructose Recognition in the GLUT3 Series.

The results of this study show that G3(7St) retains the ability to transport fructose, whereas G3(7Ed) and the other chimeras in this series do not. The K_m value obtained for fructose transport by G3(7St) was $365 \pm 21 \text{mM}$, which is approximately four-fold higher than that of wild type GLUT2 (Figure 4.4, Table 4.2).

The fact that G3(7Ed), and the other chimeras in this series, can transport deGlc with "GLUT3-like" high affinity properties precludes the possibility that lack of fructose recognition displayed by these constructs is due to a non-specific structural error which causes general transport dysfunction. Rather, we suggest that these results indicate that helix 7 plays an essential role in fructose recognition by GLUT2 (or lack of fructose recognition by GLUT3).

The observation that the K_m value for fructose transport exhibited by G3(7St) is almost five-fold higher than wild type GLUT2 suggests that the kinetics of fructose transport may also be influenced by the N-terminal half of the protein. The nature of such influence will be discussed later (section 4.6.1b).

4.5.2c Galactose Transport in the GLUT3 Series.

It can be seen from Table 4.2 that all the chimeras in the GLUT3 series retain the ability to transport D-galactose. K_m values were measured, and these results also implicate helix 7's involvement in determining the transport kinetics of this substrate. G3(7St) has a K_m value for galactose transport of $24.3 \pm 2.7 \text{mM}$ which is "GLUT2-like" (although the affinity of this construct for galactose is slightly higher than that of wild type GLUT2), whereas G3(7Ed), exhibits a marked change to "GLUT3-like" behaviour (-the G3(7Ed) galactose K_m is $2.55 \pm 0.4 \text{mM}$). The remaining chimeras in the GLUT3 series, G3(10Ed) and G3(12Ed), also exhibit similar "GLUT3-like" galactose K_m values (Table

4.2). G3(7St) and G3(7Ed) are essentially identical, except for the sequence of helix 7.

G3(7St) displays galactose transport kinetics which we have referred to as being "GLUT2-like". However, the galactose K_m value of G3(7St), although more "GLUT2-like" than "GLUT3-like", is still almost four-fold lower than that of wild type GLUT2. This suggests that the GLUT3 N-terminal half in this construct also exerts some influence on its kinetic behaviour, at least with regard to galactose transport.

To summarise, helix 7 is implicated as playing an important role in determining the substrate selectivity of GLUT2 and GLUT3, and also in determining the kinetic behaviour of these isoforms in the transport of their alternative substrates. Furthermore, the GLUT3 series data also suggests that the N-terminal half of the protein exerts an influence on the transport kinetics of alternative substrates.

4.5.3 Analysis of the GLUT2 Series.

Expression of three of the chimeras from the GLUT2 series has been problematic: functional expression of G2(7St) or G2(10Ed) has not been achieved. Furthermore, chimera G2(7Ed) gave consistently low levels of expression, (occasionally micro-injection of G2(7Ed) mRNA produced no increase in substrate uptake by oocytes at all). Possible explanations for these problems will be discussed later in this chapter (section 4.6.3).

The only member of the GLUT2 chimera series to express consistently was G2(12Ed): this molecule was "GLUT2-like" with regards to fructose recognition and deGlc transport kinetics. The problems with G2(7Ed) expression meant that only a limited number of experiments were performed on this chimera, but the results of this preliminary data suggest that this molecule is also markedly "GLUT2-like" with regard to fructose recognition

and deGlc transport kinetics (Table 4.2). The limited fructose data suggests that this chimera has a K_m value for fructose transport of $\sim 180\text{mM}$, which is higher than that noted for wild type GLUT2 ($K_m \sim 76\text{mM}$). This result is difficult to interpret in the absence of functional expression of G2(7St). Additionally, the measurement of K_m for G2(7Ed) was only performed twice, although the two values obtained for this chimera were similar ($n_1=166\text{mM}$, $n_2=195\text{mM}$), and may therefore be assumed to be reasonably accurate.

There have been no problems expressing G2(12Ed), and the kinetic characteristics of this construct have been well defined. The K_m value for fructose transport by G2(12Ed) was found to be $139\pm 21\text{mM}$. This value is higher than that of wild type GLUT2, as is the fructose K_m of G2(7Ed). This may suggest that full "GLUT2-like" behaviour would require the presence of the GLUT2 cytoplasmic C-terminal tail.

However, it should be noted that at such high substrate concentrations (i.e. $>100\text{mM}$), it becomes difficult to measure accurate K_m values. This is mostly due to the dilution of trace radiolabelled substrate with high concentrations of non-labelled substrate. For this reason, we cannot be certain that the difference between the G3(12Ed) K_m and the wild type GLUT2 K_m is significant. Also, substitution of the GLUT2 tail into a GLUT3 transporter (i.e. G3(12Ed)), clearly does not influence this isoforms deGlc transport behaviour. This therefore, suggests two possible situations: either (1) the GLUT2 tail is important for "GLUT2-like" fructose transport, but only in the context of a GLUT2 molecule, perhaps via the interaction of the tail with other GLUT2 sequences, or (2) the kinetics of G2(7Ed) and G2(12Ed) are truly "GLUT2-like", and the differences shown in the data for these and wild type GLUT2, are due to the inaccuracy of measuring K_m values at such high substrate concentrations.

The influence of the N-terminal half of the protein in the fructose transport kinetics of GLUT2 can be seen from comparison of G2(12Ed) and

G3(7St). The C-terminal six helices of these two constructs are identical: the major difference between them being that G3(7St) does not have the GLUT2 amino terminal half. This construct has a much lower affinity for fructose (K_m of $365 \pm 21 \text{mM}$) than G2(12Ed)- which does have the GLUT2 N-terminal half, and has an affinity for fructose (K_m of $139 \pm 21 \text{mM}$), which is much closer to that of wild type GLUT2 (K_m of $76 \pm 12 \text{mM}$).

Therefore, these results support the implication of the GLUT3 series, that helix 7 is necessary for fructose recognition. However, the information contained in helix 7 is not sufficient to confer complete "GLUT2-like" kinetic behaviour upon chimeric transporter molecules. Other regions in addition to helix 7 are thought to influence fructose and galactose transport kinetics: these regions lie within the N-terminal half of the protein.

4.5.4 Maltose Inhibition of DeGlc Transport.

Until now, in this chapter, it has been assumed that the parameter that is determined when measuring and comparing K_m values for deGlc transport is the affinity of the exofacial glucose binding site for deGlc. The transport of deGlc into the oocyte is rapidly followed by its phosphorylation. This phosphorylation step is not rate limiting. DeGlc-6-phosphate cannot be transported back out of the cell, and so does not interact with the endofacial binding site. Therefore, it is assumed that the measurement of K_m is a function of the affinity of the substrate at the exofacial binding site only, and that interaction of substrate with the endofacial site is negligible. In this respect, the use of deGlc is preferential to D-glucose.

However, the K_m of deGlc is a function not only of substrate binding to the exofacial site, but also of re-orientation of the transporter from the outward-facing conformation to the inward-facing conformation, and back again. So, the K_m parameter can be influenced by the catalytic turnover of the

transporter (i.e. the rate of re-orientation). In this experiment, measurement of K_m is used as a method of assessing the affinity of the exofacial binding site of chimeric transporter proteins. Therefore it may be important to determine that the observed effect on the K_m of a particular mutant is not a function of a change in catalytic turnover. Unfortunately, we have not found it possible to accurately measure transporter turnover numbers in the oocyte system (section 4.6.3).

The ability of maltose to competitively inhibit deGlc uptake can be used to identify changes in the affinity of the chimeric transporter for substrate. Maltose is a disaccharide of two molecules of D-glucose linked in $\alpha(1-4)$ glycosidic linkage (Figure 4.9). It therefore binds to the transporter in a D-glucose-like manner, but is too large to be transported. The K_i values for maltose inhibition of deGlc transport therefore, represent a true measurement of an event mediated at the exofacial binding site, which is independent of transporter turnover number (Figure 4.10). However it should be considered that the K_i value that is generated, can also be considered effectively as a measurement of the affinity of the exofacial binding site for maltose.

The maltose K_i values measured for the GLUT3 series of mutants support the premise that helix 7 is important in high affinity deGlc recognition. Chimera G3(7St) is "GLUT2-like" with respect to its maltose K_i , whereas G3(10Ed) and G3(12Ed) are "GLUT3-like". However, unlike the sharp change in deGlc K_m values observed after the substitution of helix 7, G3(7Ed) exhibits an intermediate K_i for maltose inhibition of deGlc uptake. This implies that the GLUT3 sequence that lies between the end of helix 7 and the end of helix 10 (referred to forthwith as the H7_{end}-H10_{end} sequence), is in some way responsible for the change between an intermediate maltose K_i (as in G3(7Ed)) and a "GLUT3-like" maltose K_i (as in G3(10Ed)).

As discussed before, the K_i measurement represents an effect mediated at the exofacial binding site, however, it is important to realise that this "effect"

involves the competition of two substrates* for the exofacial binding site. Therefore the intermediate K_i value exhibited by G3(7Ed) may represent two possible affinities. It may be a true representation of an intermediate affinity of the exofacial binding site, either for deGlc, or for maltose.

Firstly, let us assume that the maltose K_i value of G3(7St) represents a true measurement of affinity for deGlc at the exofacial binding site of this chimera: this K_i value suggests that the affinity of the exofacial binding site for deGlc is not truly "GLUT3-like", rather, it is intermediate between the two isoforms. Therefore, it implies that the turnover number of G3(7Ed) has increased, and it is this turnover effect which gives rise to the "pseudo-GLUT3-like" deGlc K_m value exhibited by this construct. This being the case, it has to be concluded that the sequence that lies between the H7_{end}-H10_{end} sequence is important, in the context of the GLUT3 transporter, in the formation of a high affinity deGlc binding pocket. The reason why this is not seen in the deGlc K_m data is because the turnover number of the transporter has increased, thereby artificially lowering the K_m , and thus masking the true deGlc affinity.

This explanation is possible. However, GLUT3 is a low capacity transporter, i.e. its value for the parameter of V_{max} is lower than that of GLUT2. Therefore, it seems likely that if more GLUT3 sequence is added to a chimeric transporter, the expected effect would be that the turnover number would become more "GLUT3-like" (i.e. lower), especially in a construct such as G3(7Ed), where the entire N-terminal half is also composed of GLUT3 sequence. However, in the G3(7Ed) construct (if we assume that the K_i value represents deGlc affinity), the turnover number has apparently increased. This effect does not make "isoform-specific sense".

An alternative explanation for this effect may be found if we consider that the intermediate maltose K_i value of G3(7Ed) may represent an intermediate affinity of the exofacial binding site for maltose. In this situation,

* Note that maltose is not technically a "substrate" as it is not transported.

replacing the H7_{end}-H10_{end} sequence of GLUT3 (i.e. from G3(7Ed) to G3(10Ed)), restores the affinity of the exofacial binding site of the chimeric transporter to a complete "GLUT3-like" level. It can be concluded from this that the H7-H10 sequence of GLUT3 allows a tighter binding of maltose, thereby lowering the concentration of maltose required to efficiently compete with the deGlc for the binding site, which results in a lower K_i value.

4.6 Conclusions.

4.6.1 Working Model for Substrate Recognition and Isoform-Specific Kinetics.

Based on the results of this work, we propose that helix 7 contributes to the exofacial binding site of both GLUT2 and GLUT3 in such a way as to define substrate recognition by GLUT2 (or lack of fructose recognition by GLUT3). Furthermore, helix 7 also plays an important role in defining isoform-specific kinetics.

The N-terminal half of the transporter structure is implied to exert an influence on the transport kinetics of GLUT2 and GLUT3. This influence is probably related to an involvement in the structural packing of the helices if the C-terminal half, rather than a direct involvement in the exofacial binding site (see below).

This model explains the observation that a region between the end of helix 7 and the end of helix 10 apparently contributes to the affinity of the exofacial binding site.

4.6.1a The Role of Helix 7.

The importance of helix 7 is demonstrated most dramatically in chimeras G3(7St) and G3(7Ed). These constructs are identical in all respects,

with the exception of the sequence of helix 7. In the construct G3(7St) helix 7 is composed of GLUT2 sequence, whereas in G3(7Ed) this sequence is replaced by that of GLUT3. The complete loss of fructose transport associated with the loss of the GLUT2 helix 7 sequence is compelling evidence that this single transmembrane region contains sufficient information to define fructose recognition (i.e. by GLUT2), or lack of fructose recognition (i.e. by GLUT3).

These two constructs also highlight the important role of helix 7 in contributing to the transport kinetics of deGlc by both GLUT2 and GLUT3. It has been shown that replacement of the GLUT2 helix 7 with GLUT3 sequence results in the restoration of "GLUT3-like" kinetic behaviour with regard to deGlc transport. If helix 7 is composed of GLUT2 sequence, the chimeric transporter displays "GLUT2-like" deGlc kinetics.

Inspection of the galactose data from G3(7St) and G3(7Ed) provides further evidence that helix 7 is involved in determining the galactose transport kinetics of both GLUT2 and GLUT3. These constructs show that the presence of a GLUT2 helix 7 produces "GLUT2-like" galactose transport kinetics. Replacement of the GLUT2 helix 7 with GLUT3 sequence restores "GLUT3-like" galactose transport kinetics.

This conclusion that helix 7 plays an important role in determining these aspects of the exofacial binding site is supported by a study from Hashirimoto *et al.*, which suggests that this helix is important in the interaction between GLUT1 and the exofacial ligand, ATB-BMPA (Hashiramoto *et al.*, 1992). The results presented here are also partly in agreement by work from Buchs *et al.*, which suggests that the regions responsible for the unique kinetic parameters of GLUT2 reside in the C-terminal half of the protein, specifically in a region located between the start of helix 7 and the end of helix 12. This region has been shown to exert a partial influence on the K_m and V_{max} of GLUT2 (Buchs *et al.*, 1995).

4.6.1b The Role of the N-Terminal Half of the Transporter.

The results of this study also suggest that there may be other sequences in addition to helix 7, which influence the transport kinetics of GLUT2 and GLUT3. Several observations suggest that the N-terminal half of the transporter may play such a role, at least in the transport of the "alternative" substrates of these isoforms, i.e. fructose and galactose.

This is shown by G3(7St), which is the only chimera in the GLUT3 series capable of fructose transport. The ability of this construct to recognise fructose is due to the presence of the GLUT2 helix 7 sequence. However, the K_m for fructose transport by G3(7St) is very high, which may be due to the influence of the GLUT3 N-terminal half in this construct. This suggestion is supported by the fructose transport data from G2(7Ed) and G2(12Ed), which have K_m values for fructose transport that are more "GLUT2 like" than that of G3(7St).

The influence of the N-terminal half can also be seen in the galactose transport behaviour of G3(7St). This construct has a much lower affinity for galactose (as measured by K_m) than the other constructs in the GLUT3 series. This is due to the presence of the GLUT2 helix 7 sequence, which confers upon the protein "GLUT2-like" galactose transport behaviour. However, the influence of the GLUT3 N-terminal half in this construct is implied by the K_m value for galactose transport by G3(7St), which, although more "GLUT2-like" than "GLUT3-like", is still lower than that of wild type GLUT2.

The influence of the N-terminal half in the transport kinetics of deGlc by GLUT2 and GLUT3 is difficult to determine from the present data. This is due to the lack of functional expression of G2(7St), which contains the important helix 7, but also has the N-terminal half of GLUT3. However, given that this region influences the transport kinetics of the alternative substrates of GLUTs 2 and 3, it can probably be assumed that it will play a role in the transport kinetics of the preferred substrate, deGlc.

The nature of the influence of this region is probably related to the structural packing of helices in the tertiary structure of the protein, rather than involvement of specific N-terminal domain residues in the exofacial binding site. This conclusion is based on a study from Cope *et al* (section 1.8), where it is suggested that the C-terminal half of the protein contains sufficient information to compose the exofacial and endofacial binding sites, but the presence of the N-terminal half is required for the correct structural packing of the C-terminal helices (Cope *et al.*, 1994).

One observation in this work which does not agree with the role of the N-terminal half in influencing transport kinetics is that the maltose K_i value for inhibition of deGlc transport by wild type GLUT2 is identical to that for deGlc transport inhibition by G3(7St). On the basis of the analysis of this single chimera, it is difficult to draw any certain conclusions. However, this may suggest that the structural role of the N-terminal half is more associated with the dynamics of transport, rather than the affinity of exofacial substrate binding. Until other chimeric transporters are constructed, which have junction points throughout the N-terminal half, the exact nature of the influence of this region in the transport mechanism will remain speculative.

4.6.1c Possible Involvement of the Cytoplasmic C-Terminal Tail of GLUT2.

Given that the N-terminal half comprises a large part of the transporter structure, the suggestion that it plays a role in transport kinetics as described above, seems more than likely. However, the possibility should not be dismissed that it is the lack of an appropriate cytoplasmic C-terminal tail that "restricts" the fructose transport kinetics by G2(7Ed) or G2(12Ed) from being completely "GLUT2-like", rather than the influence from the N-terminal half (see above, section 4.6.1b). Although the data presented here does not indicate that the GLUT3 tail is necessary for "GLUT3-like" behaviour, it is possible that

the GLUT2 tail interacts with other GLUT2 sequences. This possibility has also been suggested by other studies (reviewed in section 4.1.2).

4.6.1d Possible Role for the H7_{end}-H10_{end} Sequence.

Therefore, it could be concluded from this that the increase in the affinity of the exofacial binding site for maltose, which occurs upon the addition of the GLUT3 H7_{end}-H10_{end} sequence, may indicate a subtle difference in the way GLUT2 and GLUT3 can accommodate the bulky group at the C-4 position in maltose.

Therefore, we have suggested that the H7_{end}-H10_{end} sequence of GLUT3 may allow a tighter fit of maltose at the exofacial binding site, possibly because it lacks a spatial restriction that is present in the GLUT2 exofacial binding site. It has been shown previously that the interaction of the C-4 hydroxyl of glucose is less important in the exofacial binding site of the GLUT3 isoform than the GLUT2 isoform (Colville *et al.*, 1993a), an observation which may explain why GLUT3 can bind galactose, a C-4 epimer of D-glucose, with such high affinity. However, to draw the conclusion that the C-4 position of the glucose pyranose ring is normally involved in an interaction with the H7_{end}-H10_{end} sequence would be too speculative. The data does not directly suggest this, and even if we consider that this interaction does occur, the deGlc and galactose transport data would argue that the difference in the way that GLUT2 and GLUT3 bind this C-4 hydroxyl is not important in determining the specific kinetics of these isoforms.

One interesting point, when considering the nature of maltose binding is as follows. It has been shown that maltose binding produces a 10% reduction in the α -helical content of GLUT1, as measured by circular dichroism spectroscopy studies. The binding of D-glucose in contrast, produces a 10% increase in the α -helical content of GLUT1 (Pawagi & Debber, 1987, Pawagi &

Deber, 1990) (see also section 1.5.1). These observations are interpreted to indicate that the binding of maltose stabilises the transporter in the exofacial conformation, and the binding of D-glucose induces the movement of the transporter into an inward facing conformation. It is interesting to speculate (regardless of where in the transporter structure it binds) that the interaction of the C-4 position hydroxyl may be essential, or even instrumental in inducing the conformational change associated with substrate transport.

4.6.2 Speculation as to How Helix 7 Interacts with Substrate.

The defining role that helix 7 plays in fructose recognition and in the isoform specific kinetics of fructose, deGlc and galactose is striking. It is even more surprising that one single helix can mediate such influence, when the structures of these sugars are considered. It has previously been demonstrated that fructose is transported in a furanose ring form, while glucose and galactose are accepted as pyranose rings (Colville *et al.*, 1993a). With this in mind, it is interesting to speculate as to which groups of these substrates helix 7 binds to.

The major difference in the binding of fructose at the exofacial site, when compared to the binding of D-glucose, is probably the lack of hydrogen bonding between the C-1 position of fructose and the transporter. A comparison of helix 7 amino acid sequences from GLUTs 1, 2, 3, 4 and 5 is shown in Figure 4.12. From this it can be seen that there are many conserved residues in this helix throughout the family of isoforms. Notably, there is a QLS motif present in GLUTs 1, 3 and 4: these isoforms all transport deGlc with high affinity. This motif is absent in those transporters capable of fructose transport such as GLUT2 and GLUT5, and the fructose transporter of *Trypanosoma brucei* (Fry *et al.*, 1993) (section 3.1.5). The QLS motif may therefore be important in the interaction between the transporter and the C-1

position of glucopyranose. This interaction would probably involve the glutamine in the **QLS** motif, as this residue is polar and can act as a hydrogen donor or a hydrogen acceptor. In the equivalent residues of GLUT2- HVA, histidine can act as a hydrogen acceptor at neutral pH. It is tempting to speculate that this residue may be the site of hydrogen bonding between the oxygen of fructose and helix 7.

Recent advances in this laboratory indicate that this HVA motif in GLUT2 is the defining motif in fructose recognition (M.J.Seatter and G.W.Gould, unpublished data). The substitution of the GLUT2 HVA motif into the helix 7 of a GLUT3 transporter results in the ability of that molecule to accept fructose. Similarly, substitution of the GLUT3 QLS motif into a GLUT2 transporter abolishes fructose transport. It is not known at this point if substitution of the QLS motif into the GLUT2 transporter results in high affinity glucose transport.

4.6.3 Problems with this Study.

This study has been successful in that it has indicated regions of importance in the structural basis of isoform specific kinetics and substrate selectivity. This has enabled other workers in this group to search for specific motifs which may be involved in the parameters mentioned above. This approach has proved to be successful in determining the precise sequence within helix 7 which is responsible for fructose recognition in the GLUT2 isoform, and for high affinity glucose transport in the GLUT3 isoform. With regard to the other regions that are indicated in this study to be of influence in substrate transport kinetics and selectivity, it is extremely unfortunate that expression of the entire GLUT2 series was not achieved, and that a more comprehensive investigation of the remaining chimeras was hindered by problems with the expression system.

The reasons for problems with expression of the GLUT2 series constructs were not pursued in this study due to time restraints. However, several attempts have been made by other workers in this laboratory to re-check the sequence of the problematic constructs, to re-make them, and to subclone them into another vector (see Lisa Porter, PhD Thesis, to be submitted 1997, University of Glasgow). None of these procedures have been successful in locating or correcting the structural error which results in non-expression. It may be possible that it is specifically the GLUT2 N-terminus which is not efficiently processed when placed in the context of a chimeric molecule. Recently, it has been reported by Andreas Buchs (Gwyn Gould -personal communication), that from a panel of fourteen GLUT2 chimeric constructs, only a few were expressed successfully. Therefore, to overcome this problem it was decided that swapping single helices or bundles of helices within a GLUT2 molecule (or a GLUT3 molecule) would be more successful, however this approach proved to be technically difficult (Chapter 5).

General problems with the oocyte expression system impeded detailed investigation of the GLUT3 series chimeras. Seasonal variation of oocyte batches, in addition to infection and animal housing problems, resulted in this system being extremely unreliable with regard to ease of use, and in terms of reproducibility of the data generated from it. Future solutions to this problem can only be solved by subcloning of the chimeric constructs into vectors suitable for use in other cell systems. Expression of these constructs in another cell line will enable us to perform more detailed inhibition and competition studies, to further understand the relationship between the substrate binding requirements of GLUTs 2 and 3 and the regions responsible for these isoform specific differences. This is work which is underway in this laboratory.

Although several methods have been investigated, it has not been possible in this laboratory, to obtain clean plasma membrane fractions in order to determine the amount of transporter protein at the oocyte surface (see Lisa

Porter, PhD Thesis to be submitted 1997, University of Glasgow). Therefore, the use of another cell line to express these constructs, where the membrane fractionation procedures are simpler and more reproducible, will allow us to determine transporter numbers at the cell surface, which will subsequently enable the calculation of transporter turnover numbers. The measurement of this parameter is of key importance in any kinetic study. It not only has been absent in this study, but a general, reproducible, and comparable method for determining this parameter has been absent in all oocyte work to date.

CHAPTER 5.

Construction of Second Generation GLUT2/GLUT3 Chimeric Transporters.

5.1 Introduction

In an effort to test the model proposed in the last section (Chapter 4, sections 4.6.1-4.6.2), it was decided to construct a second panel of chimeras (referred to forthwith as the second generation chimeras), in which sequence regions proposed to be involved in substrate binding were swapped between GLUT2 and GLUT3. The diagram in Figure 5.1 shows the junction points of the sequence swaps in these constructs. As before, it was planned that mirror image constructs should be made.

It was thought that these constructs could be used to test various aspects of the model proposed in section 4.6: specifically, the helix 7 swap would: (1) test the hypothesis that helix 7 is solely responsible for fructose recognition in GLUT2 and for the isoform specific kinetics of galactose transport, (2) provide information on the nature and extent of influence of the N-terminal half of the transporter molecule, and (3) would indirectly test the proposal that the H7_{end}-H10_{end} sequence also influences the affinity of maltose binding.

It was proposed that the H7_{end}-H10_{end} sequence swap would: (1) specifically measure the extent of the involvement of this sequence in the exofacial binding of substrates -particularly of maltose and other C-4 substituted glucose analogues, and (2) indirectly test the proposal that it is helix 7 which is solely essential for fructose recognition by GLUT2, and the extent of the involvement of this sequence in the transport kinetics D-galactose by both isoforms.

The H10-H12 swap would: (1) test the proposal that sequences which lie beyond helix 10 (i.e. the cytoplasmic C-terminal tail) exert no effect on the substrate selection mechanism or on the transport kinetics of the two isoforms, and (2) act as a control for the mutagenesis procedure to show that the insertion of non-essential sequences did not produce any non-specific change in kinetic behaviour of each of these isoforms.

Additionally, it was hoped that expression of the GLUT2 series of these second generation constructs, would be less problematic than the first generation constructs (section 4.6.3). The foreign sequences in these new constructs would be internal, not involving the N- and C- termini. So it is possible that the targeting to, and insertion into the membrane of the oocyte might be more efficient.

5.2 Methods.

5.2.1 PCR- Primary Reactions.

To produce these constructs, a PCR based approach was used which was a modified version of a method described by Katagiri *et al* (Katagiri *et al.*, 1992). This method, outlined in Figure 5.2, involved the use of the first generation chimeric cDNAs as templates for the amplification of primary PCR products, which were then used in subsequent secondary reactions.

Oligonucleotide primers (37-61'mers) were constructed for use in the amplification of PCR fragment corresponding to the N-terminal half of the chimeric molecule. The sequences of all oligonucleotide primers are shown in Table 5.1. These primers corresponded to the positive strand of the template DNA sequence, and bound to the region of sequence next to the appropriate junction point for each construct. Note that the template used in the construction of the primary product "a", i.e. the fragment which corresponds to the N-terminal part of the protein, was the first generation chimera. The junction points are also outlined in Figure 5.1, and the primer binding regions are given in Table 5.1. Additionally, the primers were designed with "tails" -extra stretches of sequence corresponding to the positive strand of the other isoform cDNA (e.g. if the primer bound to a sequence of GLUT3 on the template cDNA, the "tail" would be composed of GLUT2 sequence).

These oligonucleotides were complimentary in sequence to other oligonucleotides (also 37-61'mers) which were designed for use in the amplification of the PCR fragment corresponding to the C-terminal half of the protein. These primers corresponded to the negative strand of the template sequence. The templates used for the construction of primary product "b" i.e. those which would correspond to the C-terminal portion of the chimeric protein, were wild type cDNA. GLUT2 encoded by pHTL217 was used as a template for the construction of the GLUT2 series, and GLUT3 encoded by pSPGT3 was used for the construction of the GLUT3 series.

The products of the primary PCR reactions were purified by agarose gel electrophoresis, the bands of appropriate size excised and the DNA recovered and purified by procedures described (section 2.6.4-2.6.6). For the helix 7 chimeras, the sizes of the primary PCR products "a" and "b" were 975bps and 725bps respectively. Likewise, for those with the helix 8 to helix 10 swaps the sizes of the fragments were 1170bps and 430bps, and for those with the helix 10 to helix 12 swaps, 1350bps and 250bps. Purified primary products for the GLUT2 mutants are shown on an agarose gel in Figure 5.3.

5.2.2 PCR- Secondary Reactions.

Primary PCR products "a" and "b" served as templates for the secondary reactions. See Figure 5.2. The last 30 bases of the 3' end of primary product "a" were complimentary to the last 30 bases of the 3' end of primary product "b". Upon the initial melt in the secondary PCR reaction, these overlapping ends anneal. Only external primers are added to the secondary reaction. These are complimentary to the 5' ends of the negative strand of the primary PCR fragments. After the initial melt and subsequent cooling the primary strands have annealed as described and the external primers have annealed as shown in the diagram. Each strand of this complex acts as a primer for extension of

the opposite strand, resulting in the amplification of a full length chimeric construct. After a few cycles of PCR a large proportion of the primary fragment strands will have annealed and been extended to form full length constructs. These serve as templates for the binding and extension of the external primers in subsequent rounds of PCR. This results in the amplification of the full length chimeric construct.

5.2.3 Vector and Cloning Procedure.

The cDNAs encoding each of the different glucose transporter isoforms have been cloned into several vectors for use in various expression systems. The vector pSP64T has been developed for expression of proteins in the *Xenopus* oocyte system. Each of the GLUT cDNA's have been cloned individually into the multiple cloning sites of pSP64T (Kayano *et al.*, 1990).

This vector contains two regions of untranslated sequence (UTR's) from the *Xenopus* β -globin gene. These sequences flank the cDNA open reading frame (ORF). The purpose of the UTR's is to aid recognition of *in vitro* transcribed mRNA by the *Xenopus* ribosome. This is thought to increase the efficiency of translation. The UTR's are also believed to further increase the efficiency of translation by increasing the stability of the mRNA in the cytosol of the oocyte, and thus prolonging the half life of the message (Kayano *et al.*, 1990).

Transcription of the coding region is driven by the powerful SP6 promoter. SP6 polymerase is commercially available. The SP64T vector encodes an ampicillin resistance gene for use in screening of positive clones. The backbone of this vector was obtained by digestion of the plasmid pSPGT4 with *Sal* I (Figure 2.1). Plasmid pSPGT4 has the cDNA of GLUT4 cloned into the pSP64T between the 5' and the 3' UTR's. *Sal* I restriction of this vector released both the GLUT4 coding sequence and a 200 base pair sequence which is part of the 3' UTR. The PCR fragments were cloned into the *Sal* I site (Figure 2.3). It was assumed that the loss of the 3' UTR sequence would not have a significant effect on the integrity of *in vitro* transcribed mRNA.

Ligations, transformations, and screening of colonies were performed as described (sections 2.5.3-2.5.8).

5.3 Results.

5.3.1 Results Using *Taq* DNA Polymerase.

Taq polymerase was the first enzyme that was used in the attempt to construct these mutants. This enzyme is commercially available. It is produced by the archaeobacterium *Thermus aquaticus*, which was originally isolated from hot springs, explaining why the polymerase displays extreme heat resistance. This property of heat resistance is exploited in PCR.

It was found that this enzyme produced high yields of primary product and secondary product for both series of chimeras. These are shown in Figures 5.3 and 5.4. The secondary products were restricted with *Sal* I and were cloned into the pSPGT vector backbone (Figure 2.3). Figure 5.4 shows samples of ligated construct and "empty" re-ligated vector as analysed by agarose gel electrophoresis. The ligated constructs were used to transform DJ15 α *E.coli* cells as described (section 2.5.7), and the plasmid DNA extracted from the resulting colonies and sequenced as described (sections 2.7.1-2.7.9). Oligonucleotides used to sequence the mutants are shown in Table 5.2.

The efficiency of production of colonies with the desired product was never 100%. The cloning of the secondary PCR fragments into the vector backbone was not directional and therefore some of the colonies recovered from transformation contained the vector with the coding sequence in the wrong orientation. These were not selected for sequencing. Often the colonies recovered from the transformation contained re-ligated vector alone.

Several clones were selected for each chimeric construct which, from agarose gel and restriction digest analysis were thought to be positive for the plasmid with the insert in the correct orientation. Sequencing of these showed that the PCR mutagenesis approach had been successful in producing each of the desired domain swaps. However, in each clone that was analysed the

fidelity of the sequence was compromised. It was found that *Taq* polymerase misincorporated bases at a rate of at least two mismatches per one thousand bases. Often in many of the clones this rate was higher.

At this point it was decided that the procedure would benefit from the use of newly commercially available polymerases- *Pfu* and *Vent*, both of which have an exonuclease proof reading activity.

5.3.2 Results Using *Pfu* DNA Polymerase.

This enzyme was used in an attempt to overcome the infidelity problems encountered with *Taq* polymerase. *Pfu* polymerase is just as thermostable as *Taq*, but has a higher fidelity of copying than *Taq* due to a 3' to 5' exonuclease proof-reading activity.

The reaction conditions used initially with this enzyme were identical to those used in a *Taq* reaction. However, the polymerase produced little or no primary PCR products with these conditions, and a large amount of primer-dimer extension product was produced. Primer-dimer extensions occur when the primers anneal to each other instead of to the template. This can occur if the annealing temperature is not correct, or if the primer anneal to themselves and begin to extend before the initial melt. To reduce the chance of this occurring the "Hot Start" PCR technique was employed (section 2.6.3). In this method the reaction mix is kept on ice until all the reagents have been added -with the exception of the polymerase. The PCR tubes are quickly transferred to the thermal cycler and an initial melt of 96°C for 10 mins is started -without the polymerase. After the initial melt all the strands of double helix DNA will have separated. On cooling down to the annealing temperature, the primers will anneal preferentially to the template rather than to themselves or to contaminating DNA fragments -events which would only occur at temperatures lower than the annealing temperature. Additionally, this

technique is thought to prolong the activity of the enzyme, since the proceeding melts after the enzyme has been added only last for a minute.

The yields of primary product were increased by the use of the hot start technique, but the yields of secondary PCR product remained extremely low. It was not possible to produce sufficient secondary PCR product for cloning into the pSPGT backbone. This problem was exacerbated by the fact that *Pfu* polymerase produces blunt-ended PCR fragments. Prior to ligation of the secondary PCR product to the vector backbone, the fragment was digested with *Sal* I to produce sticky overhangs that would be complimentary in sequence to the overhangs in the vector. However, for efficient cutting, *Sal* I requires a longer stretch of DNA sequence at each side of the restriction sequence than would be produced by a polymerase which produces blunt ended fragments. Subsequently, in an attempt to overcome the problem of low product yield, Vent polymerase was used.

5.3.3 Results Using Vent DNA Polymerase.

Vent polymerase also has a 3' to 5' exonuclease proof-reading activity, and therefore has a higher fidelity of copying than *Taq* polymerase. The manufacturers of this commercially available enzyme also claim that Vent produces higher yields of product than *Pfu*. For this reason it was decided to try Vent as an alternative to *Pfu* to overcome the problems of low yield.

The PCR parameters used with Vent were changed according to the manufacturers recommendations (section 2.6.3c), and hot start PCR was also performed. In using this enzyme, it was important that the extension time was strictly controlled to one minute per kilobase of sequence, in order that the exonuclease activity of this enzyme did not digest the ends of synthesised fragments and destroy the restriction sites, and also the regions of complimentary sequence in the primary fragments.

The yield of both primary and secondary PCR products gained with Vent was generally much higher than that obtained using *Pfu.* polymerase. Ligating the *Sal* I cut secondary PCR product was difficult, as in the case of the *Pfu.* produced fragments, possibly because Vent also produces blunt ended fragments which are difficult to restrict with *Sal* I.

Several clones from the GLUT3 series were chosen initially to screen. The DNA extracted and purified from these clones was subjected to restriction digest and agarose gel analysis, the results of which suggested that the colonies were transformants. However sequence analysis showed that the mutagenesis procedure had not been successful. The sequence that was cloned into the vector was template sequence. In all the clones analysed, the template sequence that was carried over was always the template from the production of the primary fragment "a". The reason for this is not known since theoretically carry-over of template from the primary reaction is not possible.

This approach was not pursued due to time restrictions. The amplification of secondary products and the ligation of the fragments produced in this procedure proved consistently problematic. Reasons for these difficulties may lie in the fact that the procedure requires the use of template that is the product of several previous rounds of PCR (i.e. the templates for the primary fragment "a"), and that *Sal* I is not a good choice of restriction sequence for the end primers.

Figure 5.1

Diagram of Second Generation GLUT2/ GLUT3 Chimeric Constructs.

This diagram shows a plan of the second generation GLUT2/GLUT3 chimeric constructs. The areas shown in black denote GLUT2 sequence, and the red regions GLUT3 sequence. Where the notation is GLUT2 H7, the construct is a GLUT2 molecule with a GLUT3 helix 7. Where the notation is GLUT2 H8-H10, the construct is a GLUT2 molecule with a GLUT3 sequence region from the start of helix 8 to the end of helix 10. Residue numbers of sequence regions of GLUTs 2 and 3 are shown above the corresponding junction points.

Figure 5.1

Diagram of Second Generation GLUT2/ GLUT3 Chimeric Constructs.

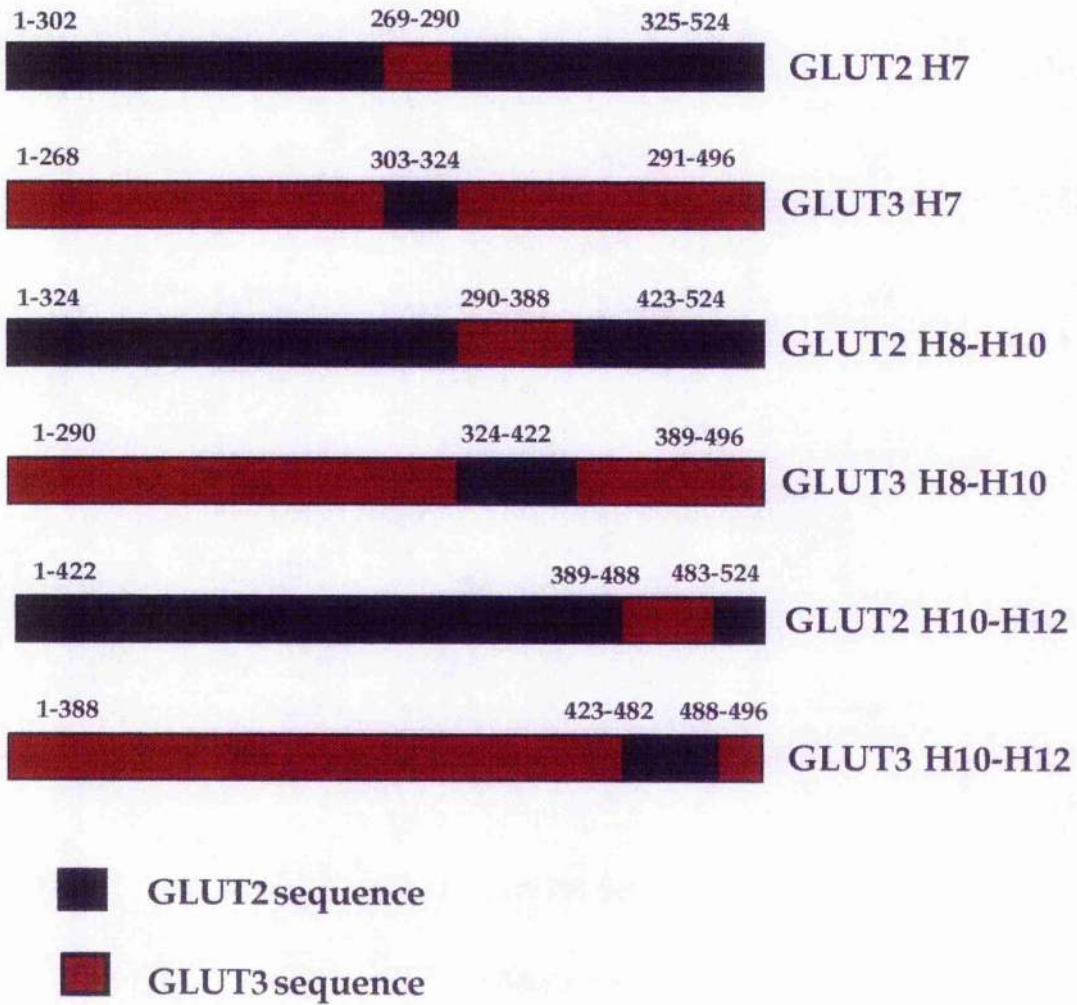


Figure 5.2.

Recombinant PCR Method Used to Construct Second Generation Chimeric Transporters.

This method was first described by Katagiri *et al* 1992, and it is similar to that used in the construction of the first generation chimeras. In this case however, the first generation chimeras themselves are used as templates for the generation of primary products "a", i.e. the fragments which correspond to the N-terminal portion of the resulting chimeric molecule. The template used for the generation of primary fragments "b" (which correspond to the C-terminal portion of the protein in the resulting chimeric protein) are wild type GLUT2 (for the GLUT2 series construction), or GLUT3 (for the GLUT3 series construction).

This diagram describes the construction of the GLUT2-H7 chimera (a GLUT2 molecule in which the helix 7 sequence is replaced with that of GLUT3), but this general method was also employed to make the other constructs.

The internal primer used to amplify primary fragment "a" for this mutant was designed to bind to the GLUT3 helix 7 sequence of the first generation chimera G2(7St). This primer also had a tail sequence which was GLUT2 in sequence. This would overlap with the GLUT2 sequence of primary product "b". Primary product "b" was amplified from GLUT2 cDNA, using a primer which bound to a region adjacent to helix 7, but which had a tail composed of GLUT3 sequence of helix 7. This sequence would overlap with the GLUT3 helix 7 sequence in primary product "a".

These primary products acted as templates in the secondary PCR reaction. After annealing, the overlapping lengths of primary sequence were extended to produce a full length chimeric construct, which was in turn amplified further in subsequent rounds of PCR. The GLUT2 external primers used in this reaction were designed with *Sal* I restriction sites. This allowed restriction of the full length PCR product to allow cloning into a *Sal* I restricted vector (Figure 2.3).

Figure 5.2 Recombinant PCR Method Used to Construct Second Generation Chimeric Transporters.

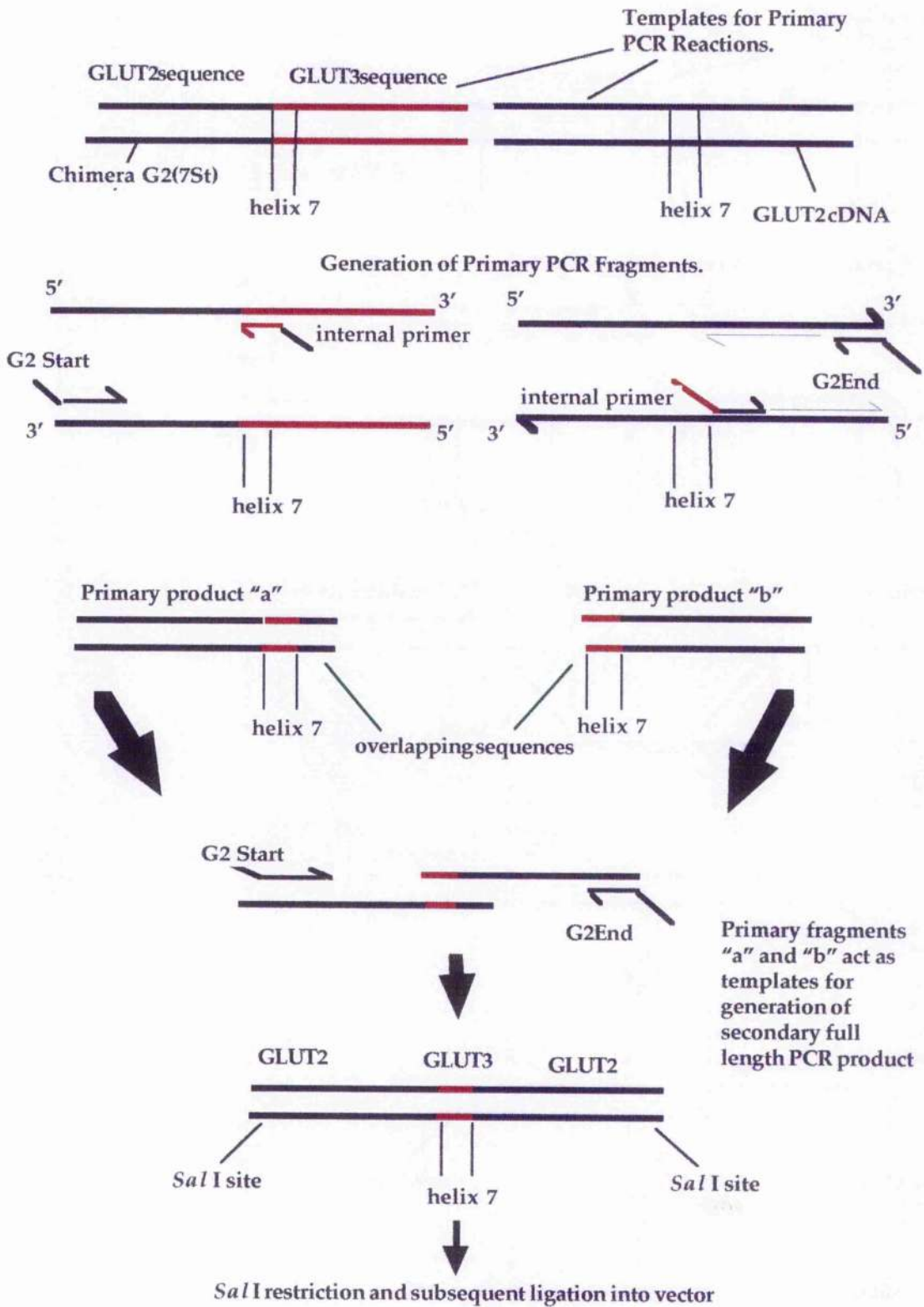


Figure 5.3

Agarose Gel of Primary *Taq* PCR Products.

Agarose gel showing the primary PCR fragments of the GLUT2 series of chimeric constructs. These fragments were run on a 1.6% agarose gel alongside *Bst*E cut λ DNA markers (not shown). The samples on the gel are as follows:

Lane	Sample	Size
1	GLUT2-H7 "a"	975bp
2	GLUT2-H8-10 "a"	1170bp
3	GLUT2-H10-12 "a"	1350bp
4	GLUT2-H7 "b"	725bp
5	GLUT2-H8-10 "b"	430bp
6	GLUT2-H10-12 "b"	250bp

Figure 5.3

Agarose Gel of Primary *Taq* PCR Fragments.

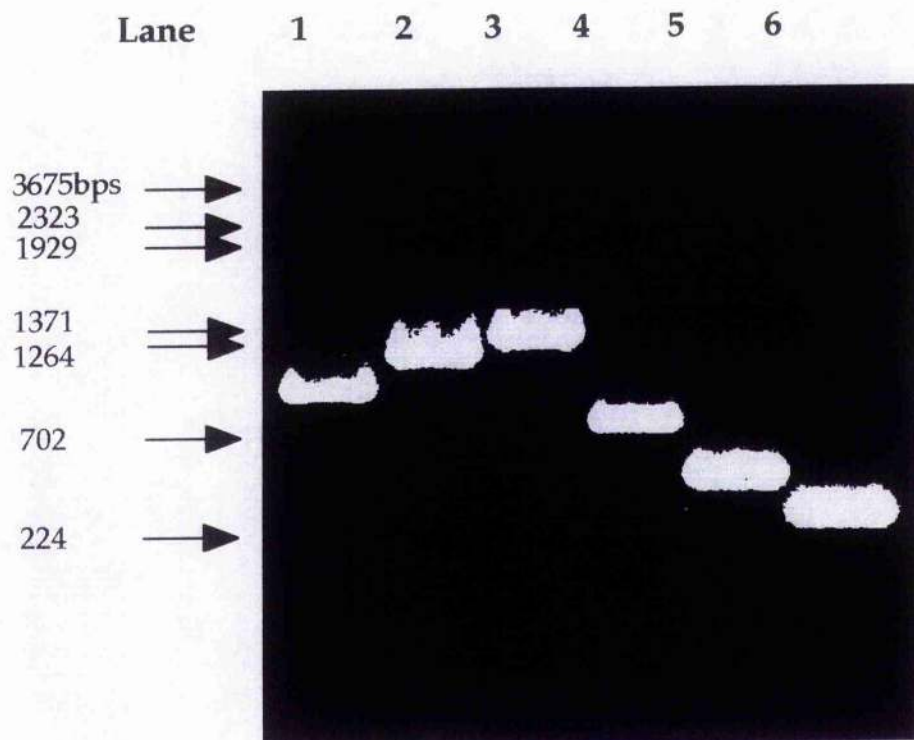


Figure 5.4

Agarose Gel of Secondary PCR Fragments, Unligated Vector and Ligated Chimeric Constructs.

This diagram shows a 1% agarose gel with samples of vector backbone (see Figure 2.3) which is self-ligated (Lane 2), uncloned secondary PCR product (Lane 3), and cloned secondary PCR product (Lane 4). *BstE* II cut lambda DNA markers are also shown on the gel (Lane 1).

Transformed DH5 α colonies which contained cloned PCR product were screened by running samples of miniprep plasmid DNA alongside self-ligated vector. Clones which contained vector + ligated PCR fragment were apparent by size.

Figure 5.4

Agarose Gel of Secondary PCR Fragments, Unligated Vector and Ligated Chimeric Construct.

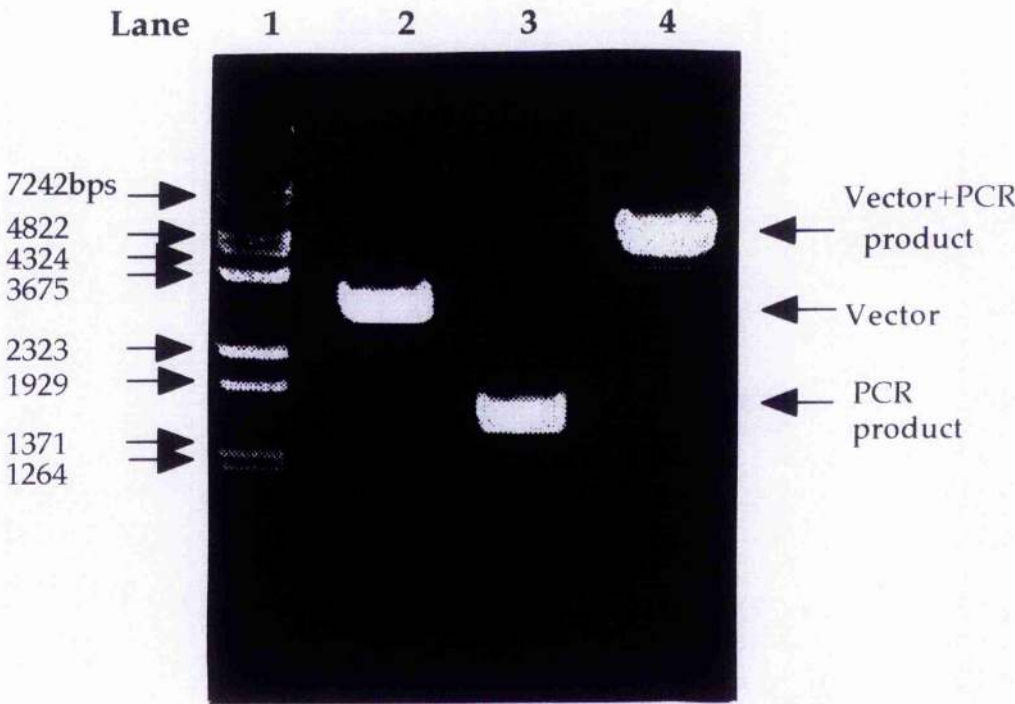


Table 5.1
Oligonucleotides Used in Recombinant PCR.

Oligonucleotides for the GLUT2 series:

External amplification oligo's:

GLUT2 Start *gtggaggtggac* TTCCGCACAGACCTGGAAATTGACA
 GLUT2 End *gtggaggtggac* CAGACGGTCCCTTAATTGTTTCTGT

Junction oligo's:

1588 (1) GCCACATGCAGCATCAGTGGCCACTAGAAATAGGCTGTGGTAGCTGGACACTCTA AAGAGC
 1585 (2) GGACGGTGGTCTTGACTGAAAAAAGCAGCCACAAATAAACAGGGAATCGGCCCTGGTCCA
 1586 (3) TCAAAAAGACCTTTCCTTTGGTTCGGAACTTGAAGAAAGTAAAAAGCCAAAGAAAGTAAATG
 1583 (4) CAGCTCTTGGATCAATGCTGTGTCTATTAACAACCAAGATTTTTCAGAGCGGCTGGT
 1589 (5) ATTGCACCAGCCCCCACTCCCTGGTTATTTGGCTGAGTTTTCAGTCAAGGACCACCGT
 1589 (6) ATTGCACCAGCCCCCACTCCCTGGTTATTTGGCTGAGTTTTCAGTCAAGGACCACCGT

Oligo's for the GLUT3 series:

External amplification oligo's:

GLUT3 Start *gtggaggtggac* TCAACCCCTAGATCTTTCCTTGAAGAC
 GLUT3 End *gtggaggtggac* CAGACGGAGAGGTGGCTTTCCTCATGCC

Junction oligo's:

1510 (1) CAATTTCCGGGAATCAATGGCAATTTTACTACTCAACAGGAATCTTCAAGGATGCAGGT
 1509 (2) ATTGGCCGAGGCCCGATCCCGTGGTCACTCCCGGAACTCTTCAGCCAGGCCCCCGGC
 1504 (3) CTCCTGGCCCTTACCCCTGTACATTTTAAAAGTCCCTGAGACCCGTTGCAGGACFTTT
 1506 (4) ACACCTGCATCCTTGAAGATTCCTGTGAGTAGTAAAAAATGCCAATTTGATTCGGAAAAAT
 1507 (5) GCCTGGGGCCCTGGCTGAAAGATTCGGCCACCATGAACCCAGGATCGGGCCCTGGCCCA
 1508 (6) TCAAAAAGTCTGCCACCGGCTCAAGGACTTTAAAAAATGTGAAACAGGTTAAAAGCCACGG

Sequences corresponding to GLUT2 are underlined. Sequences which encode a *Sma* I restriction site used in subcloning of PCR fragments are written in lower case italics. All oligo's are written 5' to 3'.

Table 5.2

Sequencing Primers.

This table shows a list of the oligonucleotide primers which were used to sequence the second generation chimeric constructs. Oligonucleotide sequences are written 5' to 3'. Primers designated "T" were of sense (top) strand sequence, and therefore bound to the antisense strand of the cDNA, and those designated "B" corresponded to the antisense (bottom) sequence, and therefore bound to the sense strand of the cDNA.

Table 5.2

Sequencing Primers.

GLUT2 Primers.

G2 9T	TCCGCACAAGACCTG
G2 7T	GCAGCTGCTCAACT
G2 6T	TTTCATCAGCTGGCC
G2 5T	GAAGAAGCATCGAGT
G2 4T	ATTGGAATGAGTGGG
G2 3T	CCACCTCCTGCTGCT
G2 2B	AATTTCCCTCAAAGA
G2 3B	AGCAGCAGGCGTGG
G2 4B	CCCACCTCATTCCAAT
G2 5B	ACTCGATGCTTCTTC
G2 6B	GGCCAGCTGATGAAA
G2 7B	AAAGCTGGAATACAG

GLUT3 Primers.

G3 7T	TCACCCCTAGATCTTTCTTGAAGAG
G3 6T	CTCTGATATTTGCCA
G3 5T	GACTGTGTAAAGTAG
G3 4T	CCAGATTTTTGCTCA
G3 3T	ATCTATGCCACCATC
G3 2T	ACTGGACCTCCAAC
G3 1B	GGGAGAGCTGGCTTT
1535	CAGTCATGAGCGGT
G3 3B	GTAGCTGGACACTCT
G3 4B	TGAGCAAAAATCTGG
G3 5B	CTACTTTACACAGTC
G3 6B	TGGCAAATATCAGAG

CHAPTER 6

Kinetic Analysis of GLUT3 Helix 8 Mutants.

6.1 Introduction.

In Chapter 4, a working model was proposed for substrate recognition by GLUT2 and GLUT3 (section 4.6). In this model, helix 7 was proposed to play an important role in substrate selection and in determining the kinetics of transport. Furthermore, a region between the end of helix 7 and the end of helix 10 was shown to influence the affinity of the exofacial binding site in GLUT2 and GLUT3 for maltose, and it is speculated that, in the exofacial binding site, this region may interact with the C-4 hydroxyl of glucose.

It has been proposed that five of the twelve putative transmembrane regions are moderately amphipathic: these are helices 3, 5, 7, 8 and 11 (Mueckler, 1985). It was hypothesised that these helices may form an aqueous channel through which glucose could move during the transport process. Recent evidence suggests however, that the C-terminal portion of the transporter is directly involved in the formation of the exofacial and the endofacial binding sites, while the N-terminal half may provide a packing surface which allows the correct alignment of the helices of the C-terminal half (Cope *et al.*, 1994) (section 1.8). Therefore, the helices in the C-terminal half of the transporter which are moderately amphipathic are helices 7, 8 and 11. Cytochalasin B is thought to bind to a region between helices 10 and 11 (Holman & Rees, 1987), and ATB-BMPA is thought to bind to a region between helices 7 and 8. (Davies *et al.*, 1991) (section 1.6).

Helices 7 and 8 contain many conserved polar residues (Figure 1.2). Several of these have been shown by site directed mutagenesis studies to be important in the formation of the exofacial and endofacial binding sites and in the conformational change of the protein which is associated with transport (Table 6.1).

On the basis of these observations it was decided that helices 7 & 8 would be excellent targets for site directed mutagenesis studies. This chapter

deals with the study of the eighth helix of GLUT3. GLUT3 was chosen for this study for the following reasons. (1) Most site directed mutagenesis studies have focused on GLUT1 as a template for mutagenesis, and so there is a lack of information on the GLUT3 isoform. (2) The study of GLUT3 may serve to build on the working model we have proposed for substrate selection by GLUT2 and GLUT3. (3) The information collected from the study of this helix in this isoform may be directly compared to data from previous GLUT1 helix 8 studies.

Additionally, it may be possible to use the substrate analogue approach to investigate the exact nature of the effect (if any) on each of the substitutions. This could provide information on the nature of substrate binding in terms of which carbon position binds to which residue, either at the exofacial binding site, at the endofacial binding site, or within the channel.

6.2.1 Use of Site Directed Mutagenesis.

Site directed mutagenesis is a powerful tool in the structural dissection of proteins. Studies have been conducted on various regions of the transporter structure throughout both the N-terminal and C-terminal halves of the protein, within the putative transmembrane helices and in the extramembranous loops. The majority of this work has used GLUT1 as a template for site directed mutagenesis, however there are some studies on the other isoforms. GLUT4 is often the focus of this type of study: however in this case the technique has been employed in attempts to identify residues of importance in targeting and translocation of this isoform to the plasma membrane in response to insulin.

Table 6.1 summarises all the information derived from site directed mutagenesis studies (i.e. single amino acid substitution studies) to date, including those mutations which were found to have no effect on structure

and transport activity. The expression system used for each mutant transporter and details of the specific effects of the mutation are shown in this table, along with references for the publication of each study. Some of the important findings of this work are discussed below.

6.2.2 Substitution of Conserved Polar Residues.

As discussed previously, helices 3, 5, 7, 8 and 11 are predicted to be moderately amphipathic and may be able to form the aqueous channel through which glucose will pass during transport. There are many conserved residues distributed throughout these helices. These include serine, threonine, asparagine, glutamine and tyrosine residues, all of which have side chains capable of interaction with glucose via hydrogen bonding.

In an effort to map the residues involved in the formation of the exofacial and endofacial binding sites, and in the formation of the channel, several of these conserved polar residues have been substituted in the GLUT1 molecule, and parameters such as ATB-BMPA binding examined.

ATB-BMPA has been shown to bind to the exofacial binding site, and it has been shown to photolabel a region between helices 7 and 8 (Davies *et al.*, 1991) (section 1.6). The site of binding and the site of photolabelling need not be identical, but it is likely that they are in close proximity.

Three conserved polar residues in helices 7 and 8 of GLUT1 have been substituted with non-polar residues. The substitutions were Asn²⁸⁸-> Ile²⁸⁸ and Gln²⁸²-> Leu²⁸² in helix 7 and Asn³¹⁷-> Ile³¹⁷ in helix 8 (Hashiramoto *et al.*, 1992) (table 6.1). The substitution of Asn²⁸⁸ and Gln²⁸² resulted in a 50% reduction in deGlc transport activity in comparison to wild type GLUT1 deGlc transport. The endofacial binding site was not disrupted by any of the three substitutions, as each of these mutants could be labelled with cytochalasin B at levels comparable to wild type GLUT1. However, the Gln²⁸² substitution

resulted in disruption of the exofacial binding site: this mutant displayed a severe loss of ability to bind ATB-BMPA, and was labelled at a level which was only 5% that of wild type GLUT1. The K_i for 4,6-*O*-ethylidene-D-glucose inhibition of deGlc transport by the Gln²⁸⁸ mutant was 10-fold higher compared with wild type GLUT1. Since this compound interacts competitively with the exofacial binding site, this is further evidence that this substitution results in disruption of the exofacial binding site. Hashirimoto *et al* concluded that Gln²⁸² (located in helix 7) is part of, or very near to, the exofacial binding site.

Other conserved polar residues in GLUT1 have been substituted: Asn¹⁰⁰ (helix 3), Gln¹⁶¹ (helix 5), Tyr²⁹² (helix 7) and Tyr²⁹³ (helix 7) have been replaced sequentially with hydrophobic residues (Mueckler, 1994a). These are shown in Table 6.1. In this study, none of the substitutions had any effect on transport activity, with the exception of Gln¹⁶¹. The non-conservative substitution of this residue with leucine produced a 50-fold decrease in the transport of deGlc with comparison to wild type GLUT1. However if this residue was substituted with asparagine which, like glutamine also has a polar side chain, the transport activity was reduced by only 10-fold. When the Gln¹⁶¹ → Asn mutant was further analysed, it was found that this decrease in transport activity was due not to a decrease in the K_m of the transporter for zero-*trans* deGlc uptake. Rather the effect was due to a decrease in turnover number by 7.5-fold with comparison to wild type GLUT1. However, it was also noted that the K_i for 4,6-*O*-ethylidene-D-glucose inhibition of deGlc transport was also increased by 18-fold with respect to wild type GLUT1. Based on these results it was suggested that Gln¹⁶¹ may comprise part of the exofacial binding site, and may also be important in the ability of the molecule to undergo the conformational change associated with transport. The importance of this residue in the conformational change mechanism was specifically suggested by the decreased turnover number of the mutant.

In marked contrast with the above study, Mori *et al* have shown that substitution of Tyr²⁹³ with Ile results in a drastic reduction in V_{\max} for deGlc transport (Mori *et al.*, 1994). Also, this reduction in transporter activity is associated with a complete loss of cytochalasin B binding, and photolabeling. Mori *et al* have interpreted this to indicate that the Tyr²⁹³ → Ile locks the transporter in an outward-facing conformation. Furthermore, Mori *et al* have observed that this mutant can still bind non-transported C-4 and C-6 substituted hexose analogues, but cannot catalyse transport. From this, they have concluded that Tyr²⁹³ may be involved in closing the exofacial binding site of the transporter around the C-4 and C-6 of D-glucose (see also section 4.6.1d for discussion of the possible involvement of the C-4 hydroxyl in exofacial binding).

Tyrosine residues Tyr²⁸ (helix 1), Tyr¹⁴³ (helix 3), Tyr²⁹² (helix 7), Tyr³⁰⁸ (helix 8) and Tyr⁴³² (helix 12) are conserved in all the GLUT isoforms (residue numbers correspond to those of GLUT1). These residues in GLUT4 have all been individually replaced with phenylalanine and expressed in LTK cells (Wandel *et al.*, 1994). Transient expression levels and subcellular distribution were found to be comparable to wild type GLUT4. Transport activity of the Tyr¹⁴³ and Tyr²⁹² mutants was decreased, as was the ability of these constructs to be photolabelled with cytochalasin B. The Tyr²⁹³ mutant also displayed loss of ability to be photolabelled by cytochalasin B but showed no decrease in transport activity. Additionally, the exofacial binding of 4,6-O-ethylidene-D-glucose and ATB-BMPA labelling were unaffected. Wandell *et al* concluded from this that Tyr¹⁴³ and Tyr²⁹³ may be important transport catalysis by GLUT4 and Tyr²⁹³ may be part of the cytochalasin B binding site.

Finally, asparagine⁴¹⁵ in helix 11 of GLUT1 was substituted with aspartate (Ishihara *et al.*, 1991). This substitution resulted in severely impaired transport activity. This was thought to be due to disruption of transporter

structure, caused perhaps by the introduction of a negative charge into a membrane spanning helix.

6.2.3 Substitution of Conserved Tryptophan Residues.

Cytochalasin B has been shown to photolabel a tryptic fragment of GLUT1 (residues 389-412), which comprises part of the loop connecting helix 10 and helix 11, and part of helix 11 itself (Holman & Rees, 1987). Trp³⁸⁸ (helix 10) and Trp⁴¹² (helix 11) are in proximity to this site, and have been implicated as being important in the transport mechanism because they have a fluorescence excitation wavelength similar to that required for cytochalasin B photoactivation (Inukai *et al.*, 1994).

It has been shown by several studies, that replacement of either of these tryptophan residues with either glycine or leucine, results in decreased deGlc or 3-O-methylglucose transport, when expressed in either *Xenopus* oocytes, CHO or COS-7 cells (Garcia *et al.*, 1992, Katagiri *et al.*, 1993, Schurman *et al.*, 1993a). The substitution of residue Trp⁴¹⁰ with leucine in GLUT3 (Trp⁴¹⁰ is the GLUT3 equivalent of Trp⁴¹² in GLUT1) also produces a decrease in deGlc transport activity (Burant & Bell, 1992b).

Although there is conflicting evidence, the substitution of Trp⁴¹², has been reported by two groups to produce a significant decrease, but not abolition of cytochalasin B binding and photolabeling (Katagiri *et al.*, 1991, Schurman *et al.*, 1993b). These studies also show that substitution of Trp⁴¹² has no effect on labelling by ATB-BMFA or IAPS-forskolin. Additionally, it has been reported that the endofacial binding of the non-transported sugar analogue n-propyl- β -D-glucoside, is significantly diminished by the Trp⁴¹² substitution (Katagiri *et al.*, 1991). These results suggest that the endofacial binding site is altered by this substitution. Also, since the decrease in transport activity reported in these studies is associated with a decrease in V_{max} , it is thought that the Trp⁴¹²

substitution alters the rate of alternation between the inward- and outward-facing conformations. The substitution of Trp³⁸⁸ in GLUT1 has also been reported to decrease photolabelling by cytochalasin B, and by forskolin (Inukai *et al.*, 1994, Katagiri *et al.*, 1993, Schurman *et al.*, 1993a). These studies, which have collectively reported a role for both Trp⁴¹² and Trp³⁸⁸ in cytochalasin B photolabeling, led Inukai *et al* to replace both of these residues in GLUT1 with leucine (Inukai *et al.*, 1994). The transport activity of this mutant is comparable to that displayed by the substitution of the single Trp⁴¹² in a mutant constructed and expressed in the same system (Inukai *et al.*, 1994). However, with the double substitution, deGlc transport is abolished, and this is associated with a complete loss of cytochalasin B photolabelling. From this, Inukai *et al* have proposed a model in which cytochalasin B can photolabel the transporter at either Trp⁴¹² or Trp³⁸⁸.

6.2.4 Substitution of Conserved Proline Residues.

It has been reported that there is a high frequency of occurrence of proline residues in the transmembrane segments of integral membrane transport proteins (Brandl & Deber, 1986, Williamson, 1994). Prolines display a unique ability to produce not only large kinks, but localised movement within their helices via *cis-trans* isomerisation of the Xaa-Pro peptide bond (Xaa = an unspecified amino acid). This has led to speculation that prolines may play a dynamic role in the molecular mechanism of the glucose transporters (Tamori *et al.*, 1994).

Based on this, the presence of several prolines in the highly conserved sequence FFEVGPPIPW (residues 378-388 in helix 10 of GLUT1), was thought to be of significance, since studies utilising tryptophan fluorescence have indicated that helix 10 may be a highly mobile region (Pawagi & Deber, 1990) (section 1.5.1).

Proline³⁸⁵ has been substituted with isoleucine and glycine, and expressed in CHO cells (Tamori *et al.*, 1994). The Pro³⁸⁵->Gly substitution produced no detectable change in transport activity or in ligand binding. However, substitution of this residue by isoleucine resulted in severely reduced transport activity and a substantial loss of ATB-BMPA labelling. Labelling with cytochalasin B was comparable with wild type levels. Tamori *et al* concluded that disruption in the transport function was therefore due to disruption of the exofacial binding site. The substitution of this proline residue by glycine was thought to maintain the atomic arrangement of the conserved motif because the glycine did not interfere with the mobility of Pro³⁸³ and Pro³⁸⁷, and thus conformational change was still possible. Therefore, it was suggested that Pro³⁸⁵ was involved in mediating a conformational change in helix 10 which facilitated the packing of helices in an arrangement which either exposed the exofacial or the endofacial binding sites.

In a subsequent study however, all the prolines in helices 6 and 10 were individually replaced either by alanine or glycine. The three proline residues in helix 6 of GLUT1 are conserved between all of the human glucose transporter isoforms, with the exception of GLUT2. Therefore, these helix 6 residues were also substituted with the equivalent residue of GLUT2 (Wellner, 1995). None of these substitutions were shown to have any effect on transport activity, but changing the helix 10 prolines with glutamine almost completely abolished deGlc transport. Since glutamine is a neutral, polar residue, it was inferred that the specific chemical structure of the substituted amino acid side chain was essential, but the unique property of proline for *cis-trans* isomerisation was not important.

It is still unknown however, if the collective role of these prolines is important in transporter function. Substitution of one proline residue for example might be adequately compensated for by neighbouring prolines. What is required to clarify this situation, is a study in which the collective role of

prolines is investigated. Such a study might involve the substitution of several or all of the prolines in the same helix, or in the entire transporter molecule.

6.2.5 Substitution of Conserved Cysteine Residues.

It has been suggested that cysteines may play a role in transporter conformational stability (reviewed in Carruthers, 1990, Walmsley, 1988), and in the oligomerisation of glucose transporters (Herbert & Carruthers, 1992).

Wellner *et al* have made the following single cysteine substitutions in GLUT1: Cys¹³³->Ser, Cys²⁰¹->Gly, Cys²⁰⁷->Ser, Cys³⁴⁷->Ser, Cys⁴²¹->Arg and Cys⁴²⁹->Ser (Wellner, 1994). None of these individual substitutions produced any change in transport activity. However, it was shown from these substitutions that Cys⁴²⁹ in the sixth external loop and Cys²⁰⁹ in the large cytoplasmic loop are those which are modified by various thiol-group reactive agents including p-chloromercuribenzenesulphonate (pCMBS) prior to transporter inactivation.

This finding that none of the individual cysteine substitutions produced any changes in on the catalytic turnover of GLUT1, questions the suggestions of Carruthers, Walmsley, and Herbert, that disulphide bridges are involved in GLUT1 intramolecular stability, and transporter oligomerisation.

Further to the above study, Due *et al* have constructed a GLUT1 transporter in which all six cysteines have been replaced. This mutant retains GLUT1 kinetics, therefore, this study also argues against the involvement of disulphide bridges in transporter stability and oligomerisation. The initial purpose of constructing this cysteineless mutant was for use in structure function studies. The cysteineless construct can serve as a template for the reintroduction of cysteines into other sites of interest. These can be chemically modified by sulphhydryl-specific agents, thereby allowing the topological mapping, and assessment of the importance of the specific residues of interest.

This technique is known as cysteine scanning mutagenesis. A modification of this technique, known as excimer fluorescence may also be applied to this cysteineless mutant. This technique has been extremely useful in the study of the tertiary structure of the lactose permease transporter of *E.coli* (section 6.6).

6.2.6 Residues in Extramembranous Regions.

It has been shown that substitution of Asn⁴⁵ in the large extracellular loop with either Asp, Trp or Gln abolishes *N*-linked glycosylation of GLUT1 (Asano *et al.*, 1991). This subsequently leads to a 2-fold decrease in the affinity of the transporter for D-glucose as measured by K_m . It is known that *N*-linked glycosidic groups can stabilise the tertiary structure of proteins and, in membrane proteins, can help to anchor the protein in the lipid environment by interaction with some lipid components (Stryer, 1988). Whether this happens with the GLUTs is not known. Certainly the glycosylation of GLUT1 is important in its function since the affinity of the aglyco-GLUT1 molecule for glucose is decreased 2-fold. This also leads us to question the effect of expression of the glucose transporters in heterologous systems such the *Xenopus* oocyte, where glycosylation may be altered.

6.2.7 The C-Terminal Cytoplasmic Tail.

The C-terminal cytoplasmic tail (residues 450-492) has been shown to be important in the ability of the molecule to undergo conformational change. The single-site alternating conformation model is shown in Figure 1.3. Oka *et al* have shown that removal of the last 37 amino acids from the C-terminal tail of GLUT1 results in abolition of transport (Oka, 1990). This loss of transport is accompanied by a complete loss of ATB-BMPA binding, however cytochalasin B binding is not reduced. Oka *et al* have concluded from this, that the

transporter is locked in an inward-facing conformation. Removal of the last 12 amino acid residues from GLUT1 does not produce this effect (Lin *et al.*, 1992).

In order to establish the minimum length of cytoplasmic tail needed for the molecule to achieve the conformational change necessary for transport, Muraoka *et al.* have constructed a range of C-terminally deleted mutants (Muraoka, 1995). It has been shown that deletion of more than 24 amino acid residues from the cytoplasmic tail results in perturbation or abolition of transport activity. Furthermore, substitutions of residues Phe⁴⁶⁷ and Arg⁴⁶⁶ produced no significant effect. These highly conserved residues are at the seemingly critical positions of 26 and 27 residues from the end of the cytoplasmic tail, and yet their substitution produced no significant effect. Therefore, Muraoka *et al.* have concluded that it is the length of the tail that is critical for function rather than the amino acid content.

Katagiri *et al.* have also investigated the importance of the C-terminal tail in transporter function. With the observation that the C-terminal cytoplasmic tail of each of the isoforms was variant in size and sequence, Katagiri *et al.* proposed that perhaps this region of the transporter was responsible in determining the specific kinetics of each isoform. The last 37 amino acids of the cytoplasmic tail of GLUT1 were replaced with those of GLUT2 (Katagiri *et al.*, 1992). This chimeric construct was expressed in CHO cells and the K_m for deGlc was found to be 3-fold higher than that of wild-type GLUT1. It was also shown that the V_{max} of this construct was ~4-fold higher than wild type GLUT1. From this, it was inferred that the C-terminal tail of GLUT2 was conferring "GLUT2-like" kinetic properties on the GLUT1 molecule. However the K_d value of this mutant for cytochalasin B was unchanged with comparison to wild type GLUT1, suggesting that the changes in transport kinetics were brought about by changes in the turnover number. As was discussed in Chapter 4, additional problems with this study result in the need for caution in the interpretation of these results.

The C-terminal cytoplasmic tail was again implicated as being important in transport kinetics in a study by Buchs *et al* (Buchs *et al.*, 1995). Replacement of the last 30 residues of the carboxy-terminus of GLUT4 with residues corresponding to GLUT2 resulted in a transporter which displayed an affinity for 3-O-methyl glucose which was intermediate between GLUT2 and GLUT4. Replacing a region from the start of the large intracellular loop of GLUT4 to the end of the carboxy-terminus with corresponding GLUT2 sequence resulted in transporter which displayed transport kinetics similar to GLUT2.

Further to the above study, Due *et al* replaced the terminal 29 amino acid residues of GLUT1 with those of GLUT4 (Due *et al.*, 1995b). This had the effect of reducing the V_{\max} of the GLUT1 molecule. Also replacing 29 or 73 amino acid residues of GLUT4 with those of GLUT1 increased V_{\max} to between a third and a half of GLUT1 wild type, although the affinity for substrate decreased by half. It was concluded from this that the C-terminal cytoplasmic tail was important in determining transporter function and the last 29 amino acid residues are important in determining the transporters affinity for substrate.

It has been shown that GLUT1 exhibits the property of accelerated exchange i.e. the presence of substrate on the opposite (*trans*) side of the membrane stimulates the transport exchange rate by increasing the rate of reorientation of carrier from the inward-facing conformation to the outward-facing conformation (or *vice versa*). This phenomenon is also known as *trans*-acceleration (section 1.4.3.3). The GLUT4 isoform does not display this phenomenon. Dauterive *et al* have examined the role of the C-terminal cytoplasmic tail in this property of murine GLUT1 (Dauterive *et al.*, 1996). In this study it was shown that replacement of the murine GLUT4 cytoplasmic tail onto a GLUT1 molecule abolished the GLUT1 property of accelerated exchange. This also had the effect of increasing turnover number by 1.6-fold. However, replacing the GLUT4 tail with that of GLUT1 did not confer the

accelerated exchange property of GLUT1 onto the GLUT4 molecule. It did however, produce an increase the turnover number of this construct. The conclusion that these authors arrived at was that the GLUT1 C-terminal cytoplasmic tail permits the accelerated exchange phenomenon, however it is not solely responsible for it, and it may require interaction with other sequences in the same GLUT1 molecule. Also, from their findings Dauterive *et al* further concluded that the C-terminal tail may act to restrict the kinetics of each transporter isoform, since mutations in both the GLUT1 and GLUT4 isoforms can act to increase the transport activity of the transporter. Thus they have taken this to indicate that the C-terminal tail may be a target for physiological factors which may, through covalent modification or direct binding, regulate the intrinsic activity of both GLUT1 and GLUT4. This aspect of transport is not discussed in this thesis, however evidence to suggest that the intrinsic activity of GLUT1 and GLUT4 is regulated by cellular factors is (reviewed in Stephens, 1995).

This has not been observed in human chimeric transporters where the carboxy-terminus is exchanged between human GLUT1 and human GLUT4, or between human-rat GLUT1-GLUT4 chimeras (Burant & Bell, 1992a, Pessino, 1991).

6.2.8 Naturally Occurring Mutations.

Two naturally occurring polymorphisms have been reported in the human GLUT2 gene (Tanizawa *et al.*, 1994). These were Ile¹¹⁰ which had mutated to Thr, and Val¹⁹⁷ which had mutated to Ile. The Ile¹¹⁰->Thr polymorphism was found to occur at equal frequencies in patients with non-insulin dependent diabetes and control subjects. The Val¹⁹⁷->Ile polymorphism was found in a female patient who developed gestational diabetes. However, the relevance of this genotype to the diabetic state of this

patient was not clear, as she made a full recovery after her pregnancy was over. Therefore, to test the specific effects of these polymorphisms on GLUT2 function, Mueckler *et al* have created the mutations individually in plasmid encoded GLUT2 and expressed these constructs in *Xenopus* oocytes (Mueckler, 1994b). They have shown that the Ile->Thr mutation results in a transporter which exhibits identical behaviour to wild type GLUT2. However, the Val->Ile mutation abolishes deGlc transport. Although Val->Ile is a conservative substitution, the increased size of the isoleucine side chain relative to valine may act to block the transport of deGlc.

6.2.9 Transmembrane Helix 8 of GLUT1.

There have been several models proposed which describe the tertiary packing of the transmembrane helices of GLUT1. Baldwin has described two possible packing schemes whereby a channel is formed by the clustering together of helices 1, 5, 6, 7, 11 and 12, or alternatively by the clustering of helices 7, 8, 10 and 11 (Baldwin, 1993). Cope *et al* have suggested that the helices of the N-terminal half of the protein do not form the channel directly, but are necessary for the overall helix packing arrangement (Cope *et al.*, 1994). Recently, Zeng *et al* have utilised advances in protein structure prediction algorithms to build two models which describe the helical packing of GLUT1 (Zeng *et al.*, 1996). These are shown in Figure 1.9. It is interesting to note that in both these models helices 7, 8 and 11 line the channel. Zeng *et al* note in their study that three of the four critical residues that have been identified by mutagenesis studies all lie in the channel lining helices of both these models. Gln²⁸² (Hashiramoto *et al.*, 1992) lies in helix 7, and Trp⁴¹² (Garcia *et al.*, 1992, Inukai *et al.*, 1994, Katagiri *et al.*, 1991, Schurman *et al.*, 1993a) and Asn⁴¹⁵ (Ishihara *et al.*, 1991) both lie in helix 11.

In view of the importance of helix 8 in the binding site of ATB-BMPA and as suggested by its place in these hypothetical models, it is surprising that no critical residues have so far been identified in this helix. In Chapter 4 a model for substrate selection and isoform specific transport kinetics was proposed in which a region between the end of helix 7 and the end of helix 10 was suggested to be involved in determining the affinity of the exofacial binding site. It is possible that helix 8 is involved in this sequence.

There are several polar residues in this helix which are conserved throughout the GLUT family. These include a tyrosine, an asparagine and two threonines, three of these residues Thr³⁰⁸, Asn³¹⁵, Thr³¹⁹ (GLUT3 residue numbers given) are predicted to lie on the polar face of the helix (Figures 6.1 and 6.2). It was decided therefore to use a site directed mutagenesis approach to investigate this helix and to attempt to determine the residues important in binding site and channel formation. Previous studies have largely used GLUT1 as a template for mutagenesis, therefore GLUT3 was chosen as a template in this mutagenesis study as there is a paucity of information available regarding this isoform. GLUT3 also has advantages over GLUT2 as a template for amino acid substitution: GLUT3 has a low K_m value for deGlc zero-*trans* entry into *Xenopus* oocytes, and therefore the kinetics of this isoform are easier to measure than the GLUT2 isoform which exhibits a very high K_m value for this transport event. Cytochalasin B also inhibits uptake of deGlc by GLUT3 more efficiently than GLUT2. This will enable us to accurately investigate the effects of amino acid substitution on the endofacial binding site. Furthermore, immunoprecipitation of GLUT2 is not possible (Jordan & Holman, 1992). To quantitate the amount of this protein at the plasma membrane by comparative immunoblot procedures a standard protein sample of known concentration is required. A GLUT2 standard is not available: quantification of the protein concentration in such a standard would require equilibrium binding studies to be carried out using [³H] cytochalasin B in the presence and absence of D-

glucose. The number of D-glucose sensitive cytochalasin B binding sites would be equivalent to the number of transporters in the sample, and protein concentration would be calculated from this by Scatchard analysis. This is not possible for GLUT2 as a consequence of the inability to immunoprecipitate it and the high K_d value of GLUT2 for cytochalasin B. The K_d for cytochalasin B dissociation from GLUT2 is $1.7\mu\text{M}$ (Axelrod & Pilch, 1983), and the concentrations of cytochalasin B required to perform equilibrium binding studies on GLUT2 exceed the solubility limit of the ligand ($\sim 50\mu\text{M}$).

6.3 Methods.

6.3.1 Alanine Scanning Mutagenesis.

It was decided to utilise an alanine scanning approach in the mutagenesis of helix 8. This approach involves the sequential replacement of each of the amino acid residues in the region of interest, in this case helix 8, alanine. Alanine is chosen because it is small in size and electro-neutral. Thus, mutating a particular residue to alanine effectively removes the side-chain properties of the original residue and leaves a "hole" in the helix. Additionally, no steric interference is introduced by alanine to confuse the results of the analysis, so that only the effect of removing the original residue of interest is measured. Since alanine is neutral, it is thought that it will not significantly disrupt either a polar or a non-polar environment. Glycine is smaller than alanine, and is also electro-neutral, however, it is thought that this residue could produce too much mobility in the α -helix.

6.3.2 Construction and Subcloning of the Helix 8 Mutants.

Each individual amino acid residue in helix 8 of GLUT3 was replaced by alanine. The construction of the mutants was carried out by Dr Michael J. Seatter (PhD Thesis, 1994, University of Glasgow). Two different site directed mutagenesis approaches were used: the first of which involved the use of Amersham's "RPN 1526 Oligonucleotide Directed Mutagenesis Kit". This kit is commercially available, and the method used was exactly according to manufacturers instructions. This method was used to make eight of the nineteen mutants but was discarded in preference to the PCR based approach described in Figure 6.3, which proved to be significantly more efficient. This method is adapted from a method described by Katagiri *et al* (Katagiri *et al.*, 1992). The remaining eleven mutants were constructed using this approach. Similar problems were encountered with this procedure as those described in Chapter 5 in the construction of the second generation chimeras. These problems were mainly associated with the low fidelity of *Taq* polymerase, however, in this case they could be resolved with the dual approach of using proof-reading polymerases and by the restriction digest and subcloning of error free sequences into appropriate restricted sites of wild type GLUT3.

The mutant constructs were cloned into the pSPGT3 vector (Figure 2.3), and the sequence checked in both directions by automated sequencing (section 2.7) for spurious mutations. (Further description of the mutagenesis and subcloning procedures can be found in M.J.Seatter, PhD thesis, November 1994, University of Glasgow.)

6.3.3 Expression of the Mutant Constructs in *Xenopus* Oocytes.

The mutant construct cDNAs were linearised with *Xba* I and used as templates for the *in vitro* transcription of cRNA (section 2.2). The cRNA was assessed for integrity and concentration by agarose gel analysis.

Due to the large number of oocytes needed to perform a K_m estimation, only three or four mutants were individually injected into oocytes taken from the same oocyte batch, i.e. from the same toad. However, each estimation of K_m for mutant injected oocytes was accompanied at least once, by an K_m estimation for wild type GLUT3 injected oocytes.

6.4 Results.

All of the helix 8 mutants were found to be successfully expressed as indicated by their ability to transport deGlc. Relative numbers of mutant and wild type transporters at the plasma membrane were not determined (section 4.6.3), and so it is not possible to say that the targeting efficiency of each mutant was similar to wild type. However, typical transport rates for the uptake of 0.1mM deGlc were in the range of 2-9 pmoles/min/oocyte. This was comparable to wild type, and was also much higher than the non-injected control rates which were typically 0.2-0.7 pmoles/min/oocyte.

An estimation of the K_m value for each of the nineteen mutants for deGlc has been obtained. Figure 6.4 shows a Lineweaver-Burk plot of the uptake of deGlc by mutant Ile³⁰⁵-injected oocytes. Figure 6.5 shows the same plot of the uptake of deGlc by oocytes injected with mutant Asn³¹⁵. Lineweaver-Burk plots for the other mutants are not shown as these are comparable to wild type GLUT3- as is the plot for mutant Ile³⁰⁵. However, K_m values for all the mutants are presented in Table 6.2. Note that on average, 50% of the "n" numbers in this study were obtained by Dr Michael J. Seatter.

Figure 6.1

Comparison of Amino Acid Sequences in Putative Transmembrane Helix 8 of the Facilitative Glucose Transporter Family.

This diagram shows a comparison between helix 8 amino acid sequences of human GLUTs 1, 2, 3, 4 and 5. Residues which are completely conserved between these isoforms are shown in bold. A consensus sequence of GLUTs 1-4 is also shown at the bottom of the diagram. Note that several polar amino acids are also conserved in this helix, including asparagine³¹⁵. The positioning of these polar amino acids is shown in Figure 6.2.

Figure 6.1

Comparison of Amino Acid Sequences in Putative Transmembrane Helix 8 of the Facilitative Glucose Transporter Family.

hGLUT1	VYATIGSGIVNTAFTVVSLFV
hGLUT2	VYATIGVGAVNMVFTA VSVFL
hGLUT3	IYATIGAGVVNTIFTVVSLFL
hGLUT4	AYATIGAGVVNTVFTLVSVLL
hGLUT5	QYVTAGTGAVNVVMTFCAVFV
GLUT1-4	XYATI GxGxVNxxxTxVSxxx

Figure 6.2

Predicted α - Helical Structure of GLUT3 Transmembrane Helix 8.

This is a helical wheel diagram which predicts the secondary structure of putative transmembrane helix 8 of GLUT3. The diagram looks down through the helix from the exofacial side of the membrane. The helix starts with Ile³⁰⁵ (numbered residue 1 on the wheel), and rotates downward in a clockwise direction to Asn³²⁵ at the bottom (Leu³²⁴ is the last residue shown on the wheel diagram, numbered residue 21). The diagram highlights a number of polar residues which cluster on one side of the helix, on the other side, the residues are largely hydrophobic in nature.

Figure 6.2

Predicted α - Helical Structure of GLUT3 Transmembrane Helix 8.

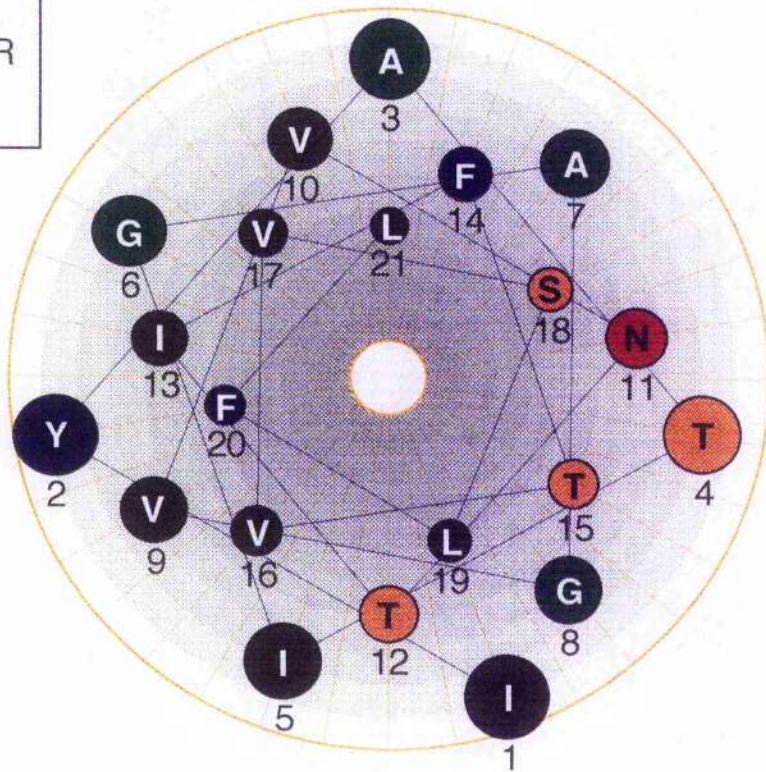
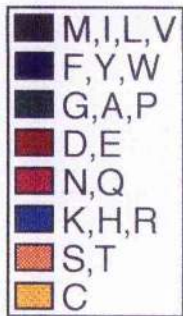


Figure 6.3.

Diagram Describing Recombinant PCR Approach.

This diagram describes the PCR approach used to construct the helix 8 mutants. The template used for the generation of primary products "a" and "b" was GLUT3 cDNA. The internal primers used in these reactions were composed of GLUT3 helix 8 sequence with the appropriate bases changed to encode for an alanine at the specific residue position of interest .

In the generation of primary product "a", the mutagenic, internal primer binds to the top (sense) strand of GLUT3, and G3 Start- the external primer, binds to the bottom (antisense) strand of GLUT3. Conversely, in the generation of primary product "b", the internal, mutagenic primer binds to the bottom (antisense) strand of GLUT3, and the external primer- G3 End, binds to the top (sense) strand. Upon melting, reannealing and extension, primary products "a" and "b" are produced which have overlapping sequences, each encoding the mutation which was incorporated in the two mutagenic primers.

These primary products serve as templates in the secondary PCR reaction. After a few PCR rounds of melting, strand dissociation and re-annealing, the overlapping sequences are extended to produce full length constructs which encode the alanine substitution. These full length fragments are further amplified in subsequent rounds of PCR by the external primers G3 Start and G3 End.

The external primers contain *Sal* I restriction sites in their tail regions. This allows the PCR product to be cloned into *Sal* I restricted vector.

Details of oligonucleotides and PCR conditions can be found in: Michael J. Seatter, PhD Thesis, November 1994, University of Glasgow.

Figure 6.3 Diagram Describing Recombinant PCR Approach.

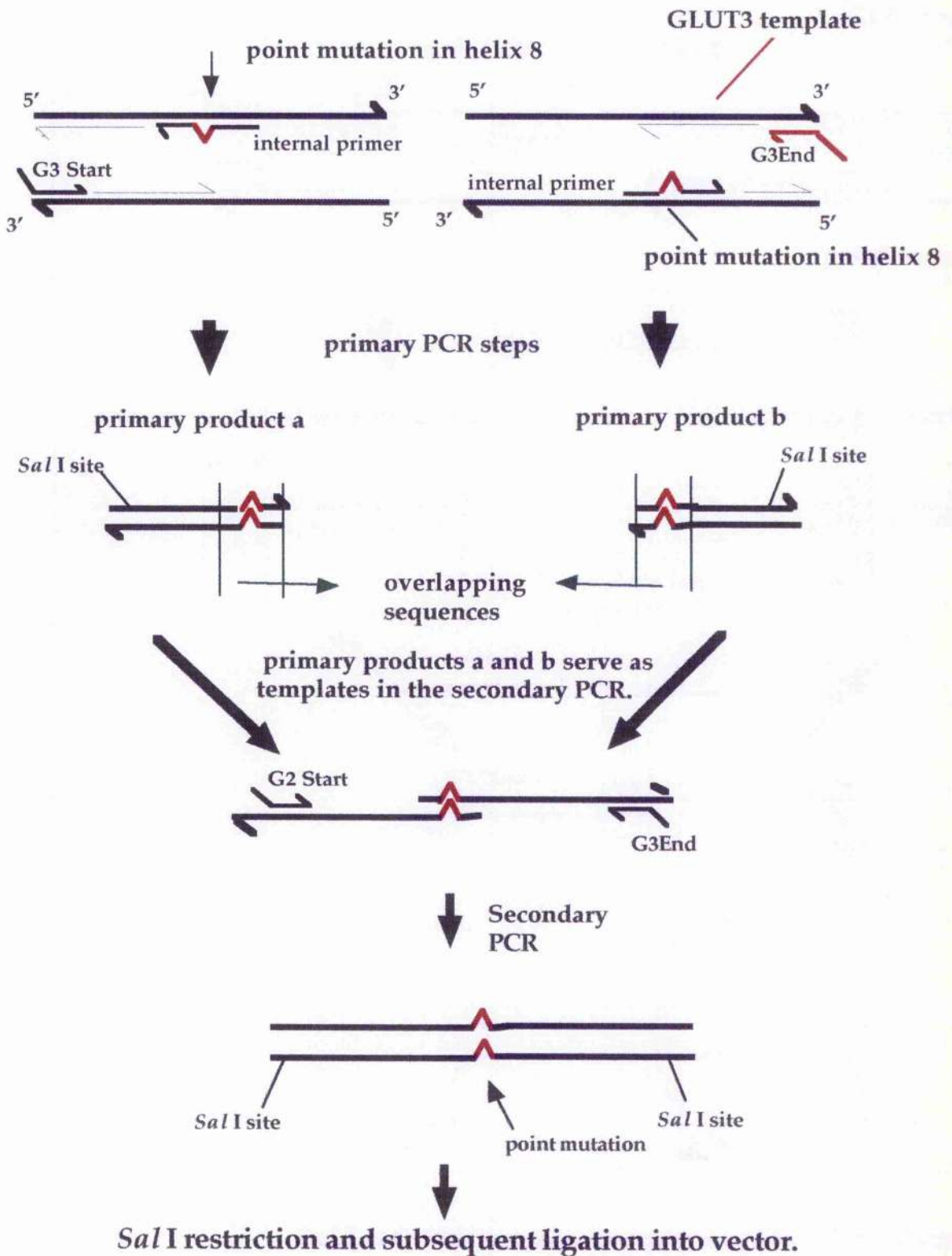


Figure 6.4.

Lineweaver-Burk Plot of the Uptake of DeGlc by Mutant Ile³⁰⁵ Injected Oocytes.

Each point is the mean transport rate determined from groups of 10 oocytes (see section 2.4). Rate of transport was determined by exposure of the oocytes to radiolabeled deGlc for 30 mins and the counts per minute determined as described (section 2.4). For each experiment endogenous oocyte transport was measured by a parallel incubation of non-injected "control" oocytes in trace radiolabeled deGlc. The values obtained for the control oocytes at each concentration were subtracted from the values obtained from the mutant-injected oocytes to obtain the heterologous transport rate. Transport rates in control oocytes were typically 10% or less of the injected oocytes. Error bars are excluded for clarity, but the range of error was typically 10%. The data shown in this particular plot and in other plots presented in this chapter, is one of at least four separate experiments.

Figure 6.4.

Lineweaver-Burk Plot of the Uptake of DeGlc by Mutant Ile³⁰⁵ Injected Oocytes.

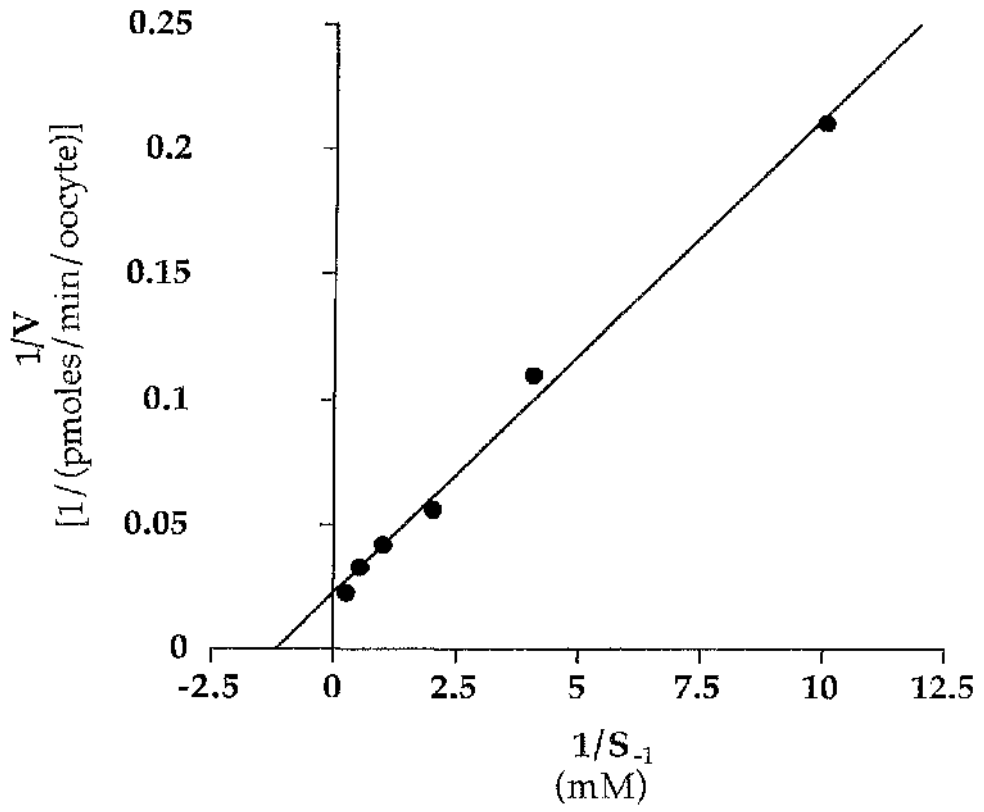


Figure 6.5.

Lineweaver-Burk Plot of the Uptake of DeGlc by Mutant Asn³¹⁵ Injected Oocytes.

Each point is the mean transport rate determined from groups of 10 oocytes (section 2.4). Rate of transport was determined by exposure of the oocytes to radiolabeled deGlc for 30 mins and the counts per minute determined as described (section 2.4). (See also Figure legend 6.6). Transport rates in control oocytes were typically 10% or less of the injected oocytes. Error bars are excluded for clarity, but the range of error was typically 10%. The data shown in this particular plot and in other plots presented in this chapter, is one of at least four separate experiments.

Figure 6.5.

Lineweaver-Burk Plot of the Uptake of DeGlc by Mutant Asn³¹⁵ Injected Oocytes.

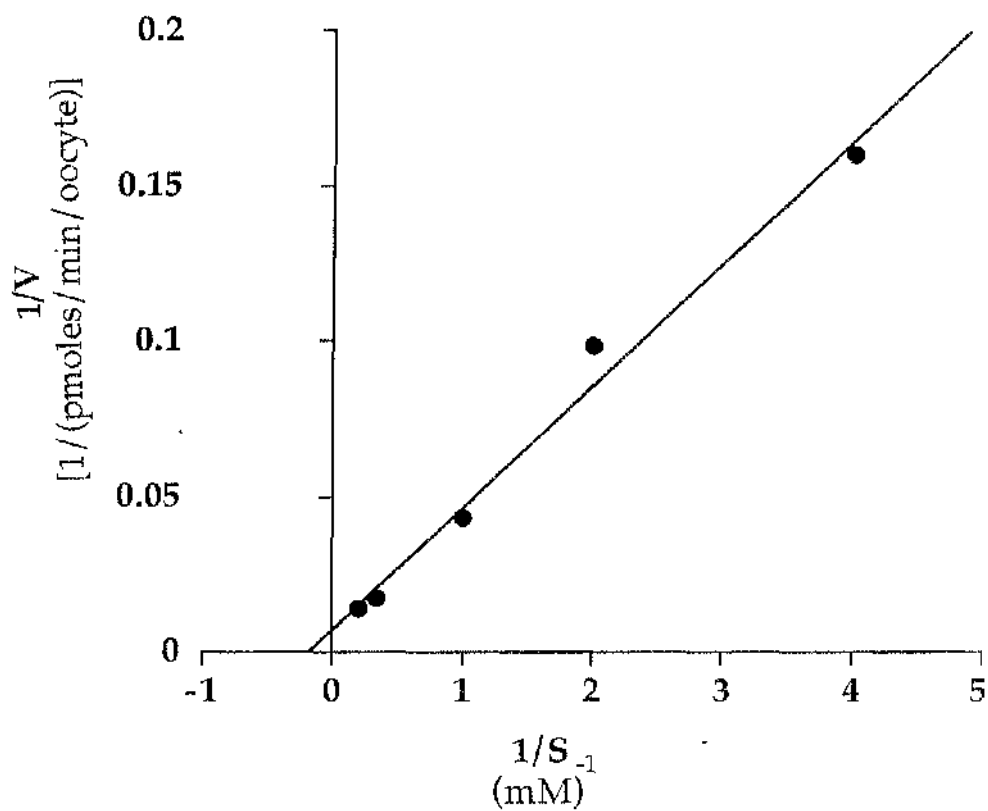


Table 6.1- Effects of Point Mutations on the Transport Activity of Glucose Transporters.

Isoform	species	residue number	mutation	Expression system	Transport activity	Vmax	Km	Turnover number	Cyto B	ATB-BMFA	ref
GLUT4	rat	28	tyr->phe	cos	wt				+		(Wandel, 1994)
GLUT1	human	48	trp->gly	oocyte	wt				+		(Garcia, 1992)
GLUT1	human	65	trp->leu	oocyte	wt				+		(Garcia, 1992)
GLUT1	human	100	asn->ile	oocyte	wt						(Mueckler, 1994)
GLUT1	human	100	asn->ser	oocyte	wt						(Mueckler, 1994)
GLUT2	human	110	thr->ile	oocyte	wt						(Mueckler, 1994)
GLUT1	human	133	cys->ser	oocyte	wt						(Wellner, 1994)
GLUT1	human	133	cys->ser	oocyte	wt						(Duc, 1995, Zottola, 1995)
GLUT4	rat	143	tyr->phe	cos	dec				+		(Wandel, 1994)
GLUT4	rat	143	tyr->phe	LTK	dec				+		(Wandel, 1994)
GLUT1	human	161	gln->leu	oocyte	-						(Mueckler, 1994)
GLUT1	human	161	gln->asn	oocyte	dec		wt(2t)	dec			(Mueckler, 1994)
GLUT1	human	165	val->ile	oocyte	dec						(Mueckler, 1994)
GLUT1	human	186	trp->gly	oocyte	wt				+		(Garcia, 1992)
GLUT1	human	186	trp->leu	oocyte	wt				+		(Garcia, 1992)
GLUT1	human	187	pro->ala	oocyte	wt						(Wellner, 1995)
GLUT1	human	187	pro->his	oocyte	wt						(Wellner, 1995)
GLUT1	human	196	pro->ala	oocyte	wt						(Wellner, 1995)
GLUT1	human	196	pro->arg	oocyte	dec				+		(Wellner, 1995)

GLUT2	human	197	val->ile	oocyte	dec													(Mueckler, 1994)
GLUT1	human	200	gln->leu	oocyte	dec													(Mueckler, 1994)
GLUT1	human	201	cys->gly	oocyte	wt													(Wellner, 1993)
GLUT1	human	201	cys->ser	oocyte	wt													(Duc, 1995)
GLUT1	human	207	cys->ser	oocyte	wt													(Wellner, 1993)
GLUT1	human	207	cys->ser	oocyte	wt													(Duc, 1995)
GLUT1	human	207	cys->ser	oocyte	wt													(Duc, 1995)
GLUT1	human	282	gln->leu	CHO	wt	wt												(Hashimoto 1992)
GLUT1	human	288	asn->ile	CHO	dec													(Hashimoto 1992)
GLUT4	rat	292	tyr->phe	LTK	wt													(Wandel, 1994)
GLUT4	rat	292	tyr->phe	cos	wt													(Wandel, 1994)
GLUT1	human	292	tyr->ile	CHO	wt	wt												(Mori, 1994)
GLUT1	human	292	tyr->phe	CHO	wt	wt												(Mori, 1994)
GLUT1	human	292	tyr->phe	oocyte	dec													(Mueckler, 1995)
GLUT1	human	292	tyr->phe	oocyte	wt													(Mueckler, 1995)
GLUT1	human	293	tyr->phe	CHO	wt	wt												(Mori, 1994)
GLUT1	human	293	tyr->ile	CHO	dec	dec												(Mori, 1994)
GLUT4	rat	293	tyr->phe	cos	dec													(Wandel, 1994)
GLUT4	rat	293	tyr->phe	LTK														(Wandel, 1994)
GLUT4	rat	308	tyr->phe	cos	wt													(Wandel, 1994)
GLUT1	human	317	asn->ile	CHO	dec													(Hashimoto 1992)
GLUT4	rat	333/ 334	arg->leu	cos (cells)	dec													(Wandel, 1995)

GLUT4	rat	333 / 334	arg->leu arg->ala	cos*	wt					wt	(Wandel, 1995)
GLUT4	rat	337	his->gln	cos*	wt					wt	(Wandel, 1995)
GLUT1	human	347	cys->ser	oocyte	wt						(Wellner, 1994)
GLUT1	human	363	trp->leu	oocyte	wt				+		(Garcia, 1992)
GLUT1	human	363	trp->gly	oocyte	wt				+		(Garcia, 1992)
GLUT1	human	383	pro->ala	oocyte	wt						(Wellner, 1995)
GLUT1	human	383	pro->gln	oocyte	dec						(Wellner, 1995)
GLUT1	human	385	pro->ala	oocyte	wt						(Wellner, 1995)
GLUT1	human	385	pro->gln	oocyte	wt						(Wellner, 1995)
GLUT1	human	385	pro->ile	CHO	dec			wt	-		(Tannori, 1994)
GLUT1	human	385	pro->gly	CHO	wt			increase	dec		(Tannori, 1994)
GLUT1	human	383 & 385	pro->ala	oocyte	wt						(Wellner, 1995)
GLUT1	human	387	pro->ala	oocyte	wt						(Wellner, 1995)
GLUT1	human	387	pro->gly	oocyte	dec						(Wellner, 1995)
GLUT1	rabbit	388	trp->leu	CHO	dec			dec		+	(Katagiri, 1993)
GLUT1	human	388	trp->leu	oocytes	dec						(Garcia, 1992)
GLUT1	human	388	trp->gly	oocytes	dec						(Garcia, 1992)
GLUT1	human	388	trp->gly	cos	dec				+		(Schümann, 1993)
GLUT1	rabbit	388 / 412	trp->leu	CHO	dec				dec		(Inukai, 1994)
GLUT3	human	410	trp->leu	oocyte							(Burant, 1992)
GLUT1	rabbit	412	trp->leu	CHO	dec			increase (zt)	dec	wt	(Katagiri, 1991)

GLUT1	human	412	trp->leu	oocyte	dec												(Garcia, 1992)
GLUT1	human	412	trp->gly	oocyte	dec												(Garcia, 1992)
GLUT1	human	412	trp->gly	cos													(Schurman, 1993)
GLUT1	human	421	cys->ser	oocyte	wt												(Due, 1995)
GLUT1	human	421	cys->arg	oocyte	wt												(Wellner, 1992, 1994)
GLUT1	human	429	cys->ser	oocyte	wt												(Wellner, 1992, 1994)
GLUT1	human	429	cys->ser	oocyte	wt												(Due, 1995, Zoltola, 1995)
GLUT1	human	467	phe->leu	CHO	dec												(Muracka, 1995)
GLUT1	human	468	arg->leu	CHO	dec												(Muracka, 1995)

* experiments performed both in COS cells and liposomes.

Table 6.2.

Kinetic Parameters of Helix 8 Mutants in Oocytes.

This table shows the K_m for deGlc for each of the helix 8 mutants when expressed in oocytes. The residue numbers given refer to GLUT3 residues. All residues are substituted by alanine, therefore since residue³⁰⁷ is alanine originally, it is not included in this study. All K_m s for deGlc are similar to wild type GLUT3, with the exception of the Asn³¹⁵ mutant, which has a K_m approximately 4-fold higher than wild type GLUT3. Note that on average, 50% of these "n" numbers were generated by Dr. Michael J. Seatter.

Table 6.2

Kinetic Parameters of the Helix 8 Mutants in Oocytes.

Residue number	Original designation	deGlcK _m (mM)
305	Ile	1.2±0.36
306	Tyr	2.1±0.6
308	Thr	1.5±0.6
309	Ile	1.1±0.3
310	Gly	1.5±0.1
312	Gly	1.5±0.02
313	Val	1.16±0.07
314	Val	2.4±0.5
315	Asn	12.2±4.9
316	Thr	2.9±1.0
317	Ile	1.53±0.3
318	Phe	1.7±0.3
319	Thr	2.7±0.4
320	Val	1.6±0.4
321	Val	2.4±0.8
322	Ser	1.4±0.5
323	Leu	1.9±0.6
324	Phe	2.6±0.3
325	Leu	1.3±0.5
wild type GLUT3		1.4±0.6

6.5 Conclusions.

All nineteen mutants have been successfully expressed in *Xenopus* oocytes. Transport rates were similar to GLUT3 wild type. K_m values for deGlc transport for each of the helix 8 mutants have been determined (Table 6.2). The substitution of Asn³¹⁵ with alanine in helix 8 of GLUT3 produced a ~3-fold increase in deGlc K_m (Figure 6.5, Table 6.2). All other substitutions produced no effect on deGlc transport rate and K_m .

6.6 Discussion.

From comparison of the helix 8 sequences in Figure 6.1, it can be seen that there are several residues which are highly conserved between the GLUT family members (there is also a high level of conservation between the species: human, rat, rabbit and mouse). Tyr³⁰⁶, Thr³⁰⁸, Gly³¹⁰, Gly³¹², Asn³¹⁵, and Thr³¹⁹ are all conserved through the whole family (human GLUT3 residue numbering). Ala³⁰⁷, Ile³⁰⁹, Val³²¹ and Ser³²² are identical in GLUTs 1-4, but not in GLUT5. Since GLUT5 is a fructose transporter and not a glucose transporter, these residues may have some importance in this regard. Also, Val³¹⁴, Thr³¹⁶ and Phe³¹⁸ are identical in GLUT1, GLUT3 and GLUT4, but not in GLUT5 or in GLUT2, both of which are capable of fructose transport.

Figure 6.2 shows a helical wheel projection of helix 8. This diagram looks down through the helix from above, with Ile³⁰⁵ at the top of the helix winding down in a clockwise direction to Asn³²⁵ at the bottom. Also shown in this diagram is the positioning of the polar residues, the majority of which cluster on one side of the helix. The other side of the helix is composed mostly of hydrophobic residues. Three of the six helix 8 polar residues that are conserved throughout the family are predicted to lie on this polar face. These residues are Thr³⁰⁸, Asn³¹⁵ and Thr³¹⁹. However, Tyr³⁰⁶ which is also capable

of hydrogen bonding, and is conserved throughout the family, is predicted to lie opposite these residues, and so according to this model would be in a lipid environment. However, the helix may rotate upon conformational change to bring this residue into a polar environment.

Substitution of the equivalent residue of Asn³¹⁵ in GLUT1 (Asn³¹⁷-> Ile, (Hashiramoto *et al.*, 1992)) produced a 50% decrease in transport activity, which the authors of this study concluded was surprising considering the absolute conservation of this residue throughout the family. This decrease in transport activity was not due to disruption of the exofacial or endofacial binding sites as labelling with ATB-BMPA and cytochalasin B was comparable with wild type. The GLUT4 residue which is equivalent to Tyr³⁰⁶ in GLUT3 (Tyr³⁰⁸->Phe, (Wandel *et al.*, 1994)), has been substituted without producing any effect on transport activity or on labelling with cytochalasin B and ATB-BMPA.

The results from the experiments presented in this chapter show that none of the nineteen substitutions of residues in helix 8 of GLUT3 have a **profound** effect on functional activity, and therefore probably not on folding and targeting of the transporter to the plasma membrane in oocytes. At present there is no available procedure for obtaining pure oocyte plasma membrane fractions, and so it cannot be directly shown that the number of transporters that reach the plasma membrane is equivalent to wild type GLUT3 (section 4.6.3). However, the deGlc transport rate of mutant-injected oocytes was always at least 5-fold greater than non-injected or water injected oocytes. Therefore, it can be assumed that the substitutions have not produced any gross defect in the protein folding or targeting mechanism.

Measurement of deGlc uptake for each of these mutants has shown that no single amino acid in helix 8 of GLUT3 is absolutely essential for transport activity. Additionally, the K_m for deGlc is unaffected by substitution of eighteen of the nineteen residues in helix 8. The only substitution which produced any effect on the K_m was that of Asn³¹⁵. This residue is conserved throughout the

GLUT family, and is predicted to be located on the polar face of helix 8. It seems possible that this residue may play a role in the exofacial binding site since the GLUT1 site of photolabeling by the exofacial ligand ATB-BMPA has been mapped to a region between helix 7 and helix 8. However, although substitution of the equivalent residue in GLUT1 produced a 50% decrease in transport activity, ATB-BMPA binding was comparable to wild type GLUT1. Therefore it may be more likely that Asn³¹⁵ in GLUT3 may participate in the transporter interactions with deGlc as it passes through the channel.

The change in K_m that resulted from substitution of Asn³¹⁵ may represent a change in the affinity of the transporter for deGlc. However, this may also be due to a change in the turnover number of the protein. At present, it is not possible to determine this due to the difficulty in obtaining the pure oocyte plasma membranes fractions needed for the quantification of protein at the cell surface.

Nevertheless, binding studies using ligands such as cytochalasin B and ATB-BMPA will provide information as to whether the substitution has resulted in perturbation of the endofacial and exofacial binding sites. It is also possible that these studies will highlight effects of the other substitutions on the exofacial and endofacial binding sites which are not necessarily accompanied by a loss of transport activity.

Measurement of the affinity of the Asn³¹⁵ mutant for other substrates such as galactose will also indicate if this residue is more critical in the transport of sugars other than deGlc. Additionally the K_i values for the inhibition of deGlc by non-transported ligands such as maltose and 4,6-O-ethylidene-D-glucose will also indicate if there are any changes in the exofacial binding site.

In Chapter 4 we have proposed a model for the structural basis of substrate binding. We have speculated the C-4 position of D-glucose may bind to a region of sequence which lies between the end of helix 7 and the end of

helix 10. Helix 8 lines the glucose transporter channel in both of the recently proposed helical packing models (Zeng *et al.*, 1996), and the presence of several highly conserved polar residues suggests a role for this helix in hydrogen bonding to the sugar. The replacement of Asn³¹⁵ with alanine is the only substitution in helix 8 which alters the K_m for deGlc. However, it is unlikely that this residue is important for C-4 binding, since the substitution of Asn³¹⁷ -the corresponding residue in GLUT1, does not affect exofacial or endofacial ligand binding. Also, it has been suggested that Tyr²⁹³ of GLUT1, which lies at the end of helix 7 may be involved in binding the sugar at the C-4 or the C-6 positions (Mori *et al.*, 1994). Nevertheless, it would be instructive to perform inhibition studies on this mutant using D-glucose analogues. The analogue approach allows us to investigate if the binding of the hydroxyls at any of the carbon positions have become less or more important in the binding of glucose to this mutant. It would be especially interesting to measure the affinity of this mutant for C-4 substituted hexoses, such as maltose and 4,6-O-ethylidene-D-glucose. A change in affinity of the mutant for these compounds compared to wild type GLUT3, may indicate a disruption of binding at the C-4 position of the sugar.

It is perhaps surprising that substitution of such highly conserved residues as those in helix 8 does not lead to greater structural and functional problems in the transporter. Indeed, of the many mutations that have been created throughout the transporter structure, remarkably few residues have been found to be of absolute importance. Clearly, there is a selective pressure maintaining the absolute conservation of these residues in the transporter structure, but perhaps their role is more collective than singular. It may be that there are few single residues that are all important for protein folding for example, but several which act in concert to allow the protein to form folding intermediates and to maintain the final tertiary structure. The residues which have been found to be absolutely critical (i.e. Gln¹⁶¹, Val¹⁶⁵, Tyr²⁹³, and Pro³⁸⁵)

may exist in locations where their precise geometry is required for function through hydrogen bonding or hydrophobic interaction (Mori *et al.*, 1994, Mueckler, 1994a, Mueckler, 1994b, Tamori *et al.*, 1994)

It is interesting in this regard to look at other transport proteins which have been subjected to site directed mutagenesis, such as the lactose (lac) permease of *E.coli*. The lac permease is a membrane transport protein that couples the transport of β -galactosides with that of H^+ . The *lac y* gene which encodes this transporter has been cloned and sequenced, and based on spectroscopic analysis of the purified protein and hydropathy analysis of the amino acid sequence, a model for the secondary structure has been proposed which is extremely similar to Muecklers model of GLUT1 (Figure 1.2) (Mueckler, 1985). As with GLUT1 the transporter is proposed to span the lipid bilayer twelve times with the N- and C-termini cytoplasmically disposed. Also similar to GLUT1 is the predicted presence of a large cytoplasmic loop between helix 6 and helix 7 (Kaback, 1996).

The lac permease has been the subject of extensive mutagenesis studies, including the use of cysteine scanning mutagenesis, second site suppresser analysis and site-directed excimer fluorescence (reviewed in Kaback, 1996, Kaback *et al.*, 1994). The cysteine scanning approach involves the use of a cysteineless permease (described in Kaback *et al.*, 1994). Each amino acid in the entire protein is then individually substituted by cysteine. Cysteine residues can be labelled with radioactive, fluorescent or spin-labelled probes, or they can be chemically modified with thiol group-modifying reagents. Additionally, with this technique it is possible to investigate the proximity of any two fluorescent-labelled cysteines in the protein. Experiments such as these have been very successful in confirming various structural features of the lac permease. It has been shown for instance, that helix 7 is probably in close proximity to helix 10 and helix 11. Helix 8 is also predicted to lie near helix 10 (Kaback, 1996).

However, in spite of the extensive mutagenesis that has been performed on this protein (over 90% of the residues have been mutated), surprisingly few single residues have been found to be essential in the active transport mechanism. Those residues which have been identified as important are mostly involved in protein folding and maintenance of the structure. Additionally, it has been shown from cysteine scanning mutagenesis studies that, with many of the residues in the lac permease, alkylation of the substituted cysteine (which replaces the original amino acid), produces slight alterations in the transport activity. It was observed that the mutants which display this slight reduction in transport activity upon alkylation appear to cluster together in the membrane, suggesting that the general shape and surface contours of the helices may be important in global transport function. It has also been suggested from such analyses that the large conformational change which occurs during transport catalysis involves widespread, multi-determined conformational changes, and does not appear to be dependent on many residue-specific side-chain/substrate, and side-chain/side-chain interaction (Frillingos & Kaback, 1996, Kaback, 1996).

It could also be said of the facilitative glucose transporters that, despite the large number of mutational studies that have been performed, remarkably few residues have been found to be important. This situation may be similar between the GLUTs and the lac permease.

CHAPTER 7.

Discussion.

Glucose is the primary energy source for the brain, and can be readily taken up and utilised by all other mammalian cells to provide immediate metabolic energy, or alternatively, it can be converted to glycogen for storage in the liver and muscle. The mechanisms which facilitate this glucose disposal are therefore crucially important in maintaining whole body glucose homeostasis. The tissue-specific expression of the mammalian facilitative glucose transporters, and the structural and functional diversity of the isoforms of this family, are key components of this mechanism. Furthermore, since the transport of glucose into certain tissues is under both acute and chronic control by circulating hormones, it is thought that aberrant expression and/or dysfunction of some isoforms may play a role in diseased states. Peripheral insulin resistance for example, a condition which leads to non insulin dependent diabetes (NIDDM), is thought to be associated with depletion or inactivation of GLUT4 in skeletal muscle and fat. In NIDDM, expression of the GLUT5 isoform in insulin responsive tissues is also impaired in the same way as GLUT4, and additionally, GLUT2, due to its presence in the liver and in the insulin secreting cells of the pancreas, is thought to play an important role in whole body glucose homeostasis.

Clearly therefore, in order to fully understand the basis of transport dysfunction, it is essential to understand the molecular mechanism by which these carriers mediate glucose transport in non-diseased states.

Investigation of the molecular basis of transport has largely focused on the GLUT1 isoform. This is due to several factors which include the abundance of this protein in the erythrocyte membrane, the ready availability of erythrocytes, and the ease with which these cells can be manipulated. Kinetic, biochemical and biophysical studies of purified GLUT1, have enabled the construction of a detailed model for the topology and transport mechanism of this isoform. The protein is proposed to have twelve membrane spanning domains which cluster together in such a way as to form a water accessible

pore through which glucose moves as it crosses the bilayer. During transport catalysis, the protein is thought to undergo a conformational change which results in the alternative exposition of an exofacial and an endofacial binding site. Glucose transport across the membrane begins by sugar binding to the exposed binding site. This is proceeded by a conformational change in the carrier which results in the appearance of glucose at the other side of the membrane. The binding sites at which glucose associate and dissociate from the transporter are structurally distinct and spatially separate. This proposed mechanism is known as the single site, alternating conformation model, and it is supported by most of the existing biochemical, biophysical and kinetic data.

Biochemical studies have mapped the exofacial and endofacial binding sites to specific regions in the transporter structure, and site directed mutagenesis studies have identified specific residues and stretches of sequence in the transporter which are important in the conformational change mechanism.

The hydropathy plots of other isoforms of the glucose transporter family are virtually superimposable with that of GLUT1. Therefore the exofacial and the endofacial binding sites of these isoforms, the conformationally active regions, the general topology, tertiary structure and mechanism of action are thought to be analogous with GLUT1. However, the glucose transporters are expressed in a highly regulated, tissue-specific manner, indicating that they may be an important component of the glucose disposal system. Previously, expression of cloned transporter cDNAs or *in vitro* transcribed mRNA in the *Xenopus* oocyte system has shown that each isoform displays slightly different transport kinetics, preferences for alternative substrates, and sensitivity to transport inhibitors. Therefore, the regulated, tissue-specific expression of the transporter isoforms probably functions to meet the specific metabolic requirements of the various tissues in which they are present.

Although the isoforms display similarities in general structure and mode of action, there clearly must be subtle structural differences which define isoform-specific behaviour. This structural basis of isoform-specific behaviour has largely been the subject of study in this thesis.

Previous work in this lab has utilised the *Xenopus* oocyte system to establish the kinetic characterisation and structural requirements for substrate binding to GLUT2 and GLUT3. This work has highlighted the disparity of these two isoforms, demonstrating for example, the fructose transport capacity of GLUT2, and the lack of fructose recognition by GLUT3. GLUT3 was shown to transport both deGlc and galactose with a much higher affinity than GLUT2. These differences provided the basis for an assay in which a panel GLUT2/GLUT3 chimeric transporters were characterised for their fructose, deGlc and galactose transport activity. This results of this study, described in chapter 4, have shown that the structural information which allows the GLUT2 isoform to accept fructose, resides entirely in helix 7. Whether other sequences in the transporter structure influence the *kinetics* of fructose transport by this isoform is not clear from the existing data. Helix 7 was also identified as being important in the ability of GLUT3 to transport deGlc and galactose with high affinity. This study is at present being taken further with ongoing work from this laboratory. On the basis of the observation that helix 7 is essential for fructose recognition, new GLUT2 and GLUT3 mutants have been constructed which have the QLS motif of helix 7 (of GLUTs 1, 3 and 4) swapped with the HVA motif of the GLUT2 helix 7. Initial analysis of these mutants suggest that it is the HVA motif of GLUT2 which is solely responsible for the ability of this isoform to accept fructose. Furthermore, the graft of the QLS motif onto a GLUT2 molecule results in high affinity deGlc transport.

The success of this study demonstrates that chimeric mutagenesis is an extremely useful approach which can be used to define regions of a protein important in specific functions. Once larger regions are mapped with this

technique, it is then possible to closely search the amino acid content of these regions for specific motifs which may be relevant to the function of interest.

Previous characterisation of fructose transport by GLUT2 had shown that this isoform transports fructose in the furanose ring form, while glucose is transported in the pyranose ring form. In a separate study it was shown that the fructose transporter of the parasite *Trypanosoma brucei* could transport both the furanose and the pyranose ring forms of fructose with approximately equal efficiency. Fructose, when in solution, exists predominantly in the pyranose ring form, and since human GLUT5 has been reported to be exclusively a fructose transporter, we have investigated which ring form of fructose is accepted by this isoform. The results of these experiments show that GLUT5, like GLUT2, transports the furanose ring form of fructose. Further experiments using fructose analogues which have carbon hydroxyls substituted by non-polar groups will provide information on the hydrogen bonding requirements of GLUT5. Previous investigations of GLUT5 have been inconclusive in determining both the substrate specificity and kinetics of fructose transport by this isoform. Since the properties of human GLUT5 have been documented only once in the literature, it was decided to examine the substrate selectivity and to measure the K_m for fructose transport of this isoform in the oocyte system. Our results from this work are in broad agreement with the previous study of human GLUT5 in oocytes from Burant *et al.*

Recently, it has been shown that the affinity of the human sodium-linked glucose transporter SGLT1 for glucose, changes in response to pH. This transporter is expressed in the gut in conjunction with GLUT5. The observation that human GLUT5 is expressed in tissues which are subject to a range of pH values (both in the gut and elsewhere), and the ambiguity in reports that this isoform can transport glucose, led us to examine the effect of varying the pH of the extracellular transport medium on the ability of GLUT5

to transport fructose and deGlc. The results of these experiments suggest that the affinity of human GLUT5 for fructose, and the lack of ability to accept deGlc does not alter in response to pH.

Finally, we have examined the effects of amino acid substitution on each residue within helix 8 of GLUT3. Helix 8 was of interest to us because of its implied role in the exofacial binding site (section 1.6). GLUT3 was chosen as a template for mutagenesis as most previous studies have focused on GLUT1. Our study would serve a dual role therefore, firstly it would investigate the structural importance of the amino acids of helix 8 to the GLUT3 molecule, and secondly, it would serve as an isoform-comparative study to the existing GLUT1 data. The experiments presented in this thesis have shown that none of the substitutions of helix 8 residues in GLUT3 have a profound effect on the folding and targeting of the transporter. Also, despite the high conservation of a number of polar amino acids in this helix, only one of the substitutions produced any effect on the K_m of GLUT3 for the transport of deGlc. The substitution of Gln³¹⁵ with Ala resulted in a 4-fold increase in the K_m for transport of deGlc. This is analogous to the results of previous studies on the helix 8 of GLUT1.

In conclusion therefore, the chimeric approach has been extremely successful in identifying the domains involved in fructose recognition. Future work with the existing chimeras may involve the use of glucose analogues to study the interaction of individual sugar hydroxyls with the chimeric transporters. The precise effects of swapping individual helices within GLUT2 and GLUT3 could not be determined in this study due to methodology problems. However, the enzymes which are commercially available for recombinant PCR are being quickly improved in terms of proof-reading capacity, and so it should soon be possible to construct error-free single domain swap mutants.

Future studies of the existing chimeras and of single domain swap chimeras, would probably benefit from use of another expression system. The *Xenopus* oocyte system has proven to have extreme drawbacks. The seasonal variation of oocyte batches meant that reliable data could only be obtained during a very limited time period within the year. This restriction was compounded by animal housing problems: *Xenopus laevis* are extremely sensitive to their environment, and this has a direct effect on the quality of the oocytes that are produced.

Expression of chimeras in another system such as CHO cells would also enable the measurement of plasma membrane protein concentration, which would allow other kinetic parameters to be determined- such as V_{\max} and transporter turnover. More accurate and detailed kinetic studies would therefore be possible in another cell system.

References.

- Ahlborg, G., & Bjorkman, O. (1990) *J. Appl. Physiol.* **69**, 1244-1251.
- Allard, W. J., & Lienhard, G. E. (1985) *J. Biol. Chem.* **260**, 8668-8675.
- Appleman, J. E., & Lienhard, G. E. (1989) *Biochemistry* **28**, 8221-8227.
- Asano, A., Katagiri, H., Takata, K., Lin, J.-L., Ishihara, H., Inukai, K., Tsukuda, K., Kikuchi, M., Hirano, H., Yazaki, Y., & Oka, Y. (1991) *J. Biol. Chem.* **266**, 24632-24636.
- Asano, T., Shibasaki, Y., Kasuga, M., Kanazawa, Y., Takaku, F., Akanuma, Y., & Oka, Y. (1988) *Biochem. Biophys. Res. Comm.* **154**, 1204-1211.
- Axelrod, J. D., & Pilch, P. F. (1983) *Biochemistry* **22**, 2222-2227.
- Baker, G. F., & Widdas, W. F. (1973) *J. Physiology* **231**, 143-165.
- Baldwin, J. M., Gorga, J. C., & Lienhard, G. E. (1981) *J. Biol. Chem.* **256**, 3685-3689.
- Baldwin, S. A. (1993) *Biochim. Biophys. Acta.* **1154**, 17-49.
- Baldwin, S. A., Baldwin, J. M., Gorga, F. R., & Lienhard, G. E. (1979) *Biochim. Biophys. Acta* **552**, 183-188.
- Baldwin, S. A., & Henderson, P. J. F. (1989) *Ann. Rev. Physiol.* **51**, 459-471.
- Baldwin, S. A., & Lienhard, G. E. (1989) *Methods Enzymol.* **174**, 39-50.
- Barnett, J. E. G., Holman, G. D., Chalkley, R. A., & Munday, K. A. (1975) *Biochem. J.* **145**, 417-429.
- Barnett, J. E. G., Holman, G. D., & Munday, K. A. (1973) *Biochem. J.* **131**, 211-221.
- Birnbaum, M. J. (1989) *Cell* **57**, 305-315.

- Birnbaum, M. J., Haspel, H. C., & Rosen, O. M. (1986) *Proc. Natl. Acad. Sci. USA* **83**, 5784-5788.
- Bloch, R. (1973) *Biochemistry* **12**, 4799-4801.
- Brandl, C. J., & Deber, C. M. (1986) *Proc. Natl. Acad. Sci. USA* **83**, 917-921.
- Buchel, D. F., Gronenborn, B., & Muller-Hill, B. (1980) *Nature (London)* **283**, 541-545.
- Buchs, A., Lu, L., Morita, H., Whitesell, R. R., & Powers, A. C. (1995) *Endocrinology* **136**, 4224-4230.
- Burant, C. F., & Bell, G. I. (1992a) *Biochemistry* **31**, 10414-10420.
- Burant, C. F., & Bell, G. I. (1992b) *Biochemistry* **31**, 10412-10420.
- Burant, C. F., Takeda, J., Brot-Laroche, E., Bell, G. I., & Davidson, N. O. (1992) *J. Biol. Chem.* **267**, 14523-14526.
- Cairns, M. T., Alvarez, J., Panico, M., Gibbs, A. F., Morris, H. R., Chapman, D., & Baldwin, S. A. (1987) *Biochim. Biophys. Acta.* **905**, 295-310.
- Carruthers, A. (1990) *Physiological Review* **70**, 1135-1176.
- Carruthers, A. (1991) *Biochemistry* **30**, 3898-3906.
- Carruthers, A., & Helgerson, A. L. (1991) *Biochemistry* **30**, 3907-3915.
- Charron, M. J., Brosius III, F. C., Alper, S. L., & Lodish, H. F. (1989) *Proc. Natl. Acad. Sci. USA* **86**, 2535-2539.
- Chin, J. J., Jhun, B. J., & Jung, C. Y. (1992) *Biochemistry* **31**, 1945-1951.
- Chin, J. J., Jung, E. K. Y., & Jung, C. Y. (1986) *J. Biol. Chem.* **261**, 7101-7104.
- Clark, A. E., & Holman, G. D. (1990) *Biochem. J.* **269**, 615-622.

- Colville, C. A., Seatter, M. J., & Gould, G. W. (1993a) *Biochem. J.* **194**, 753-760.
- Colville, C. A., Seatter, M. J., Jess, T. J., Gould, G. W., & Thomas, H. M. (1993b) *Biochem. J.* **290**.
- Connolly, T. J., Carruthers, A., & Melchoir, D. I. (1985) *J. Biol. Chem.* **260**, 2617-2620.
- Cope, D. L., Holman, G. D., Baldwin, S. A., & Wolstenholme, A. J. (1994) *Biochem. J.* **300**, 291-294.
- Corpe, C. P., Basaleh, M. M., Affleck, J., Gould, G. W., Jess, T. J., & Kellet, G. L. (1996) *Eur. J. Physiol.* **432**, 192-201.
- Crouzoulon, G., & Korieh, A. (1991) *Comp. Biochem. Physiol.* **100A**, 175-182.
- Cushman, S. W., & Wardzala, L. J. (1980) *J. Biol. Chem.* **255**, 4758-4762.
- Dauterive, R., Laroux, S., Bunn, R. C., Chaisson, A., Sanson, T., & Reed, B. (1996) *J. Biol. Chem.* **271**, 11414-11421.
- Davidson, N. O., Hausman, A. M. L., Ifkovits, C. A., Buse, J. B., Gould, G. W., Burant, C. F., & Bell, G. I. (1992) *Am. J. Physiol.* **262**, C795-C800.
- Davies, A. F., Davies, A., Preston, R. A. J., Clark, A. E., Holman, G. D., & Baldwin, S. A. (1991) in *Molecular Basis of Biological Membrane Function meeting*, SERC, U.K.
- Dohm, G. L., Tapscott, E. B., Pories, W. J., Flickinger, E. G., Meelheim, D., Fushiki, T., Atkinson, S. M., Elton, C. W., & Caro, J. F. (1988) *J. Clin. Invest.* **82**, 486-494.
- Due, A. D., Cook, J. A., & Fletcher, S. J. (1995a) *Biochem. Biophys. Res. Comm.* **208**, 590-596.
- Due, A. D., ZhiChao, Q., Thomas, J. M., Buchs, A., Powers, A. C., & May, J. M. (1995b) *Biochemistry* **34**, 5462-5471.

- Edwards, P. A. W. (1973) *Biochim. Biophys. Acta* **307**, 415-418.
- Elliott, K. R. F., & Craik, J. D. (1983) *Biochem. Soc. Trans.* **10**, 12-13.
- Frillingos, S., & Kaback, H. R. (1996) *Biochemistry* **35**, 5333-5338.
- Fry, A. J., Towner, P., Holman, G. D., & Eisenthal, R. (1993) *Mol. Biochem. Parasitol.* **60**, 9-18.
- Fukumoto, H., Kayano, T., Buse, J. B., Edwards, Y., Pilch, P. F., Bell, G. I., & Seino, S. (1989) *J. Biol. Chem.* **264**, 7776-7779.
- Fukumoto, H., Seino, S., Imura, H., Seino, Y., Eddy, R. L., Fukushima, Y., Byers, M. G., Shows, T. B., & G.I., B. (1988) *Proc. Natl. Acad. Sci. USA* **85**, 5434-5438.
- Garcia, J. C., Strube, M., Leingang, K., Keller, K., & Mueckler, M. M. (1992) *J. Biol. Chem.* **267**, 7770-7776.
- Geck, P. (1971) *Biochim. Biophys. Acta* **241**, 462-472.
- Gibbs, A. F., Chapman, D., & Baldwin, S. A. (1988) *Biochem. J.* **256**, 421-427.
- Gould, G. W., Brant, A. M., Kahn, B. B., Shepherd, P. R., McCoid, S. C., & Gibbs, F. M. (1992) *Diabetologia* **35**, 304-309.
- Gould, G. W., & Holman, G. D. (1993) *Biochem. J.* **295**, 329-341.
- Gould, G. W., Thomas, H. M., Jess, T. J., & Bell, G. I. (1991) *Biochemistry* **30**, 5139-5145.
- Griffith, J. K., Baker, M. E., Rouch, D. D., M.G.P., P., Skurray, R. A., Paulson, I., Chater, K. F., Baldwin, S. A., & Henderson, P. J. F. (1992) *Curr. Opin. Cell. Biol.* **4**, 684-695.
- Halperin, M. L., & Cheema-Dhadli, S. (1982) *Biochem. J.* **202**, 717-721.

Hashiramoto, M., Kadowaki, T., Clark, A. E., Muraoka, A., Momomura, K., Sakura, H., Tobe, K., Akanuma, Y., Yazaki, Y., Holman, G. D., & Kasuga, M. (1992) *J. Biol. Chem.* **267**, 17502-17507.

Hebert, D. N., & Carruthers, A. (1992) *J. Biol. Chem.* **267**, 23829-23838.

Hebert, D. N., & Carruthers, A. (1991) *Biochemistry* **30**, 4654-4658.

Helgeson, A. L., & Carruthers, A. (1987) *J. Biol. Chem.* **262**, 5464-5475.

Hellwig, B., Brown, F. M., A., S., & al, e. (1992) *Biochim. Biophys. Acta.* **1111**, 178-184.

Henderson, P. J. F., Baldwin, S. A., Cairns, M. T., Charalambous, B. M., Dent, H. C., Gunn, F. J., Liang, W. J., Lucas, V. A., G.E., M., McDonald, T. P., McKeown, B. J., Muiry, J. A., Petro, K. R., Roberts, P. E., Shatwell, K. P., Smith, G., & Tale, C. G. (1992) *Int. Rev. Cytol.* **137**, 149-208.

Herbert, D. N., & Carruthers, A. (1992) *J. Biol. Chem.* **267**, 23829-23838.

Hirayama, B. A., Loo, D. D. F., & Wright, E. M. (1994) *J. Biol. Chem.* **269**, 21407-21410.

Hirshman, M. F., Goodyear, L. J., Wardzala, L. J., Horton, E. D., & Horton, E. S. (1990) *J. Biol. Chem.* **265**, 987-991.

Hodgson, P. A., Osguthorpe, D. J., & G.D., H. (1992) in *11th Annual Molecular Graphics, Society Meeting Abstracts*.

Holman, G. D., Kozka, I. J., Clark, A. E., Flower, A. F., Saltis, J., Habberfield, A. D., Simpson, I. A., & Cushman, S. W. (1990) *J. Biol. Chem.* **265**, 18172-18179.

Holman, G. D., & Midgley, P. J. W. (1985) *Carbohydrate Research* **135**, 337-341.

Holman, G. D., Parker, B. A., & Midgley, P. J. W. (1986) *Biochim. Biophys. Acta.* **855**, 115-126.

- Holman, G. D., & Rees, W. D. (1987) *Biochim. Biophys. Acta.* **897**, 395-405.
- Honneger, P., & Semenza, G. (1973) *Biochim. Biophys. Acta.* **318**, 390-410.
- Hresko, R. C., Kruse, M., Strube, M., & Mueckler, M. (1994) *J. Biol. Chem.* **269**, 20482-20488.
- Hundal, H. S., Ahmed, A., Guma, A., Mitumoto, Y., Marette, A., Rennie, M. J., & Klip, A. (1992) *Biochem. J.* **286**, 339-343.
- Hussain, S. (1989) *Physiol. Behav.* **46**, 65-68.
- Inukai, K., Asano, T., Katagiri, H., Anai, M., Funaki, M., Ishihara, H., Tsukuda, K., Kikuchi, M., Yazaki, Y., & Oka, Y. (1994) *Biochem. J.* **302**, 355-361.
- Inukai, K., Katagiri, H., Takata, K., Asano, T., Anai, M., Ishihara, H., Nakazaki, M., Kikuchi, M., Yazaki, Y., & Oka, Y. (1995) *Endocrinology* **136**, 4850-4857.
- Ishihara, H., Asano, T., Katagiri, H., Lin, J. L., Tsukuda, K., Shibasaki, Y., & Oka, Y. (1991) *Biochem. Biophys. Res. Commun.* **176**, 922-930.
- Jacquez, J. A. (1984) *Am. J. Physiol.* **246**, R289-298.
- James, D. E., Strube, M., & Mueckler, M. (1989) *Nature* **338**, 83-87.
- Joost, H. G., Weber, T. M., & Cushman, S. W. (1988) *Biochem. J.* **249**, 155-161.
- Jordan, N. J., & Holman, G. D. (1992) *Biochem. J.* **286**, 649-656.
- Jung, C. Y. (1971) *J. Membr. Biol.* **5**, 200-214.
- Kaback, H. R. (1996) *Handbook of Biological Physics.*, Elsevier, Amsterdam.
- Kaback, H. R., Frillingos, S., Jung, H., Jung, K., Prive, G. G., Ujwal, M. L., Weitzman, C., Wu, J., & Zen, K. (1994) *J. Exp. Biol.* **196**, 183-195.
- Kaestner, K. H., Christy, R. J., McLenithan, J. C., Braiterman, J. T., Cornelius, P., Pekla, P. H., & Lane, M. D. (1989) *Proc. Natl. Acad. Sci. USA* **86**, 3150-3154.

- Kahlenberg, A., & Dolansky, D. (1972) *Can. J. Biochem.* **50**, 638-643.
- Karim, A. R., W.D., R., & Holman, G. D. (1987) *Biochim. Biophys. Acta.* **902**, 402-405.
- Kasahara, M., & Hinkle, P. C. (1977) *J. Biol. Chem.* **252**, 7384-7390.
- Katagiri, H., Asano, T., Ishihara, H., & al, e. (1993) *Biochem. J.* **291**, 861-867.
- Katagiri, H., Asano, T., Ishihara, H., Tsukuda, K., Lin, J.-L., Inukai, K., Kikuchi, M., Yazaki, Y., & Oka, Y. (1992) *J. Biol. Chem.* **267**, 22550-22555.
- Katagiri, H., Asano, T., Shibasaki, Y., Lin, J.-L., Tsukuda, K., Ishihara, H., Akanuma, Y., Takaku, F., & Oka, Y. (1991) *J. Biol. Chem.* **266**, 7769-7773.
- Kayano, T., Barrant, C. F., Fukumoto, H., Gould, G. W., Fan, Y.-S., Eddy, R. L., Byers, M. G., Shows, T. B., Seino, S., & Bell, G. I. (1990) *J. Biol. Chem.* **265**, 13276-13282.
- Kayano, T., Fukumoto, H., Eddy, R. L., Fan, Y.-S., Byers, M. G., Shows, T. B., & Bell, G. I. (1988) *J. Biol. Chem.* **263**, 15245-15248.
- Keller, K., Strube, M., & Mueckler, M. (1989) *J. Biol. Chem.* **264**, 18884-18889.
- King, A. P. J., Tai, P.-K., K, & Carter-Sue, C. (1991) *Biochemistry* **30**, 11546-11553.
- Klip, A., Ramlal, T., Young, D. A., & Holloszy, J. O. (1987) *FEBS letts.* **224**, 224-230.
- Kreig, P. A., & Melton, D. A. (1984) *Nucleic Acids Research* **12**, 7057-7070.
- Krupka, R. M. (1971) *Biochemistry* **10**, 1143-1153.
- Krupka, R. M. (1972) *Biochim. Biophys. Acta.* **282**, 326-336.
- LeFevre, P. G. (1961) *Pharmacol.Rev* **13**, 39-70.

- LeFevre, P. G., & Marshall, J. K. (1959) *Journal of Biological Chemistry* **234**, 3022-3027.
- Li, J., & Tooth, P. (1987) *Biochemistry* **26**, 4816-4823.
- Lin, J.-L., Asano, T., Katagiri, H., Tsukuda, K., Ishihara, H., Inukai, K., Yazaki, Y., & Oka, Y. (1992) *Biochem. Biophys. Acta.* **184**, 865-870.
- Lowe, A. G., & Walmsley, A. R. (1986) *Biochim. Biophys. Acta.* **857**, 146-154.
- Lund-Anderson, H. (1979) *Physiol. Rev.* **59**, 305-352.
- Maher, F., Vannucci, S. J., & Simpson, I. A. (1994) *FASEB Journal* **8**.
- Maher, F., Vannucci, S. J., Takeda, J., & Simpson, I. A. (1992) *Biochem. Biophys. Res. Comm.* **182**, 703-711.
- Maiden, M. C. J., Davis, E. O., Baldwin, S. A., Moore, D. C. M., & Henderson, P. J. F. (1987) *Nature* **325**, 641-643.
- Martin, G. E. M., Seamon, K. B., Brown, F. M., Shanahan, M. F., Roberts, P. E., & Henderson, P. J. H. (1994) *J. Biol. Chem.* **269**, 24870-24877.
- Mavrias, D. A., & Mayer, R. J. (1973) *Biochim. Biophys. Acta.* **291**, 538-544.
- May, J. M. (1988) *J. Biol. Chem* **263**, 13635-13640.
- May, J. M. (1989) *J. Biol. Chem.* **263**, 875-881.
- May, J. M., Buchs, A., & Carter-Sue, C. (1990) *Biochemistry* **29**, 10393-10398.
- May, J. M., & Mikulecky, D. C. (1982) *J. Biol. Chem* **257**, 11601-11608.
- Merrall, N. M., Plevin, R. J., & Gould, G. W. (1993) *Cellular Signalling* **5**, 667-675.
- Midgley, P. J. W., Parkar, B. A., & Holman, G. D. (1985) *Biochim. Biophys. Acta.* **812**, 33-41.

- Miyamoto, K., Tatsumi, S., Morimoto, A., Minami, H., Yamamoto, Y., Sone, K., Taketani, E., Nakabou, Y., Oka, T., & Takeda, E. (1994) *Biochem. J.* **303**, 877-883.
- Mori, H., Hashiramoto, M., Clark, A. E., Yang, J., Muraoka, A., Tamori, Y., Kasuga, M., & Holman, G. D. (1994) *J. Biol. Chem.* **269**, 11578-11583.
- Mueckler, M., Caruso, C., Badlwin, S.A., Panico, M., Blench, I., Morris, H.R., Allard, W.J., Leinahrd, G.E., Lodish, H.F. (1985) *Science* **229**, 941-945.
- Mueckler, M., Weng, W., Kruse, M. (1994a) *J. Biol. Chem.* **269**, 10533-10538.
- Mueckler, M., Kruse, M., Strube, M., Riggs, A.C., Chiu, K.C., Permutt, M.A. (1994b) *J. Biol. Chem.* **269**, 17765-17767.
- Muraoka, A., Hashiramoto, M., Clark, A.E., Edwards, L.C., Sakura, H., Kadowaki, T., Holman, G.D., Kasuga, M. (1995) *Biochem. J.* **311**, 699-704.
- Nagamatsu, S., Kornhauser, J.M., Burant, C.F., Seino, S. Mayo, K.E., Bell, G.I. (1992) *J. Biol. Chem.* **267**, 467-472.
- Nishimura, H., Pallardo, F.V., Seidner, G.A., Vannucci, S., Simpson, I.A., Birnbaum, M.J. (1993) *J. Biol. Chem.* **268**, 8514-8520.
- Oka, Y., Asano, T., Shibasaki, Y., Lin, J-L., Tsukuda, K., Katagiri, H., Akanuma, Y., Takaku, F. (1990) *Nature* **345**, 550-553.
- Orci, L., Thorens, B., Ravazzola, M., Lodish, H.F. (1989) *Science* **245**, 295-297.
- Pawagi, A. B., & Debber, C. M. (1987) *Biochem. Biophys. Res. Comm.* **145**, 1087-1091.
- Pawagi, A. B., & Deber, C. M. (1990) *Biochemistry.* **29**, 950-955.
- Pederson, O., & Gliemann, J. (1981) *Diabetologica.* **20**, 630-635.
- Pessino, A., Hebert, D.N., Woon, C.W., Harrison, S.A., Clancy, B.M., Buxton, J.M., Carruthers, A. & Czech, M.P. (1991) *J. Biol. Chem.* **266**, 20213-20217.

Peterson, R. N., & Freund, M. (1975) *Human Semen and Fertility Regulation in Men*, Mosby, St. Louis.

Ploug, T., Galbo, H., Vinten, J., Jorgensen, M. & Richter, E.A. (1987) *Am. J. Physiol. (Endocrinol. Metab.)* **253** (16), E12-E20.

Preston, R. A., & Baldwin, S. A. (1993) *Biochem. Soc. Trans.* **21**, 309-312.

Rand, E. B., Depaoli, A.M., Davidson, N.O., Bell, G.I. & Burant, C.F. (1993) *Am. J. Physiol.* **264**, G1169-G1176.

Rogers, B. J., & Perreault, S. D. (1990) *Biol. Reprod.* **43**, 1064-1069.

Schultz, S. G., & Strecker, C. K. (1970) *Biochim. Biophys. Acta.* **367**, 247-254.

Schurman, A., Keller, K., I., M., & al, e. (1993a) *Biochem. J.* **290**, 497-501.

Schurman, A., Keller, K., Monden, I., & al., e. (1993b) *Biochem. J.* **290**, 497-501.

Sergeant, S., & Kim, H. D. (1985) *J. Biol. Chem.* **260**, 14677-14682.

Shanahan, M. F. (1982) *J. Biol. Chem.* **257**, 7290-7293.

Shanahan, M. F., Morris, D. P., & Edwards, B. M. (1987) *J. Biol. Chem.* **262**, 5978-5984.

Shepherd, P. R., Gould, G.W., Colville, C.A., McCoid, S.C., Gibbs, E.M., Kahn, B.B. (1992a) *Biochem. Biophys. Res. Comm.* **188**, 149-154.

Shepherd, P. R., Gibbs, E.M., Waslau, C., Gould, G.W., Kahn, B.B. (1992b) **41**, 1360-1365.

Sigrist-Nelson, K., & Hopfer, U. (1974) *Biochim. Biophys. Acta.*, 98-112.

Simpson, I. A., & Cushman, S. W. (1986) *Annu. Rev. Biochem.* **55**, 1059-1089.

Sogin, D. C., & Hinkle, P. C. (1978) *J. Supramol. Struct.* **8**, 447-453.

- Stephens, J. M., Pilch, P.F. (1995) *Endocrine Rev.* 16, 529-546.
- Stryer, L. (1988) *Biochemistry.*, 3rd ed., W.H. Freeman and Co., New York.
- Suzue, K., Lodish, H. F., & Thorens, B. (1989) *Nucleic Acids Research* 17, 10099.
- Suzuki, K., & Kono, T. (1980) *Proc. Natl. Acad. Sci. (USA)* 77, 2542-2545.
- Takata, K., Kasahara, T., Kasahara, M., Ezaki, O., & Hirano, H. (1990) *Biochem. Biophys. Res. Commun.* 173, 67-73.
- Tamori, Y., Hashiramoto, M., Clark, A. F., Morei, H., Muraoka, A., Kadowaki, T., Holman, G. D., & Kasuga, M. (1994) *J. Biol. Chem.* 269, 2982-2986.
- Tanizawa, Y., Riggs, A. C., Chiu, K. C., Janssen, R. C., Bell, D. S. H., Go, R. P. C., Roseman, J. M., Acton, R. T., & Permutt, M. A. (1994) *Diabetologia* 37, 420-427.
- Taylor, L. P., & Holman, G. D. (1981) *Biochim. Biophys. Acta.* 642, 325-335.
- Thorens, B., Sarkar, H.K., Kaback, H.R., Lodish, H.F. (1988) *Cell* 55, 281-290.
- Thorens, B., Cheng, Z-Q., Brown, D., Lodish, H.F.,. (1990) *American Journal of Physiology* 260, C279-C285.
- Vischer, U., Blondel, B., Wollheim, C. B., Hoppner, E., Seitz, H. J., & Lijnen, P. B. (1987) *Biochem. J.* 241, 249-255.
- Waddell, I. D., Zomerschoe, A.G., Voice, M.W. & Burchell, A. (1992) *Biochem. J.* 286, 173-177.
- Wadzinski, B. E., Shanahan, M. F., & Ruoho, A. E. (1987) *J. Biol. Chem.* 262, 17683-17689.
- Wadzinski, B. E., Shanahan, M. F., Seamon, A. B., & al, e. (1990) *Biochem. J.* 272, 151-158.
- Walmsley, A. R., Lowe, A.G. (1987) *Biochim. Biophys. Acta.* 901, 229-238.

- Walmsley, A. R. (1988) *Trends. Biochem. Sci.* **13**, 226-231.
- Wandel, S., Schurmann, A., Becker, W., Summers, S. A., Shanahan, M. F., & Joost, H. G. J. N. F. L. (1994) **348**, 114-118.
- Wang, J.-F., Falke, J.J., Chan, S.I. (1986) *Proc. Natl. Acad. Sci. (USA)* **83**, 3277-3281.
- Weiler Guttler, H., Zinke, H., Mockel, B., Frey, & Gassen, H. G. (1989) *Biol. Chem. Hoppe. Seyler.* **370**, 467-473.
- Wellner, M., Monden, I., Keller, K. (1994) *Biochem. J.* **299**, 813-817.
- Wellner, M., Monden, I., & Keller, K. (1992) *FEBS Letters* **309**, 293-296.
- Wellner, M. M., I;Mueckler, MM;Keller, K. (1995) *European Journal of Biochemistry* **227**, 454-458.
- Wheeler, T. J., Hinkle, P.C. (1981) *J. Biol. Chem.* **256**, 8907-8914.
- Whitesell, R. R., & Gliemann, J. (1979) *J. Biol. Chem.* **254**, 5276-5283.
- Widdas, W. F. (1952) *J. Physiology* **118**, 23-39.
- Widdas, W. F. (1955) *J. Physiol. (London)*. **127**, 318-327.
- Williamson, M. P. (1994) *Biochem. J.* **297**, 249-260.
- Wright, E. M., Turk, E., Zabel, B., Mundlos, S., & Dyer, J. (1991) *J. Clin. Invest* **88**, 1435-1440.
- Yano, H., Seino, Y., Inagaki, N., Hinokio, Y., Yamamoto, T., Yasuda, K., Masuda, K., Someya, Y. & Imura, H. (1991) *Biochem. Biophys. Res. Commun.* **174**, 470-477.
- Zeng, H., Parthasarathy, R., Rampal, A. L., & Jung, C. Y. (1996) *Biophys. J.* **70**, 14-21.

Zoccoli, M. A., Baldwin, S. A., & Lienhard, G. E. (1978) *J. Biol. Chem.* **253**, 6923-6930.

Zottola, R. J., Cloherty, E. K., Coderre, P. E., Hansen, A., Hebert, D. N., & Carruthers, A. (1995) *Biochemistry* **34**, 9734-9747.